JPRS L/10269

21 January 1982

USSR Report

PHYSICS AND MATHEMATICS

(FOUO 1/82)

FBIS FOREIGN BROADCAST INFORMATION SERVICE

FOR OFFICIAL USE ONLY

APPROVED FOR RELEASE: 2007/02/09: CIA-RDP82-00850R000500020038-3

NOTE

JPRS publications contain information primarily from foreign newspapers, periodicals and books, but also from news agency transmissions and broadcasts. Materials from foreign-language sources are translated; those from English-language sources are transcribed or reprinted, with the original phrasing and other characteristics retained.

Headlines, editorial reports, and material enclosed in brackets [] are supplied by JPRS. Processing indicators such as [Text] or [Excerpt] in the first line of each item, or following the last line of a brief, indicate how the original information was processed. Where no processing indicator is given, the information was summarized or extracted.

Unfamiliar names rendered phonetically or transliterated are enclosed in parentheses. Words or names preceded by a question mark and enclosed in parentheses were not clear in the original but have been supplied as appropriate in context. Other unattributed parenthetical notes within the body of an item originate with the source. Times within items are as given by source.

The contents of this publication in no way represent the policies, views or attitudes of the U.S. Government.

JPRS L/10269

21 January 1982

USSR REPORT

PHYSICS AND MATHEMATICS

(FOUO 1/82)

CONTENTS

CRYSTALS AND SEMICONDUCTORS

UDC 539.2

PRINCIPLES OF THERMODEPOLARIZATION ANALYSIS

Moscow OSNOVY TERMODEPOLYARIZATSIONNOGO ANALIZA in Russian 1981 (signed to press 3 Mar 81) pp 2-8

[Annotation, preface and table of contents from book "Principles of Thermodepolarization Analysis", by Yuriy Andreyevich Gorokhovatskiy, Izdatel'stvo "Nauka", 2800 copies, 176 pages]

[Text] The monograph contains a systematized exposition of the theory of thermostimulated depolarization and the method based on this phenomenon for studying electrophysical properties of dielectrics, semiconductors, and also various devices and components of integrated circuits that contain such materials. The principal capabilities and fields of application of the method of thermostimulated depolarization are pinned down. A special section deals with exposition of the peculiarities and "stumbling blocks" of the experimental technique. Modifications of thermodepolarization analysis are described--thermostimulated depolarization under conditions of self-consistent and fractional heating, which can appreciably improve the information content of the method. An extensive bibliography is presented on thermostimulated depolarization.

Figures 47, table 1, references 321.

Preface

The method of thermostimulated depolarization (TSD) has found extensive application in recent years in the investigation of electrophysical phenomena in semiconductors, dielectrics, and also in a variety of devices and elements of integrated circuits made on the basis of such materials.

The TSD method attracts researchers by its high informativeness combined with comparative simplicity of hardware realization and processing of experimental data. However, it is not always that this method is effectively used to the full extent of its capabilities; in some cases the experimental technique is misused, and the experimental data are improperly interpreted. These negative tendencies are due both to a lack of the necessary analysis of the theory of the physical phenomenon of TSD, and to inavailability of special literature on the experimental methods of TSD.

In monographs dealing with thermoactivation spectroscopy, which includes the TSD method, this technique has remained practically unanalyzed with the exception of

a recently published book by V. N. Vertoprakhov and Ye. G. Sal'man [Ref. 49]. This situation can be attributed first of all to the fact that the TSD method began to be intensively used only in the late sixties, and secondly to the fact that until recently it has been used primarily only in research on the electret effect [Ref. 91, 118, 129, 310], in which the first attempts have been made at outlining the theory and experimental methods of TSD.

However, because of the topical thrust of this research, the TSD method has been superficially treated, and as a rule from a quite specific standpoint (in both theory and experiment).

In this book the author has set himself the task of more detailed and systematic analysis of the theory of the phenomenon and experimental technique of TSD for the purpose of further development, explanation of fundamental peculiarities, capabilities and drawbacks of the method of thermostimulated depolarization.

The book consists of five chapters.

The first chapter presents the essence of the TSD effect, and of the technique based on this effect for studying electrophysical properties of dielectrics and semiconductors. The author describes processes of polarization that take place in objects that contain polar defects and free charge carriers. The class of phenomena is pointed out for which the TSD method can be used in research, the advantages that the TSD method has over other techniques usually used for these purposes are enumerated. A Bibliography is given under headings of years, subject matter and scientific collectives. A sample of terminology is presented at the conclusion of the first chapter.

The second chapter examines the elementary theory of TSD of homogeneous material (semiconductor or dielectric) that contains a single kind of electrically active defects. An analysis is made of electronic and ionic processes associated both with orientation and with space-charge polarization. Expressions are derived that describe the TSD current for different models of charge migration and ionization. The author discusses the ways that the behavior of curves for TSD current is influenced by conditions of the contacts (blocking or non-blocking electrodes), equilibrium conductivity and disruption of electrical neutrality of a specimen. A list is given of research papers on TSD in which an examination is made of different limiting cases and approximations.

In the third chapter, a brief examination is made of the major methods of analyzing experimental curves to determine the parameters of electrically active defects (concentration, activation energy, frequency factor). An estimate is made of the errors of the methods that are considered. A technique is described for determining the nature of the polarization process from TSD curves by varying the conditions of polarization of the object.

The content of the first three chapters is essentially an introduction to thermodepolarization analysis, providing the requisite theoretical and procedural basis for going further into the specifics of the theory and the experimental technique with more complicated objects, as presented in the fourth and fifth chapters.

In particular, the fourth chapter examines the way that curves of TSD current are influenced by quasicontinuous energy distribution of electrically active defects in the object. A method is described for evaluating the parameters of this distribution from the initial section of the TSD current peak. Results are given on the use of computers for calculating TSD current curves in the case of a still more complicated model of the dielectric (semiconductor) object with two-dimensional quasicontinuous distribution of electrically active defects with respect to activation energy and with respect to frequency factor. Possible causes of the phenomenon of TSD current inversion frequency observed in experiments are discussed. In addition, the fourth chapter examines the phenomenon of repolarization in the internal electric field, the strong internal field effect, association and dissociation of complexes of electircally active defects, and their influence on the TSD current curves.

The fifth chapter describes some modifications of thermodepolarization analysis --TSD under conditions of self-consistent and fractional heating--which considerably increase the information content of the method and reduce ambiguity in the interpretation of experimental data. It is shown that the use of self-consistent heating enables determination of the order of the kinetics of the relaxation process, and accordingly affords unambiguous calculation of the activation energy and frequency factor of electrically active defects. Use of the fractional heating state enables reconstruction of the behavior of the distribution of electrically active defects with respect to activation energy or frequency factor, as well as establishment of the fact of existence of bivariate distribution. An examination is made of the question of choosing the optimum mode of fractional heating that minimizes measurement error while maximizing the resolution of the method. At the end of the chapter, a brief survey is given of different complexes of methods of studying dielectrics and semiconductors, including the TSD method, and their capabilities are analyzed.

The experimental data used in the book serve as an illustration of the theoretical principles and experimental technique of thermodepolarization analysis. An extensive survey of experimental material on investigation of some inorganic substances and compounds by methods of thermoactivation spectroscopy, and in particular by the method of TSD, can be found in Ref. 49.

The book is based on the results of studies done with direct participation of the author. A list of fundamental and additional literature is given. The additional literature is given as an aid to the reader for more detailed and complete acquaintance with some questions that are only touched upon in the text, but are not taken up in depth because of the limited scope of the book.

The author considers it his pleasant duty to thank the people at the Scientific Research Institute of Solid State Physics of Latvian State University imeni P. Stuchka and the Physics Department of Moscow Institute of Electronic Machine Building, who were of help to the author in his studies, and who also took part in discussing the results of these studies.

The author is particularly grateful to associate members of the USSR Academy of Sciences G. A. Smolenskiy and Yu. A. Osip'yan, as well as to Candidate of Physical and Mathematical Sciences E. L. Lutsenko for thorough and extremely useful analysis of the manuscript of the book during its review.

The author owes a debt of thanks to doctors of physical and mathematical sciences, professors A. N. Gubkin and Yu. R. Zakis, and to Candidate of Physical and Mathematical Sciences, Docent V. E. Eirap, who acquainted themselves with the manuscript of the book and made a number of constructive comments.

Contents page

6610
CSO: 1862/44

ELECTRICITY AND MAGNETISM

UDC 621.373.1

INERTIAL PILE-DRIVER ACCUMULATOR FOR PRODUCING HIGH-ENERGY ELECTRIC PULSES

Moscow PRIBORY I TEKHNIKA EKSPERIMENTA in Russian No 3, May-Jun 81 (manuscript received 22 Feb 80) pp 199-201

[Article by V. N. Kunin, V. V. Dorozhkov and M. V. Sergeyeva, Vladimir Polytechnical Institute]

[Text] A pulse generator is described that consists of a DC electromagnet with armored magnetic circuit, and a working coil. Pulses are generated when the electromagnet falls into a coaxial coil. Mass of the facility is four metric tons, and the maximum height to which a 1350 kg electromagnet is raised is nine meters. The facility generates bell-shaped current pulses with energy of up to 50 kJ and duration of 50-100 ms.

An inertial accumulator is described below in which the kinetic energy of a falling electromagnet is converted to the energy of an electric pulse [Ref. 1]. The accumulator is a system that consists of a DC electromagnet with armored magnetic circuit and a coaxial working coil. When the electromagnet falls into the coil, an electromotive induction force arises that is closed to a low-resistance active load.

The magnetic circuit of the electromagnet is cast from grade St.20 steel, has an outside diameter of 930 mm (Fig. 1 [photo not reproduced]) and masses 1350 kg. The magnetizing coil contains 125 turns of copper wire with 50 mm^2 cross section. Experiments have shown that the leakage coefficient of the magnetic field is 1.5-1.7.

In the accumulator the electromagnet moves under the force of gravity along guide columns by means of centering rollers on bearings. The columns are mounted on a foundation that also carries the working coil. The facility is fastened on a concrete base with shock-absorbing layer of wooden beams. The electromagnet is raised by a winch with electric drive. The hoisting cable is equipped with a lock that permits release of the electromagnet from the cable at a predetermined height. The operation of the facility is remotely controlled from a panel situated in a laboratory. The mass of the facility is four metric tons, and the height to which the electromagnet can be raised is nine meters.

Fig. 2 shows oscillograms of the current and voltage across an active load, produced by the K-115 light-beam oscilloscope. At a magnetizing current of 400 A, voltage of 30 V and height of elevation of the electromagnet of 2.0 m, the current pulse amplitude was 3 kA at voltage of 100 V. Pulse duration was 0.11 s, and the energy

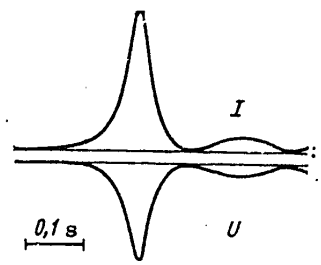

Fig. 2. Oscillograms of current I and voltage U across resistive load

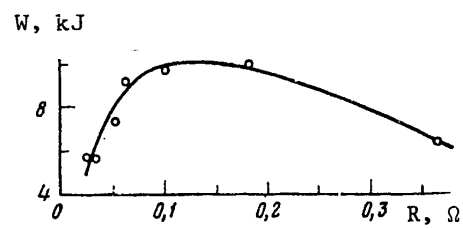

Fig. 3. Energy W released in load as a function of load resistance R

released in the load was 10.1 kJ. Thus the coefficient of amplification with respect to electric power in this experiment is equal to 25. This parameter reaches 90 in experiments with maximum heights of magnet elevation.

The coefficient of conversion of accumulated mechanical energy to the energy of an electric pulse is 38%. The load resistance and resistance of the working coil are approximately equal (maximum power mode), and therefore about 40% of the stored energy is released in the working coil as heat. The remaining 22% of the energy is mechanical losses and losses in the connecting wires.

The efficiency of the pile-driver accumulator also depends on losses associated with residual kinetic energy of the falling magnet. Actually, generation of the minimum attainable working voltage necessitates a certain residual velocity of the magnet v_{res} relative to the working coil, and therefore energy $mv_{res}^2/2$ is expended, where m is the mass of the magnet. For example when the accumulator is used for feeding arc sources, the arc is extinguished at a voltage where $v_{res} = 0.2v_{max}$ [Ref. 2], and the losses amount to 4%. Quenching of v_{res} requires transfer of momentum $P = mv_{res}$ from the magnet to the base by inelastic impact. If the braking path is about 10% of the working stroke, then in case of triangular shape of the generated pulse a constant force is required that is equal to half the

maximum working force of 100 metric tons. Such a force can be easily provided by brakes of various designs, such as a rubber bumper. However, the construction must provide for accident prevention in case the working electric circuit is ruptured, when all the energy accumulated by the magnet is transferred to the base. In this case the braking force is five times the maximum working force. Experience has shown that the required conditions are met by a lead crusher 100 mm in diameter and 80 mm high that spreads out between the flats of the base and the magnet upon impact. Energy of 1.2 kJ is expended on deformation of such a crusher by 90%, ensuring efficient braking under extreme experimental conditions.

The base of the accumulator is the same kind of electromagnet as the working unit, but turned through 180°. Shorting of its coils ensures efficient braking of the working magnet on the concluding segment of the working stroke, when the working magnet begins to induce magnetic flux in the base. The force of electromagnetic braking is proportional to the velocity of approach of the working magnet and base, which is favorable with regard to extremum situations when the approach takes place at v_{max}.

When the magnet strikes the base, a seismic wave arises that represents a certain danger to brick structures. Therefore the accumulator is situated at a distance of 30 m from the laboratory.

To reduce the power of the seismic wave, the base of the accumulator in the ground bears on the foundation through a wooden floor 50 mm thick. The foundation is built up of concrete blocks with total mass of 11 metric tons buried in the ground and laid on a sandstone bed. To reduce losses on formation of the pulsed magnetic field around the wires of the working circuit, and to alleviate the danger of harmful action of this field on the health of experimental workers, the forward and return working wires are stretched over the entire length in direct proximity to one another.

The pulse power under conditions of maximum generator power is determined by the expression

$$N = 2B^2v^2V_p/\rho,$$

where B is the induction in the working gap, v is the velocity of magnet motion, V_p is the volume of copper in the working coil and ρ is resistivity.

A disadvantage of a converter of this type is that the magnetic circuit is open before the working stroke begins. As a result, the total reluctance of the magnetic circuit includes the reluctance of an air gap equal to the width of the working coil (in our converter $\Delta l = 150$ mm), which appreciablyreduces the working value of B, and as a consequence the power of the resultant pulse.

Among the advantages of this design is moderate sensitivity of accumulator current pulse parameters to the magnitude of the external load. Fig. 3 shows how the energy released in the load depends on load resistance. In the experiments that yielded this curve, H = 2 m, and the current in the magnetizing coil was 400 A.

It can be seen from Fig. 3 that the energy maximum is rather flat, and when the load changes from 0.06 to 0.28 Ω, i. e. by a factor of 4, the power changes by

only 20%. In producing powerful pulses, we have to reconcile ourselves to the fact that about half the stored energy is expended on internal losses. Nonetheless, with respect to the ratio of electric energy in a pulse to weight of the facility, the described design corresponds approximately to a capacitive accumulator based on IMU5-140 capacitors. The maximum stored potential energy for this facility is about 110 kJ. The inertial pile-driver accumulator enables generation of bell-shaped current pulses with energy up to 50 kJ and duration of 50-100 ms.

REFERENCES

1. Dorozhkov, V. V., Kunina, M. V., "Sbornik. Voprosy nizkotemperaturnoy plazmy i magnitogidrodinamiki" [Collection. Problems of Low-Temperature Plasma and Magnetohydrodynamics], Ryazan', Radio Engineering Institute, 1978, p 37.

2. Kunin, V. N., Zalazayev, P. M., Gradusov, B. F. et al., "Sbornik. Voprosy nizkotemperaturnoy plazmy i magnitogidrodinamiki", Ryazan', Radio Engineering Institute, 1978, p 3.

6610
CSO: 8144/0423

LASERS AND MASERS

UDC 533.951.2.3

PRODUCING BAND-LIKE HIGH CURRENT ION BEAMS IN TETRODE WITH NON-SELFDESTRUCTING ANODE FOR GAS LASER PUMPING

Tomsk IZVESTIYA VYSSHIKH UCHEBNYKH ZAVEDENIY: FIZIKA in Russian Vol 24, No 9, Sep 81 p 138

[Abstract of article by V. M. Bystritskiy, Ya. Ye. Krasik and S. S. Sulakshin]

[Text] The work is devoted to the study of a new type of high current proton beam generator developed for gas laser pumping. A band-like form of proton beams was produced, and the energy, time and spatial characteristics of the beam were studied. It is shown that the resources of the generator exceed the operation by 100 to 1,000 times. The possibility of focusing a high current proton beam by two types of magnetic lenses is considered. It is noted that the application of the developed generator for Ar-N2 and XeCl laser pumping allows new results in laser research to be obtained.

CSO: 1862/50-P

UDC 621.373.826.038.823

CONTROLLING DIVERGENCE AND SPECTRUM OF XeCl LASER

Moscow KVANTOVAYA ELEKTRONIKA in Russian Vol 8, No 9(111), Sep 81 (manuscript received 1 Nov 80) pp 1861-1866

[Article by V. Yu. Baranov, V. M. Borisov and Yu. Yu. Stepanov, Institute of Atomic Energy imeni I. V. Kurchatov, Moscow]

[Text] The paper gives the results of a study of divergence and spectral composition of radiation from an electric-discharge XeCl laser with non-dispersive and dispersive cavities. It is shown here for the first time that the spectrum of the XeCl laser can be considerably narrowed by merely reducing the level of stimulated emission in a non-dispersive cavity. It is found that discharge inhomogeneity in the direction across the current has an effect on laser emission divergence. Lasing is achieved with line width of 0.1 cm^{-1} and divergence close to the diffraction limit.

Introduction

At the present time, excimer lasers are in fairly wide use in photochemistry [Ref. 1], laser purification of material [Ref. 2, 3], separation of uranium isotopes [Ref. 4] and also in laser-driven fusion programs [Ref. 5, 6]. Naturally, each of the possible applications imposes certain requirements on laser characteristics. The distinguishing feature in use of excimer lasers for nuclear fusion is that the laser cannot be used as an amplifier in the conventional arrangement of series amplification of a short pulse because of the short radiation lifetime of excimer molecules. Under discussion at present are various methods of converting or compressing an intense excimer laser pulse with duration of 100-500 ns into a pulse with duration of 1 ns [Ref. 5-7]. For example, Ref. 8 suggests time compression of a KrF laser pulse in stimulated Raman scattering of amplification of opposed beams. An approach of this kind is one of the most promising. To realize stimulated Raman scattering of amplification of opposed beams in methane, as experimentally shown in Ref. 8, the spectrum of the KrF laser must be narrowed from its initial free-running width of $\Delta\nu = 50$ cm^{-1} to $\Delta\nu = 0.1$ cm^{-1}. Such narrowing should be done in a master laser with subsequent injection of the narrow-band radiation into an amplifier.

The following circumstances must be taken into consideration in developing a master laser with narrow spectrum and divergence close to the diffraction limit. The time

of formation of inversion in electric discharge excimer lasers is ordinarily 10-20 ns [Ref. 10]. Heating of stimulated emission from the level of spontaneous noise at a characteristic cavity length of about 1 m takes place in approximately 3-4 double passes of the cavity. Under these conditions, appreciable narrowing of the spectrum and reduction of divergence can be achieved by using strongly dispersive elements, which should be accompanied by a considerable reduction of lasing energy. For this reason, for such a master laser particular attention should be given to reducing non-selective losses in the cavity and ensuring a high level of stimulated emission of the electric-discharge system.

The purpose of our research is to develop a master laser using XeCl that gives the requisite emission parameters. It has been recently demonstrated that an electron beam-pumped XeCl laser may have efficiency as high as that of the KrF laser [Ref. 9]. Besides, the XeCl laser has certain advantages: its lasing mixture is more resistant to dissociation, and withstands a much greater number of flashes than the KrF laser mixture, the free-running width is narrower--$\Delta\nu \cong 15$ cm^{-1}. Therefore, to do experiments on stimulated Raman compression of excimer laser emission we have selected the XeCl laser.

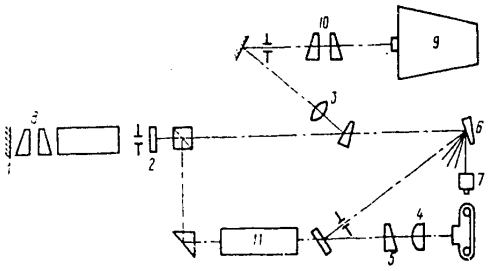

Fig. 1. Optical system of the facility: 1, 2--flat mirrors of the cavity (R_1 = 99%, R_2 = 85%); 3, 4--lenses (f_3 = 614 mm, f_4 = 340 mm); 5, 6--optical wedges (ϕ_5 = 47', ϕ_6 = 20'); 7--calorimeter; 8, 10--Fabry-Perot interferometers; 9--spectrograph; 11--He-Ne laser

Description of Facility and Method of Measurements

The optical arrangement of the facility is shown in Fig. 1. This arrangement made it possible for us to measure energy, spectrum and divergence of laser radiation in each pulse. A laser was used with UV pre-ionization by four rows of sparks; the electric circuit for producing the discharge is analogous to that of Ref. 11. The discharge was set up in a volume of $40 \times 5 \times 0.7 = 140$ cm^3, where 5 cm is the interelectrode spacing. Mainly, a cavity with external mirrors was used, and LiF windows were installed in the chamber. The laser operated on a mixture of HCl:Xe:He = 1:15:500 at pressure of 1.5-2.0 atm. To narrow the lasing spectrum, one or two IT-28-30 Fabry-Perot interferometers (8) were placed in the cavity with mirror reflectivities of 70%. The spectrum was monitored by the STE-1 spectrograph (9) with crossed IT-28-30 Fabry-Perot interferometer (10). To reduce absorption of laser emission, the aluminum coatings of the interferometer mirrors were replaced by multilayer interference coatings. Divergence of laser radiation was determined by photometry of one of the spots produced in the focus of lens 4 after passing through wedge 5. Divergence was determined with respect to the level at half intensity. Laser emission was attenuated upon reflection from wedge 6 and transmission through wedge 5. Both wedges were made of quartz and had 70% interference coatings on each face. The system comprising wedge 5, lens 4 and the camera, was aligned

with respect to the beam of He-Ne laser 11, coinciding with the excimer laser beam. The spectrograms and focal spot were photographed on KN-2 film at normal exposures. The laser pulse energy was measured by KTP calorimeter 7 with F116/1 microvoltmeter. The duration of the light pulse was determined by coaxial photocell FK-3 and an I2-7 timer. The glass window of the FK-3 strongly attenuated the laser emission, and therefore duration could be measured only for pulses with power greater than 0.1 W.

Narrowing of the Radiation Pattern

Usually electrical-discharge excimer lasers give strongly diverging radiation ($\theta = 5$-10 mrad [Ref. 11, 12]). Ref. 13 describes a laser with unstable cavity (magnification 20-30) on which a divergence of $\theta = 0.5$ mrad was attained with output aperture 5 mm in diameter. To narrow the lasing spectrum, a Fabry-Perot etalon must be placed in the laser cavity, but as pointed out in Ref. 14, the size of the base of the Fabry-Perot etalon placed in an unstable cavity is limited by the angle of aperture of the spherical wave in this cavity. On the other hand it is known [Ref. 14] that the limiting divergence is attained more easily in lasers with flat cavities than in those with unstable cavities. Therefore in our research we studied the divergence and spectrum of the XeCl laser with flat cavity.

Cavity characteristics			Lasing energy, mJ	Pulse duration at level 0.5, ns	Divergence θ_1 with respect to larger dimension, mrad	Divergence θ_2 with respect to smaller dimension, mrad
R_1, %	R_2, %	l, cm				
99	8	67	200	25	4	0.6
99	85	110	5	27	2.2	0.35
99	85	110	3	16	0.7	0.3

Note: In the last case a Fabry-Perot interferometer was placed in the cavity, $d = 0.3$ mm

The table summarizes the energy, time and space characteristics of laser operation with stimulated emission over the entire discharge aperture (50×7 mm) for different cavities. As usual for lasers of this kind, the maximum lasing energy is realized with a short cavity with weak coupling. In this case the cavity mirrors were installed directly on the discharge chamber. Radiation divergence was rather large, and on the larger dimension of the aperture it was seven times the divergence with respect to the smaller dimension. For a cavity with external mirrors and strong coupling, divergence was about two times lower. In this case there was a sharp reduction in lasing energy. It was found that divergence θ_1 with respect to the larger dimension of the aperture is nearly independent of the level of energy input, and for central regions of the discharge is about double the level for the edge regions, i. e. in the vicinity of the electrodes. On the other hand, divergence θ_2 with respect to the smaller dimension of the aperture shows little difference in the center and on the edges of the aperture, but is appreciably dependent on the level of energy input. For example, when the charging voltage is increased

from 50 to 60 kV, θ_2 increases by 50%. The transverse dimension of the discharge in this case does not change; visually it shows a large number of luminescent channels, and the increase in divergence is apparently mainly due to this deterioration of discharge homogeneity.

To further reduce divergence, a circular diaphragm is placed in the cavity. In addition, the use of a Fabry-Perot interferometer for frequency selection of the radiation is also accompanied by angular selection. By way of example, the table presents the characteristics of lasing without a diaphragm when one Fabry-Perot interferometer is installed in the cavity. The interferometer base d = 0.3 mm, and reflectivity of the mirrors was 70%. The Fabry-Perot interferometer was installed in such a way that angular selection was in the direction of greater divergence θ_1. It can be seen that divergence actually decreases with some fall-off of energy and shortening of the laser pulse. By way of illustration, Fig. 2 [photo not reproduced] shows focal spots produced at the focus of lens 4 (see Fig. 1) for various cavities and dimensions of the intracavity diaphragm D. In the case of large image magnification (Fig. 2a-c) the focal spots consist of individual points, i. e. lasing has inhomogeneous spatial distribution. Moreover, for lasing with non-dispersive cavity the focal spots in individual cases were stretched out in the direction across the discharge current. The observed distortions of shape amounted to 30-60%. The deformation of the focal spot, and accordingly the increase in θ, are obviously related to discharge inhomogeneity.

It was possible to eliminate deformation of the focal spot by shifting the diaphragm in the direction across the discharge. The reduction in θ in one of the directions when a single Fabry-Perot interferometer was installed in the cavity was accompanied by compression of the spot in this direction (see Fig. 2c). The focal spot corresponding to the state with minimum divergence and θ close to the diffraction limit is shown in Fig. 2d.

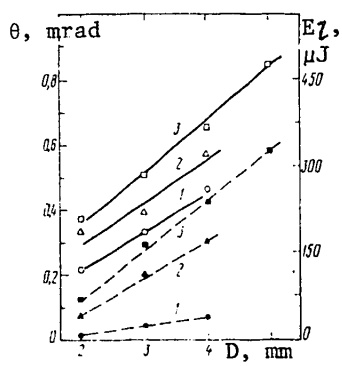

Fig. 3. Divergence θ (solid lines) and lasing energy E_ζ (dashed lines) as functions of the diameter of the intracavity diaphragm: 1--cavity with two Fabry-Perot interferometers, d = 2 mm; 2--cavity with one Fabry-Perot interferometer, d = 0.3 mm; 3--non-dispersive cavity

Fig 3 shows dependences of θ and lasing energy E_ζ on the size of diaphragm D for different lasing modes; each of the points on the graph is the average of 5-7 measurements. For a cavity with a single Fabry-Perot interferometer, θ is given for the larger dimension of the spot (see Fig. 2c). All cavities show a common pattern: decreasing θ with decreasing D. This is apparently due to a reduction in the number of transverse modes. Divergence close to the diffraction limit is obtained only at D = 2 mm and additional angular selection with respect to two directions by using two Fabry-Perot interferometers (d = 2 mm). Inclusion of the Fabry-Perot interferometers also reduces the energy and brightness of the emission. But whereas the

total energy due to suppression of transverse modes falls off rapidly, the emission brightness decreases to a lesser extent, and the spectral brightness increases. For example for D = 2 mm with transition from wide-band to narrow-band lasing with two Fabry-Perot interferometers, the energy decreases by about two orders of magnitude, whereas the brightness falls off only to one-half, and the spectral brightness increases by a factor of 20.

In the mode with minimum divergence, the laser pulse had an energy of about 10 μJ. Although this is not much energy, according to Ref. 15 it is completely adequate for injection into an amplifier that produces a pulse with energy of ~100 mJ. It is known from Ref. 15 that for a KrF amplifier an injected pulse with narrow spectrum and energy of the order of a few tens of microjoules is capable of controlling the spectrum of a pulse with energy of ~400 mJ; on the other hand, we know that all major characteristics of excimer molecules XeCl and KrF and of lasers based on these molecules are similar. Therefore we have good reason to assume that the resultant pulse with energy of ~10 μJ can be used for effective injection into a powerful XeCl amplifier.

Narrowing of the Spectrum

Ref. 15 and 16 report on getting narrow-band stimulated emission in KrF and XeCl master lasers; radiation divergence was not measured in these lasers. We have studied the spectral composition of XeCl laser radiation for stimulated emission both with a non-dispersive cavity and with intracavity Fabry-Perot interferometers. The width of each lasing line was determined from a system of interference rings obtained from the control Fabry-Perot interferometer (10) in the focal plane of the STE-1 spectrograph (see Fig. 1). Systems of rings from different lines were separated by the spectrograph. Line width was determined with respect to the level of half-intensity. Fabry-Perot interferometers were used with bases d = 1, 2, 5, 10 and 20 mm; reflectivity of the mirrors was 85%.

An attempt was made to increase the spectral power of the XeCl laser by reducing the pressure of the mixture as was done for an XeF laser in Ref. 12. Reducing the pressure of the mixture from 3 to 0.4 atm did not lead to any appreciable narrowing of the lasing spectrum.

As an example, Fig. 4 [photo not reproduced] shows spectrograms of free-running emission and lasing with a single Fabry-Perot interferometer (d = 0.3 mm) in different positions. With a non-dispersive cavity, the XeCl laser usually emits two lines: 308.0 and 308.2 nm, corresponding to transitions (0-1) and (0-2) [Ref. 17]. The width of each line under our conditions was 7-8 cm^{-1} at lasing power density of 1-3 mW/cm^2. With a Fabry-Perot interferometer (d = 0.3 mm), the spectrum shows several components. For some positions of the Fabry-Perot interferometer (see for example Fig. 4b, c), a single component remains with a reduction in lasing level by a factor of 3-4.

Fig. 5 shows the dependence of lasing line width $\Delta\nu$ on lasing energy density E_{ls} for cavities with a diaphragm. For a non-dispersive cavity and a cavity with a single Fabry-Perot interferometer (d = 2 mm) the spectrum consists of two lines of approximately equal width. The figure shows the $\Delta\nu$ for one of these. A common feature of all curves is that as E_{ls} increases, so does $\Delta\nu$. This shows up most

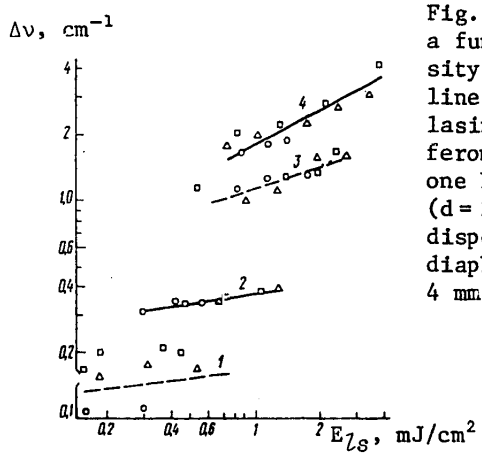

Fig. 5. Lasing line width Δν as a function of lasing energy density E_{ls}: 1, 3--lasing on one line; 2, 4--on two lines; 1--lasing with two Fabry-Perot interferometers (d = 2 mm); 2--with one Fabry-Perot interferometer (d = 2 mm); 4--lasing with non-dispersive cavity; intracavity diaphragm (D = 2 (○); 3 (△) and 4 mm (□))

weakly in the case of selection by two Fabry-Perot interferometers (curve 1, the straight line is an arbitrary approximation). The quantity Δν shows the greatest dependence on E_{ls} for a non-dispersive cavity (curve 4). As E_{ls} decreases from 4 to 0.8 mJ/cm^2, the width of each of the two lasing lines falls to half. If we consider the fact that for E_{ls} = 20-60 mJ/cm^2, Δν = 7-8 cm^{-1} for each line, we can see that by merely reducing the lasing level we can narrow the spectrum of the XeCl laser by a factor of 4-5. Such a technique may be useful for some applications.

The width of the spectrum can be further reduced by using a Fabry-Perot interferometer; however, narrowing of the spectrum in not in proportion to the resolution of the interferometer (curves 2 and 3). This can be attributed to the fact that an isolated Fabry-Perot interferometer in the cavity selects the mode composition only with respect to one direction (see Fig. 3), while selection with respect to the other direction is considerably poorer. Only under conditions of "rigid" selection by two Fabry-Perot interferometers is the spectrum narrowed in proportion to the resolution of the interferometer. Typically, emission is on only one line in this case, and a fairly strong relation shows up between Δν and θ (see points above curve 1; here an increase in θ by a factor of two with a change from D = 2 to D = 4 leads to doubling of Δν as well).

And so, in this paper we have investigated the conditions of narrowing of the spectrum and radiation pattern of the XeCl master laser. We have attained the required parameters: lasing line width of 0.1 cm^{-1} and divergence near the diffraction limit.

In conclusion, the authors thank S. N. Borisov for assistance with the experiments.

REFERENCES

1. Wampler, F. B., Tiee, J. J., Rice, W. W., Oldenborg, R. C., J. CHEM. PHYS., Vol 71, 1979, p 3926.

2. Donohue, T., OPTICAL ENG., Vol 18, 1979, p 181.

3. Clark, J. H., Andersen, R. G., APPL. PHYS. LETTS., Vol 32, 1978, p 46.

4. LASER FOCUS, Vol 16, No 5, 1980, p 18.

5. Murray, J. R., Goldhar, J., Eimerl, D., Szöke, A., IEEE J., Vol QE-15, 1979, p 342.

6. Ewing, J. J., Haas, R. A., Swingl, J. C., George, E. V., Krupke, W. F., IEEE J., Vol QE-15, 1979, p 368.

7. Krupke, W. F., George, E. V., Haas, R. A., "Laser Handbuch", Amsterdam, Vol 3, 1979, p 627.

8. Murray, J. R., Goldhar, J., Szöke, A., APPL. PHYS. LETTS., Vol 32, 1978, p 551.

9. Bothe, D. E., West, J. B., Bhaumik, M. L., IEEE J., Vol QE-15, 1979, p 314.

10. Lakoba, I. S., Yakovlenko, S. I., KVANTOVAYA ELEKTRONIKA, Vol 7, 1980, p 677.

11. Borisov, V. M., Vysikaylo, F. I., Mamonov, S. G., Napartovich, A. P., Stepanov, Yu. Yu., KVANTOVAYA ELEKTRONIKA, Vol 7, 1980, p 593.

12. Baranov, V. Yu., Borisov, V. M., Kiryukhin, Yu. B., Stepanov, Yu. Yu., KVANTOVAYA ELEKTRONIKA, Vol 5, 1978, p 2285.

13. James, D., McKee, T. J., Skrlac, W., IEEE J., Vol QE-15, 1979, p 335.

14. Anan'yev, Yu. A., "Opticheskiye rezonatory i problema raskhodimosti lazernogo izlucheniya" [Optical Cavities and the Problem of Laser Emission Divergence], Moscow, Nauka, 1979.

15. Goldhar, J., Rapoport, W. R., Murray, J. R., IEEE J., Vol QE-16, 1980, p 235.

17. Tellinghuizen, J., Hoffman, J. M., Tisone, G. C., Hays, A. K., J. CHEM. PHYS., Vol 64, 1976, p 2484.

6610
CSO: 1862/41

UDC 621.373.826.038.823

OPTIMIZING AVERAGE POWER OF EXCIMER PULSE-PERIODIC KrF AND XeCl LASERS

Moscow KVANTOVAYA ELEKTRONIKA in Russian Vol 8, No 9(111), Sep 81 (manuscript received 5 Jan 81) pp 1909-1912

[Article by V. Yu. Baranov, V. M. Borisov, F. I. Vysikaylo, Yu. B. Kiryukhin and N. Ya. Smirnov]

[Text] An examination is made of the possibilities for increasing the average power of KrF and XeCl lasers in the pulse-periodic mode without increasing the rate of circulation of the gas mixture in a closed loop. Improvement of the homogeneity and stability of the volumetric discharge resulted in an average power of about 40 W with several hours of laser operation.

There has recently been an upsurge of interest in pulse-periodic inert halide gas lasers because of a wide range of possible applications. Attainment of a high average power in such lasers involves rapid circulation of the gas mixture. For example in Ref. 1 an average power of 24 W was attained at a gas mixture flowrate of about 25 m/s. In this paper an examination is made of the possibilities for increasing average laser power [Ref. 2] at low gas mixture pumping velocity (about 6 m/s). On a fairly simple and compact laboratory facility, the main thrust is at attainment of good homogeneity and stability of the volumetric discharge with high efficiency of converting electrical energy to lasing.

Fig. 1 shows the construction of the pulse-periodic excimer laser. Chamber 1 is made of stainless steel, and the removable cover 4 holding high-voltage electrode 3 is made of glass-textolite. The surface of the cover that faces the discharge was covered with sheet Teflon, improving passivation of the loop and extending the service life of the laser. Pre-ionization, as in Ref. 2, was produced by four rows of sparks formed between the electrodes and four rows of pins that were introduced into the chamber. The length of the row was equal to the length of the grounded (2) and high-voltage (3) electrodes (720 mm). The closed stainless steel loop contained simple heat exchanger 8 and compressor 9.

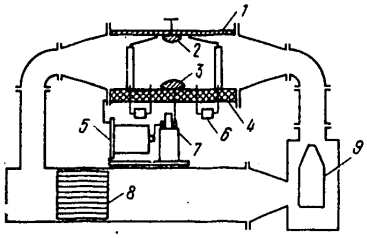

Fig. 1. Design of pulse-periodic excimer laser

The electric power supply contained an IOM-100 high-voltage source of supply that charged storage capacitor C_0 (7) in a resonant diode system. Peaking capacitor C was structurally accommodated on the removable cover and made on the basis of KVI-3 capacitors (6). A TGI-2500/50 thyratron (5) was used as the commutator. Firing of the thyratron flash-charged the low-inductance peaking capacitor, and the energy stored in it by the time of breakdown of the main interelectrode gap ensured high current density of the volumetric discharge. The amplitude of the current pulse, its rise time and duration are thus functions of the parameter C/C_0. As measurements show, this parameter has an appreciable effect on both the energy input to the volumetric discharge and its stability in the pulse recurrence mode, i. e. it determines the average power of the laser. In the measurements that we made, $C_0 = 0.5$ μF did not vary, but capacitance C was varied. The limiting current through the volumetric discharge reached 35 kA at a half-width duration of ~60 ns.

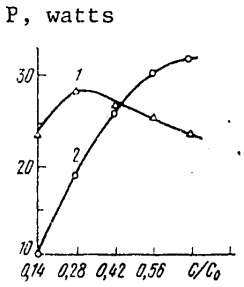

Fig. 2. Lasing output power as a function of ratio C/C_0 in mixture F_2:Kr:He = 1:25:500 (1) and HCl:Xe:He = 1:20:500 (2); p = 2 atm; U_0 = 45 kV

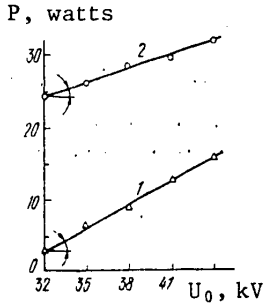

Fig. 3. Lasing output power as a function of charge voltage for unilateral (1) and bilateral (2) illumination of the active volume

The behavior of curves for $P = f(C/C_0)$ (Fig. 2) depends strongly on the composition of the working mixture. The presence of a pronounced maximum for the KrF laser (curve 1) can be explained as follows. KrF* molecules are formed only as a result of inelastic collisions of F_2 with Kr*. Excitation of Kr* atoms requires electrons of fairly high energies. At values of E/p lower than 2.5 V/(cm·mm Hg) the number of such electrons falls rapidly with increasing E/p due to collisions (with energy transfer) of electrons with light helium atoms [Ref. 3]. Therefore the reduction in lasing power for the KrF laser as C/C_0 increases past 0.28 can be attributed to the low value of E/p in the discharge, which is due to the stretching of the voltage front as C increases, resulting in breakdown of the gas gap at lower voltages across the high-voltage electrode. At the same time, there is no power maximum for the XeCl* molecule as a function of C/C_0 (curve 2) in the investigated range of values of C/C_0.

We also studied the influence that the level of pre-ionization of the discharge gap had on lasing power. The level of pre-ionization was varied, as in experiments with a monopulse laser [Ref. 4] by shorting out a row of pins to one side of the high-voltage electrode, which cut the intensity of UV radiation in half, since the sources on both sides of the electrode are identical. It should be noted that in this case there could be a change in the degree of homogeneity of photoelectron

distribution by changing the lighting geometry. As can be seen from Fig. 3, in the case of unilateral illumination the lasing power is more sharply dependent on the charge voltage across the storage capacitor, the lasing power remaining much lower than with bilateral lighting.

The considerable dependence of average laser power on homogeneity and the level of pre-ionization shown qualitatively in Fig. 3 prompted us to use a discharge over the surface of a dielectric as a pre-ionizer and plasma electrode. Such a discharge has already proved its effectiveness as a powerful homogeneous source of UV radiation in the monopulse mode [Ref. 5].

The electrode system with pre-ionization by discharge over the surface of a dielectric that we used for work under conditions of high pulse recurrence rate is shown

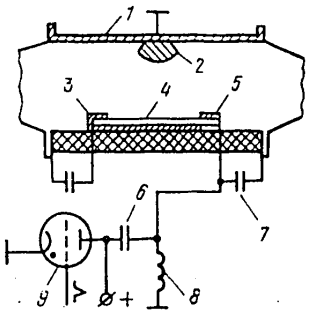

Fig. 4a. Construction of chamber with discharge over dielectric surface: 1--stainless steel chamber; 2--grounded electrode; 3--low-voltage electrode; 4--dielectric; 5--high-voltage electrode; 6--storage capacitor; 7--ceramic-capacitor peaking line; 8--charging inductance; 9--thyratron commutator

in Fig. 4a. As the dielectric 4, we used a ceramic plate with $\varepsilon = 150$ of dimensions 165 x 100 x 5 mm. Located on the plate were two metal electrodes 3 and 5, between which an auxiliary planar discharge was developed on the surface of the dielectric. In laser chamber 1 along its optical axis were four plates. Metal electrode 2 was located at a distance of 2.6 cm from the ceramic plate. The discharge over the surface of the dielectric was formed upon charging of peaking capacitor 7. Detailed studies (the results of which will be published separately) have shown that a surface discharge with high homogeneity is stable under certain conditions even at quite high pulse recurrence rates ($f \cong 10$ kHz). Fig. 4b [photo not reproduced] shows luminescence of four sections of the plasma electrode at $f = 200$ Hz. A volumetric discharge arose between the plasma and grounded electrodes. Observations of the volumetric discharge with plasma electrode showed that it is quite homogeneous and stable. It is interesting to note that the previously observed growth of a spark filament from the metal surface of the high-voltage electrode (at elevated energy inputs) [Ref. 2] is absent on the plasma electrode.

In Ref. 6 an examination is made of the problem of the possibility of arisal of local perturbations (near the electrode) under conditions of volumetric plasma stability. The principal causes of universal instability observed in Ref. 6 are current focusing in the region with elevated conductivity (in the presence of field gradients along and across the current). The threshold conditions derived in Ref. 7 for a self-maintained discharge

$$\hat{\nu}_i \varkappa L_a > 1, \ \hat{\nu}_i = \partial \ln \nu_i / \partial \ln E, \qquad (1)$$

and for a semi-self-maintained discharge

$$\varkappa^2 \nu_i \hat{\mu}_e L_a > \nu_i;\ \hat{\mu}_e = \partial \ln \mu_e / \partial \ln E;\ \text{usually}\ \hat{\mu}_e < 0, \qquad (2)$$

show the appreciable dependence of these conditions on the field gradient (or on κ, $E = E \exp(-\kappa x)$ and plasma concentration along the current; the X axis is directed from the electrode being considered). Here L_α is a dimension of the electrode layer; $\nu_i(E/N)$ is the frequency of independent ionization from the intensity of the normalized electric field; ν_i is the ion drift rate; μ_e is electron mobility.

In our experiments the use of a plasma electrode increases the electron concentration in the electrode region, and in this way apparently reduces the field gradients along the current, which leads to stability of the electrode regions of the plasma and increases the stability of the discharge at large f. The limiting possible f for the investigated system with pre-ionization discharge over the surface of a dielectric were not attained in our experiments due to absence of cooling of the dielectric, as such cooling was technically difficult in the available chamber.

An important aspect of the pulse-periodic lasers is the work life without changing the gas mixture. Fig. 5 shows how the average power of the XeCl laser depends on

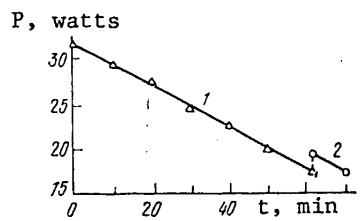

Fig. 5. Emission output power as a function of laser operating time at f = 100 Hz, U_0 = 45 kV, p = 2 atm: 1--mixture HCl:Xe:He = 1:20:500; 2--mixture after an hour of operation with addition of HCl of from 50 to 100% with respect to its initial concentration

working time without changing the gas mixture in the loop. The total volume of gas mixture in the loop is about 200 liters, the active volume occupied by the discharge is 70 x 0.8 x 3 cm, or 168 cm^3, where 3 cm is the interelectrode spacing. It can be seen from the figure that in an hour of operation the laser power falls from 30 to 20 W. In Ref. 8 with the same volume of mixture in a closed loop, the power of 14 W attained in the laser fell by 20% over a time of about 2.5 hours. Such a discrepancy can be attributed to lower average power and higher purity of the gases used in Ref. 8.

It was noted in Ref. 2 that one of the causes of a reduction in lasing power may be a reduction in the concentration of halide in connection with its drift to the walls of the chamber. Therefore we added different amounts of HCl to the gas volume of the laser after an hour of operation; however, there was either no increase in lasing power at all, or it was only slight (see curve 2 on Fig. 5). This is an indication that in our case there is an accumulation of plasma-chemical reaction products that may absorb on the laser emission wavelength, as well as products that are capable of quenching the excited XeCl* molecules in the discharge.

With operation under forced conditions (charge voltage about 45 kV at interelectrode spacing of about 4 cm), the power produced on the laser amounted to 40 W at efficiency of about 0.9%, and after an hour of operation it had decreased by 40-50% without a change of gas mixture in the loop. Gradual replacement of the gas mixture in the

loop during laser operation enables many hours of operation without any appreciable reduction of power.

Thus the results of this research show that the average power of pulse-periodic excimer lasers can be considerably increased without increasing the rate of circulation merely by increasing the homogeneity and stability of the volumetric discharge. This is done by choosing the optimum relation between parameters of the electric circuit for a specific laser mixture, and by providing a high level of uniform pre-ionization.

REFERENCES

1. Wang, C. P., Gibb, O. L., IEEE J., Vol QE-15, 1979, p 318.

2. Baranov, V. Yu., Baranov, G. S., Borisov, V. M., Kiryukhin, Yu. B., Mamonov, S. G., KVANTOVAYA ELEKTRONIKA, Vol 7, 1980, p 896.

3. Sze, R. C., Scott, P. B., REV. SCI. INSTR., Vol 49, 1978, p 772.

4. Baranov, V. Yu., Vysikaylo, V. I., Mamonov, S. G., Napartovich, A. P., Stepanov, Yu. Yu., KVANTOVAYA ELEKTRONIKA, Vol 7, 1980, p 593.

5. Baranov, V. Yu., Borisov, V. M., Khristoforov, O. B., KVANTOVAYA ELEKTRONIKA, Vol 8, 1981, p 165.

6. Vysikaylo, V. I., Dykhne, A. M., Napartovich, A. P., "Tezisy dokladov pyatoy Vsesoyuznoy konferentsii po fizike nizkotemperaturnoy plazmy" [Abstracts of Papers to the Fifth All-Union Conference on Low-Temperature Plasma Physics], Kiev, 1978, p 165.

7. Dykhne, A. M., Napartovich, A. P., DOKLADY AKADEMII NAUK SSSR, Vol 247, 1979, p 837.

8. Miller, J. L., Dickie, J., Davin, J., Swingle, J., Kan, T., APPL. PHYS. LETTS., Vol 35, 1979, p 912.

6610
CSO: 1862/41

UDC 621.378.32

MULTIPASS NEODYMIUM GLASS AMPLIFIER

Moscow KVANTOVAYA ELEKTRONIKA in Russian Vol 8, No 9(111), Sep 81 (manuscript received 17 Mar 81) pp 1962-1967

[Article by A. V. Kil'pio, A. V. Larikov, A. A. Malyutin and P. P. Pashinin, Institute of Physics imeni P. N. Lebedev, USSR Academy of Sciences]

[Text] The paper describes the design of a multipass amplifier that uses prism optics for organizing passes. The calculated and experimental characteristics of the amplifier are given. A gain of $\sim 2 \cdot 10^4$ is achieved (with consideration of losses--$\sim 2.5 \cdot 10^3$) for pulse duration of 25 ns with energy of 4 mJ.

As multipass devices are well known and extensively used in optics, it is no wonder that the idea of using multipass devices for amplifying electromagnetic radiation was suggested even before lasers put in their appearance. In quantum electronics, the use of a Fabry-Perot interferometer as a resonator has helped us to make lasers even on media with quite weak amplification.

At the present time, the upsurge of interest in multipass devices has been prompted by development of powerful laser facilities for nuclear fusion [Ref. 1], where the use of this idea promises a considerable reduction in cost and an improvement in the efficiency and reliability of systems. At the same time, the use of multipass amplifiers is also attractive for other types of facilities, since this reduces overall dimensions, while simultaneously improving radiation power and energy.

Three major types of multipass amplifiers are known. The first type--regenerative amplifiers--is analogous to the conventional laser with Fabry-Perot cavity. Input and output of radiation in these devices is by electro-optical shutters [Ref. 2]. The second type is amplifiers with telescopic optics (spherical or cylindrical) [Ref. 3]. Both these types of amplifiers have considerable drawbacks. In regenerative amplifiers, the limitations on aperture and stability of electro-optical shutters preclude the attainment of high emission power. Work with large-aperture beams is difficult. Another considerable disadvantage is the leakage of radiation from preceding passes into the output channel of the amplifier, in the former case due to the finite contrast of the shutter, and in the second case--to diffraction effects on the mirrors. The tendency to self-excitation appreciably reduces the advantage of these types of multipass amplifiers.

The third type is multipass amplifiers with spatial separation of beams. Here the power limitations are determined only by the stability of the reflective

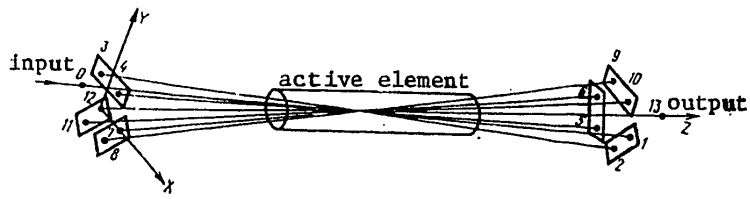

Fig. 1. Diagram of multipass amplifier; numbers 1-12 indicate the successive positions of beam 0,13 on the "hypotenuse" faces of the prisms.

components, and if arrangements are used with separation of beams in the far zone, there is no leakage of radiation from preceding passes into the output channel of the amplifier. A disadvantage of this type of multipass amplifier (as of the other two types) is high sensitivity of the direction of the output beam to stability of the components used for organizing passes through the active element.

This article is devoted to a multipass amplifier based on neodymium glass that uses prism optics for organizing passes. The proposed design can be used with other types of active media as well.

There are a number of advantages to using prisms as reflective elements. First of all, their radiation resistance is higher than for mirror reflectors. Secondly, the stability of the direction of the output radiation of the amplifier can be considerably improved. Besides, the described multipass amplifier design rotates the image [Ref. 4], which considerably improves uniformity of amplification over the beam cross section. The proposed design can be used with fairly large beam apertures.

If for any reason the use of prisms is impossible (for example because of high absorption of the amplified emission), the design can use mirror reflectors that are equivalent in action to the prisms.

The proposed amplifier with prism optics uses seven passes through the active element (Fig. 1). This number of passes corresponds to "dense packing" of the amplified beams since in this case the beam axis in any cross section of the active element forms a regular hexagonal structure with the center in successive passes. The system of laser beam reflectors is made in the form of two modules of identical prisms with total internal reflection. Fig. 1 shows only the "hypotenuse" faces of these prisms. The path of a beam through an individual prism and the active element is shown on Fig. 2.

Obviously the following relations must be satisfied for compactness of the system:

$$a=2r_0;\ H+2r_0=h;\ H-2(R_0-r_0)=(L-L_a)\ \mathrm{tg}\gamma;\ 2(R_0-r_0)/L_a=\mathrm{ctg}\ \theta;\ \theta=90^\circ-\\ -\arcsin(\sin\gamma/n),$$

which can be used to find any five parameters of the amplifier if the five others are known. It is convenient to take as the starting parameters the dimensions of the active element (length and diameter), the aperture of the beam to be amplified, the base of the amplifier and the index of refraction n. The base of the

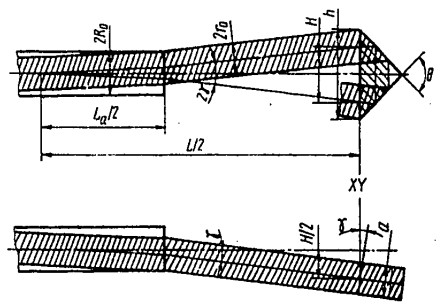

Fig. 2. Beam travel through active element and individual prism: L--base of amplifier (distance between prism modules); L_a--length of active element; R_0--radius of cross section of active element; r_0--radius of cross section of beam being amplified; h, a--height and width of prism; θ--angle between reflective faces of prism; H--distance between beam centers on hypotenuse face of prism; 2γ--angle of convergence of beams being amplified; n--index of refraction of material of active element and prisms (taken as equal for the sake of simplicity)

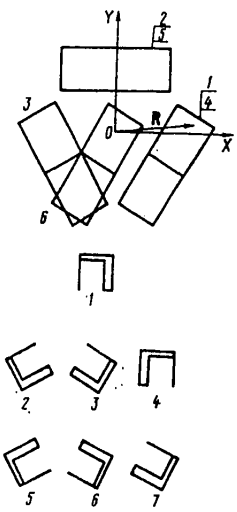

Fig. 3. Arrangement of prisms in modules (above or to the side of the amplifier input) and orientation of the beam being amplified on different passes (the numbers of the passes are indicated by the numerals)

amplifier is made as short as possible consistent with practical considerations. The aperture of the beam to be amplified must be taken somewhat larger in the calculation with consideration of the necessary alignments and the structure that holds the prisms in a group.

Fig. 3 shows the arrangement of the prisms in groups. Even numbers correspond to the input group of prisms, and odd numbers--to the output group. With this arrangement, the prism optical system of the amplifier rotates the cross section of the amplified beam as a whole relative to the axis of the system.

It can be shown that transformation of the coordinates of points of the beam after a system of k prisms arranged as in Fig. 3 takes place according to the law

$$R_k = \left(\prod_{j=1}^{k} T_j \right) R_0, \qquad (1)$$

where $\vec{R} = \{x,y\}$ is the radius vector of beam points in a unified coordinate system (such a system is shown in Fig. 3); $\vec{R}_0$ corresponds to the points at the input to the system; $k \leqslant 6$;

$$T_j = \begin{pmatrix} \cos 2\alpha_j & \sin 2\alpha_j \\ \sin 2\alpha_j & -\cos 2\alpha_j \end{pmatrix}$$

is the matrix of transformation of the j-th prism. Components T_j are defined by the angles α_j formed by the edges of the prism (line of intersection of reflecting faces) with the X axis. For our system, we have $\alpha_1 = \alpha_4 = \alpha_6 = -\pi/6$, $\alpha_2 = \alpha_5 = \pi/2$, $\alpha_3 = -5\pi/6$. Fig. 3 also shows the positions of the cross section of the beam being amplified (for an arbitrary image) on all seven passes.

The arrangement of the prisms ensures high stability of the direction of the output beam under condition that they are tightly secured in the modules, since their orientation in the module is similar to the orientation of the faces of a triple prism. An exception is the last prism on the beam path (No 6) that directs the amplified beam along the axis of the active element.

Obviously beam rotation and the different inclinations of the beam to the axis of the system ensure uniform amplification even in the case of nonuniform distribution of inversion with respect to the active element. Qualitative evaluation of the relative role of rotation of the beam cross section and oblique passage through the active element with nonuniform distribution of inversion in a specific system of a seven-pass amplifier is done by calculation.

Distribution of inversion was taken in the form

$$\Delta(x, y) = \Delta_0 + \Delta_1(x^2 + y^2) + \Delta_2 x^2 y^2,$$

which corresponds to the model of a four-lamp illuminator. The magnitudes and signs of Δ_1 and Δ_2 determine the specific behavior of inversion. In particular, in the calculations it was assumed that $\Delta_1 < 0$ and $\Delta_2 > 0$, which is equivalent to an increase of inversion from the center to the edge in planes passing through the lamps, and to a fall-off between them. Fig. 4 shows the results of calculation.

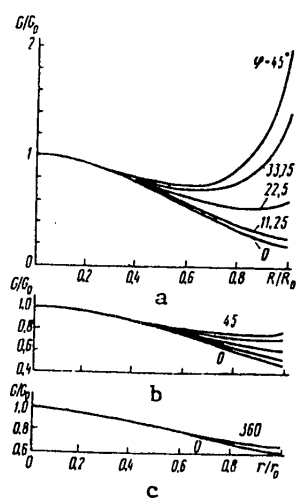

Fig. 4. Normalized amplification of laser beam G/G_0 as a function of normalized radius R/R_0 and r/r_0 with nonuniform distribution of inversion: a--normal passage through active element; b--oblique passage, and c--oblique passage with field rotation. Calculation done for seven passes, $G_0 = 3000$ is gain in the center of the beam, $r_0/R_0 = 0.67$.

We can see that while amplification on the edge of the active element varies by an order of magnitude depending on azimuthal angle ϕ, amplification on the edge of the beam with consideration of rotation and oblique path differs by less than 10%. Rotation of the field leads to a change in the output beam with respect to azimuthal angle with period π rather than $\pi/2$, as assumed for distribution of inversion in the active element.

The prism optics of the amplifier also transforms beam polarization. If polarization of emission is given by the vector

$$\mathbf{P}=\begin{pmatrix}\rho\\ re^{i\delta}\end{pmatrix},\quad \text{where } \rho^2+r^2=1,$$

then after passes through k prisms of the system we will have

$$\mathbf{P}_k=\mathbf{P}_0\prod_{j=1}^{k} D_j^{-1}\Phi\mathrm{I}D_j, \tag{2}$$

where $\mathrm{I}=\begin{pmatrix}1 & 0\\ 0 & -1\end{pmatrix}$ is the unit matrix; $\Phi=\begin{pmatrix}\exp(i\Delta_x) & 0\\ 0 & \exp(i\Delta_y)\end{pmatrix}$ is the matrix of the phase advance, and D_j and D_j^{-1} are the direct and inverse matrices of rotation through angle α_j: $D_j=\begin{pmatrix}\cos\alpha_j & \sin\alpha_j\\ -\sin\alpha_j & \cos\alpha_j\end{pmatrix}$; $\mathbf{P}_0$ is polarization at the input.

Let us note that the matrix given above $T_j=D_j^{-1}\mathrm{I}D_j$. Quantities $\Delta_x=141.38°$, $\Delta_y=69.44°$ are determined by angle $\theta=88°55'$ of the reflective prisms.

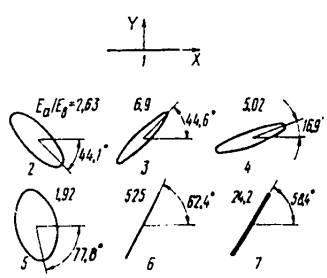

Fig. 5. Change of beam polarization by passes (calculation); input beam polarized linearly with respect to X axis; coordinate system the same as in Fig. 3.

Emission polarizations by passes calculated from (2) are shown on Fig. 5. It was assumed that radiation at the input to the amplifier is linearly polarized along the X axis. It should be noted that although the phase delay that arises in the case of total internal reflection in the prisms is fairly large (on the fifth pass we have polarization close to circular), the polarization at the output of the system is again close to linear and is rotated relative to the input polarization through an angle of about 60°.

An important characteristic of the amplifier from the standpoint of its operation at high power densities of laser emission is the nonlinear phase advance [Ref. 5].

$$B=248{,}3\int_0^L (I(z)\,n_2/n)\,dz, \tag{3}$$

where I(z) [W/cm^2] is beam intensity; n and n_2 [CGSE units] are the linear and nonlinear parts of the index of refraction of the active element and reflective prisms. If the aperture of the beam being amplified does not change during amplification, calculation of (3) presents no difficulty. For practical purposes it is convenient to use multipass amplifiers for amplifying divergent beams, e. g. as a preamplifier, i. e. immediately after the master laser in a laser unit. If we assume gaussian distribution of the beam at input to the multipass amplifier

$$J(r,\ t)=J_0 \exp\left[-(t/\tau_0)^2\right]\exp\left[-(r/r_0)^2\right]$$

(τ_0 is half-duration of the beam at intensity level J_0/e; r_0 is the half-width of the beam at this same level; J_0 is intensity at the maximum), and consider besides that r_0 varies during propagation in accordance with the law

$$r_0^2=a^2\left[1+(z-z_0)^2/k^2a^4\right]$$

(a is the dimension of constriction of the gaussian beam), which is close to the case of practical interest of using a laser with zero transverse mode as the master laser, then analytical calculation of (3) is impossible. Therefore integration of (3) in this case must be done numerically

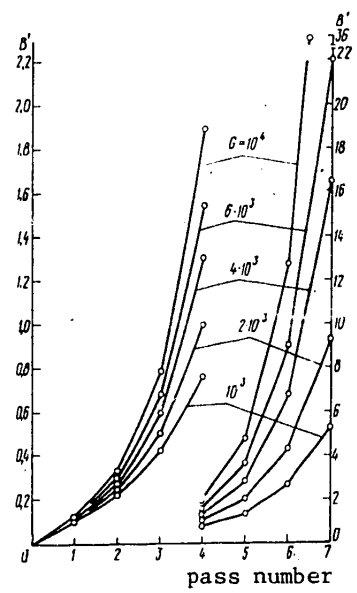

Fig. 6. Change in integral B by passes through the amplifier for gauusian pulse of duration τ with input energy E_{in} (calculated), $B' = B\tau 10^8/E_{in}$, $r_{in} = 1.5$ mm, $r_{out} = 13.5$ mm, length of active element 34 cm, length of pumped part of active element 28 cm, optical path in prisms 75 mm, base of amplifier 1.5 m, n = 1.5, $n_2 = 10^{-13}$ CGSE unit, scale on the left for passes 1-4, on the right for passes 4-7

The results of a computer calculation for a seven-pass amplifier are shown in Fig. 6. The calculation shows that nonlinear effects are negligible ($B \lesssim 1$) at peak power of pulses at the input up to 10 MW and amplification of $(2-3)\cdot 10^3$. If we consider the fact that the prism optics of the amplifier produces elliptical polarization, nonlinear effects are still further reduced (for circular polarization on all passes, the integral B would be reduced by a factor of $\sqrt{2}$).

The experimentally studied multipass amplifier used a GLS-22 neodymium glass active element with dimensions of $L_a = 340$ mm, $2R_0 = 45$ mm. The base of the amplifier was 1.5 m. At dimensions of the hypotenuse face of the reflective prisms of 7 cm and angle $\theta = 88°55'$, the maximum possible aperture of the amplified beam $2r_0 = 25$ mm. The hypotenuse faces of the prisms were anti-reflection coated (reflection <0.3%); the end faces of the active element were not coated, but were beveled relative to the axis of the active element by 7.5°. Pumping of the active element was by four IFP-8000-1 lamps (illuminator geometry same as for GOS-1001 laser).

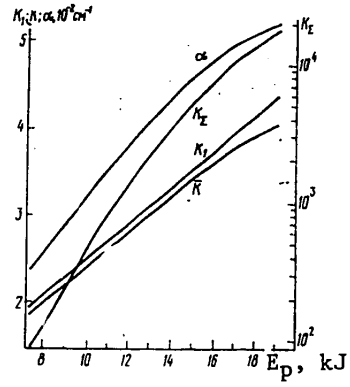

Fig. 7. Experimental values of gain K_1, K_Σ, $\bar{K} = \sqrt[7]{K_\Sigma}$ and α.

Gain measurements were made with a beam having divergence predetermined at the input to the amplifier. Beam diameter at the input was ~3 mm, at the output ~20 mm (with respect to half-intensity level). Radiation energy at the input was ~4 mJ at pulse duration of 25 ns. Measurements were made of amplification on the first pass K_1, and the total amplification on seven passes K_Σ. If K_1 was measured in the weak-signal case, then K_Σ, especially at high amplifier pumping energies E_p, could be considered as measured at signal saturation. Fig. 7 shows the pumping energy dependences of K_1 and K_Σ, together with $\bar{K} = \sqrt[7]{K_\Sigma}$ and $\alpha = \ln \bar{K}/L_p$ ($L_p = 28$ cm is the length of the pumped section of the active element). Amplification is normalized to the amplifier output, i. e. no consideration is taken of losses to absorption in optical elements of the system, Fresnel reflection or scattering. The latter is apparently responsible for most of these losses since accounting for inactive absorption (the nameplate for the active element gives $\alpha = 10^{-3}$ cm^{-1}), Fresnel reflection on the end faces of the active element and faces of the prisms gives losses of ~0.56. Accuracy of measurement of K_1 and K_Σ was ±5%. We can see that $\bar{K}$ is somewhat lower than K_1 and has a bend due to saturation at high pumping energies: output energy with pumping of 19.2 kJ is ~10 J. The difference between $\bar{K}$ and K_1 can apparently be attributed to reduction of inversion in the region of overlapping of the amplified beams in the active element (see Fig. 1).

We also measured polarization at the amplifier output with linear polarization of emission at the input. The orientation of the ellipse and the ratio of its semimajor and semiminor axes are close to the calculated values (Fig. 4).

Stability of the multipass amplifier to misalignment of its base is confirmed by prolonged operation as part of the Kamerton facility [Ref. 6]: alignment of the prism modules need not be done for a year or more.

The amplifier design completely precludes self-excitation. Suppression of amplified spontaneous emission can be effectively handled by saturable filters that can be installed both within the amplifier and at its output.

In conclusion the authors thank D. V. Bardin and V. N. Lukanin for assistance with the work.

REFERENCES

1. Lawrence Livermore Laboratory. Annual Report UCRL-50021-76, 1976.

2. Makukha, V. K., Smirnov, V. A., Tarasov, V. M., Troshin, B. I., in: "Lazernyye sistemy" [Laser Systems], Novosibirsk, Nauka, 1980, p 47.

3. Anan'yev, Yu. A., Sventsitskaya, N. A., Sherstobitov, V. Ye., ZHURNAL EKSPERIMENTAL'NOY I TEORETICHESKOY FIZIKI, Vol 56, 1968, p 131.

4. Danileyko, Yu. K., Lobachev, V. A., KVANTOVAYA ELEKTRONIKA, Vol 1, 1974, p 74.

5. Bliss, E. S., Speck, D. R., Holzrichter, J. F., Erkkala, J. H., Glass, A. J., APPL. PHYS. LETTS., Vol 25, 1974, p 448.

6. Bulatov, E. D., Vodop'yanov, K. L., Kil'pio, A. V., Malyutin, A. A., Otlivanchik, M. A., Pashinin, P. P., Filippov, A. N., Shpuga, S. M., "Proc. XIII European Conf. on Laser Interaction with Matter", Leipzig, 1979, p K13.

6610
CSO: 1862/41

UDC 535.36.621.373.826.038.824

STIMULATED SCATTERING OF LIGHT BY TEMPERATURE WAVES EXCITED IN THERMODYNAMICALLY NONEQUILIBRIUM MEDIA DUE TO ENTHALPY OF LIGHT-CONTROLLED CHEMICAL REACTIONS

Moscow KVANTOVAYA ELEKTRONIKA in Russian Vol 8, No 9(111), Sep 81 (manuscript received 15 Apr 81) pp 1968-1977

[Article by V. S. Zuyev and Ye. P. Orlov, Institute of Physics imeni P. N. Lebedev, USSR Academy of Sciences]

[Text] Based on the example of working gas mixtures of iodine photodissociation lasers it is demonstrated that in thermodynamically nonequilibrium media where the chemical reaction rate depends on the intensity of the electromagnetic field, there may be stimulated scattering of light by temperature waves that are excited due to the enthalpy of the thermodynamically nonequilibrium medium. A theoretical investigation is made of the spectrum of the scattered light; it is shown that light amplification is realized on the anti-Stokes frequency, and the gain of stimulated scattering under typical conditions characteristic of iodine lasers at a pressure of the working mixture of ~0.5 atm may reach 100-400 cm/MW.

1. Introduction

It was observed in Ref. 1 that in the active medium of iodine photodissociation lasers when a certain pumping power level is exceeded, small-scale optical inhomogeneities arise, and laser emission divergence is shaprly increased. In Ref. 2, and later in Ref. 3 it was established that this effect is associated with the presence of exothermal reactions in the active medium with rates that depend on the intensity of the laser field. The initial working gas mixture of iodine photodissociation lasers consists of buffer gases such as SF_6 or CO_2 with a small amount of molecules of type n-C_3F_7I. Upon photolysis of n-C_3F_7I molecules, excited iodine atoms are formed, some of which make a transition to the unexcited state under the action of the resonant laser field. Exothermal reactions take place between iodine atoms and n-C_3F_7 radicals, the unexcited iodine atoms reacting with the radicals many times faster than the excited atoms. Dependence of the rates of these reactions on the intensity of the laser field is due to the fact that in causing induced transitions, this field changes the concentrations of excited and unexcited iodine atoms.

It has been shown in Ref. 2 and 3 that inhomogeneities of laser field intensity lead to gasdynamic perturbations of the medium due to thermal expansion with nonuniform heating, which show up as small-scale optical inhomogeneities. In Ref. 2, consideration was given to the fact that this gives rise to nonlinear defocusing self-stress of light, and the arisal of small-scale optical inhomogeneities was attributed to instability of the laser emission wave front, assuming positive feedback and the possibility of parametric buildup of small-scale optical inhomogeneities because of the response lag of the medium.

In Ref. 4 it was demonstrated that the phenomenon observed in iodine photodissociation lasers may represent a new kind of stimulated scattering of light, i. e. it was shown that interaction of a laser field with the active medium of the laser takes place in such a way that the gasdynamic perturbations of the medium are replenished by the enthalpy of light-controlled chemical reactions, and energy is pumped from the wave of the stimulating laser field to the wave of radiation scattered by gasdynamic perturbations. It has been proposed that this effect be called enthalpy-stimulated scattering. As an example, an investigation was made in Ref. 4 of stimulated scattering of the given type by ultrasonic waves excited in the thermodynamically nonequilibrium active medium of iodine photodissociation lasers.

A fundamental qualitative difference between the enthalpy-stimulated scattering considered in Ref. 4 and conventional types of stimulated scattering (stimulated Mandelstam-Brillouin scattering, stimulated temperature scattering [Ref. 5-7], stimulated absorption scattering [Ref. 8], etc.) is that internal oscillations of the medium may be excited exclusively due to the energy of processes that occur in a thermodynamically nonequilibrium medium. In this regard, the light acts as a controlling element: it controls the process rates.

The threshold of enthalpy-stimulated scattering is quite low. For example in the active medium of iodine photodissociation lasers at pressures of 0.5-1 atm this effect has been observed at a laser field intensity of about 10 kW/cm^2 [Ref. 2]. The gain of enthalpy-stimulated scattering on ultrasound at scattering angles of about 10 mrad reaches 10 cm/MW [Ref. 4], which is almost 10^4 times higher than the gain of stimulated Mandelstam-Brillouin scattering in gases at the same pressures, and two or three orders of magnitude higher than in liquids and compressed gases [Ref. 9, 10]. The intensity of ultrasound reaches tenths of a watt per square centimeter. This is implied by experimental data on the relative change in gas density in small-scale optical inhomogeneities [Ref. 1, 2], where it is 1%, and the known speed of sound, and is also demonstrated by theoretical analysis [Ref. 11].

Ultrasonic waves are not the only partial waves of the medium that are excited under the given conditions. Since fluctuations of electromagnetic field intensity in enthalpy-stimulated scattering lead to nonuniform heating of the medium due to the energy of light-controlled processes, the excitation of ultrasound should be accompanied by excitation of isobaric density and temperature waves [Ref. 5] which, as noted in Ref. 4, should also give rise to stimulated scattering of light.

This is the phenomenon that we will study in this article.

2. Formulation of the Problem and Principal Equations

Among the chemical reactions that occur in the active region of iodine photodissociation lasers [Ref. 12], we will consider only the two fastest reactions in our examination of enthalpy-stimulated scattering on temperature waves:

$$R + J \rightarrow RJ, \quad (1)$$

$$R + R \rightarrow R_2 \quad (2)$$

where R are organofluorine radicals. The contributions made by other radicals to this stimulated scattering process can be disregarded.

The rate of energy release in a unit volume as a result of reactions (1) and (2) is

$$Q = q_1 \mathcal{K}_1 [R][J] + q_2 \mathcal{K}_2 [R]^2, \quad (3)$$

where [J], [R] are the concentrations of unexcited iodine atoms and radicals; $\mathcal{K}_1$ and $\mathcal{K}_2$ are the rate constants of reactions (1) and (2); $q_{1,2}$ is the energy released in recombination of one iodine atom and a radical into the initial RJ molecule, and of two radicals into an R_2 molecule respectively. (Let us note that in this article the quantities Q and $\mathcal{K}_2$ replace $\dot{Q}$ and $\mathcal{K}_2/2$ from Ref. 4.)

To find [R] and [J], we start from equations that describe the concentrations of particles of the working substances [N], excited iodine atoms [J*], iodine atoms in the unexcited state [J] and radicals [R]:

$$\frac{\partial [N]}{\partial t} - D_N \nabla^2 [N] = -w[N] + \mathcal{K}_1 [R][J]; \quad (4)$$

$$\frac{\partial [J^*]}{\partial t} - D_{J^*} \nabla^2 [J^*] = w[N] - \sigma_y \left([J^*] - \frac{g_2}{g_1} [J] \right) \frac{ncE^2}{4\pi\hbar\omega_0} - \frac{[J^*]}{\tau_p}; \quad (5)$$

$$\frac{\partial [J]}{\partial t} - D_J \nabla^2 [J] = \sigma_y \left([J^*] - \frac{g_2}{g_1} [J] \right) \frac{ncE^2}{4\pi\hbar\omega_0} - \mathcal{K}_1 [R][J] - \frac{[J^*]}{\tau_p}; \quad (6)$$

$$\frac{\partial [R]}{\partial t} - D_R \nabla^2 [R] = w[N] - \mathcal{K}_1 [R][J] - 2\mathcal{K}_2 [R]^2, \quad (7)$$

where w is the probability of photodissociation of molecules of the working gas under the action of ultraviolet pumping radiation; σ_y is the cross section of the laser transition; g_1/g_2 is the ratio of statistical weights of the upper and lower laser levels; τ_p is the time of nonradiative relaxation of the upper laser level; $\vec{E}$ is the total field of the exciting ($\vec{E}_0$) and scattered ($\vec{E}_S$) electromagnetic waves; n is the index of refraction of the medium; $\hbar\omega_0$ is the energy of a quantum of the laser field; D_N, D_{J^*}, D_J, D_R are the coefficients of diffusion of molecules of the working substance, excited and unexcited iodine atoms, and radicals in the buffer gas.

Equations (3)-(7) in combination with the thermal diffusivity and Maxwell's equations

$$\frac{\partial T}{\partial t} - \chi \nabla^2 T = \frac{1}{\rho c_p} Q, \quad (8)$$

$$\frac{n^2}{c^2} \frac{\partial^2 \mathbf{E}}{\partial t^2} - \nabla^2 \mathbf{E} = -\frac{1}{c^2} \frac{\partial^2}{\partial t^2} \left[\left(\frac{\partial \varepsilon}{\partial T} \right)_p T \mathbf{E} \right] \quad (9)$$

form the complete closed system of equations necessary for solving the problem of stimulated scattering by temperature waves. Here T is the deviation of the temperature of the medium from its equilibrium value T_0; χ is the coefficient of thermal diffusivity; ρ is the density of the medium; c_p is specific heat at constant pressure; $\varepsilon = n^2$. Let us note that in (9) we have left out the term corresponding to amplification on the resonant transition of atomic iodine, since accounting for amplification in the final results presents no difficulty.

3. Linearized Equations

Obviously we cannot get a general solution of system (3)-(9) in analytical form. Therefore we linearlize the system, assuming that the intensity of stimulated scattering $\sim\vec{E}_S^2$ is considerably less than the intensity of the stimulating light $\sim\vec{E}_0^2$. Then the deviations of particle concentrations from those that would have taken place in the absence of the scattered field are small, and equations (3)-(7) can be linearized. After linearization, they will take the form

$$\mathscr{K}_1[J]_0[R]_1 + \mathscr{K}_1[R]_0[J]_1 - \left(\frac{\partial}{\partial t} - D_N\nabla^2 + w\right)[N]_1 = 0; \tag{10}$$

$$\frac{g_2}{g_1}\sigma_y I_0[J]_1 - \left(\frac{\partial}{\partial t} - D_J\cdot\nabla^2 + \sigma_y I_0 + \frac{1}{\tau_p}\right)[J^*]_1 + w[N]_1 = \sigma_y\Delta_0 I_1; \tag{11}$$

$$\mathscr{K}_1[J]_0[R]_1 + \left(\frac{\partial}{\partial t} - D_J\nabla^2 + \mathscr{K}_1[R]_0 + \frac{g_2}{g_1}\sigma_y I_0\right)[J]_1 - \\ -\left(\sigma_y I_0 + \frac{1}{\tau_p}\right)[J^*] = \sigma_y\Delta_0 I_1; \tag{12}$$

$$\left(\frac{\partial}{\partial t} - D_R\nabla^2 + \mathscr{K}_1[J]_0 + 4\mathscr{K}_2[R]_0\right)[R]_1 + \mathscr{K}_1[R]_0[J]_1 - w[N]_1 = 0; \tag{13}$$

$$Q = Q_0 + Q_1, \tag{14}$$

where $[N]_0$, $[J^*]_0$, $[J]_0$, $[R]_0$ are the concentrations of particles in the absence of a scattered field; $[N]_1$, $[J^*]_1$, $[J]_1$, $[R]_1$ are the deviations of particle concentrations from $[N]_0$, $[J^*]_0$, $[J]_0$, $[R]_0$; $\Delta_0 = [J^*]_0 - [J]_0 g_2/g_1$; $I_0 = nc\mathrm{E}_0^2/4\pi\hbar\omega_0$ is the intensity of the exciting wave; $I_1 = 2nc(\mathrm{E}_0\mathrm{E}_S)/4\pi\hbar\omega_0$ is deviation of the intensity of the resultant field from I_0 due to interference of the exciting and scattered waves; $Q_0 = q_1\mathscr{K}_1[R]_0[J]_0 + q_2\mathscr{K}_2[R]_0^2$; $Q_1 = q_1\mathscr{K}_1([J]_0[R]_1 + [R]_0[J]_1) + 2q_2\mathscr{K}_2[R]_0[R_1]$.

In linearlizing equations (8) and (9) we will assume that Q_0 heats the medium to temperature T'. We denote the deviation from T' due to Q_1 by T_1. Then equation (8) is transformed to

$$\partial T_1/\partial t - \chi\nabla^2 T_1 = Q_1/\rho c_p, \tag{15}$$

and equation (9), transformed to the equation for $\vec{E}_S$, in the approximation of the given field $\vec{E}_0$, takes the form

$$\frac{n^2}{c^2}\frac{\partial^2\mathrm{E}_S}{\partial t^2} - \nabla^2\mathrm{E}_S = -\frac{1}{c^2}\left(\frac{\partial\varepsilon}{\partial T}\right)_p\frac{\partial^2}{\partial t^2}(\mathrm{E}_0 T). \tag{16}$$

In this article we will limit ourselves to the case of a monochromatic stimulating field, and will consider only the steady-state theory. The conditions of

applicability of the steady-state theory will be made clear below. Let total field $\vec{E}$ consist of linearly polarized stimulating ($\vec{E}_0$) and scattered ($\vec{E}_S$) waves with the same polarization. Then we can consider only scalar waves. Let us represent E as

$$E = {}^1/_2 E_0 \exp(i\omega_0 t - i\mathbf{k}_0\mathbf{r}) + {}^1/_2 E_S \exp(i\omega_S t - i\mathbf{k}_S\mathbf{r}) + \text{compl. conj.}, \quad (17)$$

where ω_0 and ω_S are the frequencies of the stimulating and scattered light waves; $\vec{k}_0$ and $\vec{k}_S$ are their wave vectors. Here $I_0 = ncE_0^2/8\pi\hbar\omega_0$, and

$$I_1 = {}^1/_2 \tilde{I} \exp(i\Omega t - i\mathbf{q}\mathbf{r}) + \text{comp. conj.}, \quad (18)$$

where $\tilde{I} = 2ncE_0E_S^*/8\pi\hbar\omega_0$; $\Omega = \omega_0 - \omega_S$; $\mathbf{q} = \mathbf{k}_0 - \mathbf{k}_S$.

Let us represent $[N]_1$, $[J^*]_1$, $[J]_1$, $[R]_1$, T_1, Q_1 in the same form as I_1:

$$\begin{gathered}
[N]_1 = {}^1/_2[\tilde{N}]\exp(i\Omega t - i\mathbf{q}\mathbf{r}) + \text{comp. conj.};\\
[J^*]_1 = {}^1/_2[\tilde{J}]\exp(i\Omega t - i\mathbf{q}\mathbf{r}) + \text{comp. conj.};\\
[J]_1 = {}^1/_2[\tilde{J}]\exp(i\Omega t - i\mathbf{q}\mathbf{r}) + \text{comp. conj.};\\
[R]_1 = {}^1/_2[\tilde{R}]\exp(i\Omega t - i\mathbf{q}\mathbf{r}) + \text{comp. conj.};\\
T_1 = {}^1/_2\tilde{T}\exp(i\Omega t - i\mathbf{q}\mathbf{r}) + \text{comp. conj.};\ Q_1 = {}^1/_2\tilde{Q}\exp(i\Omega t - i\mathbf{q}\mathbf{r}) + \text{comp. conj.}
\end{gathered} \quad (19)$$

Substituting (17)-(19) in equations (10)-(16), we get the following system of linear equations relative to

$$\mathcal{K}_1[J]_0[\tilde{R}] + \mathcal{K}_1[R]_0[\tilde{J}] - (i\Omega + D_N\mathbf{q}^2 + w)[\tilde{N}] = 0; \quad (20)$$

$$\frac{g_2}{g_1}\sigma_y I_0[\tilde{J}] - \left(i\Omega + D_J\mathbf{q}^2 + \sigma_y I_0 + \frac{1}{\tau_p}\right)[\tilde{J}^*] + w[\tilde{N}] = \sigma_y\Delta_0\tilde{I}; \quad (21)$$

$$\begin{gathered}
\mathcal{K}_1[J]_0[\tilde{R}] + \left(i\Omega + D_J\mathbf{q}^2 + \mathcal{K}_1[R]_0 + \frac{g_2}{g_1}\sigma_y I_0\right)[\tilde{J}] -\\
-\left(\sigma_y I_0 + \frac{1}{\tau_p}\right)[\tilde{J}^*] = \sigma_y\Delta_0\tilde{I};
\end{gathered} \quad (22)$$

$$(i\Omega + D_R\mathbf{q}^2 + \mathcal{K}_1[J]_0 + 4\mathcal{K}_2[R]_0)[\tilde{R}] + \mathcal{K}_1[R]_0[\tilde{J}] - w[\tilde{N}] = 0; \quad (23)$$

$$\tilde{Q} = q_1\mathcal{K}_1([J]_0[\tilde{R}] + [R]_0[\tilde{J}]) + 2q_2\mathcal{K}_2[R]_0[\tilde{R}]; \quad (24)$$

$$(i\Omega + \chi\mathbf{q}^2)\tilde{T} = \tilde{Q}/\rho c_p; \quad (25)$$

$$\frac{\partial E_S^*}{\partial\zeta} = i\frac{k_S}{4n^2}\left(\frac{\partial\varepsilon}{\partial T}\right)_p \tilde{T}E_0^*. \quad (26)$$

where ζ is the coordinate in direction $\vec{k}_S$; I_0 and $\tilde{I}$ are determined by using E_0 and E_S above. In deriving (25), we have limited ourselves to the case where there is no amplification of the temperature wave during propagation, and in deriving (26), consideration was taken of the fact that the relative change in amplitude of the scattered field is small at distances of the order of a wavelength of light, and therefore only the first spatial derivative of amplitude has been retained in (26).

4. Scattering Spectrum

Solving equations (20)-(23) relative to $[\tilde{R}]$ and $[\tilde{J}]$, and substituting the solutions in equation (24), we get the complex amplitude of the variable component of the rate of specific energy release $\tilde{Q}$:

$$\tilde{Q} = q_1 \mathcal{K}_1 [R]_0 \sigma_y \Delta_0 \frac{i\Omega + D_{J*}\mathbf{q}^2}{\mathrm{Det}\,|a_{ik}|} \Big[i\Omega + D_R \mathbf{q}^2 + \\ + 4\mathcal{K}_2 [R]_0 \left(1 - \frac{q_2}{2q_1} \frac{i\Omega + D_N \mathbf{q}^2}{i\Omega + D_N \mathbf{q}^2 + w} \right) \Big] \tilde{I}. \tag{27}$$

where the matrix

$$|a_{ik}| = \begin{vmatrix} i\Omega + D_R\mathbf{q}^2 + 4\mathcal{K}_2[R]_0 & -(D_J - D_{J*})\mathbf{q}^2 & -(i\Omega + D_{J*}\mathbf{q}^2) \\ \mathcal{K}_1[J]_0 & i\Omega + D_J\mathbf{q}^2 + \mathcal{K}_1[R]_0 + \\ & + \left(1 + \frac{g_2}{g_1}\right)\sigma_y I_0 + \frac{1}{\tau_p} & -\left(\sigma_y I_0 + \frac{1}{\tau_p}\right) \\ \frac{(i\Omega + D_N\mathbf{q}^2)\mathcal{K}_1[J]_0}{i\Omega + D_N\mathbf{q}^2 + w} & \frac{(i\Omega + D_N\mathbf{q}^2)\mathcal{K}_1[R]_0}{i\Omega + D_N\mathbf{q}^2 + w} + & (i\Omega + D_{J*}\mathbf{q}^2) \\ & + (D_J - D_{J*})\mathbf{q}^2 & \end{vmatrix}. \tag{28}$$

Substituting (27) in (25), we find the complex amplitude of temperature, and by using (26) we find that in the region of nonlinear interaction, the scattered field intensity proportional to $|E_S|^2$ varies in accordance with the law

$$|E_S(\zeta)|^2 = |E_S(\zeta = 0)|^2 \exp[g(\Omega)\zeta], \tag{29}$$

where

$$g(\Omega) = k_S \left(\frac{\partial \varepsilon}{\partial T}\right)_p \frac{q_1 \mathcal{K}_1 [R]_0 \sigma_y \Delta_0}{\varepsilon \rho c_p} \mathrm{Re} \Big\{ i \frac{i\Omega + D_{J*}\mathbf{q}^2}{(i\Omega + \chi\mathbf{q}^2)\,\mathrm{Det}\,|a_{ik}|} \Big[i\Omega + D_R\mathbf{q}^2 + \\ + 4\mathcal{K}_2 [R]_0 \left(1 - \frac{q_2}{2q_1} \frac{i\Omega + D_N\mathbf{q}^2}{i\Omega + D_N\mathbf{q}^2 + w} \right) \Big] \Big\} I_0. \tag{30}$$

5. Principal Results

Let us analyze the major features of the kind of scattering considered above. We will make the following assumption to simplify the analysis: all coefficients of diffusion will be taken as equal, i. e. $D_R = D_N = D_{J*} = D_J = D$. Then (30) takes the form

$$g(\Omega) = k_S \left(\frac{\partial \varepsilon}{\partial T}\right)_p \frac{q_1 \mathcal{K}_1 [R]_0 \sigma_y \Delta_0}{\varepsilon \rho c_p} \mathrm{Re} \left\{ \frac{\beta^{(1)}\Omega + i(\Omega^2 - \beta^{(2)})}{(i\Omega + \chi\mathbf{q}^2)(\alpha^{(1)}\Omega^2 - \alpha^{(3)} + i\Omega(\Omega^2 - \alpha^{(2)}))} \right\} I_0, \tag{31}$$

where

$$\alpha^{(1)} = \mathcal{K}_1 [J]_0 + \mathcal{K}_1 [R]_0 + 4\mathcal{K}_2 [R]_0 + w + (1 + g_2/g_1)\sigma_y I_0 + 3D\mathbf{q}^2 + 1/\tau_p; \tag{32}$$

$$\alpha^{(2)} = (D\mathbf{q}^2 + w)(D\mathbf{q}^2 + (1 + g_2/g_1)\sigma_y I_0 + 1/\tau_p) + (D\mathbf{q}^2 + 4\mathcal{K}_2[\mathrm{R}]_0)\times$$
$$\times(2D\mathbf{q}^2 + w + (1 + g_2/g_1)\sigma_y I_0 + 1/\tau_p) + \mathcal{K}_1[\mathrm{J}]_0(2D\mathbf{q}^2 + (1 + g_2/g_1)\sigma_y I_0 +$$
$$+ 1/\tau_p) + \mathcal{K}_1[R]_0(2D\mathbf{q}^2 + w + 4\mathcal{K}_2[R]_0 + \sigma_y I_0 + 1/\tau_p); \quad (33)$$
$$\alpha^{(3)} = [(D\mathbf{q}^2 + 4\mathcal{K}_2[\mathrm{R}]_0)(D\mathbf{q}^2 + w) + \mathcal{K}_1[\mathrm{J}]_0 D\mathbf{q}^2](Dq^2 + (1 + g_2/g_1)\sigma_y I_0 + 1/\tau_p) +$$
$$+ \mathcal{K}_1[R]_0 4\mathcal{K}_2[\mathrm{R}]_0(D\mathbf{q}^2 + w + \sigma_y I_0 + 1/\tau_p); \quad (34)$$
$$\beta^{(1)} = 2D\mathbf{q}^2 + 4\mathcal{K}_2[\mathrm{R}]_0(1 - q_2/2q_1) + w; \quad (35)$$
$$\beta^{(2)} = (D\mathbf{q}^2)^2 + (4\mathcal{K}_2[\mathrm{R}]_0(1 - q_2/2q_1) + w)D\mathbf{q}^2 + 4\mathcal{K}_2[\mathrm{R}]_0 w. \quad (36)$$

After calculating the real part of the complex expression in braces in (31), we represent the dependence $g(\Omega)$ in the form

$$g(\Omega) = k_S\left(\frac{\partial\varepsilon}{\partial T}\right)_p \frac{q_1\mathcal{K}_1[\mathrm{R}]_0\sigma_y\Delta_0}{\varepsilon\rho c_p}\frac{\Omega}{\Omega^2 + (\chi q^2)^2}\frac{W^{(1)}\Omega^4 + W^{(3)}\Omega^2 + W^{(5)}}{\Omega^{(6)} + W^{(2)}\Omega^4 + W^{(4)}\Omega^2 + W^{(6)}} I_0, \quad (37)$$

where $W^{(1)} = (\alpha^{(1)} - \beta^{(1)}) + \chi\mathbf{q}^2$; $W^{(2)} = \alpha^{(1)2} - 2\alpha^{(2)}$; $W^{(3)} = (\beta^{(1)}\alpha^{(2)} - \alpha^{(1)}\beta^{(2)}) - \alpha^{(3)} - (\alpha^{(2)} - \alpha^{(1)}\beta^{(1)} + \beta^{(2)})\chi\mathbf{q}^2$; $W^{(4)} = \alpha^{(2)2} - 2\alpha^{(1)}\alpha^{(3)}$; $W^{(5)} = \alpha^{(3)}\beta^{(2)} + (\alpha^{(2)}\beta^{(2)} - \alpha^{(3)}\beta^{(1)})\chi\mathbf{q}^2$; $W^{(6)} = \alpha^{(3)2}$.

It can be seen from (37) that dependence $g(\Omega)$ is antisymmetric relative to the sign of Ω, i. e. $g(\Omega) = -g(-\Omega)$. This means that $g(\Omega)$ will be positive either in the Stokes region or in the anti-Stokes region, depending on the sign of $(\partial\varepsilon/\partial T)_p$, i. e. amplification of the scattered light waves is realized. Consequently, the temperature waves stimulated in media in which the chemical reaction rates depend on laser field intensity should give rise to stimulated scattering of light.

Formula (37) is much simplified in two cases: when $\chi\mathbf{q}^2 < \bar{\Omega} = \min\{|W^{(k)}/W^{(j)}|^{1/(k-j)}\}$, where $j = 1, 2, 3, 4$; $k = 5, 6$, and when diffusion time $\tau_D = (D\mathbf{q}^2)^{-1}$ is considerably less than the time of chemical reactions, the time of photodissociation and the lifetime of iodine atoms in the excited state.

Actually, cofactor $f(\Omega) = (W^{(1)}\Omega^4 + W^{(3)}\Omega^2 + W^{(5)}/(\Omega^6 + W^{(2)}\Omega^4 + W^{(4)}\Omega^2 + W^{(6)})$ in (37) varies insignificantly in frequency band $|\Omega| \lesssim \Omega$: $f \approx W^{(5)}/W^{(6)}$, and cofactor $f_\tau(\Omega) = \Omega/(\Omega^2 + (\chi\mathbf{q}^2)^2)$ reaches extremum values at $\Omega = \pm\chi\mathbf{q}^2$. Therefore if angle θ between the wave vectors of the stimulating and scattered light waves is such that $\chi\mathbf{q}^2 < \bar{\Omega}$, the gain $g(\Omega)$ can be approximated as

$$g(\Omega) \approx k_S\left(\frac{\partial\varepsilon}{\partial T}\right)_p \frac{q_1\mathcal{K}_1[\mathrm{R}]_0\sigma_y\Delta_0}{\varepsilon\rho c_p}\frac{W^{(5)}}{W^{(6)}}\frac{\Omega}{\Omega^2 + (\chi q^2)^2} I_0. \quad (38)$$

The maximum gain is

$$g_{\max} = k_S\left|\frac{\partial\varepsilon}{\partial T}\right|_p \frac{q_1\mathcal{K}_1[\mathrm{R}]_0\sigma_y\Delta_0}{2\varepsilon\rho c_p\chi\mathbf{q}^2}\left|\frac{W^{(5)}}{W^{(6)}}\right| I_0. \quad (39)$$

The time of establishment of the steady state in this case is determined by the time of damping of the thermal wave: $t_{\text{уст}} \gg \tau_\tau = (\chi\mathbf{q}^2)^{-1}$.

In the second case, the gain $g(\Omega)$ can be represented as

$$g(\Omega) \approx k_S\left(\frac{\partial\varepsilon}{\partial T}\right)_p \frac{q_1\mathcal{K}_1[\mathrm{R}]_0\sigma_y\Delta_0}{\varepsilon\rho c_p}\frac{\Omega(D\mathbf{q}^2 + \chi\mathbf{q}^2)}{(\Omega^2 + (\chi\mathbf{q}^2)^2)(\Omega^2 + (D\mathbf{q}^2)^2)} I_0. \quad (40)$$

The frequencies at which $g(\Omega)$ reaches extremum values in this case are equal to

$$\Omega = \pm \frac{q^2}{\sqrt{6}} \sqrt{D^2+\chi^2} \left(\sqrt{1+12\chi^2 D^2/(D^2+\chi^2)^2} - 1\right)^{1/2}. \qquad (41)$$

If $D \cong \chi$, the frequencies determined by (41), $\Omega = \pm\chi q^2/\sqrt{3}$, i. e. the frequency shift is considerably different from that with stimulated temperature scattering or stimulated concentration scattering [Ref. 13, 14]. The maximum $g(\Omega)$ is

$$g_{\max} = k_S \left| \frac{\partial \varepsilon}{\partial T} \right|_p \frac{q_1 \mathcal{X}_1 [R]_0 \sigma_y \Delta_0}{\varepsilon \rho c_p} \frac{3\sqrt{3}}{8} \frac{l_0}{(\chi q^2)^2}, \qquad (42)$$

and the half-width of the scattering spectrum can be determined from the equation

$$\xi^4 + 2\xi^3 + 3\xi^2 - 2\xi - 1 = 0, \qquad (43)$$

where $\xi = \sqrt{3}\delta\Omega'/(2\chi q^2)$; $\delta\Omega'$ is the difference between the frequency where $|g(\Omega)|$ is maximum and the frequency where it has fallen to half. The real roots of equation (43) $\xi_1 \cong 0.7$ and $\xi_2 \cong -0.35$, implying that the half-width of the scattering spectrum $\delta\Omega \approx 2.1\chi q^2/\sqrt{3}$, i. e. approximately three times lower than with stimulated temperature scattering. The time of settling of the steady state is accordingly as many times longer.

6. Discussion of the Results

It can be seen from (37) that in media that do not absorb the energy of the electromagnetic field, there is non-zero gain of stimulated scattering by temperature waves. Just like ultrasonic waves [Ref. 4], temperature waves are stimulated in this case not by the energy of the electromagnetic field as occurs in stimulated temperature scattering or stimulated absorption scattering, but rather by the energy of chemical reactions controlled by the electromagnetic field, i. e. by the energy of the thermodynamically nonequilibrium medium. It is clear from this that the given stimulated scattering cannot be reduced to either stimulated temperature scattering or stimlated Mandelstam-Brillouin scattering. Moreover, if the amplification of scattered light waves is realized in the anti-Stokes region $\Omega < 0$, then every second an amount of energy equal to $\hbar(\omega_S - \omega_0) g I_S dV$ is added to the energy of the electromagnetic field because of stimulated scattering from every element of volume dV. It can be easily seen that in an ideal (nonabsorbing) medium the only source of increase in the energy of the electromagnetic field is from chemical reactions.

Thus by using the given kind of stimulated scattering, it is possible in principle to convert energy of chemical reactions to energy of an electromagnetic field.

Let us evaluate the gain of enthalpy-stimulated scattering on temperature waves in the active medium of iodine photodissociation lasers operating in the quasi-steady amplification mode.

We note that special studies [Ref. 16] have shown that no absorption of laser emission is observed in the active medium of these lasers, or at any rate the coefficient of absorption does not exceed 10^{-4} cm^{-1}. Consequently we should not observe ordinary stimulated absorption scattering [Ref. 8] in these lasers at typical radiation intensities of 10-100 kW/cm^2.

Our estimates are for lasers with a working gas mixture consisting of $n\text{-}C_3F_7I$ at a pressure of 0.03 atm and CO_2 at pressure of 0.47 atm. In this mixture with flash-lamp pumping for a time of ~100 μs the energy extracted from 1 cm^3 reaches ~0.05 J, which corresponds to probability of photodissociation of $n\text{-}C_3F_7I$ molecules $w \sim 4 \cdot 10^3$ s^{-1}, amplification cross section $\sigma_y = 10^{-18}$ cm^2, N_0 (initial concentration of $n\text{-}C_3F_7I$ molecules) equal to $7.5 \cdot 10^{17}$ cm^{-3}, $\mathcal{K}_1 = 7\ 10^{-12}$ cm^3/s, $\mathcal{K}_2$ $2 \cdot 10^{-12}$ cm^3/s [Ref. 17], $q_1 = 3.8 \cdot 10^{-19}$ J, $q_2 = 6.7 \cdot 10^{-19}$ J [Ref. 18], $\lambda = 1.315$ μm [Ref. 12].

Since the gain of a resonant transition of the iodine atom $\sigma_y \Delta_0$ depends on the intensity of the stimulating field I_0, we consider two separate cases. In the first case we will assume that I_0 is much greater than the intensity of the saturating signal $I_H \approx (\sigma_y \tau_p)^{-1} \sim 10^{14}$ quanta/$cm^2 \cdot s$ ($\tau_p \gtrsim 10^{-4}$ s [Ref. 19]). In this case for quasisteady concentrations $[R]_0$, $[J]_0$ and for the product $\sigma_y \Delta_0 I_0$ from equations (4)-(7), using a method analogous to that in Ref. 12, in the case of free-running emission we get the relations

$$[R]_0 \approx \sqrt{\left(\frac{1}{2}\left(1+\frac{g_2}{g_1}\right)\frac{\sigma_y I_0}{w+\sigma_y I_0}\frac{w}{\mathcal{K}_1}\right)^2 + \frac{\sigma_y I_0 w N_0}{2\beta \mathcal{K}_2 (w+\sigma_y I_0)}} - \frac{1}{2}\left(1+\frac{g_2}{g_1}\right)\frac{\sigma_y I_0}{w+\sigma_y I_0}\frac{w}{\mathcal{K}_1}; \quad (44)$$

$$[J]_0 \approx 2\beta \mathcal{K}_2 [R]_0/\mathcal{K}_1; \quad \sigma_y \Delta_0 I_0 \approx 2\beta \mathcal{K}_2 [R]_0^2, \quad (45)$$

where constant β is weakly dependent on initial conditions and lies in a range of 10-25. In estimates of $[R]_0$ and $[J]_0$ we will take $\beta \cong 20$. Then $[R]_0 \cong 5.6 \cdot 10^{15}$ cm^{-3}, and $[J]_0 \cong 6.4 \cdot 10^{16}$ cm^{-3}. We take $I_0 = 1.33 \cdot 10^{23}$ quanta/$cm^2 \cdot s$ (20 kW/cm^2).

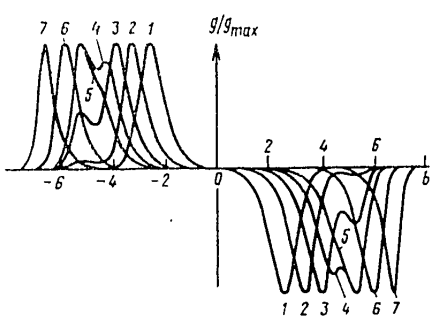

Fig. 1. Scattering spectra at $I_0 \gg I_H$ and $\theta = 1$ (1), 2.5 (2), 5 (3), 7.4 (4), 10 (5), 50 (6) and 100 mrad (7). Along the axis of ascissas $b = (\Omega/|\Omega|) \times \lg(1+|\Omega|)$, so that for $|\Omega| \ll 1$ the scale is linear with respect to frequency, while for $|\Omega| \gg 1$ we have a logarithmic scale.

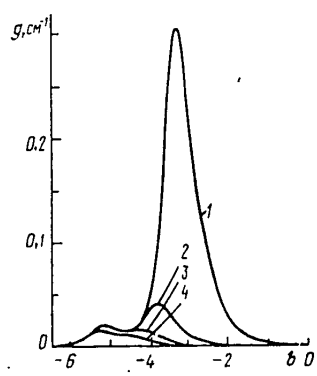

Fig. 2. Frequency dependence of gain in enthalpy-stimulated scattering at $I_0 \gg I_H$ and $\theta = 2.5$ (1), 5 (2), 7.5 (3) and 10 mrad (4). Scale along the axis of abscissas same as in Fig. 1.

Characteristic dependences $g(\Omega)$ described by formula (37) for different scattering angles θ are shown in Fig. 1 and 2. It can be seen that amplification is realized in the anti-Stokes region, the dependence of gain on Ω showing two maxima in the range of scattering angles $0 < \theta \leqslant 10$ mrad. For one of these maxima, the frequency shift and amplification are nearly independent of θ and accordingly $\Omega_1 \cong 10^5$ rad/s and $g(\Omega_1) \cong 2 \cdot 10^{-2}$ cm^{-1}. The second amplification maximum occurs at a lower absolute value of the frequency shift Ω_2, where $|\Omega_2|$ decreases with decreasing angle, while amplification increases. At $\theta \cong 5$ mrad the amplification of scattered waves shifted in frequency by $\Omega_1 \cong 10^4$ rad/s becomes greater than the amplification of waves shifted by Ω_1, and with a further reduction of θ the displacement $|\Omega_2|$ decreases as θ^2, and amplification increases as θ^{-2} (see (39)). At angles $\theta > 10$ mrad, as we see from Fig. 2, amplification falls off sharply (as θ^{-4}, see (42)). Thus for typical scattering angles of $\theta = 5$-10 mrad the gain of enthalpy-stimulated scattering $g \cong (1.5\text{-}4) \times 10^{-2}$ cm^{-1}.

Let us now consider the case where $I_0 \ll I_H$. Here concentrations $[J^*]$, $[R]_0 \gg [J]_0$. The unsaturated gain of the resonant transition of the iodine atom, as implied by (4)-(7), $\sigma_y \Delta_0 \approx \sigma_y w N_0 \tau_p / (1 + g_2/g_1 + w\tau_p) \approx 0.16$ cm^{-1}, and $[R]_0 \approx [(1 + g_2/g_1) w N_0 / (2\mathcal{K}_2 (1 + g_2/g_1 + w\tau_p))]^{1/2} \approx 2.4 \cdot 10^{16}$ cm^{-3}. In this case $g \propto I_0$, and a more convenient characteristic of amplification of enthalpy-stimulated scattering is $G = g/\hbar\omega_0 I_0$. In the range of $\theta \cong 5$-10 mrad, $G \cong 100$-400 cm/MW.

For purposes of comparison, let us estimate under the same conditions the gain of enthalpy-stimulated scattering by ultrasonic waves stimulated by light-controlled chemical reactions. For characteristic scattering angles $\theta \cong 5$-10 mrad, the maximum gain in accordance with Ref. 4 can be calculated from the formula

$$g_{\text{зв}} = k_S \left(\rho \frac{\partial \varepsilon}{\partial \rho} \right)_T \frac{q_1 \mathcal{K}_1 [R]_0 \sigma_y \Delta_0}{\varepsilon \rho c_p T_0} \frac{I_0}{2\delta\Omega_{\text{МБ}} \Omega_{\text{МБ}}}, \qquad (46)$$

where $\Omega_{\text{МБ}} = v_{\text{зв}} q$; $v_{\text{зв}}$ is the speed of sound; $2\delta\Omega_{\text{МБ}} = \Gamma q^2$ is the half-width of Mandelstam-Brillouin scattering [Ref. 20]; $\Gamma = (4/3\eta + \eta')/\rho$; η and η' are the shear and volumetric coefficients of viscosity. Substituting the same values in (46) as in the case of scattering by temperature waves, we get for $I_0 \gg I_H$, $g_{\text{зв}} \cong (0.5\text{-}4) \cdot 10^{-2}$ cm^{-1}, and for $I_0 \ll I_H$ the quantity $G_{\text{зв}} \cong 10$-70 cm/MW, i. e. under the same conditions amplification of stimulated scattering by temperature waves at $I_0 \gg I_H$ is comparable with, and at $I_0 \ll I_H$ is even much greater than amplification with scattering by ultrasound.

Thus the arisal of small-scale optical inhomogeneities in the active medium of iodine photodissociation lasers during stimulated emission or amplification of light pulses [Ref. 1] may in principle be due to enthalpy-stimulated scattering both by ultrasonic and by temperature waves. In connection with this, let us note that prevention of the development of small-scale optical inhomogeneities by reducing the initial inhomogeneity of the laser field intensity, as suggested in Ref. 3, may not be successful. The fact of the matter is, that in Ref. 3 no consideration was taken of the possibility of existence of positive feedback between perturbations of the medium and the electromagnetic field, or the possibility of arisal of instability. This precludes consideration of the part played by spontaneous processes in development of the given effect and, in particular, the role of the spontaneous process corresponding to enthalpy-stimulated scattering. This

spontaneous process is probably due to the discreteness of the process of stimulated emission analogously to the way that discreteness of the process of absorption of the electromagnetic field in an absorbing medium causes the spontaneous process corresponding to stimulated scattering caused by absorption of light [Ref. 8].

In conclusion it should be noted that enthalpy-stimulated scattering examined in Ref. 4 and in this paper is not specific to iodine lasers. As noted in Ref. 2 and 4, analogous effects should arise in other types of powerful lasers as well, and in general in media in which energy release depends on intensity of laser radiation, for example in CO_2 lasers due to VT relaxation. In this connection we note Ref. 21 which reports on an experimental study of perturbations of the index of refraction of the active medium of a CO_2 laser produced by the difference in heat release between lasing and non-lasing regions due to VT relaxation, and also Ref. 22, which examines the question of excitation of ultrasound in CO_2 lasers with unstable cavity.

The authors thank N. G. Basov for support of the work, and O. Yu. Nosach and K. S. Korol'kov for constructive discussions.

REFERENCES

1. Borovich, B. L., Zuyev, V. S., Katulin, V. A., Nosach, V. Yu., Nosach, O. Yu., Startsev, A. V., Stoylov, Yu. Yu., KVANTOVAYA ELEKTRONIKA, Vol 2, 1975, p 1281.

2. Zuyev, V. S., Netemein, V. N., Nosach, O. Yu., KVANTOVAYA ELEKTRONIKA, Vol 6, 1979, p 875.

3. Alekhin, B. V., Borovkov, V. V., Lazhintsev, B. V., Nor-Arevyan, V. A., Sukhanov, L. V., Ustinenko, V. A., KVANTOVAYA ELEKTRONIKA, Vol 6, 1979, p 1948.

4. Basov, N. G., Zuyev, V. S., Nosach, O. Yu., Orlov, Ye. P., KVANTOVAYA ELEKTRONIKA, Vol 7, 1980, p 2614.

5. Starunov, V. S., Fabelinskiy, I. L., USPEKHI FIZICHESKIKH NAUK, Vol 98, 1969, p 441.

6. Zaytsev, G. I., Kyzylasov, Yu. I., Starunov, V. S., Fabelinskiy, I. L., PIS'MA V ZHURNAL EKSPERIMENTAL'NOY I TEORETICHESKIY FIZIKI, Vol 6, 1967, p 802.

7. Herman, R. M., Gray, M.A .,PHYS. REV. LETTS, Vol 19, 1967, p 829.

8. Zel'dovich, B. Ya., Sobel'man, I. I., USPEKHI FIZICHESKIKH NAUK, Vol 101, 1970, p 3.

9. Gangardt, M. G., Grasyuk, A. Z., Zubarev, I. G., KVANTOVAYA ELEKTRONIKA, No 6, 1971, p 118.

10. Ragul'skiy, V. V., TRUDY FIZICHESKOGO INSTITUTA IMENI P. N. LEBEDEVA AKADEMII NAUK SSSR, Vol 85, 1976, p 3.

11. Zuyev, V. S., Orlov, Ye. P., Preprint FIAN [Lebedev Physics Institute], Moscow, 1981, p 158; KVANTOVAYA ELEKTRONIKA, Vol 8, 1981, p 1978.

12. Borovik, B. L., Zuyev, V. S., Katulin, V. A., Mikheyev, L. D., Nikolayev, F. A., Nosach, O. Yu., Rozanov, V. B., "Itogi nauki i tekhniki. Seriya Radiotekhnika" [Advances in Science and Technology. Electronics Series], Moscow, Izdatel'stvo VINITI, Vol 15, pp 135, 153-156.

13. Aref'yev, I. M., Morozov, V. V., PIS'MA V ZHURNAL EKSPERIMENTAL'NOY I TEORETICHESKOY FIZIKI, Vol 9, 1969, p 448.

14. Starunov, V. S., ZHURNAL EKSPERIMENTAL'NOY I TEORETICHESKIY FIZIKI, Vol 57, 1969, p 1012.

15. Likhanskiy, V. V., Napartovich, A. P., KVANTOVAYA ELEKTRONIKA, Vol 8, 1981, p 637.

16. Zuyev, V. S., Korol'kov, K. S., Nosach, O. Yu., Orlov, Ye. P., KVANTOVAYA ELEKTRONIKA, Vol 7, 1980, p 2604.

17. Kuznetsova, S. V., Maslov, A. I., KVANTOVAYA ELEKTRONIKA, Vol 5, 1978, p 1587.

18. Gurvich, L. V., Karachevtsev, G. V., Kondrat'yev, V. N., Lebedev, Yu. A., Medvedev, V. A., Potapov, V. K., Khodeyev, Yu. S., "Energiya razryva khimicheskikh svyazey. Potentsialy ionizatsii i srodstvo k elektronu" [Breaking Energy of Chemical Bonds. Ionization Potential and Electron Affinity], Moscow, Nauka, 1974, pp 72, 91.

19. Zuyev, V. S., Katulin, V. A., Nosach, V. Yu., Petrov, A. L., TRUDY FIZICHESKOGO INSTITUTA IMENI P. N. LEBEDEVA AKADEMII NAUK SSSR, Vol 125, 1980, p 46

20. Landau, L. D., Lifshits, Ye. M., "Elektrodinamika sploshnykh sred" [Electrodynamics of Continuous Media], Moscow, GIFML, 1959, p 501.

21. Roper, V. G., Lamberton, N. M., Parcelland, E. W., Manley, A. W. J., OPTICS COMMS, Vol 25, 1978, p 235.

22. Likhanskiy, V. V., Napartovich, A. P., KVANTOVAYA ELEKTRONIKA, Vol 8, 1981, p 170.

6610
CSO: 1862/41

UDC 534.61:621.373.826.038.823

INTENSITY OF ULTRASOUND EXCITED IN STIMULATED LIGHT SCATTERING BY LIGHT-CONTROLLED CHEMICAL PROCESSES

Moscow KVANTOVAYA ELEKTRONIKA in Russian Vol 8, No 9(111), Sep 81 (manuscript received 15 Apr 81) pp 1978-1984

[Article by V. S. Zuyev and Ye. P. Orlov, Institute of Physics imeni P. N. Lebedev, USSR Academy of Sciences]

[Text] Relations are derived for the intensity of ultrasound and the number of phonons falling to each scattered quantum of light with stimulated scattering in thermodynamically nonequilibrium media in which chemical reaction rates depend on light intensity. Estimates showed that in gas mixtures of CO_2 with n-C_3F_7I at a total pressure of 0.5 atm in which exothermic reactions arise between iodine atoms and organofluorine radicals upon photolysis of n-C_3F_7I, light with intensity of ~10^5 W/cm^2, resonantly interacting with iodine atoms, may excite ultrasound with intensity of tenths of a watt per square centimeter on a frequency of ~1 MHz; in this case ~10^4 phonons fall to each scattered photon.

1. Introduction

In this paper we continue our examination of enthalpy-stimulated scattering of light [Ref. 1, 2] (Ref. 2 is the preceding article in this issue of KVANTOVAYA ELEKTRONIKA) that arises in thermodynamically nonequilibrium media where reaction rates depend on the intensity of light.

As before, we study enthalpy-stimulated scattering in the active medium of iodine photodissociation lasers, which as a rule consists of SF_6 or CO_2 doped with a small amount of n-C_3F_7I vapor. Upon photolysis of n-C_3F_7I molecules, free radicals R≡n-C_3F_7 are formed along with stimulated iodine atoms J*, some of which make the transition to the unexcited state in the field of resonant laser radiation. As this happens, exothermal reactions take place in the mixture between iodine atoms and organofluorine radicals n-C_3F_7, the unexcited iodine atoms J reacting with the radicals many times faster than the excited atoms. The dependence of the rates of these reactions on laser field intensity is due to the fact that in causing stimulated transitions, this field changes the concentrations of excited and unexcited iodine atoms.

In development of enthalpy-stimulated scattering, both ultrasonic [Ref. 1] and temperature waves [Ref. 2] may arise. It will be shown in this paper that the enthalpy of chemical reactions gives rise to many phonons for each scattered photon rather than just one phonon as is the case in stimulated Mandelstam-Brillouin scattering. Relations will be derived for the intensity of ultrasound excited during enthalpy-stimulated scattering, and it will be shown how many phonons are produced for each scattered quantum of light, including numerical estimates of these quantities for specific experimental conditions.

2. Formulation of the Problem and Initial Equations

Since we need account for only the two fastest of all chemical reactions that occur in the active region of photodissociation lasers [Ref. 3] when considering enthalpy-stimulated scattering, i. e.

$$R+J\rightarrow RJ, \tag{1}$$

$$R+R\rightarrow R_2, \tag{2}$$

the power released in a unit of volume can be represented as

$$Q=q_1\mathscr{K}_1[R][J]+q_2\mathscr{K}_2[R]^2. \tag{3}$$

All symbols used in (3) are explained in Ref. 1 and 2.

Since [J] depends on the intensity of the resonant laser field, intensity fluctuations according to (3) lead to energy release that is nonuniform with respect to volume. As a consequence of thermal expansion of the gas in nonuniform heating, ultrasonic waves arise which, as shown in Ref. 1, are replenished by the enthalpy of chemical reactions (1), (2), and the energy of the stimulating emission is transferred to the electromagnetic wave scattered by ultrasound, i. e. enthalpy-stimulated scattering arises.

To find the intensity of the ultrasound that arises in enthalpy-stimulated scattering due to the enthalpy of chemical reactions, let us consider in more detail the effect of the laser field on processes of energy release in the nonlinear active medium of iodine photodissociation lasers. Let two waves propagate in this medium: a powerful stimulating laser wave $^1/_2(\mathbf{E}_L\exp(i\omega_L t-i\mathbf{k}_L\mathbf{r})+$ comp. conj.) and a stimulated scattering wave $^1/_2(\mathbf{E}_S\exp(i\omega_S t-i\mathbf{k}_S\mathbf{r})+$ comp. conj.), both waves being planar and linearly polarized. If the intensity of the scattered wave, which is proportional to $\vec{E}_S^2$, is much less than the intensity of the stimulating wave, which is proportional to $\vec{E}_L^2$, then the deviations of particle concentrations from those that would have occurred in the absence of a scattered field are small, and (3) can be represented as

$$Q=Q_0+Q_1, \tag{4}$$

where $Q_0=q_1\mathscr{K}_1[R]_0[J]_0+q_2\mathscr{K}_2[R]_0^2$, $Q_1=q_1\mathscr{K}_1[R]_0[J]_1+(q_1\mathscr{K}_1[J]_0+2q_2\mathscr{K}_2[R]_0)[R]_1$; $[J]_0$, $[R]_0$ are the concentrations of particles in the absence of a scattered field; $[J]_1$, $[R]_1$ are the deviations of concentrations from $[J]_0$, $[R]_0$.

We will limit ourselves to consideration of ultrasound whose frequency $\Omega=\omega_L-\omega_S$ is much greater than the probabilities of recombination of iodine atoms and radicals

which, according to Ref. 1, are equal to $\mathscr{K}_1[R]_0$ and $\mathscr{K}_1[J]_0+4\mathscr{K}_2[R]_0$, and also much greater than the probability of induced transitions $\sigma_y I_L/\hbar\omega_L$, where σ_y is the cross section of amplification of the laser field; I_L is the intensity of laser emission; is the energy of a quantum of the laser field. Utrasound excited in iodine photodissociation lasers, as shown by experiments [Ref. 4, 5], satisfies these conditions. Actually, from the increase in divergence of laser emission and from the characteristic transverse dimension of small-scale optical inhomogeneities we can conclude that scattering occurs at angles of 5-10 mrad to the direction of propagation of the stimulating radiation. At a laser emission wavelength of $\lambda = 1.315$ μm [Ref. 3] in mixtures with CO_2, where the speed of sound $v_{ЗВ} \cong 260$ m/s, this corresponds to $\Omega \cong (6\text{-}12)\cdot 10^6$ rad/s, while the characteristic values of $\mathscr{K}_1[R]_0 \sim \mathscr{K}_1[J]_0 + 4\mathscr{K}_2[R]_0 \approx 10^5\ s^{-1}$, and probability $\sigma_y I_L/\hbar\omega_L \leqslant 10^8 s^{-1}$ right up to laser radiation intensities of $\sim 10^5$ W/cm^2.

Within the framework of this limitation, as implied by Ref. 1, in the steady state $[J]_1 \backsim 1/\Omega$, while $[R]_1 \backsim 1/\Omega^2$, and as a result the second term in the expression for Q_1 can be disregarded compared with the first, and the equation for $[J]_1$ can be approximated by

$$\partial[J]_1/\partial t = \sigma_y \Delta_0 I_1/\hbar\omega_L, \tag{5}$$

where $\Delta_0 = [J^*]_0 - (g_2/g_1)[J]_0$; $[J^*]_0$ is the concentration of excited iodine atoms in the absence of a scattered field; g_2/g_1 is the ratio of the statistical weights of the upper and lower lasing levels; $I_1 = [(nc\mathbf{E}_L\mathbf{E}_S^*/8\pi)\exp(i\Omega t - i\mathbf{qr}) + \text{comp. conj.})$ is the deviation of intensity of the overall field from I_L; n is the index of refraction of the medium; $\mathbf{q} = \mathbf{k}_L - \mathbf{k}_S$. Substituting $[J]_1$ found by using (5) in Q_1, we get

$$Q_1 = -i\,\frac{q_1\mathscr{K}_1[R]_0\sigma_y\Delta_0}{\hbar\omega_L\Omega}\,\frac{nc}{8\pi}\,\mathbf{E}_L\mathbf{E}_S^*\exp(i\Omega t - i\mathbf{qr}) + \text{comp. conj.} \tag{6}$$

The linearized equation of gas dynamics with consideration of the power Q released in the medium takes the form [Ref. 6]

$$\frac{\partial^2\rho}{\partial t^2} - v_{ЗВ}^2\nabla^2\rho - \Gamma\frac{\partial}{\partial t}\nabla^2\rho = \frac{1}{T}\left(\frac{\partial p}{\partial S}\right)_\rho \nabla^2\int Q\,dt, \tag{7}$$

where ρ is the density of the material; $\Gamma = 4\eta/3 + \eta'$; η and η' are the shear and volumetric coefficients of viscosity; T is absolute temperature; $(\partial p/\partial S)\rho$ is the derivative of pressure p with respect to entropy S at constant density ρ. Using (7) with consideration of (4) and (6) we find the change in density of the material in the ultrasonic wave, and then the intensity of ultrasound.

3. Principal Results

Let us consider the steady-state case, i. e. we will assume that the duration of a pulse of stimulating radiation is much greater than phonon lifetime $1/2\alpha v_{ЗВ}$, where α is the coefficient of absorption of sound. In this case the deviation of ρ from the equilibrium value ρ_0 will be sought in the same form as Q_1, i. e.

$$\delta\rho = {}^1/_2\tilde{\rho}\exp(i\Omega t - i\mathbf{qr}) + \text{comp. conj.}, \tag{8}$$

where the complex amplitude of $\tilde{\rho}$ is time-independent. If we assume in this case that the amplitudes of light and sound waves as well as concentrations [J] and [R] change slowly over distances of the order of a wavelength of sound, then we get an equation for $\tilde{\rho}$ from equation (7) when (8) is substituted into (7) with consideration of (6):

$$\frac{1}{q}(\mathbf{q}\nabla)\tilde{\rho}+\left(i\frac{\Omega^2-\Omega_{\text{МБ}}^2}{2v_{\text{зв}}\Omega_{\text{МБ}}}+\alpha\frac{\Omega}{\Omega_{\text{МБ}}}\right)\tilde{\rho}=-\frac{i}{T}\left(\frac{\partial p}{\partial S}\right)_\rho\frac{q_1}{\hbar\omega_L}\frac{\mathcal{K}_1[\text{R}]_0\sigma_y\Delta_0\Omega_{\text{МБ}}}{v_{\text{зв}}^3\Omega^2}\frac{cn}{8\pi}\mathbf{E}_L\mathbf{E}_S^*, \tag{9}$$

where the derivation is based on relations $\alpha v_{\text{зв}}={}^1/_2\Gamma\mathbf{q}^2$ and $\Omega_{\text{МБ}}=v_{\text{зв}}|\mathbf{q}|$ [Ref. 7, 8].

We select a right-handed rectangular cartesian coordinate system in which the operator ∇ acts in such a way that the direction of the X axis of this system coincides with the direction of vector $\vec{q}$, while the Z axis lies in the plane passing through vectors $\vec{k}_L$, $\vec{k}_S$, $\vec{q}$. Then

$$(\mathbf{q}\nabla)\tilde{\rho}/q=d\tilde{\rho}/dx,$$

and, using the thermodynamic identity

$$\frac{1}{T}\left(\frac{\partial p}{\partial S}\right)_\rho=-\frac{v_{\text{зв}}^2}{\rho_0 c_p}\left(\frac{\partial \rho}{\partial T}\right)_p,$$

where c_p is specific heat at constant pressure, we transform (9) to

$$\frac{\partial\tilde{\rho}}{\partial x}+\left(i\frac{\Omega^2-\Omega_{\text{МБ}}^2}{2v_{\text{зв}}\Omega_{\text{МБ}}}+\alpha\frac{\Omega}{\Omega_{\text{МБ}}}\right)\tilde{\rho}=\frac{i}{\rho_0 c_p}\left(\frac{\partial\rho}{\partial T}\right)_p\frac{q_1}{\hbar\omega_L}\frac{\mathcal{K}_1[\text{R}]_0\sigma_y\Delta_0\Omega_{\text{МБ}}}{v_{\text{зв}}\Omega^2}\frac{cn}{8\pi}\mathbf{E}_L(x,z)\mathbf{E}_S^*(x,z). \tag{10}$$

Equation (10) is a linear first-order differential equation with solution that can be represented as

$$\rho(x)=\tilde{\rho}(0)\exp\left(-\frac{\alpha\Omega}{\Omega_{\text{МБ}}}x-i\frac{\Omega^2-\Omega_{\text{МБ}}^2}{2v_{\text{зв}}\Omega_{\text{МБ}}}x\right)+\frac{i}{\rho_0 c_p}\left(\frac{\partial\rho}{\partial T}\right)_p\frac{q_1}{\hbar\omega_L}\frac{\mathcal{K}_1[\text{R}]_0\sigma_y\Delta_0}{v_{\text{зв}}\Omega^2}\times$$
$$\times\Omega_{\text{МБ}}\frac{cn}{8\pi}\int_0^x\mathbf{E}_L(x',z)\mathbf{E}_S^*(x',z)\exp\left[-\frac{\alpha\Omega}{\Omega_{\text{МБ}}}(x-x')-i\times,\right.$$
$$\left.\times\frac{\Omega^2-\Omega_{\text{МБ}}^2}{2v_{\text{зв}}\Omega_{\text{МБ}}}(x-x')\right]dx'. \tag{11}$$

Let us assume that the rate of acoustic losses is greater than the rate of change in E_L and E_S in the direction of sound wave propagation, i. e.

$$\frac{\alpha|\Omega|}{\Omega_{\text{МБ}}}\gg\frac{1}{E_L}\left|\frac{\partial\mathbf{E}_L}{\partial x}\right|,\quad\frac{1}{E_S}\left|\frac{\partial\mathbf{E}_S}{\partial x}\right|.$$

Let us further take into consideration that the factor $\exp[-\alpha\Omega(x-x')/\Omega_{\text{МБ}}]$ makes the principal contribution to (11) in region $|x-x'|\leqslant\Omega_{\text{МБ}}/\alpha|\Omega|$. Then $\mathbf{E}_L(x',z)\mathbf{E}_S^*(x',z)$ can be brought out of the integrand, and its value can be taken at $x=x'$. Then in region $x\gg\Omega_{\text{МБ}}/\alpha|\Omega|$ we will have

$$\tilde{\rho}(x,z)=\frac{i}{\rho_0 c_p}\left(\frac{\partial\rho}{\partial T}\right)_p\frac{q_1}{\hbar\omega_L}\frac{\mathcal{K}_1[\text{R}]_0\sigma_y\Delta_0}{\Omega}\frac{cn}{8\pi}\frac{\mathbf{E}_L(x,z)\mathbf{E}_S^*(x,z)}{i(\Omega-\Omega_{\text{МБ}})+\delta\Omega_{\text{МБ}}}, \tag{12}$$

where it is taken into consideration that in iodine lasers amplification of the scattered field is realized on the Stokes frequency [Ref. 1], and the half-width of thermal Mandelstam-Brillouin scattering [Ref. 9] is

Substituting (12) in the known relation for sound wave intensity [Ref. 10]

$$I_{\text{зв}} = v_{\text{зв}}^3 \overline{(\delta\rho)^2}/\rho_0 = v_{\text{зв}}^3 |\tilde{\rho}|^2/2\rho_0,$$

where the vinculum over $(\delta\rho)^2$ denotes averaging over the period of the sound wave, we get

$$I_{\text{зв}}(\Omega) = \frac{v_{\text{зв}}^3}{2\rho_0}\left(\frac{1}{\rho_0 c_p}\left(\frac{\partial\rho}{\partial T}\right)_p \frac{q_1}{\hbar\omega_L}\frac{\mathcal{K}_1 [R]_0 \sigma_y \Delta_0}{\Omega}\right)^2 \frac{I_L I_S}{(\Omega-\Omega_{\text{МБ}})^2 + (\delta\Omega_{\text{МБ}})^2}, \quad (13)$$

where $I_L = cnE_L^2/8\pi$, $I_S = cnE_S^2/8\pi$.

Using the expression obtained in Ref. 1 for the gain of enthalpy-stimulated scattering

$$g(\Omega) = \frac{1}{2} k_S \frac{(\partial\varepsilon/\partial\rho)_T}{c_p T n^2}\frac{q_1}{\hbar\omega_L}\frac{\mathcal{K}_1 [R]_0 \sigma_y \Delta_0}{\Omega}\frac{\delta\Omega_{\text{МБ}}}{(\Omega-\Omega_{\text{МБ}})^2 + (\delta\Omega_{\text{МБ}})^2} I_L, \quad (14)$$

we transform (13) to

$$I_{\text{зв}}(\Omega) = K\frac{g(\Omega)\,\Omega}{2\alpha\omega_S} I_S, \quad (15)$$

where

$$K = \frac{2cnv_{\text{зв}}^2}{(\rho\partial\varepsilon/\partial\rho)_T c_p T}\left(\frac{T}{\rho}\frac{\partial\rho}{\partial T}\right)_p^2 \frac{q_1}{\hbar\omega_L}\frac{\mathcal{K}_1 [R]_0 \sigma_y \Delta_0}{\Omega^2}. \quad (16)$$

Considering that the product $g(\Omega)I_S = P_S$ is the density of power transferred to the scattered field with frequency ω_S, and the product $2\alpha I_{\text{зв}}(\Omega) = P_{\text{зв}}$ is the density of power transferred to the ultrasonic wave with frequency Ω, we get the following relation from (15):

$$P_{\text{зв}} = KP_S\Omega/\omega_S, \quad (17)$$

from which we see that K is numerically equal to the number of phonons produced upon scattering of each light quantum.

4. Discussion of the Results

If we were to have K = 1 in (17), it would then mean that a single phonon is produced when one photon is scattered, and (17) would be the well known Manley-Rowe relation, which holds in particular in the case of stimulated Mandelstam-Brillouin scattering [Ref. 8]. Let us estimate K in enthalpy-stimulated scattering in the thermodynamically nonequilibrium active medium of iodine photodissociation lasers operating in the quasi-steady state amplification mode.

To do this, we express $[R]_0$ and Δ_0 in (16) in terms of the parameters of the working substance, the pumping source and the intensity of the stimulating field. We limit

ourselves to the case where $I_L \gg I_H = \varepsilon_H/\tau_p$ (I_H and $\varepsilon_H = \hbar\omega_L/\sigma_y$ are the intensity and energy of saturation of the laser transition [Ref. 11]); τ_p is the time of nonradiative relaxation; $I_H \lesssim 10^3$ W/cm^2 since τ_p, as implied by Ref. 12, is at least 10^{-4} s, $\sigma_y = 10^{-18}$ cm^2, $h\omega_L = 15 \cdot 10^{-20}$ J [Ref. 3]. In this case, if we disregard the accumulation of molecular iodine in the amplification process, the quasi-steady concentrations $[R]_0$ and Δ_0 can be estimated by the formulas [Ref. 2, 3]:

$$[R]_0 \approx \sqrt{\left(\frac{1}{2}\left(1+\frac{g_2}{g_1}\right)\frac{I_L}{I_L+w\varepsilon_H}\frac{w}{\mathcal{K}_1}\right)^2 + \frac{wN_0I_L}{2\beta\mathcal{K}_2(I_L+w\varepsilon_H)}} - \frac{1}{2}\left(1+\frac{g_2}{g_1}\right)\frac{I_L}{I_L+w\varepsilon_H}\frac{w}{\mathcal{K}_1}; \quad (18)$$

$$\Delta_0 \approx 2\beta\mathcal{K}_2[R]_0^2\varepsilon_H/I_L, \quad (19)$$

where N_0 is the initial concentration of working substance, w is the probability of photodissociation of molecules of the working substance under the effect of UV pumping radiation; $\beta = 10$–25 is a constant that depends slightly on initial conditions [Ref. 3].

Substituting (19) in (16) and taking consideration of the fact that $\Omega \cong v_{3B}q$, and $q = 2\pi/\Lambda$, where Λ is the wavelength of ultrasound, we get the dependence of K on $[R]_0$:

$$K = \frac{cn}{\pi^2}\left(\frac{T}{\rho}\frac{\partial\rho}{\partial T}\right)_p^2 \frac{q_1\mathcal{K}_1\mathcal{K}_2\beta[R]_0^3}{(\rho\partial\varepsilon/\partial\rho)_T c_p T}\frac{\Lambda^2}{I_L}. \quad (20)$$

With consideration of (18), formula (20) gives the dependence K(w), from which we see that K increases with increasing w. The figure (curves 1, 2) shows the dependences K(w) for a mixture of n-C_3F_7I at pressure of 0.03 atm and a buffer gas of CO_2 at pressure of 0.7 atm, which can be treated at T ≅ 300 K as an ideal gas with properties determined by the buffer gas. The thermodynamic parameters appearing in (20) are as follows: $\left(\frac{T}{\rho}\frac{\partial\rho}{\partial T}\right)_p = -1$; $\left(\rho\frac{\partial\varepsilon}{\partial\rho}\right)_T = 4{,}5\cdot10^{-4}$; $c_p = 0{,}2$ kcal/g deg [Ref. 13]; $k_L = 4.78\cdot10^4$ cm^{-1}; n = 1; $q_1 = 3.8\cdot10^{-19}$ J [Ref. 14]; $g_2/g_1 = 0.5$ [Ref. 3]. The reaction rate constants $\mathcal{K}_1$ and $\mathcal{K}_2$ for the n-C_3F_7I molecule are $7\cdot10^{-12}$ cm^3/s and $2\cdot10^{-12}$ cm^3/s [Ref. 15]; $N_0 = 7.5\cdot10^{17}$ cm^{-3}. In the calculations β was taken as equal to the geometric mean of the minimum and maximum values, i. e. $\beta = \sqrt{250} \cong 16$. The quantity I_L was varied over limits such that on the one hand the condition $I_L \gg I_H \cong 10^3$ W/cm^2 was satisfied, and on the other hand the condition $\sigma_y I_L \ll \hbar\omega_L\Omega$ was not violated, where formula (6) is valid.

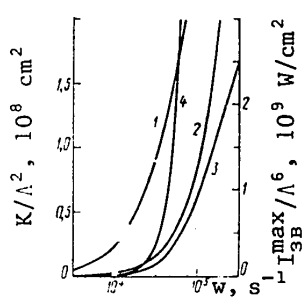

Curves for the number of phonons produced in scattering of a single light quantum normalized to Λ^2 (1, 2) and for intensity of ultrasound normalized to Λ^6 (3, 4) as functions of the probability of photodissociation of n-C_3F_7I molecules at a laser field intensity of $I_L = 10$ (1, 3) and 100 kW/cm^2 (2, 4)

Under typical experimental conditions [Ref. 5], where photodissociation of n-C_3F_7I molecules is produced by ultraviolet radiation of an open discharge, $w \cong 5\cdot10^4$ s^{-1}, and $I_L \cong 10^5$ W/cm^2. In this case, as can be seen from the figure, at characteristic scattering angles of θ ≅ 5–10 mrad, from $5\cdot10^3$ to $2\cdot10^4$ phonons are produced for each scattered light quantum. These quantities may be off from the true values by a factor of 1.26 due to uncertainty of β.

Let us now estimate the intensity of ultrasonic waves. To do this, we represent formula (13) for $I_{ЗВ}(\Omega)$ with consideration of (19) in the form

$$I_{ЗВ}(\Omega)=\frac{1}{2\rho_0}\left(\left(\frac{T}{\rho}\frac{\partial\rho}{\partial T}\right)_p\frac{q_1\mathcal{K}_1\mathcal{K}_2}{c_pT}\right)^2\frac{v_{ЗВ}^3\beta^2[R]_0^6}{\Omega^2((\Omega-\Omega_{МБ})^2+(\delta\Omega_{МБ})^2)}\frac{I_S}{I_L}. \quad (21)$$

It is clear from (21) that the ultrasonic waves with maximum intensity are those with frequency $\Omega=\Omega_{МБ}=v_{ЗВ}q$. Considering the relation $2\delta\Omega_{МБ}=\Gamma q^2$, we find that the maximum intensity

$$I_{ЗВ}^{max}=\frac{\Lambda^6}{32\pi^6}\left[\left(\frac{T}{\rho}\frac{\partial\rho}{\partial T}\right)_p\frac{q_1\mathcal{K}_1\mathcal{K}_2}{c_pT}\right]^2\frac{v_{ЗВ}\beta^2[R]_0^6}{\rho_0\Gamma^2}\frac{I_S}{I_L}. \quad (22)$$

When (18) is substituted in (22), we get the dependence $I_{ЗВ}^{max}(w)$. Since $[R]_0$ appears as its sixth power in (22), the intensity of ultrasound is quite strongly dependent on the probability of photodissociation of molecules of the working substance. This is illustrated on the figure by curves 3 and 4, which show the dependences $I_{ЗВ}^{max}(w)$ as calculated from (22) for the same experimental conditions as K. The following parameters of the medium were additionally used in the calculations: $\rho_0 \cong 10^{-3}$ g/cm^3, $v_{ЗВ}=2.6\cdot10^4$ cm/s, $\eta=1.49\cdot10^{-4}$ g/cm·s [Ref. 13]. The volumetric coefficient of viscosity η' is taken as equal to η. In this situation the coefficient of absorption of ultrasound agrees well with reality at the given pressures of CO_2 and frequencies of sound [Ref. 16, 17]. The ratio I_S/I_L was preassigned as equal to 0.1.

From the curves on the figure we can see that when $w=5\cdot10^4$ s^{-1}, $I_L \cong 10^5$ W/cm^2 and $\theta \sim 5$-10 mrad, we have $I_{ЗВ}^{max} \sim 0.01$-0.7 W/cm^2. This corresponds to experimental data on relative change of gas density in small-scale optical inhomogeneities [Ref. 4, 5], where it is equal to 1%. Since β appears in (22) as its square, the resultant values may be off from the true values by a factor of 2.5 due to uncertainty of β.

It can also be seen from the figure that at $I_L=10^5$ W/cm^2, a reduction in w by a factor of only 5 leads to a reduction of the intensity of ultrasound by a factor of more than 100, i. e. $I_{ЗВ}^{max} \backsim w^3$. But if $I_S \equiv 0$ at the amplifier input, and enthalpy-stimulated scattering starts with spontaneous noises, then as w decreases there will also be a reduction of I_S in the volume of the amplifier, and as a result the dependence $I_{ЗВ}^{max}(w)$ will be still sharper. In this sense, enthalpy-stimulated scattering is a threshold process with respect to the probability of photodissociation of molecules of the working substance, i. e. with respect to pumping power, which agrees with experiment. As we know, small-scale optical inhomogeneities in iodine photodissociation lasers are observed only when a certain level of pumping power is exceeded [Ref. 4, 5].

In conclusion the authors thank N. G. Basov for supporting the work, and O. Yu. Nosach for constructive discussions and assistance with the work.

REFERENCES

1. Basov, N. G., Zuyev, V. S., Nosach, O. Yu., Orlov, Ye. P., KVANTOVAYA ELEKTRONIKA, Vol 7, 1980, p 2614.

2. Zuyev, V. S., Orlov, Ye. P., KVANTOVAYA ELEKTRONIKA, Vol 8, 1981, p 68.

3. Borovich, B. L., Zuyev, V. S., Katulin, V. A., Mikheyev, L. D., Nikolayev, F. A., Nosach, O. Yu., Rozanov, V. B., "Itogi nauki i tekhniki. Seriya Radiotekhnika" [Advances in Science and Technology. Electronics Series], Moscow, Izdatel'stvo VINTI, Vol 15, 1978, pp 153-177.

4. Borovich, B. L., Zuyev, V. S., Katulin, V. A., Nosach, V. Yu., Nosach, O. Yu., Startsev, A. V., Stoylov, Yu. Yu., KVANTOVAYA ELEKTRONIKA, Vol 2, 1975, p 1282.

5. Zuyev, V. S., Netemin, V. N., Nosach, O. Yu., KVANTOVAYA ELEKTRONIKA, Vol 8, 1979, p 875

6. Zel'dovich, B. Ya., Sobel'man, I. I., USPEKHI FIZICHESKIKH NAUK, Vol 101, 1970, p 3.

7. Starunov, V. S., ZHURNAL EKSPERIMENTAL'NOY I TEORETICHESKOY FIZIKI, Vol 57, 1969, p 1012.

8. Starunov, V. S., Fabelinskiy, I. L., USPEKHI FIZICHESKIKH NAUK, Vol 98, 1969, p 441.

9. Landau, L. D., Lifshits, Ye. M., "Elektrodinamika sploshnykh sred" [Electrodynamics of Continuous Media], Moscow, GIFML, 1959, p 501.

10. Yavorskiy, B. M., Detlaf, A. A., "Spravochnik po fizike" [Physics Handbook], Moscow, Nauka, 1971, pp 543-544.

11. Kryukov, P. G., Letokhov, V. S., USPEKHI FIZICHESKIKH NAUK, Vol 99, 1969, p 169.

12. Zuyev, V. S., Katulin, V. A., Nosach, V. Yu., Petrov, A. L., TRUDY FIZICHESKOGO INSTITUTA IMENI P. N. LEBEDEVA AKADEMII NAUK SSSR, Vol 125, 1980, p 46.

13. Kikoin, I. K., academician, ed., "Tablitsy fizicheskikh velichin" [Tables of Physical Quantities], Moscow, Atomizdat, 1976, p 635.

14. Gurvich, L. V., Karachevtsev, G. V., Kondrat'yev, V. N., Lebedev, Yu. A., Medvedev, V. A., Potapov, V. K., Khodeyev, Yu. S., "Energiya razryva khimicheskikh svyazey. Potentsialy ionizatsii i srodstvo k elektronu" [Breaking Energy of Chemical Bonds. Ionization Potentials and Electron Affinity], Moscow, Nauka, 1974, p 91.

15. Kuznetsov, S. V., Maslov, A. I., KVANTOVAYA ELEKTRONIKA, Vol 5, 1978, p 1587.

16. Fabelinskiy, I. L., "Molekulyarnoye rasseyaniye sveta" [Molecular Scattering of Light], Moscow, Nauka, 1965, p 237.

17. Mezon, U., ed., "Fizicheskaya akustika. Tom II, ch. A. Svoystva gazov, zhidkostey i rastvorov" [Physical Acoustics. Vol 2, Part A. Properties of Gases, Liquids and Solutions], Moscow, Mir, 1968, p 175.

6610
CSO: 1862/41

UDC 621.373.8.029.071

NONLINEAR OPTICAL INHOMOGENEITIES IN ACTIVE MEDIA OF GAS LASERS

Moscow KVANTOVAYA ELEKTRONIKA in Russian Vol 8, No 9(111), Sep 81 (manuscript received 13 Mar 81) pp 1987-1989

[Article by L. A. Vasil'yev, M. G. Galushkin, A. M. Seregin and N. V. Cheburkin]

[Text] A theoretical examination is made of the mechanism of formation of nonlinear optical inhomogeneities in active media of gas lasers that is associated with the influence of emission intensity on the relaxation rate of excited molecules. Density perturbations of the amplifying medium of a CO_2 laser are calculated, and an estimate is made of the change in phase characteristics of its emission.

An important factor that determines the phase characteristics of output radiation of high-pressure gas lasers is the formation of gasdynamic perturbations caused by the limited range of energy input [Ref. 1]. Therefore the radiation usually takes up only part of the volume of the active medium for elimination of their effect.

However, under certain conditions in molecular lasers and amplifiers the dynamics of heat release depends on emission intensity as well, which also may lead to spatial nonuniformity of temperature, pressure and density of the working substance. In the CO_2 laser the rate of nonradiative relaxation of CO_2 molecules from the lower lasing level may be an order of magnitude greater than the rate of relaxation from the higher level, and therefore induced transitions are conducive to faster transition of CO_2 molecules from the upper laser level to ground level. As a result, the rate of heat release in the emission zone may be considerably greater than in the remaining region of the active medium, and during a pulse, more thermal energy may be released in a unit of volume of this zone than in the near vicinity [Ref. 2]. For this reason, a temperature differential arises on the edge of the laser beam, resulting in formation of perturbations of density of the gas medium.

For quantitative analysis of this mechanism of formation of nonlinear optical inhomogeneities in an amplifying medium, we use a model of kinetics of an electron beam-controlled CO_2 laser in the quasi-cw mode [Ref. 3] where a change of its phase characteristics is most appreciable:

$$\frac{d\varepsilon_2}{dt} = \frac{2p_1 + p_3}{m} + \frac{p}{m}\left[-3D + \sum_M \gamma_M k_{20M}(\varepsilon_{2T} - \varepsilon_2)\right] + \frac{2\alpha J}{m\gamma_1(\theta_3 - \theta_1)kN}; \quad (1)$$

$$\frac{d\varepsilon_3}{dt} = p_3 + p\,[D - \gamma_2 k_{12}(\varepsilon_3 - \varepsilon_4)] - \frac{\alpha J}{\gamma_1(\theta_3 - \theta_1)kN}; \quad (2)$$

$$\frac{d\varepsilon_4}{dt} = p_4 + p\,[\gamma_1 k_{12}(\varepsilon_3 - \varepsilon_4) + \gamma_3 k_{23}(\varepsilon_{4T} - \varepsilon_4)]; \quad (3)$$

$$\frac{dT}{dt} = (\gamma - 1)\,p\theta_2\gamma_1 \sum_M \gamma_M k_{20M}(\varepsilon_{2T} - \varepsilon_2); \quad (4)$$

$$\frac{dJ}{dt} = cJ\,(\alpha - k_{\text{п}}), \quad (5)$$

where

$$D = \frac{(1-\beta_2)^3}{8(1-\beta_3)} \sum_M \gamma_M k_{32M} \left\{ \frac{\beta_3 \varepsilon_2^3 (1+\varepsilon_3)}{\beta_2^3} - \varepsilon_3 (2+\varepsilon_2)^3 \right\};$$

$$m = (3\varepsilon_2^2 + 6\varepsilon_2 + 2)/2(1+\varepsilon_2)^2; \quad \beta_i = \exp(-\theta_i/T);$$

ε_i is the average number of vibrational quanta per molecule in the corresponding vibrational modes; subscripts $i = 2, 3, 4$ refer respectively to deformational and antisymmetric modes of oscillations of CO_2, and to the type of normal oscillations of N_2; p, T are the pressure and temperature of the gas; $\gamma_{1,2,3}$ are the mole fractions of CO_2, N_2 and He respectively in the mixture; $k_{\text{п}}$ is threshold gain; $\theta_1 = 1980$ K; $\theta_2 = 960$ K; $\theta_3 = 3360$ K; $Nk = p/T$; $p_i = jE\delta_i/\gamma_i kN\theta_i$; α is gain; j, E are the current density and electric field strength in the discharge; δ_i is the relative fraction of pumping power that goes to the ν_i-mode; J is intensity of laser emission; γ is the adiabatic exponent of the gas; ε_{iT} is the equilibrium number of quanta in the modes.

System of equations (1)-(5) was numerically solved in the radiation-filled region at threshold gain $k_{\text{п}} = 1.46 \cdot 10^{-3}$ cm^{-1} and at different pumping values $N_1 = jE\tau_H/p$, where τ_H is pumping duration. A solution was also found for system of equations (1)-(4) at $J = 0$, referring to the region where there is no radiation.

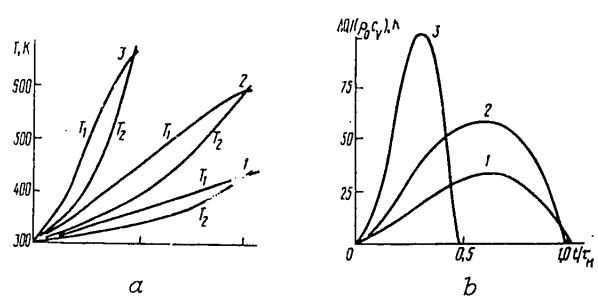

a b

Time dependence of T_1, T_2 (*a*) and thermal energy differece ΔQ (*b*) for $N_1 = 1.5$ (1), 5 (2) and 10 (3). Mixture $CO_2:N_2:He = 1:5:4$, $p_0 = 0.1$ MPa, $T_0 = 300$ K, $\tau_H = 50$ μs.

Figure *a* shows the time dependences of the temperature of the mixture in the region of radiation T_1 and outside it T_2 for pumping values that are constant during the pulse and in space, varying over a range of $1.5 \leqslant N_1 \leqslant 10$.

Figure *b* shows the time change in the difference of thermal energy in a unit of volume $\Delta Q(t) = Q_1(t) - Q_2(t)$, where $Q_1(t)$ refers to the region of radiation, and $Q_2(t)$ refers to the vicinity of the laser beam. For all investigated cases the dependences $T_1(t)$, $T_2(t)$, $\Delta Q(t)$ show qualitatively simplar behavior.

Considering the nature of the time dependence of function $\Delta Q(t)$, in calculating the distortion of gas density on the boundary of the luminous region we will use an approximation of the form $\Delta Q_a(t) = \alpha_0 t(1 - t/\tau)$, where τ corresponds to lasing duration, and α_0 can be determined from the condition of equality of the maximum values of functions $\Delta Q(t)$ and $\Delta Q_a(t)$ from the values of $\Delta Q(t)$ calculated from equations (1)-(5).

In the acoustic gasdynamics approximation in the case of cylindrical symmetry

$$\frac{\partial(\delta\rho)}{\partial t} + \frac{\rho_0}{r}\frac{\partial(rv)}{\partial r} = 0; \tag{6}$$

$$\rho_0\frac{\partial v}{\partial t} + a^2\frac{\partial(\delta\rho)}{\partial r} + \frac{\partial p_T}{\partial r} = 0, \tag{7}$$

where $p_T = (\gamma - 1)\Delta Q(t) \approx (\gamma-1)\alpha_0 t(1-t/\tau)$; $\delta\rho=\rho-\rho_0$; ρ_0 is initial gas density, v is its radial velocity and a is the speed of sound.

Let us solve equations (6), (7) under condition of a sharp drop in radiation intensity on the edge of the laser beam, since in this case the density perturbations have the strongest effect on the optical properties of the medium. We introduce a new coordinate $\eta = r - R$ (R is the radius of the laser beam). Density distribution $\delta\rho(\eta, t)$ in the perturbed region ($|\eta| \leqslant at$) will be determined for the unsteady case ($t \ll R/a$), where motion can be considered two-dimensional. The solutions of equations (6), (7) are waves traveling in opposite directions from the edge of the laser beam, and the change of density in region $r < R$ [Ref. 4]:

$$\delta\rho = -\frac{\gamma-1}{2a^2}\alpha_0 t\left[\left(1-\frac{|\eta|}{at}\right) - \left(1-\frac{|\eta|}{at}\right)^2\frac{t}{\tau}\right],\ |\eta| \leqslant at;$$

$$\delta\rho = 0,\ |\eta| > at. \tag{8}$$

By simple transformations, (8) can be reduced to the form

$$\delta\rho = \frac{(\gamma-1)\alpha_0}{2a^4\tau}\left(|\eta| + \frac{a\tau}{2} - at\right)^2 - \frac{(\gamma-1)\tau\alpha_0}{8a^2}, \tag{9}$$

from which we see that the change in index of refraction with respect to coordinate η has a parabolic profile.

It is known that an inhomogeneous square-law medium characterized by index of refraction $n = n_0 - \frac{1}{2}n_1\eta^2$ in the case $n_1RL \ll 1$ can be replaced by a thin lens with focal length $f = n_0/n_1L$, where L is the length of the inhomogeneous medium along the beam [Ref. 5]. Taking into consideration the relation $\delta_n = \beta_0\delta\rho$, where β_0 is the Gladstone-Dale constant, we find that the perturbations arising on the boundary of the laser beam act as a thin dispersing lens with focal length $f = n_0\tau a^4/\alpha_0\beta_0(\gamma-1)L$ that moves at the speed of sound toward the beam axis. During a pulse, such a lens benetrates into the laser beam to distance $a\tau$, and causes distortion of its wave front. By the end of the pulse ($t = \tau$), the center of the lens is at distance $R - r = a\tau/2$ from the edge of the beam. Hence the maximum angle of beam deviation is

$$\theta_{max} = a\tau/2f = (\gamma-1)\beta_0\alpha_0 L/2n_0a^3. \tag{10}$$

Let us estimate angles θ_{max} for the three cases shown in Fig. *a* where $\alpha_0 = 13.3$, 3.2 and 2.1 kW/cm^3. After substituting values from (10), we get $\theta_{max}/L = 1.5 \cdot 10^{-2}$, $0.36 \cdot 10^{-2}$ and $0.24 \cdot 10^{-2}$ m^{-1} respectively.

Thus under typical experimental conditions the nonlinear optical inhomogeneities that arise on the boundary of the luminous region due to a difference in the rates of relaxation of excited molecules may have a considerable effect on the phase characteristics of radiation. This mechanism of formation of nonlinear optical inhomogeneities shows up in greatest measure in gas lasers with unstable confocal cavity in which the width Δ of an annular beam ($\Delta < R$) may be comparable with the length traveled by a sound beam during the pulse.

REFERENCES

1. Glotov, Ye. P., Danilychev, V. A., Kruglyy, A. Ye., Pustovalov, V. V., Soroka, A. M., Cheburkin, N. V., KVANTOVAYA ELEKTRONIKA, Vol 5, 1978, p 1924.

2. Lamberton, H. M., Roper, V. G. in: "Gas-Flow and Chemical Lasers", J. F. Wendt, ed., Hemisphere Publ. Corp., Washington-New York-London, 1978, p 471.

3. Biryukov, A. S., TRUDY FIZICHESKOGO INSTITUTA IMENI P. N. LEBEDEVA AKADEMII NAUK SSSR, Vol 83, 1975, p 12.

4. Rayzer, Yu. P., ZHURNAL EKSPERIMENTAL'NOY I TEORETICHESKOY FIZIKI, Vol 52, 1967, p 470.

5. Markuze, D., "Opticheskiye volnovody" [Optical Waveguides], Moscow, Mir, 1974.

6610
CSO: 1862/41

UDC 621.375.8

FEASIBILITY OF DEVELOPING EXCIMER LASERS WITH IONIZATION BY EXTERNAL LOW-POWER SOURCE

Moscow KVANTOVAYA ELEKTRONIKA in Russian Vol 8, No 9(111), Sep 81 (manuscript received 6 May 81) pp 1992-1993

[Article by A. Yu. Aleksandrov, N. G. Basov, V. A. Danilychev, O. M. Kerimov and A. I. Milanich, Institute of Physics imeni P. N. Lebedev, USSR Academy of Sciences]

[Text] A method of pumping excimer lasers is proposed that is based on accumulation of negative ions, and model experiments are done using an electron beam as an external ionizer. Lasing on transitions of the XeF excimer ($\lambda = 353$ nm) was observed at the minimum negative ion concentration of $\sim 10^{11}$ cm^{-3}.

The development of electroionization and electron-beam pumped excimer lasers has now reached a qualitatively new stage associated with the fact that with respect to some important parameters like efficiency (11% [Ref. 1]), specific energy output (~40 J/ℓ [Ref. 1]) and others, they have come close to electroionization CO_2 lasers. However, there are a number of obstacles in the way of development and extensive industrial introduction of such lasers, the main one certainly being destruction of the foil that separates the vacuum space of the electron gun from the laser chamber. The foil is destroyed because the current densities of the electron gun that are required for exciting the active medium of an excimer laser are considerably greater than those required by electroionization CO_2 lasers (by a factor of 10^2-10^3). This paper is devoted to a study of one possibility of reducing the current density of the electron gun.

Several methods can be suggested for attaining this goal with the common feature of setting up another channel for electron production besides direct ionization by high-energy electrons. For example an earlier paper [Ref. 2] proposed using photoionization of metastable states of noble gas atoms as such an additional channel. Analogous results can be achieved by using Penning-discharge ionization, photoionization of an easily ionizable additive and so on. In this paper we study the feasibility of accumulating negative ions (which are essentially an easily ionizable additive), and using them as electron donors.

Let us write a system of equations that describe the change in concentration of electrons n and negative ions H^- in the active medium of an excimer laser:

$$\frac{dn}{dt} = q - \alpha n H;$$
$$\frac{dH^-}{dt} = \alpha n H - \beta H^- (n + H^-),$$

where α is the sticking constant ($1.5 \cdot 10^{-9}$ cm^3/s for NF_3 [Ref. 3]); β is the recombination constant ($5 \cdot 10^{-6}$ cm^3/s for He at p = 2 atm [Ref. 4]); q is the concentration of electron-ion pairs created by the ionizer in a unit of time; H is the concentration of halogen-containing molecules.

The equilibrium concentration of electrons $n = q/(\alpha H)$ is reached in time $\tau_\alpha \cong (\alpha H)^{-1} \cong$ 10 ns in mixtures that are typical for excimer lasers.

The equilibrium concentration of negative ions

$$H^- = \sqrt{\frac{q}{\beta} + \frac{q^2}{4\alpha^2 H^2}} - \frac{q}{2\alpha H} \qquad (1)$$

is reached in time $\tau_\beta \cong [q\beta + q^2\beta^2/(4\alpha^2 H^2)]^{-1/2}$.

After the action of the external ionizer stops, the concentrations of electrons and negative ions decrease from the initial values of n_0 and H_0^- by the laws

$$n = n_0 \exp(-\alpha H t), \qquad H^- = H_0^-/(1 + H_0^- \beta t). \qquad (2)$$

It was shown in Ref. 5 that effective operation of an excimer laser requires a concentration of negative ions of $\sim 5 \cdot 10^{11}$ cm^{-3}, which according to (1) corresponds to an external ionizer with $q \cong 5 \cdot 10^{17}$ cm$^{-3} \cdot$s^{-1}.

In the case of a helium laser mixture at a pressure of p = 2 atm when using an electron beam as an external ionizer, the current density of the electron gun should be equal to $j \cong 1$ mA/cm^2. Then the concentration of negative ions is settled within $\tau_\beta \cong 1$ μs.

Thus by using a relatively low-power ionizer we can accumulate negative ions and then, by applying a voltage pulse with $E/p \cong 5$ kV/(cm·atm) to the discharge gap, we can loosen the electrons from the negative ions, multiply them, and finally stimulate the active medium of such a laser.

In our research, we did experiments to simulate the operation of such an excimer laser. To do this, after exposing the active medium of the XeF excimer laser to an electron beam for 50 ns (λ = 353 nm, mixture $He:Xe:NF_3 = 350:2.5:1$, p = 2 atm, volume of active region 0.5 x 1.5 x 18 cm $\cong$ 14 cm^3), a voltage pulse was applied to the discharge gap with delay controllable over wide limits (up to ~10 μs). By combining signals from voltage meters across the peaking capacitance of the electron gun [Ref. 6] and across the cathode of the discharge gap, we monitored the time delay and voltage amplitude across the discharge gap. Fig. 1 shows a typical oscillogram of the voltage pulses [photo not reproduced].

The dependence of lasing energy on delay time at different electron beam current densities is shown on Fig. 2. This curve implies that the minimum concentration of negative ions at which lasing is just observed is about 10^{11} cm^{-3}, which agrees with the results of Ref. 5. It should be noted that we did not optimize the mixture

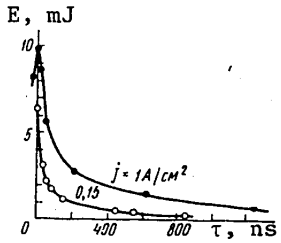

Fig. 2. Dependence of lasing energy on delay time; mirror reflectivities ~100% and ~90%

with respect to maximum attainable initial negative ion concentration. Moreover, an appreciable increase in lasing energy when the voltage pulse across the discharge gap is superimposed on the electron beam pulse shows the considerable part played in the multiplication process by the initial concentration of electrons produced directly by the electron beam.

And so, in our research we have suggested ways to eliminate the drawbacks of the electric-discharge laser with ultraviolet pre-ionization -- restrictions due to the short mean free path of the UV photon (~10 cm [Ref. 7]) on the maximum volume, degradation of the mixture as a consequence of the high spark temperature of the ultraviolet ionizer, inefficient utilization of the ultraviolet ionizer because of its nonuniformity [Ref. 5], etc.--by using an external homogeneous ionizer.

Moreover, when using present-day sources of ionizing radiation (electron guns that operate in both the cw and pulse-periodic modes, continuous-duty nuclear reactors, pulsed x-ray units and so on), we can realize the pulse-periodic operation of excimer lasers with pulse-recurrence rate of tens of kilohertz and an average radiation power of several kilowatts.

REFERENCES

1. Tisone, G. C., Patterson, E. L., Rice, J. K., APPL. PHYS. LETTS, Vol 35, 1979, p 437.

2. Basov, N. G., Glotov, Ye. P., Danilychev, V. A., Milanich, A. I., Soroka, A. M., PIS'MA V ZHURNAL TEKHNICHESKOY FIZIKI, Vol 5, 1979, p 449; Danilychev, V. A., Glotov, Ye. P., Milanich, A. I., Soroka, A. M., IEEE J, Vol QE-16, 1980, p 154.

3. Basov, N. G., Vasil'yev, L. A., Volkov, V. N., Danilychev, V. A., Kerimov, O. M., Milanich, A. I., Lomakin, V. N., Ustinov, N. D., Kachapuridze, T. S., IZVESTIYA AKADEMII NAUK SSSR: SERIYA FIZICHESKAYA, Vol 43, 1979, p 239.

4. Flannery, M. R., Yang, T. P., APPL. PHYS. LETTS, Vol 32, 1978, p 327.

5. Hsia, J. A., APPL. PHYS. LETTS., Vol 30, 1977, p 101.

6. Basov, N. G., Brunin, A. N., Danilychev, V. A., Kerimov, O. M., Milanich, A. I., Khodkevich, D. D., PIS'MA V ZHURNAL TEKHNICHESKOY FIZIKI, Vol 3, 1977, p 1297.

7. Andrews, A. J., Kearsley, A. J., Webb, C. E., Haydon, S. C., OPT. COMMS, Vol 20, 1977, p 265.

6610

CSO: 1862/41

UDC 621.373.826

MEASURING COPPER VAPOR CONCENTRATION AND DEGREE OF GAS HEATING IN TRANSVERSE-DISCHARGE COPPER-VAPOR LASER

Moscow KVANTOVAYA ELEKTRONIKA in Russian Vol 8, No 9(111), Sep 81 (manuscript received 9 Dec 80) pp 1996-2000

[Article by B. L. Borovich, L. A. Vasil'yev, V. Ye. Gerts, S. A. Negashev, S. N. Regeda and L. N. Tunitskiy]

[Text] Copper vapor distribution over the discharge gap cross section is measured in a transverse-discharge copper-vapor laser on the basis of integral absorption in the resonant line. The gas temperature profile in the discharge is determined, and an estimate is made of the coefficient of conversion of electric energy to heat in a nanosecond pulse-periodic discharge (about 30%). The gas in the center of the discharge gap is heated to a temperature of about 2500°C.

Emission parameters that have so far been achieved in copper-vapor lasers [Ref. 1, 2] are still far from those expected, especially with respect to efficiency and specific energy output. At the same time, there are not enough experimental data on characteristics of the active medium to construct an adequate model of physical processes in such lasers. Further progress in increasing efficiency of lasers of this kind can be assured only by a detailed study of physical processes and parameters that determine the particulars of their operation, such as concentration of working particles and electrons, degree of heating of the gas, electron energy and so on.

This paper gives the results of measurements of the distribution of copper vapor concentration in a laser with transverse discharge [Ref. 2]. We also determine the gas temperature profile in working modes, and the coefficient of conversion of the electric energy invested in the discharge into heat. Measurements were based on the well known spectral method of determining particle concentration from the integral absorption of probing radiation in the resonant line [Ref. 4] (for copper we used the line $4^2S_{1/2}-4^2P_{3/2}$, $\lambda = 324.7$ nm). Under the conditions of the experiment, the size of the transilluminated zone and the concentration of copper vapor were such that the index of absorption in the center of the line k_0L was large ($\sim 10^5$), and the intensity of the transmitted light was determined by absorption in the far wings of the line, i. e. by the lorentzian part of the line contour.

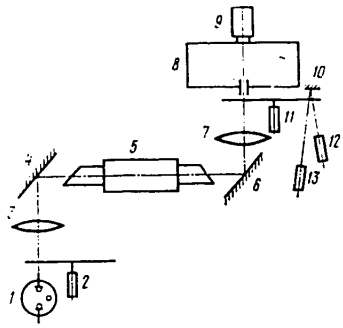

Fig. 1. Schematic of measurement system: 1--DKSSh-3000 lamp; 2--disk modulator; 3 and 7--quartz lenses; 4, 6 and 10--mirrors; 5--laser chamber; 8--MDP-2 monochromator; 9--FEU-36 photomultiplier; 11--disk shutter; 12--photodiode; 13--LG-13 laser

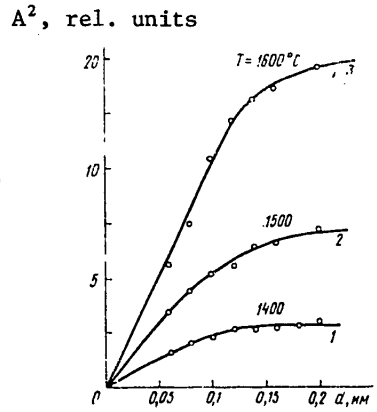

Fig. 2. Integral absorption as a function of width of the monochromator slit

In this case the strong absorption approximation is applicable, and assuming that the width of the slit of the spectral instrument is sufficiently great, the concentration of copper vapor is

$$N_{cu} = A^2 mc^3/\lambda_0^4 e^2 f \gamma L, \quad (1)$$

where $A = \int[(I_0 - I)/I_0]d\lambda$ is integral absorption (the parameter to be measured); I_0 and I are the spectral intensities of the probing radiation at input and output of the chamber respectively; m and e are the electronic mass and charge; c is the speed of light; λ_0 is the wavelength in the center of the line; f is the oscillator strength of the given transition; $\gamma = aN_{Cu} + bN_{Cu}$ is the lorentzian width of the line determined by collisions with neon and copper atoms [Ref. 5].

A schematic of the system for copper vapor concentration measurements is shown in Fig. 1. The emission source was DKSSh-3000 xenon lamp 1 with continuous spectrum. The quartz lenses and mirrors 3, 4, 6, 7 shaped the probing beam and focused it on the input slit of MDP-2 monochromator 8. The radiation receiver was FEU-36 photomultiplier 9. Every effort was made to suppress spurious background illumination, the main source being luminescence on the probed transition excited by the laser pumping source--a high-voltage nanosecond pulse generator. Two techniques were used to enhance the signal-to-noise level. First, the emission of the xenon lamp was modulated at a frequency of 87 Hz by a mechanical modulator 2, and the photomultiplier signal was recorded by a resonant voltmeter with passband of 4.35 Hz. Secondly, A disk shutter 11 was placed in front of the monochromator input slit. Signals to trigger the voltage pulse generator were supplied from

photodiode 12 at the instant when the recording arrangement was covered by the disk. The recording system was uncovered ~100 μs after the excitation pulse, with duration of ~100 ns. Thus the measurements were taken in the space between pulses when the luminescence intensity had fallen to a negligible level. Pulse recurrence rate was 2.8 kHz.

To determine the distribution of copper vapor concentration over the cross section, diaphragms were installed on the laser chamber windows. The neon pressure in the chamber was monitored by a laboratory voltmeter. The temperature T of the walls of the acitve zone of the chamber, determined by copper vapor concentration in the working zone, was measured by an LOP-72 pyrometer. In each working mode, the copper concentration was measured 5-6 times, and then the average was taken.

The width of the monochromator slit was selected on the basis of two considerations. On the one hand it had to be large enough so that the entire section of the spectrum cut off by the absorption line would fit into the spectral width of the recording system. On the other hand, 2.7 nm from the line to be used is another resonant line $4^2S_{1/2}-4^2P_{1/2}$, $\lambda = 327.4$ nm, and we had to be sure that the wings of this line would not fall into the region of registration. This imposes constraints from above and below on the width of the monochromator slit, and consequently on the measurable copper vapor concentration. Fig. 2 shows typical dependences of the square of the integral absorption on the width d of the monochromator output slit at different temperatures of the discharge chamber walls. At a wall temperature below 1500°C, dependence $A^2(t)$ shows pronounced saturation, which demonstrates the feasibility of using the selected strong absorption approximation. At higher temperatures, and consequently at higher copper concentrations, saturation is not reached because of the contribution that the adjacent line makes to absorption, and the proposed method of measurement is inapplicable.

The copper vapor concentration was determined by using values of the line width from Ref. 5, and specifically $\gamma = 4 \cdot 10^9$ cm^{-1} at $N_{Ne} = 1.3 \cdot 10^{18}$ cm^{-3}.

Another source of errors in determining N_{Cu} is the inconstancy of copper vapor concentration lengthwise of the region being probed due to the inconstancy of the temperature of the walls of the discharge zone of the chamber. Special measurements of the wall temperature made with a pyrometer and graphite rods with a depression simulating an absolutely black body gave a temperature spread over a range of 20 K with the exception of the end regions taking up about 20% of the entire length of the chamber. Temperature falls off sharply on the ends. With consideration of the temperature dependence of copper vapor concentration in the given region, the error in determination of the average copper concentration due to edge effects apparently does not exceed 10%.

The overall absolute accuracy of determining copper vapor concentration is apparently not worse than 40%. Experimental confirmation of this value can be seen from Fig. 3, which shows the measured dependence of copper vapor concentration on temperature of the walls of the discharge zone without switching on the discharge. Also shown on this figure is the saturated copper vapor concentration from Ref. 6. The difference between the two curves does not exceed 30%. Let us note that the accuracy of determining temperature profile is considerably higher than the accuracy of absolute measurements.

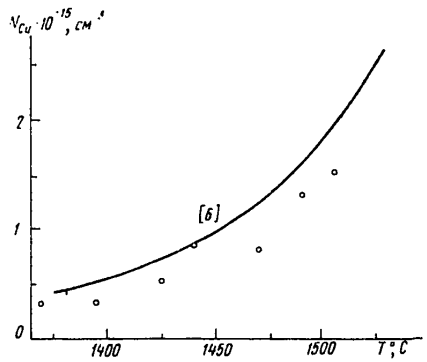

Fig. 3. Copper vapor concentration as a function of the temperature of the chamber walls (without discharge)

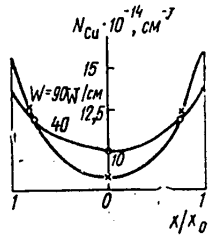

Fig. 4. Distribution of copper vapor concentration over the cross section of the discharge gap

Fig. 4 shows the distribution of copper vapor concentration over the horizontal cross section of a discharge zone of 6 x 6 cm for different pumping powers. A typical feature of these dependences is a dip in concentration at the center of the discharge zone. The depth of the dip increases with increasing power input. This behavior of the distribution can be attributed to the fact that in the center of the discharge gap the temperature of the gas is higher than on the edge since when the pressure is constant through the volume, the particle concentration is lower where the temperature is higher.

The change in copper concentration when pumping is started (or stopped) enabled measurement of the gas heating temperature. For this purpose, the change of integral absorption was measured when pumping was started (stopped). Recording was done several seconds after starting (stopping). During this time, the gas had time to heat up to the steady-state temperature, but the wall temperature of the discharge zone (and hence the saturated vapor concentration) did not change appreciably. According to measurements, in 10-20 s the wall temperature changed by only 5-10 K. Under the given conditions, the copper vapor could be treated as an ideal gas, and we could assume that $\Delta N_{Cu}/N_{Cu} = \Delta T_g/T_g$, where T_g is gas temperature. If the experiment is done under conditions where impact broadening of the line by copper atoms is insignificant, then, considering the temperature dependence of the cross section of impact broadening of the line by neon atoms ($\sigma \sim T_g^{-1/5}$), we can readily get an expression for the gas heating temperature from (1):

$$T_g = T_{g0} (A_0/A)^{20/17},$$

where A_0 and A are the integral absorptions without and with discharge respectively.

Fig. 5 shows the gas temperature distribution over the horizontal cross section of the discharge zone for different pumping powers. The latter was determined from the current-voltage characteristics of the discharge. In virtue of the specifics of the measurement technique in these experiments, the pumping power was measured only by varying the amplitude of the voltage generator pulses. The recurrence rate of the pulses was 2.8 kHz. The figure shows that the gas temperature in the

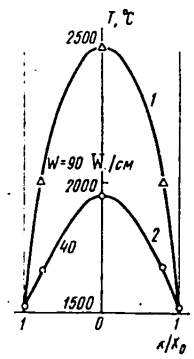

Fig. 5. Gas temperature profile

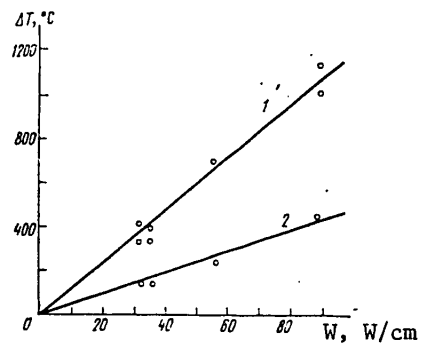

Fig. 6. Dependence of gas temperature on power invested in the discharge: in the center of the gap (1) and at a distance of 0.2 x_0 from the walls of the chamber (2)

center of the discharge gap is much higher than the temperature of the chamber walls. Under conditions that are optimum with respect to lasing power, the temperature of the center of the discharge zone reaches about 2500°C, i. e. the gas in the center is heated by 1000 K. Under such conditions the thermal population of the lower metastable level of copper (for the green emission component) is about 1%. The resultant data also imply that the degree of heating of gas by the discharge is a linear function of the electric power invested in the discharge (Fig. 6).

On the basis of the temperature gradient on the walls of the discharge zone and the coefficient of thermal conductivity of neon at working temperatures, we can readily get the overall value of the heat flux carried off from the discharge gap. By comparing the heat flux with the average power invested in the discharge, we get the coefficient of conversion of electrical energy to heat (heating of heavy particles) in the investigated pulse-periodic discharge--about 30%. The rest of the energy invested in the discharge is apparently re-radiated and carried off to the walls of the chamber by radiant heat conduction.

Thus, in the operation of a copper-vapor laser, rather appreciable heating of gas takes place in the central zone of the diacharge, which apparently leads to direct population of lower metastable laser levels, and in addition slows down the rate of plasma relaxation in the period between pulses, which may cause considerable population of metastable levels by electron impact. Besides, there is a nonuniform change of plasma conductivity over the cross section of the discharge gap, which leads to nonuniform energy release in the discharge, and to redistribution of the electric field with respect to the height of the gap. All these factors can appreciably reduce laser operating efficiency at high levels of pumping power.

REFERENCES

1. Isayev, A. A., Lemmerman, G. Yu., KVANTOVAYA ELEKTRONIKA, Vol 4, 1977, p 1413.

2. Artem'yev, A. Yu., Babeyko, Yu. A., Bakhtin, O. M., Borovich, B. L., Vasil'yev, L. A., Gerts, V. Ye., Nalegach, Ye. P., Ratnikov, G. Ye., Tatarintsev, L. V., Ul'yanov, A. N., KVANTOVAYA ELEKTRONIKA, Vol 7 80, p 1948.

3. Isayev, A. A., Kazaryan, M. A., Petrash, G. G., KVANTOVAYA ELEKTRONIKA, No 6(18), 1973, p 112.

4. L'vov, B. V., "Atomno-absorbtsionnyy spektral'nyy analiz" [Atomic-Absorption Spectral Analysis], Moscow, Nauks, 1966.

5. Nerheim, N. M., J. APPL. PHYS., Vol 48, 1977, p 3244.

6. Nesmeyanov, A. N., "Davleniye parov khimicheskikh elementov" [Vapor Pressure of Chemical Elements], Moscow, Izd. AN SSSR, 1961.

6610
CSO: 1862/41

UDC 621.378.8

SUBNANOSECOND ATOMIC IODINE PHOTODISSOCIATION LASER

Moscow KVANTOVAYA ELEKTRONIKA in Russian Vol 8, No 9(111), Sep 81 (manuscript received by PIS'MA V ZHURNAL TEKHNICHESKOY FIZIKI 19 Sep 80; by KVANTOVAYA ELEKTRONIKA 6 Mar 81) pp 2034-2035

[Article by V. I. Annenkov, A. V. Belotserkovets and S. V. Grigorovich]

[Text] The paper gives the results of studies of an iodine photodissociation laser in the mode of periodic Q-switching by a ¼-wave Pockels cell. The modulating voltage was formed by discharge of a cable line, and was a series of damped pulses of trapezoidal shape with steep fronts. The recurrence period of the Q-switch transmission was matched to the round-trip time of light through the cavity. The mixture used was C_3F_7I (7-15 mm Hg) and Ar at total pressure of 1 atm. A train of subnanosecond laser pulses was produced, consisting of 3-4 peaks. Total energy of the train was 10-20 mJ, and minimum duration of an individual pulse was 0.4 ns.

The main requirements on the master oscillator of a laser facility for controlled nuclear fusion are high quality of the beam, regular pulse duration (0.3-1 ns) and high contrast of emission ($\geqslant 10^7$).

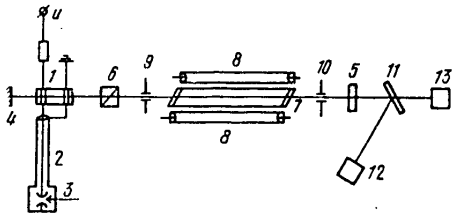

Fig. 1. Optical diagram of the facility: 1--DKDP crystal; 2--shaping line; 3--discharger; 4, 5--cavity mirrors; 6--polarizer; 7--cell; 8--pumping lamp; 9, 10--diaphragms; 11--beam splitter; 12-- calorimeter; 13--SDF-11 photocell

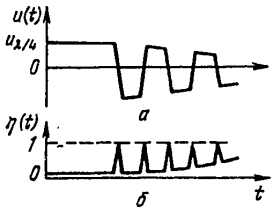

Fig. 2. Voltage waveshape across the shutter (a) and transmission function of the shutter (b)

These requirements are met by a neodymium glass laser with periodic Q-switching [Ref. 1]. The purpose of this article is to explain the working capabilities of an iodine photodissociation laser in the periodic Q-switched mode, and to study its characteristics. A diagram of the measurement facility is shown in Fig. 1.

The research was based on laser chamber 7 with inside diameter of 9 mm and length of the active section of 1 m, with windows beveled at the Brewster angle. The pumping source was two xenon flashlamps 8. The lamps were placed so as to minimize the magnetic field on the axis of the cell. The lamp supply was from a 3 μF capacitor charged to 50 kV through a low-inductance discharger. The main pumping energy was released within the first half-period of the discharge current of 4 μs duration.

Periodic Q-switching was accomplished by a ¼-wave Pockels shutter based on DKDP crystal 1. Shaping line 2 with shorting discharger 3 produced the controlling electric pulses across the shutter with period T_{el} of shape shown in Fig. 2a. The corresponding transmission function of the shutter is shown in Fig. 2b. The characteristics of the controlling electric pulses are as follows: charging voltage 4.5 kV, pulse rise time 1-2 ns, damping of pulse amplitude by a factor of e takes place in time of $15T_{el}$.

The working medium was a mixture of C_3F_7I (7-15 mm Hg) and Ar at a total pressure of 1 atm. Gain of the active medium was selected so that the lasing threshold was slightly exceeded during pumping with the shutter closed.

Q-switching was started at the instant of the first zero of the pumping current. This led to rapid development of a train of subnanosecond laser pulses with period equal to the round-trip time of light through the cavity. Each train consisted of 3-4 laser pulses. The pulses reached maximum amplitude after 10-15 round trips through the cavity. The overall energy of the train was 10-20 mJ with a diaphragm 3 mm in diameter and cavity length of 220 cm. An instrument with time resolution of ~0.3 ns was used to record the duration of an individual laser pulse. Pulse duration was appreciably dependent on matching T_{el} with the round-trip time of light through the cavity T_{light}; in the case of optimum matching, pulse duration reached a minimum value of 0.4 ns at half-amplitude (without consideration of the time resolution of the instrument). It should be noted that there was little change in pulse duration when T_{light} and T_{el} were matched within 0.1 ns. A typical lasing oscillogram is shown in Fig. 3 [photo not reproduced].

Measurements of the angular distribution of lasing showed that radiation divergence is close to the diffraction limit.

Results on energy, pulse duration and divergence show that this laser could be extensively used in multistage iodine laser facilities [Ref. 2, 3], e. g. for laser-driven fusion.

REFERENCES

1. Basov, N. G., Bykovskiy, N. Ye., Danilov, A. Ye., Kalashnikov, M. P., Krokhin, O. N., Kruglov, B. V., Mikhaylov, Yu. A., Osetrov, V. P., Pletnev, N. V., Rode, A. V., Senatskiy, Yu. V., Sklizkov, G. V., Fedotov, S. I., Fedorov, A. N., TRUDY FIZICHESKOGO INSTITUTA IMENI P. N. LEBEDEVA AKADEMII NAUK SSSR, Vol 103, 1978, p 3.

2. Katulin, V. A., Nosach, V. Yu., Petrov, A. L., KVANTOVAYA ELEKTRONIKA, Vol 3, 1976, p 1829.

3. Belotserkovets, A. V., Gaydash, V. A., Kirillov, G. A., Kormer, S. B., Krotov, V. A., Kuratov, Yu. V., Lapin, S. G., Murugov, V. M., Rukavishnikov, N. N., Samylin, V. A., Cherkesov, N. A., Shemyakin, V. I., PIS'MA V ZHURNAL TEKHNICHESKOY FIZIKI, Vol 5, 1979, p 204.

6610
CSO: 1862/41

UDC 621.373.826.038.823

USING ARGON IN WORKING MIXTURES OF CW ELECTRON BEAM-CONTROLLED CO_2 PROCESS LASERS

Moscow KVANTOVAYA ELEKTRONIKA in Russian Vol 8, No 9(111), Sep 81 (manuscript received 2 Feb 81) pp 2063-2065

[Article by A. P. Averin, N. G. Basov, Ye. P. Glotov, V. A. Danilychev, N. N. Sazhina, A. M. Soroka and V. I. Yugov, Institute of Physics imeni P. N. Lebedev, USSR Academy of Sciences]

[Text] It is shown that the use of argon in working mixtures of cw electroionization CO_2 lasers considerably enhances the specific volumetric energy output (by a factor of 1.5-2) without detriment to the physical efficiency of the laser. Substituting argon for helium considerably reduces the cost of processes of laser technology.

At present one of the main factors that determine the cost of laser technology is the high price of helium, which has a content of 40-80% in typical laser mixtures [Ref. 1]. Therefore a very important practical problem is total or partial substitution of less expensive gases for helium in the working mixtures of electroionization process lasers. One possible way to do this is to use helium-free mixtures such as CO_2-N_2, i. e. to replace helium with nitrogen. However, this considerably reduces lasing efficiency, due chiefly to an increase in the threshold pumping energy W_*, i. e. the energy carried off by the gas flow from the active volume, a quantity that increases with the ratio of concentration of nitrogen and CO_2: $W_* \sim (m+1)$, where $m = [N_2]/[CO_2]$. When helium is replaced with nitrogen, we can retain the ratio of $[N_2]/[CO_2]$ and accordingly the threshold pumping energy as a result of increasing the CO_2 content in the mixture. However, this would require a corresponding increase in electron beam current density because of the accelerated loss of electrons in the electroionization discharge plasma as a result of sticking to molecules of carbon dioxide (the electron sticking rate constant $\beta \sim [CO_2]$). In existing cw electroionization lasers, the current density of the electron beam j_e is limited by overheating of the separative foil of electron guns on a level of 10-15 $\mu A/cm^2$ (in the plane of the anode of the discharge chamber). Therefore the content of carbon dioxide in optimum laser mixtures at the present time does not exceed a few percent [Ref. 2], and an increase in CO_2 concentration leads to reduced pumping power, emission power and lasing efficiency.

In Ref. 3 an investigation was made of the possibility of increasing the specific characteristics of helium-free mixtures of CO_2 electroionization lasers by trace

doping with hydrogen, whose molecules effectively depopulate the lower lasing level, which is very important for laser operation in the powerful short pulse mode. In CO_2 cw electroionization lasers hydrogen doping cannot improve lasing parameters since H_2 molecules sharply increase the relaxation rate of the upper lasing level, and accordingly the power of relaxation losses that determine operation of the cw electroionization laser [Ref. 2].

It was experimentally established in Ref. 1 that using xenon additives in the laser mixture improves the characteristics of the electroionization discharge by reducing electrode potential drops [Ref. 4]. However, the use of Xe leads to still greater increase in laser cost as it is priced 600 times as high as helium.

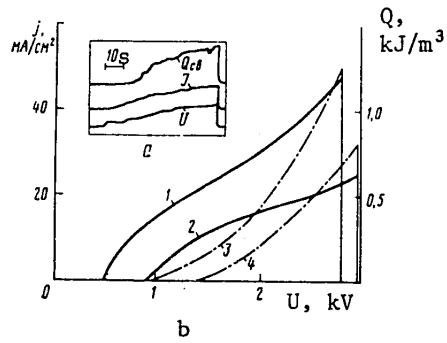

Fig. 1. Typical loop oscillograms of voltage U, discharge current J and lasing power Q_{CB} (*a*) and dependences of discharge current density (1, 2) and specific lasing energy (3, 4) as functions of the voltage across the discharge chamber (b) for laser mixtures $CO_2:N_2:He:Ar = 1:29:0:30$ (1, 3) and 1:29.30:0 (2, 4) at pressure of 60 mm Hg; interelectrode spacing 10 cm

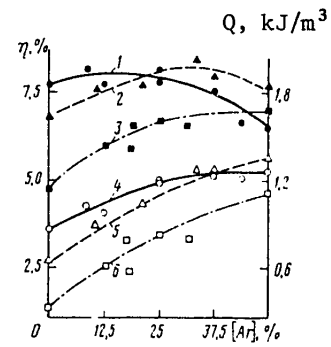

Fig. 2. Lasing efficiency η (1-3) and maximum specific energy output Q_{CB} (4-6) as functions of the argon concentration in laser mixtures $CO_2:N_2:(He+Ar) = 1:29:30$ (1, 4), 1:14:15 (2, 5) and 1:4:5 (3, 6)

In this paper an experimental investigation is made of the possibility of replacing helium with argon, and it is shown that the use of argon not only is not detrimental to the specific characteristics of the cw electroionization laser, but also increases the specific lasing output without reducing efficiency as a result of increasing the power of the energy contribution at unaltered electron beam current. This is due to an increase in the density of the laser mixture and accordingly in the number of electron-ion pairs γ formed per unit of length of the mean free path of a beam electron (for mixture $CO_2:N_2:He = 1:30:29$ when argon is substituted for helium its molecular weight increases from 16.76 to 34, i. e. more than doubles). The other discharge parameters remain practically unchanged [Ref. 5].

Experiments were done on a process cw laser facility (duration of a single operating run about 10 minutes). Fig. 1*a* shows loop oscillograms of the luminosity-current-voltage characteristics for a laser mixture $CO_2N_2:Ar = 1:29:30$ at pressure p = 60 mm Hg

and electron beam current density $j_e = 12\ \mu A/cm^2$. Voltage U and discharge current J were measured by an ohmic divider and a shunt respectively. Lasing power was measured by a wire-type duct bolometer [Ref. 6]. Fig. 1b shows curves for discharge current density and lasing energy taken from a unit of volume of the circulating gas as functions of the voltage across the discharge chamber for two mixtures. It can be seen that in the mixture containing argon, the non-self-maintained discharge changes from "Thomson" burning, where nearly all the applied voltage is shielded by the cathode layer, to "electroionization" burning [Ref. 7] at a slightly lower voltage than in a mixture of CO_2-N_2-He (510 V instead of 960). This is due to an increase of electron density in the discharge due to more efficiency in use of the electron beam. At the working voltages of an electroionization laser the discharge current in a mixture of CO_2-N_2-Ar is more than double the current in the CO_2-N_2-He mixture. The curve of lasing power as a function of voltage for the mixture containing argon is also everywhere higher than for the CO_2-N_2-He mixture. However, the maximum working voltage in the CO_2-N_2-Ar mixture in all the experiments was 10-15% lower than in the CO_2-N_2-He mixture. This is not due to a reduction in electric strength of the mixture, and can be attributed to the fact that the gas density at the end of the active volume in the first case as a result of energy input drops more strongly, and accordingly there is a stronger increase in the normalized field strength E/N. The results of the experiments are in good qualitative agreement with the formula that defines the dependence of breakdown voltage U_* on pumping power:

$$U_*(w) = \frac{(E/\rho)_* d\rho_0}{1 + w/(qc_pT_0)},$$

where $(E/\rho)_*$ is the normalized breakdown field strength; w is pumping power; q is gas flowrate; T_0 is the initial temperature of the laser mixture; c_p is specific heat of the gas at constant pressure; d is the spacing between electrodes.

Fig. 2 shows the curves for maximum specific energy outputs Q corresponding to limiting field strength, and lasing efficiency as functions of the argon content in laser mixtures with predetermined concentrations of carbon dioxide and nitrogen. The total content of helium and argon was 50%. The energy output increases monotonically with increasing Ar content in the mixture. For a mixture with high carbon dioxide content $CO_2:N_2:(He+Ar) = 1:4:5$, complete replacement of helium with argon leads to an increase in lasing power by a factor of 2.5, which is associated with an increase in energy input almost without any change in pumping efficiency; in this case the laser efficiency also increases. In a mixture of $CO_2:N_2:(He+Ar) = 1:29:30$ (curve 1) the lasing efficiency with substitution of argon for helium falls from 8 to 6.5%, which is due on the one hand to overheating of the laser mixture, and on the other hand--to a reduction in the rate of depopulation of the lower lasing level in the absence of helium. In the mixture $CO_2:N_2:(He+Ar) = 1:14:15$ (curve 2) the dependence of efficiency on argon concentration has a flat maximum. The comparatively wide scatter of the experimental points is due to unstable behavior of the threshold voltage of streamer breakdown of the discharge gap, which depends not only on pumping power, but also on electrode surface state, which could not be controlled during the experiments.

Thus, substitution of argon for helium in working mixtures of cw process lasers increases pumping power by a factor of 1.5-2 without any change of electron beam current, and with almost no reduction in lasing efficiency. This is especially

important for prolonged cw laser operation when pumping power falls to half because of the formation of nitrogen oxides [Ref. 8] even when a regenerator is used. The cost of the laser mixture in this case decreases by more than an order of magnitdue, and the total cost of processes of laser technology is cut in half.

REFERENCES

1. Basov, N. G., Babayev, I. K., Danilychev, V. A., Mikhaylov, M. D., Orlov, V. K., Savel'yev, V. V., Son, V. G., Cheburkin, N. V., KVANTOVAYA ELEKTRONIKA, Vol 6, 1976, p 772.

2. Averin, A. P., Glotov, Ye. P., Danilychev, V. A., Sazhina, N. N., Soroka, A. M., Yugov, V. I., PIS'MA V ZHURNAL TEKHNICHESKOY FIZIKI, Vol 7, 1981, p 769.

3. Danilychev, V. A., Kovsh, I. B., Sobolev, V. A., TRUDY FIZICHESKOGO INSTITUTA IMENI P. N. LEBEDEVA AKADEMII NAUK SSSR, Vol 116, 1980, p 98.

4. Averin, A. P., Glotov, Ye. P., Danilychev, V. A., Koterov, V. N., Soroka, A. M., Yugov, V. I., PIS'MA V ZHURNAL TEKHNICHESKOY FIZIKI, Vol 6, 1980, p 405.

5. McDaniel, I. I., "Protsessy stolknoveniy v ionizovannykh gazakh" [Collision Processes in Ionized Gases], Moscow, Mir, 1967.

6. Kuz'michev, V. M., Perepechay, M. P., KVANTOVAYA ELEKTRONIKA, Vol 1, 1974, p 2407.

7. Aleksandrov, V. V., Koterov, V. N., Soroka, A. M., ZHURNAL VYCHISLITEL'NOY MATEMATIKI I MATEMATICHESKOY FIZIKI, Vol 5, 1978, p 1214.

8. Glotov, Ye. P., Danilychev, V. A., Kholin, I. V., TRUDY FIZICHESKOGO INSTITUTA IMENI P. N. LEBEDEVA AKADEMII NAUK SSSR, Vol 116, 1980, p 189.

6610
CSO: 1862/41

NUCLEAR PHYSICS

PAPERS ON HIGH-ENERGY PHYSICS

Leningrad FIZIKA VYSOKIKH ENERGIY in Russian 1981 (signed to press 9 Mar 81) pp 2-3, 22-24, 26, 50-51, 54, 81-83, 115, 162-163, 200

[Excerpts from book "High-Energy Physics (Materials of the 16th Winter School of Leningrad Institute of Nuclear Physics imeni P. N. Konstantinov)", edited by V. Ye. Bunakov, M. M. Makarov, A. N. Moskalev and G. Ye. Solyakin, LIYaF, 500 copies, 231 pages]

[Text] The materials of this volume include papers dealing with various aspects of high-energy physica. These articles discuss deeply inelastic processes at high energies, problems of e^+e^- annihilation, processes with large transverse momentum. Material is given on three-baryon resonances. In addition, papers are presented that are fundamental in nature even though not directly related to processes between elementary particles at high energies. Among these are items on neutrino experiments at low energies, and effects of parity violation in nuclei.

The papers are intended for theoreticians and experimental researchers dealing with problems of high-energy physics, elementary particles and the atomic nucleus. With respect to level of presentation, they are accessible to scientific workers and graduate students.

UDC 539.12

DEEP INELASTIC PROCESSES IN THE LOW-x REGION

[Article by L. V. Gribov, Ye. M. Levin and M. G. Ryskin]

[Excerpts] An examination is made of the structure function of deep inelastic scattering at low x in QCD perturbation theory. Diagrams are summed in which the smallness of the coupling constant α_s is compensated by large logarithms: $\ln s$ and $\ln q^2$. It is shown that the increase in the structure function at small x is masked by multiple-ladder diagrams. As a result of this screening, the unitarity conditions are not violated. The paper discusses the resultant solution and its physical consequences for "rigid" processes.

Conclusion. In this paper we have attempted to demonstrate a method of calculating the asymptotic behavior of scattering amplitude at high energies within the framework of QCD perturbation theory. It has been shown that in these calculations, it

is not only the Feynman diagrams in which the smallness of the coupling constant α_s is compensated by a large energy logarithm $\left(\ln\frac{s}{q^2} = \ln\frac{1}{x}\right)$ that are important, but also graphs in which each power of α_s has its own logarithm of virtuality (i. e. $\alpha_s \ln q^2 \sim 1$), as well as a more complex class of diagrams in which the probability of parton rescattering

$$W = \int^{q^2} \frac{\alpha_s(q'^2)}{q'^2} \phi\left(\ln\frac{1}{x}, q'^2, q_0^2\right) dq'^2$$

reaches values of the order of unity due to an increase in parton density ϕ. It should be emphasized that no other large parameters arise in the problem.

Summation of diagrams of QCD perturbation theory that contain at least one large logarithm $\left(\ln q^2 \text{ or } \ln\frac{1}{x}\right)$ for each power of α_s is accomplished by using system of equations (11). The parton density $\phi\left(\ln\frac{1}{x}, q^2, q_0^2\right)$ obtained as a result of such summation is the Green's function of an effective pomeron in QCD.

To calculate contributions of order W^n to the amplitude, a diagram method was developed analogous to V. N. Gribov's reggeon diagram method [Ref. 3], where the part of a pomeron is played by the "ladder" of Fig. 2a, and the vertex of interaction of effective pomerons is calculated by QCD perturbation theory (for example see Fig. 4 and expression (16) for G_{3p}). Let us note that by gradually increasing energy in QCD perturbation theory, we again reproduced the "reggeon" diagram method. However, in contrast to the Reggeon field theory [RFT] that has recently been popular, we started from low energies and calculated the Green's function of an effective pomeron and the vertex of its interaction within the framework of perturbation theory. Our main theoretical goal has been to find the sum of the "reggeon" diagrams at high energy, whereas RFT introduces a seed amplitude at energy $s \to \infty$ and phenomenological vertices of interaction of pomerons, and investigates the feasibility of self-consistency of such a theory.

In this paper we have restricted ourselves to calculation of the cross sections of deeply inelastic processes in order to avoid discussing the "confinement" problem and the region of small virtualities where α_s may be large. For this reason we have not been able to get to the region of positive t or to verify t-channel unitarity conditions.* Nonetheless, s-channel unitarity, the relation between processes with different multiplicity (Abramovskiy-Gribov-Kancheli rules of Regge cuts [Ref. 11]), is totally conserved here. Moreover, our diagram method coincides with the old reggeon approach from the phenomenological standpoint since it conserves such features of the reggeon theory as introduction of a new quantum number (signature), classification of asymptotic behavior in accordance with quantum numbers of the t-channel, etc. In particular, exchange of a secondary "reggeon" corresponds to the ladder diagrams of Fig. 11 constructed from a quark and an antiquark. The asymptotic behavior of these diagrams differs appreciably from the vacuum channel (Fig. 2a), and in the case of $|t| > \Lambda^2$, the amplitude takes the form

*This limitation is fundamental, and does not allow us to move into the region of $q_0^2 \sim \Lambda^2$. On the other hand, limitation $\ln 1/x < \ln^2 q^2$ (the region below curve 2 in Fig. 1) is due exclusively to the fact that we have not yet been successful in summing amplified "reggeon" diagrams.

$$\left(\frac{s}{t}\right)^{\sqrt{2c_F \frac{\alpha_s(t)}{\pi}}}$$

[this formula is readily obtained by the method developed in Ref. 12]. From the standpoint developed here, we get a natural explanation of the difference in nature of constriction of the diffraction cone in the vacuum and non-vacuum channel. It is a commonly known experimental fact that $\alpha_D' \ll \alpha_R'$, where the α' are the slopes of the trajectories of the pomeron and secondary R-reggeon. In QCD, the secondary reggeon corresponds to the above asymptotic formula, which leads to large $\alpha_R' \sim \frac{1}{t \ln^2 t}$. Let us recall that an effective pomeron in this same approximation is standing, i. e. $\alpha' = 0$. We take this example as an argument in favor of the phenomenological value of considering asymptotic behavior within the limits of QCD perturbation theory.

UDC 539.12.1

OLD PARTICLES AT NEW ENERGIES OF e^+e^- ANNIHILATION

[Article by Ya. I. Azimov, Yu. L. Dokshitser and V. A. Khoze]

[Excerpts] The authors consider new experimental results accumulated in e^+e^- annihilation over the past year. Prospects for studying intermediate bosons of weak interaction and processes of multiple formation of old hadrons are discussed.

Conclusion. Over the past year many important and interesting results have been obtained in e^+e^- annihilation. There is no question that the main one has been confirmation that has been found for the existence of the gluon, which we promised at the last "school." It would also seem that we are on the verge of discovering intermediate Z^0 and $W^\pm$ bosons, and there is a general consensus that the results of this search will be reported no later than the 20-th School of Leningrad Institute of Nuclear Physics.

Even now experiments are coming close to studying such important problems of chromodynamics as the physics of the color neutralizing process, the individual life of a gluon jet, direct observation of gluon self-stress, specifics of heavy quark production and the like. Of course, detailed investigation of many of these processes will require still higher e^+e^- beam energies.

By the same token, the new energies will lead to some new difficulties in interpreting the results of observations. At $\sqrt{S} \gtrsim 50$ GeV the electromagnetic and weak contributions to quark production become comparable. The raw data will be a mixture of weak, one-photon and two-photon mechanisms of formation of hadron jets that are buried under the radiation tail of the Z^0 boson besides (at $\sqrt{S} > M_Z$). At $\sqrt{S} > 2M_W$ we also get the formation and subsequent decays of W^+W^- pairs. Nevertheless, the various contributions can be distinguished, in particular by using the kinematics specific to their corresponding final states. Polarization of the initial e^- and e^+ beams may also play an important part in this noble cause.

The authors thank B. L. Ioffe, L. M. Kurdadze, A. P. Onuchin, I. B. Khriplovich, and especially M. G. Ryskin for useful discussions.

UDC 539.12.1

LARGE P_T AND JETS IN HADRON-HADRON COLLISIONS

[Article by V. Yu. Glebov]

[Excerpts] The paper is a survey of experimental data obtained in the physics of large P_T in 1978-1980. The author discusses inclusion spectra of hadrons with very large P_T, the ratio of particle yields in πp and pp interactions, and measurements of yields of direct photons. Methods of distinguishing jets in hadron interactions are analyzed. Characteristics of jets in pp, e^+e^- and νp interactions are compared.

Conclusion. Over the past two years, a number of important advnaces have been made in the physics of large P_T from both the theoretical and experimental standpoints.

Advances in theory have been due to using QCD for describing processes of particle production with large P_T. At the present time QCD is capable of not only qualitative but also quantitative description of inclusive formation of isolated hadrons with very large P_T, formation of symmetric hadron pairs with moderate P_T, ratio of particle yields in πp and pp collisions, and production of direct photons with large P_T.

A great move forward has been the detailed study of the structure of jets with large P_T. One of the principal ideas of the quark-parton approach to rigid processes--universality of jets in e^+e^- annihilation, deeply inelastic scattering of leptons by nucleons and production of particles with large P_T in hadron-hadron collisions--has found reliable experimental confirmation.

A specific feature of the QCD quark model is the presence of gluons in hadrons. QCD calculations show that contributions of quark-gluon and gluon-gluon scattering are not small in the inclusive production of particles with large P_T. However, it is the gluon effects that are difficult to isolate. The process of formation of direct photons with large P_T was observed in 1979. In QCD, the gluon Compton effect is responsible for this production process. This opens up a unique possibility for verifying a fundamental prediction of QCD: the existence of gluons in hadrons.

But despite advances in both theory and experiment, there are still a number of unresolved questions. Three-jet events have been observed in e^+e^- annihilation. Their analog is five-jet events in particle production with large P_T in pp collisions. How does a small admixture of such events influence the structure of events treated as containing only two jets with large P_T? At what P_T and energies will formation of a third jet with large P_T be noted? What are the regions of applicability of QCD with respect to the scale of energies and transverse momenta from below? What is the mechanism of transition from "small" to "large" P_T? These and other questions so far remain unanswered.

On the whole the picture of particle production with large P_T is still incomplete, and further theoretical and experimental efforts are needed for a deeper understanding of the nature of processes that occur.

In conclusion the authors consider it their pleasant duty to express sincere gratitude to Ye. M. Levin, A. K. Likhoded, N. N. Nikolayev, M. G. Ryskin and R. M. Sulyayev for numerous constructive discussions, and to L. N. Shevchenko for assistance in preparing the manuscript for printing.

UDC 539.12, 539.171

DO THREE-BARYON RESONANCES EXIST?

[Article by L. A. Kondratyuk and L. V. Shevchenko]

[Excerpt] The authors discuss the predictions of a stretched rotating 9-quark bag model for the spectrum of 3-baryon resonances with zero strangeness. An analysis is made of the reaction of pd-backscattering in the region $T_p = 0.3$-1 GeV, and arguments are given to support the hypothesis that the observed structure in the energy dependence of the cross section of this reaction at $\sqrt{S} = 3$-3.5 GeV is due to the contribution of 3-baryon resonances.

UDC 539.173

NEUTRINO EXPERIMENTS AT LOW TEMPERATURES

[Article by L. A. Popenko and A. V. Derbin]

[Excerpt] This paper reviews neutrino experiments carried out up to the present on reactors. An examination is made of the major goals of studying ν- and $\tilde{\nu}$-interactions at low energies. The authors discuss the feasibility of setting up neutrino experiments with the use of a silicon multidetector and radioactive sources of ν_e and $\tilde{\nu}_e$ in the energy range from 0.2 to 3 MeV. An examination is made of some technical problems of detector design and construction of a radioactive source with activity of several megacuries.

Introduction. The fourth of December 1980 was the fiftieth anniversary of the "discovery" of the neutrino as recounted in a letter by W. Pauli dated 4 Dec 1930, where he asks experimenters to look in nuclei for a neutral particle with spin $S = \frac{1}{2}$, mass of no more than 1/100 of the mass of the proton, and ionization effect no greater than for a gamma particle.

The establishment and confirmation of this particle over the course of the fifty years has been associated with the names of W. Pauli, E. Fermi, B. Pontecorvo and F. Reines. Over the past few years in connection with the sharp upsurge of interest in neutrino data, construction has started on new detectors to supplement the CERN neutrino detectors such as VEVS, CDHS, CHARM and many others in the United States and the USSR. We have begun to treat the neutrino as an equal with the electron, gamma quantum and other particles, dropping the "mystical" epithet that continuously accompanied the neutrino through nearly the entire fifty years from the time of its discovery at the "penpoint" of E. Fermi and W. Pauli.

We are now seeing a revival of the neutrino in connection with indications of an experiment at the Institute of Theoretical and Experimental Physics [ITEF] to the effect that the neutrino has a rest mass of the order of 30 eV [Ref. 1]. This fact

could radically alter our ideas about the universe. In this case it is a neutrino-determined universe according to estimates by Ya. B. Zel'dovidh.

Recent indications of neutrino oscillations implied by experiments of F. Reines have given the square of the mass difference of the electron-type antineutrino and the μ-meson type in a range of 1 eV^2 [Ref. 2], which has indirectly confirmed the fairly large rest mass of the neutrino. However, the results of a new experiment done in Grenoble [Ref. 3] have not confirmed these data, and the limit on this parameter is 0.13 eV^2. All this shows that we are extremely uncertain of experimental data both on the physical properties of the neutrino and on its interactions. In connection with this, at low energies we can distinguish two classes of problems that must be experimentally studied:

--the problem of neutrino mass and oscillation;
--effects with neutral currents, including interference effects of neutral and charged currents.

UDC 539.141

PARITY VIOLATION EFFECTS IN COMPOUND NUCLEI

[Article by O. P. Sushkov and V. V. Flambaum]

[Excerpt] The authors discuss effects of violation of spatial parity in interaction of neutrons with a nucleus--P-odd asymmetry in fission of nuclei, parity violation when neutrons are coherently scattered by nuclei (in neutron optics), and also effects of parity violation in the reaction (n, γ).

6610
CSO: 1862/39

ALL-UNION SEMINAR ON PHYSICS AND ENGINEERING OF INTENSIVE SOURCES OF IONS AND ION BEAMS

Moscow FIZIKA PLAZMY in Russian Vol 7, No 5, Sep-Oct 81 p 1175

[Article by M. D. Gabovich and N. N. Semashko]

[Text] During 21-23 October 1980, the Third Session of the All-Union Seminar on the Physics and Engineering of Intensive Sources of Ions and Ion Beams was held at the Physics Institute of the UkSSR Academy of Sciences in Kiev. It was organized by a decree of the USSR Academy of Sciences Scientific Council on the Problem of "Plasma Physics". The seminar leaders were: A. I. Morozov, N. N. Semashko (Institute of Atomic Energy imeni I.V. Kurchatov), and M.D. Gabovich (Physics Institute of the UkSSR Academy of Sciences). Approximately 150 scientists--representatives of scientific establishments from Moscow, Leningrad, Novosibirsk, Khar'kov, Kiev and other cities--took part in the session. Forty-eight papers were presented on the following topics: (1) high-current, quasi-stationary ion sources; (2) high-current impulse ion sources; (3) negative ion sources; (4) sources of multiply-charged ions; (5) collective processes in an ion-beam plasma; and (6) industrial ion beams.

Significant advances were made in the above areas. In particular, the following results should be mentioned:

1. Obtainment of quasi-stationary beams of positive ions up to 100 A, intended for the injectors of thermonuclear plants (Institute of Atomic Energy imeni I.V. Kurchatov; Institute of Nuclear Physics, Siberian Department, USSR Academy of Sciences).

2. Development of methods of obtaining intensive negative ion beams (Institute of Atomic Energy imeni I. V. Kurchatov; Institute of Nuclear Physics, Siberian Department, USSR Academy of Sciences).

3. Research of the collective processes in an ion-beam plasma (Physics Institute of the UkSSR Academy of Sciences).

4. Obtainment of intensive fluxes of multiply-charged ions (Moscow Engineering Physics Institute; Joint Institute of Nuclear Research and others).

It should be mentioned also that advances have been made in the creation of high-current impulse ion fluxes, in particular, at the Institute of Nuclear Physics at Tomsk Polytechnical Institute.

The next session of the seminar is planned for October 1981 in Kiev.

CSO: 1862/72-P

OPTICS AND SPECTROSCOPY

UDC 535.37:621.375.826

DETERMINING SPECTRAL DEPENDENCES OF ABSOLUTE QUANTUM YIELDS OF XeF EXCIMER FORMATION (B, C, D) IN XeF_2 PHOTOLYSIS

Moscow KVANTOVAYA ELEKTRONIKA in Russian Vol 8, No 9(111), Sep 81 (manuscript received 9 Mar 81) pp 1945-1951

[Article by N. K. Bibinov, I. P. Vinogradov, L. D. Mikheyev and D. B. Stavrovskiy, Institute of Physics imeni P. N. Lebedev, USSR Academy of Sciences]

[Text] Interest in photolysis of XeF_2 accompanied by production of excited molecules of XeF (B, C, D) is occasioned by the use of this reaction in excimer lasers with optical pumping. In this paper an investigation is made of photolysis of gaseous XeF_2 in the spectral range of 108-220 nm. It is established that the maximum quantum yields of production of XeF(B) and XeF(C) are 30 ± 9 and $3.5 \pm 1\%$ respectively in the region of 140-180 nm ($\lambda_{max} \cong 165$ nm). The quantum yield of formation of XeF(D) in this region does not exceed 1.5%. The authors discuss the mechanism of dissociation of XeF_2 molecules. It is shown that several electron transitions contribute to the absorption band of XeF_2 that has a maximum at 158 nm. It is suggested that a transition in this band to states $^1\Pi_g$ or $^3\Pi_u$ leads to formation of XeF(D), and a transition to $^1\Pi_u$ leads to formation of XeF (X or A), transitions to $^1\Sigma_u^+$ and $^3\Sigma_u^+$ lead to formation of XeF(B) and XeF(C) respectively.

1. Introduction

Interest in spectroscopy of XeF excimer at the present time stems from intensive development of research on excimer lasers. Lasing has been achieved on two electron transitions of XeF X-B ($\lambda \cong 350$ nm) and C-A ($\lambda \cong 480$ nm) with different methods of creating inverse population: in an electric discharge [Ref. 1-3], under the action of a beam of fast electrons [Ref. 4, 5] and by optical pumping [Ref. 6-9]. (We will denote the electronic states of XeF by letters of the Latin alphabet as has been done for example in Ref.10, 12.)

Optically pumped XeF lasers use XeF_2 photolysis. To study the kinetics of these lasers and determine their limiting characteristics, data on absolute values and spectral dependences of quantum yields of different photolysis products are of great significance. The reaction of photodissociation of XeF_2 was experimentally studied in Ref. 10-12. In Ref. 10, 11, formation of XeF(B) was observed when XeF_2 was exposed to light on wavelengths of 123.6, 160-180, 184.9 and 193 nm. According

to estimates by the authors of Ref. 10, the quantum yield of the process is close to unity; however, it has not been measured directly. The absolute values of quantum yields of formation of XeF in excited electronic states B, C and D were measured in Ref. 12. It was found that upon photolysis in the region of 145-175 nm the quantum yields of XeF(B) > 90%, XeF(C) < 5%, and XeF(D) < 3%.

This paper gives the results of a study of photodissociation of XeF_2 with formation of excited fragments of XeF(B, C, D) in the spectral band of 220-108 nm.

2. Experimental Part

Descriptions can be found in previous papers [Ref. 13, 14] for most of the experimental facility for measuring absorption cross sections, luminescence spectra and spectral dependences of absolute quantum yields of luminescence of the molecules, atoms and radicals formed upon photolysis of vapor in the XUV region of the spectrum. Only the cell part was changed. In this research a cell was used that was separated from the rest of the experimental facility by LiF and MgF_2 windows. The cell was made of brass and plated with nickel. The optical length of the absorbing layer was 6.7 cm. Before starting the work, the cell and the inlet system were evacuated to a pressure of 10^{-5} mm Hg and passivated with fluorine to such a degree that dissociation of XeF_2 was no more than 10% over the time of one complete measurement (30 minutes). The curves presented in the work were obtained in pure XeF_2 vapor by averaging four measurements. Scanning over the spectrum was done both toward shorter and toward longer wavelenghts. The random error of relative measurements did not exceed ±8%.

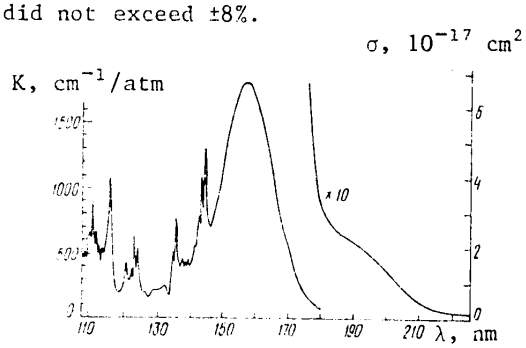

Fig. 1. Absorption spectrum of XeF_2 vapor taken with resolution of $\Delta\lambda \cong 0.3$ nm

Results of Measurements and Their Discussion

Fig. 1 shows the absorption spectrum that we obtained for XeF_2 in the region of 108-225 nm. The error in determining the absolute value of the cross section is 10%. Absorption in the region of 220 nm is due to the forbidden transition $5\pi_u \rightarrow 7\sigma_u$, $^{1,3}\Pi \leftarrow {}^1\Sigma_g^+$ [Ref. 15]. The coefficient of absorption of XeF in this wavelength region is quite low (~4-5 cm^{-1}/atm). In the region of 210-145 nm an intense broad absorption band is observed with maximum at 158 nm, corresponding according to Ref. 15 to transition $10\sigma_g \rightarrow 7\sigma_u$, $^1\Sigma_u^+ \leftarrow {}^1\Sigma_g^+$. According to our measurements, the absorption at the band maximum is 1810 cm^{-1}/atm, which agrees with the results of Ref. 12, but is 2 times lower and 1.4 times greater respectively than according to the data of Ref. 15 and 16. Shorter than 145 nm, we observe the Rydberg band series identified in Ref. 15: $\pi_u(3/2, 1/2) \rightarrow$ ns, nd and $\sigma_g \rightarrow$ np with well-resolved vibrational structure.

Under the action of XUV radiation, the following reactions are possible in XeF_2, leading to formation of primary excited products [Ref. 10, 12]:

$$XeF_2 + h\nu \xrightarrow{\sigma} XeF_2^*, \quad (1)$$

$$XeF_2^* \xrightarrow{\varphi_B} XeF\,(B) + F\,(^2P_u), \quad (2)$$

$$XeF_2^* \xrightarrow{\varphi_C} XeF\,(C) + F\,(^2P_u), \quad (3)$$

$$XeF_2^* \xrightarrow{\varphi_D} XeF\,(D) + F\,(^2P_u), \quad (4)$$

where σ is the cross section of absorption of light by a molecule of XeF_2, ϕ_B, ϕ_C, ϕ_D are the quantum yields of formation of the corresponding excited states of XeF.

The resultant excited molecules of XeF either expend the energy of excitation in collisions with XeF_2, or emit a quantum of light [Ref. 12, 17, 18]:

$$XeF\,(B) + XeF_2 \underset{k_{CB}}{\overset{k_{BC}}{\rightleftarrows}} XeF\,(C) + XeF_2, \quad (5)$$

$$XeF\,(B) + XeF_2 \xrightarrow{k_B} XeF\,(X,\ A^3/_2,\ A^1/_2) + XeF_2, \quad (6)$$

$$XeF\,(C) + XeF_2 \xrightarrow{k_C} XeF\,(X,\ A^3/_2,\ A^1/_2) + XeF_2, \quad (7)$$

$$XeF\,(D) + XeF_2 \xrightarrow{k_D} XeF\,(X,\ A^3/_2,\ A^1/_2) + XeF_2, \quad (8)$$

$$XeF\,(B) \xrightarrow{W_{BX}} XeF\,(X) + h\nu\,(\lambda \sim 350\ \text{nm}), \quad (9)$$

$$XeF\,(B) \xrightarrow{W_{BA}} XeF\,(A^1/_2) + h\nu\,(\lambda \sim 470\ \text{nm}), \quad (10)$$

$$XeF\,(C) \xrightarrow{W_{CA}} XeF\,(A^3/_2) + h\nu\,(\lambda \sim 470\ \text{nm}), \quad (11)$$

$$XeF\,(D) \xrightarrow{W_{DX}} XeF\,(X) + h\nu\,(\lambda \sim 260\ \text{nm}), \quad (12)$$

$$XeF\,(D) \xrightarrow{W_{DA}} XeF\,(A^1/_2) + h\nu\,(\lambda \sim 290\ \text{nm}), \quad (13)$$

where k_{BC}, k_{CB}, k_B, k_C, k_D are the reaction rate constants, W_{BX}, W_{BA}, W_{CA}, W_{DX}, W_{DA} are the probabilities of radiative transitions.

Fig. 2 shows the luminescence spectra that we obtained for XeF corresponding to the transitions $B \to X$ and $D \to X$. The spectra are plotted with consideration of the spectral dependence of sensitivity of the recording channel. The luminescence spectrum that we observed on transitions $C \to A$ and $B \to A$ was analogous to that obtained in Ref. 17, being a broad structureless band in the region of 360-550 nm with maximum at 450 nm. It can be seen that with an increase in the energy of a quantum of photolyzed radiation there is an increase in the width of the luminescence band $XeF(B \to X)$ due to an increase in vibrational excitation of XeF(B). A structureless band observed in the vicinity of 290 nm may be due to luminescence on transition $D \to A^1/_2$, as is predicted by the calculation done in Ref. 18.

In the experiment we determined the ratios of intensity of the absorbed light and luminescence intensity: $S_1 = I_0\sigma Q/W_{BX}B$ ($\lambda \sim 350$ nm); $S_2 = I_0\sigma Q/(W_{BA}B + W_{CA}C)$ ($\lambda \sim 470$ nm);

$S_3 = I_0\sigma Q/W_{DX}D$ ($\lambda \sim 260$ nm). Here B, C, D are the concentrations of XeF in the corresponding electron states; Q is the concentration of XeF_2; I_0 is the intensity of the photolyzing radiation. In measuring the luminescence intensity, the radiation was recorded in the corresponding luminescence band in a spectral range of ~9 nm. The percentage of photons reaching the given spectral range was calculated from the luminescence spectrum. Consideration was taken of the change in the luminescence spectrum as a function of the wavelength of the photolyzing radiation. Linear dependences of S_1, S_2, S_3 on XeF_2 pressure were observed in the investigated pressure range of 0-1 mm Hg.

The following relations obtained in analysis of the kinetics of processes (1)-(13) were used in processing the measurement results

$$S_1 = \frac{1}{\varphi_B}\left(1 + \frac{W_{BA}}{W_{BX}}\right) + \frac{k_B + k_{BC}}{\varphi_B W_{BX}} Q, \qquad (14)$$

$$\lim_{Q\to 0} S_2 = \frac{W_{BX} + W_{BA}}{(W_{BX} + W_{BA})\varphi_C + W_{BA}\varphi_B}, \qquad (15)$$

$$S_3 = \frac{1}{\varphi_D}\left(1 + \frac{W_{DA}}{W_{DX}}\right) + \frac{k_D}{\varphi_D W_{DX}} Q. \qquad (16)$$

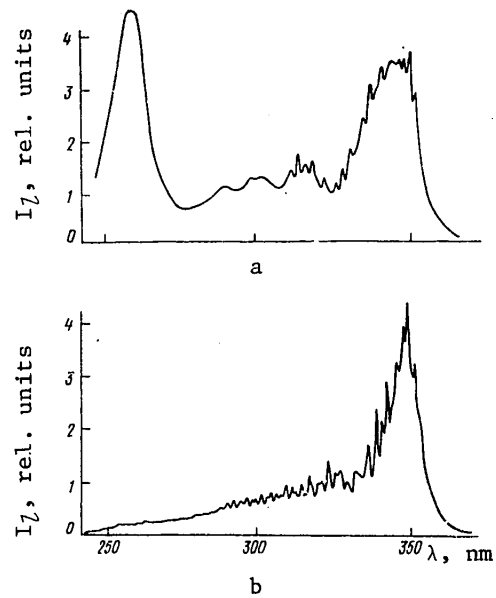

Fig. 2. Luminescence spectrum of XeF on transitions $B \to X$ ($\lambda \sim 350$ nm), $D \to X$ ($\lambda \sim 250$ nm) and possibly $D \to A^1_2$ ($\lambda \sim 290$ nm); $\lambda_{exc} = 116$ (a) and 160.8 nm (b)

The values of ϕ_B, ϕ_C, ϕ_D, $(k_B + k_{BC})$, k_D are determined from a comparison of the experimental and theoretical relations. It should be noted that terms of the order of Q^2 and higher, as well as the term $k_{CB}\phi_C(W_{BX} + W_{BA})Q/(\phi_B^2 W_{BX} W_{CA})$ have been omitted in the second member of expression (14). Estimates show that the contribution of these terms is small compared with the random error of the experiment. Calculations and estimates used the following data taken from the literature: $W_{BX} = 7.5\cdot 10^7$ s^{-1}, $W_{CA} = 9.9\cdot 10^6$ s^{-1} [Ref. 12], $W_{BA} = 2.9\cdot 10^6$ s^{-1}, $W_{DX} = 1.05\cdot 10^8$ s^{-1}, $W_{DA} = 1.33\cdot 10^7$ s^{-1} [Ref. 18], $\phi_C/\phi_B < 0.1$, $k_{BC}/k_{CB} = 22.8$ [Ref. 12].

Our value of $k_B + k_{BC} = (5.0 \pm 0.4)\cdot 10^{-10}$ $cm^3/s\cdot mol$. differs from the values cited in the literature: $(3.5 \pm 0.2)\cdot 10^{-10}$ [Ref. 11], $(7.4 \pm 0.3)\cdot 10^{-10}$ [Ref. 12], $(2.6 \pm 0.3) \times 10^{-10}$ [Ref. 19]. It should be noted that the authors of Ref. 11, 12, 19 did not consider reaction (5), and give the values of k_B, when they actually measured the sum $k_B + k_{BC}$ as well. As far as we know, no one has yet determined the ratio between constants k_B and k_{BC}.

The value that we got for k_D was $(1.6 \pm 0.16)\cdot 10^{-9}$ $cm^3/s\cdot mol$. In calculating k_D, we used the lifetime $\tau_D = 1/W_{DX}$ found theoretically in Ref. 18. We know of no experimentally determined value of τ_D. A value of $\tau_D = 13 \pm 1$ ns was found in Ref. 20 by using the τ_D measured in an inert gas matrix and extrapolating to the gas phase.

This value is apparently unreliable since the value of $\tau_B = 8$ ns given in the same paper differs strongly from the τ_B measured directly in the gas phase; for example Ref. 12 gives $\tau_B = 13.3 \pm 0.2$ ns.

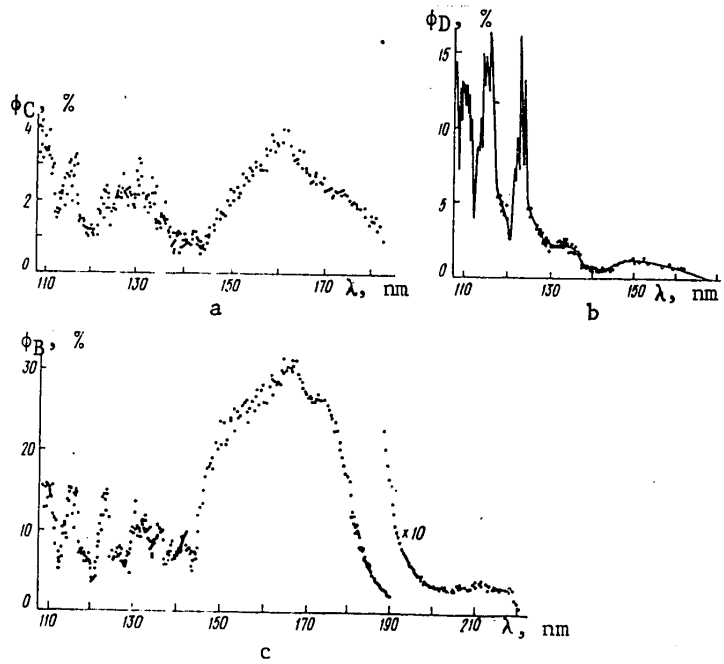

Fig. 3. Spectral dependences of quantum yields of formation of XeF(C) (a), XeF(D) (b) and XeF(B) (c)

The spectral dependences of ϕ_B, ϕ_C, ϕ_D are shown in Fig. 3. By using the value of the photon energy corresponding to the threshold of formation of XeF(B) ($\lambda_{thr} = 220 \pm 2$ nm), we can estimate the energy required for breaking the chemical bond Xe-F in the XeF molecule: it is <2.2 eV. This value is obtained with consideration of the results of Ref. 21, according to which the difference in energies of states B (v' = 0) and X (v'' = 0) of XeF is 28,865 cm^{-1}.

Fig. 4 shows spectra of luminescence excitation of XeF on transitions $B \rightarrow X$ and $D \rightarrow X$. The luminescence excitation spectra on transitions $C \rightarrow A$ and $B \rightarrow X$ are similar. Comparison of the absorption spectrum of XeF_2 (see Fig. 1) with the luminescence excitation spectra of XeF ($B \rightarrow X$, $D \rightarrow X$) shows the complicated nature of the absorption band with maximum at 158 nm. Photolysis of XeF_2 in this band is accompanied by formation of three excited products XeF(B, C, D), the maximum in the luminescence excitation spectrum of XeF($B \rightarrow X$) being shifted toward the long-wave region, while the maximum of the excitation spectrum XeF($D \rightarrow X$) is shifted toward the short-wave region as compared with the maximum of the absorption spectrum.

Subtracting the curve of the partial cross section of formation of XeF(B) + XeF(C) from the curve of the absorption cross section of XeF_2, we get the difference band

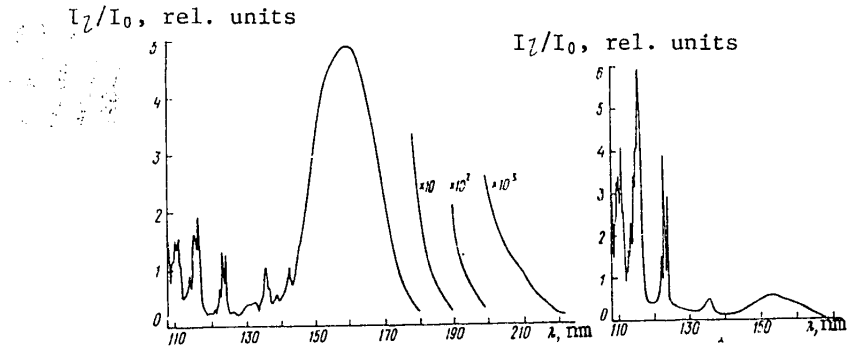

Fig. 4. Luminescence excitation spectrum of XeF(B→X) (a) and XeF(D→X) (b)

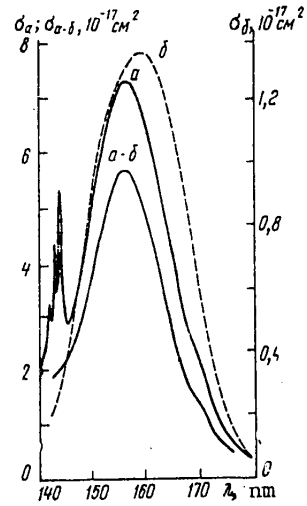

Fig. 5. Absorption cross section of XeF_2 (a), partial cross section of formation of XeF(B, C) in photolysis of XeF_2 (b), and their difference curve (a - b)

shown in Fig. 5. (The partial cross section of formation of a product is found by multiplying the absorption cross section by the quantum yield of product formation.) Excitation of XeF_2 in this difference band does not lead to formation of radiating fragments (the partial cross section of formation of XeF(D) can be disregarded as the quantum yield of process (4) in the vicinity of 140-180 nm does not exceed 1.5%). Thus we have grounds for assuming that the band with maximum at 158 nm is due to several electron transitions, and therefore we must re-examine the identification of this band given in Ref. 15. It can be assumed that the transitions are effected in four dispersion electron states of XeF_2: α, β, γ and δ, the first two dissociating with formation of XeF(B) and XeF(C), the third yielding no radiating products, and the fourth dissociating with formation of XeF(D). The electronic states of the XeF_2 molecule were calculated in Ref. 22, and the photoelectron spectrum of XeF_2 was studied in Ref. 23. According to the results of these studies, the following electronic transitions are possible in the region of 140-180 nm: $10\sigma_g \to 7\sigma_u(^{1,3}\Sigma_u^+ \leftarrow {}^1\Sigma_g^+)$, $3\pi_g \to 7\sigma_u(^{1,3}\Pi_u \leftarrow {}^1\Sigma_g^+)$, $4\pi_u \to 7\sigma_u(^{1,3}\Pi_g \leftarrow {}^1\Sigma_g^+)$ (transitions are arranged in order of increasing photon energy).

Since the partial cross sections of formation of non-radiating products and XeF(B) are large, states γ and α are apparently associated with the ground state $XeF_2(^1\Sigma_g^+)$ by allowed transitions. We assume that state α is $^1\Sigma_u^+$, and state γ is $^1\Pi_u$. As to states β and δ, we assume that β is $^3\Sigma_u^+$, and δ is $^1\Pi_g$ or $^3\Pi_u$. This assumption allows us to explain the low values of the quantum yields of formation of XeF(C) and XeF(D) in photolysis of XeF_2 in the region of 140-180 nm (see Fig. 3a, b) since the cross sections of light absorption on forbidden transitions $^3\Sigma_u^+ \leftarrow {}^1\Sigma_g^+$ and $^3\Pi_u$, $^1\Pi_g \leftarrow {}^1\Sigma_g^+$ are a small fraction of the total absorption cross section above 140 nm.

It should be noted that our assumed identification of states α, β, γ, δ agrees with the rules of correlation of states of the unified molecule and the states of the fragments [Ref. 24].

There is one more circumstance that supports our proposed identification of state γ. Excitation of XeF_2 on 144.5 nm to the Rydberg state $^1\Pi_u$ corresponding to transition $\pi_u{}^{3}/_{2} \rightarrow 6s$ does not lead to formation of excited fragments. Therefore it can be assumed that predissociation from the Rydberg state $^1\Pi_u$ takes place to a dispersion state of the XeF_2 molecule correlating with non-radiating fragments of XeF(X or A) + $F(^2P_u)$. Predissociation to state $^1\Pi_u$ is more probable than to $^1\Sigma_u^+$, since heterogeneous predissociation ($\Delta\Lambda = \pm 1$) is possible in electron-rotational interaction that shows up markedly in diatomic molecules, and is quite weak in polyatomic molecules [Ref. 24].

In the spectral region below 145 nm, the luminescence excitation spectra of XeF(B, C, D) show intense bands corresponding to transitions to the Rydberg states $\pi_u{}^{3}/_{2}, {}^{1}/_{2} \rightarrow ns$ and $\sigma_g \rightarrow np$. The only exceptions are the transitions $\pi_u{}^{3}/_{2} \rightarrow 6s$, 7s on 144.5 and 115.9 nm respectively (see Fig. 4).

The absolute values of quantum yields of XeF luminescence shown on Fig. 3 were obtained by a relative method. The reference standard was the quantum yield of formation of $OH(A^2\Sigma^+)$, equal to $5.2 \pm 0.6\%$ on line L_α (121.6 nm) in photolysis of water [Ref. 13]. The overall maximum quantum yield of formation of XeF upon excitation in the absorption band with maximum at 158 nm is equal to 0.34 ± 0.1 (principal contribution is from the process of formation of XeF(B), $\phi_B{}^{max} = 0.30 \pm 0.09$).

The quantum yield of formation of $OH(A^2\Sigma^+)$ that we used agrees well with the value of 5% obtained in Ref. 25. However, Lee et al., [Ref. 26, 27], in studying the photolysis of water on individual lines, give absolute values of quantum yields of formation of $OH(A^2\Sigma^+)$ that average 1.35 times higher than in Ref. 13. If we use the results of Ref. 26 and 27, the maximum quantum yield of XeF(B) luminescence may reach 40%.

The values of the quantum yield of luminescence that we obtained by using luminescence of the OH radical as a standard diverge considerably from the results of Ref. 12, where calibration was done with respect to luminescence of the XeO excimer in photolysis of a gas mixture of N_2O-Xe, and the total quantum yield of XeF(B,C,D) was close to 100% in the region of 145-175 nm. The reason for such a considerable discrepancy is not clear. It is also difficult to understand why the authors of Ref. 12 failed to observe the wavelength dependence of quantum yield.

REFERENCES

1. Burnham, R., Harris, N. W., Djeu, N., APPL. PHYS. LETTS., Vol 28, 1976, p 86.

2. Fisher, C. H., Center, R. E., Mullaney, G. L., McDaniel, J. P., APPL. PHYS. LETTS., Vol 35, 1979, p 26.

3. Burnham, R., APPL. PHYS. LETTS., Vol 35, 1979, p 48.

4. Brau, C. A., Ewing, J. J., APPL. PHYS. LETTS., Vol 27, 1975, p 435.

5. Ernst, W. E., Tittel, F. K., APPL. PHYS. LETTS., Vol 35, 1979, p 36.

6. Basov, N. G., Zuyev, V. S., Mikheyev, L. D., Stavrovskiy, D. B., Yalovoy, V. I., KVANTOVAYA ELEKTRONIKA, Vol 4, 1977, p 2453.

7. Eden, J. G., OPTICS LETTS., Vol 3, 1978, p 94.

8. Basov, N. G., Zuyev, V. S., Kanayev, A. V., Mikheyev, L. D., Stavrovskiy, D. B., KVANTOVAYA ELEKTRONIKA, Vol 6, 1979, p 1074.

9. Bishel, W. K., Nakano, H. H., Eckstrom, D. J., Hill, R. M., Huestis, D. L., Lorents, D. C., APPL. PHYS. LETTS., Vol 34, 1979, p 565.

10. Brashears, H. C., Jr., Setser, D. W., Desmarteau, D., CHEM. PHYS. LETTS., Vol 48, 1977, p 84.

11. Burnham, R., Harris, N. W., J. CHEM. PHYS., Vol 66, 1977, p 2742.

12. Lorents, D. C., Black, G., Sharples, R., Huestis, D., Gutcheck, R., Helms, D., Bonifield, T., Walters, G. W., "Proc. Int. Conf. on Lasers 79," Orlando, Florida, Dec 17-21, 1979, p 143.

13. Vinogradov, I. P., Vilesov, F. I., OPTIKA I SPEKTROSKOPIYA, Vol 44, 1978, p 1119.

14. Bibinov, N. K., Vilesov, F. I., Vinogradov, L. D., Mikheyev, L. D., Pravilov, A. M., KVANTOVAYA ELEKTRONIKA, Vol 6, 1979, p 1430.

15. Nielsen, U., Schwarz, W., J. CHEM. PHYS., Vol 13, 1976, p 195.

16. Pysh, E., Jortner, J., Rice, S., J. CHEM. PHYS., Vol 40, 1964, p 2018.

17. Brashears, H. C., Jr., Setser, D. W., APPL. PHYS. LETTS., Vol 33, 1978, p 821.

18. Dunning, T. H., Jr., Hay, P. J., J. CHEM. PHYS., Vol 69, 1978, p 134.

19. Eden, J. G., Waynant, R. W., OPTICS LETTS., Vol 2, 1978, p 13.

20. Goodman, J., Brus, L. E., J. CHEM. PHYS., Vol 65, 1976, p 3808.

21. Zuyev, V. S., Kanayev, A. V., Mikheyev, L. D., Stavrovskiy, D. B., TRUDY FIZICHESKOGO INSTITUTA AKADEMII NAUK SSSR IMENI P. N. LEBEDEVA, Vol 125, 1980 p 3.

22. Scheire, L., Phariseau, P., Nuyts, R., PHYSICA, Vol 101A, 1980, p 22.

23. Brundle, C. R., Robin, M. B., Jones, G. R., J. CHEM. PHYS., Vol 52, 1970, p 3383.

24. Gertsberg, G., "Elektronnyye spektry i stroyeniye mnogoatomnykh molekul" [Electron Spectra and Structure of Polyatomic Molecules], Moscow, Mir, 1969.

25. Carrington, T., J. CHEM. PHYS., Vol 41, 1964, p 2012.

26. Lee, L., Oren, L., Phillips, E., Judge, D., J. PHYS. B, Vol 11, 1978, p 47.

27. Lee, L. C., J. CHEM. PHYS., Vol 72, 1980, p 4334.

6610
CSO: 1862/41

UDC 621.375.826:535.24:519

DIFFRACTOMETER WITH THERMOMAGNETIC REGISTRATION FOR CHECKING WAVEFRONT DISTORTIONS OF PULSED LASER EMISSION

Moscow IZMERITEL'NAYA TEKHNIKA in Russian No 10, Oct 81 (signed to press 1 Oct 81) pp 27-28

[Article by Ye. P. Antonets, B. M. Stepanov and V. A. Fabrikov]

[Text] Certain applications of powerful pulsed lasers require an undistorted wavefront that is close to planar. Such a wavefront is produced when a laser operates on the TEM_{00} mode alone. Tuning of lasers to single-mode operation is checked by analyzing diffraction patterns from the simplest apertures. In this paper, an investigation is made of the feasibility of using a diffractometer with thermomagnetic registration of pulsed emission for these purposes.

Cw gas lasers are tuned to single-mode lasing with radiation of the lower TEM_{00} mode by comparing the measured diffraction pattern of the investigated emission on a circular aperture with the calculated Airy pattern [Ref. 1, 2]. Tuning precision is evaluated from the degree of swelling of the first maximum. Amplitude distribution in the Airy pattern is described by the formula

$$E(r) = \gamma E_0 \frac{r_0}{r} J_1\left(1{,}22 \frac{r}{r_1}\right), \qquad (1)$$

where γ is an immaterial phase multiplier; E_0 is the field amplitude of the incident wave in the plane of the diaphragm; r_0 is the radius of the diaphragm; r is the modulus of the radius vector $\vec{r}$ of the observation point in the focal plane of the objective lens; $J_1(x)$ is a first-order Bessel function of the first kind of argument x; $r_1 = 1.22f/kr_0$ is the radius of the first dark ring in the Airy pattern; f is the focal length of the objective lens that shapes the diffraction pattern; $k = 2\pi/\lambda$ is the wave number.

Energy distribution in the diffraction pattern of continuous radiation is measured by a photomultiplier that is mechanically displaced in the transverse plane [Ref. 1]. The photomultiplier is used to ensure the dynamic measurement range necessary for analyzing distortion of the Airy pattern. However, the procedure based on using a scanning device with photomultiplier is not applicable in the pulsed mode of laser operation. The diffraction pattern to be measured must be first recorded on a medium that has a sufficient dynamic range, resolution and sensitivity to radiation in the investigated wavelength band.

We used magnetic films with strip domains as the recording mediu. Registration was done at an emission wavelength of 1.06 μm. However, the thermomagnetic method used for recording on these films [Ref. 3] enables registration of diffraction patterns in the longer-wave band as well. The recording range offered by the films ($E_{max}/E_{min} \cong 30$) is not wide enough for simultaneous Airy-pattern registration of the zero maximum with respect to which the degree of swelling of zero rings is found, and the first maximum that serves as a reference point. This explains why the diffraction pattern from two holes of the same diameter is chosen instead of the Airy pattern as a gage for diagnosing mode purity of pulsed laser emission. The ratio of the first maximum to the zero maximum in this pattern is close to 0.5 for a distance between the centers of the holes of $4k_0$. This is considerably greater than in the Airy pattern, where this ratio is 0.0175. The distance between the centers of the holes can be selected differently as well, and with increasing distance there is an increase in the ratio of the first maximum to the zero maximum.

As we know, the Fraunhofer diffraction pattern is the Fourier transform of the aperture function with spatial frequency $\vec{\omega} = k\vec{r}/f$. In the case of two holes of identical shape, the aperture function $\psi(\vec{r})$ is written as [Ref. 4, 5]

$$\psi(\vec{r}) = g(\vec{r}) \ast \{\delta(\vec{r}+\vec{a}) + \delta(\vec{r}-\vec{a})\}, \qquad (2)$$

where $g(\vec{r})$ is the aperture function of one hole; $\vec{a}$ and $-\vec{a}$ are the radius vectors of the centers of the holes; $\delta(\vec{r})$ is the Dirac delta function; the symbol $\ast$ denotes the operation of convolution of two functions with respect to variable $\vec{r}$. In the given case

$$g(\vec{r}) = \mathrm{cire}\left(\frac{r}{r_0}\right) = \begin{cases} 1 & r < r_0 \\ 0 & r > r_0, \end{cases}$$
$$\vec{a} = \vec{i}a = \vec{i}2r_0,$$

$\vec{i}$ is the unit vector along the x-axis joining the centers of the holes. The Fourier transform of the convolution is equal to the product of the Fourier transforms of the convoluted functions. From (1) and (2) with consideration of the formula of Fourier transformation for amplitude distribution in the diffraction pattern from two apertures we get

$$E(x, y) = 2\gamma E_0 \frac{r_0}{r} J_1\left(1{,}22\frac{r}{r_1}\right) \cos\frac{kr^2 r_0}{f}, \qquad (3)$$
$$\text{where } r = \sqrt{x^2+y^2}.$$

This distribution serves as a gage in diagnosing laser radiation in the proposed method. Experiments in diffraction pattern recording on magnetic films used a neodymium-doped glass laser with pyroceramic diffuse pumping reflector and a passive modulator based on dyes. The diameter of the holes in the aperture diaphragm was 0.6 mm, and the distance between centers of the holes was 1.2 mm. Recording and visualization of the diffraction patterns were done by a procedure described in Ref. 3. A preliminary check on tuning of the laser to operation close to single-mode was done by recording the radiation on photosensitive paper.

Fig. 1 shows a diagram of a magnetic-film diffractometer, where 1 is a pulse laser; 2 is a beam expander; 3--is a screen with diaphragms; 4 is the magnetic film;

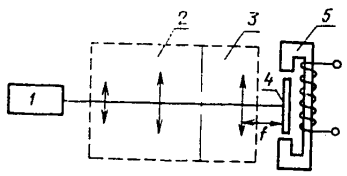

Fig. 1

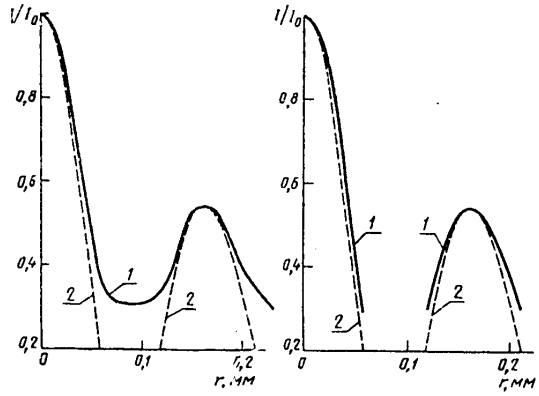

a b

Fig. 2

5 is the reco ing device. Fig. 2 shows the intensity distribution along the x axis in diffr ion patterns recorded on films with multimode (a) and single-mode (b) laser emi n (curve 1--experiment; curve 2--calculation). In the given case, single-mode radi ion is understood to be emission in which the main part of the energy is concentrated in the lower mode that produces an axisymmetric spot in the recording on photographic paper. Single-mode operation was achieved by using a selecting diaphragm with aperture diameter of less than 2 mm. Multimode emission that produced a spot of diffuse shape on the photographic paper was achieved by increasing the diameter of the diaphragm to 4-5 mm. This spot had a structure in which the traces of higher spatial modes could be clearly delineated.

In the diffraction patterns recorded on magnetic tape the position of the maxima and minima coincided with the calculated values determined from Ref. 3. The relative levels of the maxima also coincided, but the depths of the minima differed strongly. The ratio of the radiation intensity in the first minimum of the diffraction pattern to the intensity in the zero maximum in multimode radiation was about 30%. In single-mode operation, this ratio is less than 0.03, i. e. it lies beyond the limits of the dynamic range of the films. The depth of the minimum of the recorded diffraction pattern varies with a change in diameter of the selecting diaphragm close to 2 mm, and may serve as an indicator of the accuracy of tuning the optical system to single-mode operation. The sensitivity of the method as estimated from the relative power of higher transverse modes is close to 10%.

REFERENCES

1. Heineman, H., Redline, H., TIIER, Vol 53, No 88, 1965.

2. Hurd, G., "Izmereniye lazernykh parametrov" [Measurement of Laser Parameters], Moscow, "Mir", 1970.

3. Klyuchkin, L. M. et al., "Fotografirovaniye na magnitnyye plenki" [Photography of Magnetic Films], Moscow, Atomizdat, 1971.

4. Williams, R. P., "Transform Approach to Paraxial Optics", CONTEMPORARY PHYSICS, Vol 15, 1974.

5. Papulis, A., "Teoriya sistem i preobrazovaniy v optike" [Theory of Systems and Transformations in Optics], Moscow, "Mir", 1971.

6610
CSO: 1862/38

UDC 535.853.5:621.375.826

INSTRUMENT FOR MEASURING LASER EMISSION WAVELENGTHS

Moscow IZMERITEL'NAYA TEKHNIKA in Russian No 10, Oct 81 (signed to press 1 Oct 81) pp 28-29

[Article by L. Ya. Gustyr', V. N. Puchkov, A. K. Toropov and Yu. A. Fedorov]

[Text] To measure laser radiation wavelength, facilities have been developed in which (as for example in Ref. 1, 2) continual refinements are made in the value of the wavelength found by preliminary measurement with a low-accuracy monochromator, or a method of comparison with the wavelength of a reference laser is used [Ref. 3 4]. Efforts to get high accuracy in measurements (the error of wavelength measurement in Ref. 1 is $\pm 3.5\ 10^{-6}$ μm, and in Ref. 4 it is $\pm 10^{-7}$ μm) in realization of these methods, and to provide capabilities for operation with pulsed and cw radiation over a wide spectral range lead to development of unique measurement facilities. In many practical cases the use of such facilities is inadvisable.

In this article a device is described that is intended for automatically checking the wavelengths of tunable cw lasers in different technological applications, as well as in developing and making such lasers. The instrument is based on an interference method of getting successive approximations of the wavelength by using a scanning Fabry-Perot interferometer with known distance between mirrors. The essence of the method is as follows. The fractional part ε of the interference order is determined from the magnitude of the scanning interval from its beginning to the closest transmission maximum of the interferometer. Then the preliminary value $\lambda_{пр}$ of the wavelength to be measured is determined from the size of the interval between two adjacent interference maxima. The integral part K of the interference order is found from the equation

$$\frac{2L-\varepsilon}{\lambda_{пр}}+0{,}5=K+\delta, \qquad (1)$$

(by dropping the fractional part δ), where L is the length of the interferometer, and the refined value of the wavelength is determined from the formula

$$\lambda=\frac{2L-\varepsilon}{K} \qquad (2)$$

Addition of the fraction 0.5 to the first member of equation (1) allows us to replace the operation of rounding off the resultant number with the operation of separating the integral part of the number, which is an operation that can be done in a computer.

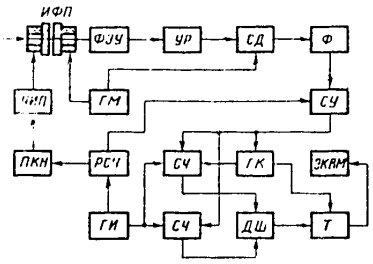

The figure shows a block diagram of the instrument for measuring wavelengths. The laser emission whose wavelength is to be measured is directed at a multi-beam scanning plane-parallel Fabry-Perot interferometer *ИФП*. Both mirrors of the interferometer are fastened on piezoelectric elements. A linearly varying voltage of triangular shape with frequency of 1 Hz is sent to the piezodrive of one of the mirrors. This voltage is formed by the principle of digital-analog conversion by a channel consisting of pulse generator *ГИ*, reversible counter *РСЧ*, code-to-voltage converter *ПКН* and controllable power supply *УИП*. The clock pulses from the pulse generator are counted by the binary 11-digit reversible counter. The parallel code from the counter outputs is sent to the 11-digit code-to-voltage converter. When the reversible counter is filled with ones or zeros, reversal takes place automatically, and a step voltage of triangular shape is formed at the output of the code-to-voltage converter. The number of steps on the leading and trailing edges of this voltage is the same, and is equal to the number of pulses coming to the input of the reversible counter from the output of the pulse generator in one half-period of scanning of the Fabry-Perot interferometer. In the controllable power supply, the amplitude of the scanning voltage is boosted to the requisite value for scanning two orders of the interference pattern.

The use of a digital-analog converter in the scanning voltage shaper channel ensures rigid one-to-one correspondence (forced synchronization) between the number of pulses and the increment in length of the Fabry-Perot interferometer. The measure of the increment in length of the interferometer by values equal to the fractional ε and integral $\lambda_{пр}$ parts of the interference order is the number of pulses that will fit from the beginning of a scan to the first interference maximum and between two adjacent maxima respectively, which is recorded by counters *СЧ*. The distribution of pulses between these counters is handled by control circuit *СУ* under condition that optical radiation is acting on the input of the device.

The interference pattern after the Fabry-Perot interferometer is registered by photomultiplier *ФЭУ*. The instant that the mirror passes through the maximum is determined by differentiating the signal with respect to the first derivative on the modulation frequency. To do this, an audio frequency signal (5 kHz) is sent to the piezodrive of the second mirror from oscillator *ГМ*. Resonant amplifier *УР* is tuned to the first harmonic of the modulating frequency. The first derivative of the signal shape is sent from the output of synchronous detector *СД* to shaper *Ф* that generates a short pulse to trigger the control circuit *СУ* at the instant when the derivative passes through zero. Filling of one of the counters *СЧ* begins at the beginning of each scanning period, and ends upon passage through the first interference maximum (measurement of ε). At this instant, the second of counters *СЧ* is energized, and it is de-energized at the instant of transition through the second maximum (measurement of $\lambda_{пр}$). The counter content is transcribed by translator *Т* via decoder *ДШ* into store *ЭКВМ*. The sequence of transcription is determined by command generator *ГК* which is also controlled by *СУ*.

Solution of (1) and (2) is accomplished by a program that is compiled for the store that is used, and that is introduced into the store beforehand. Solution is done

automatically by commands from ПК. The value of the measured wavelength is shown digitally on the display of the store.

The wavelength measuring device uses the Iskra-123 store. Information input to the device is through an auxiliary built-in plug to which wires are led directly from the keyboard contacts. Binary information is transmitted thorugh a decoder that converts binary-decimal code to decimal code. The translator is based on RES-55 relays that simulate keyboarding. With this setup, the maximum rate of information transmission is 100 decimal digits per second.

This type of data input through a keyboard does not interfere with use of the store for extraneous calculations at the instant of cessation of running measurements, and upon disconnecting the automation device. In principle, such an arrangement can be used with any store regardless of its specific structure or element base.

In calculating the value of the wavelength, consideration is taken of the nonlinearity of the piezodrive. The dependence of the overall elongation ΔL of the piezoceramic elements of the drive on the applied voltage, or what amounts to the same thing, the number of pulses n of generator ГИ, is completely satisfactorily approximated by a cubic polynomial

$$\Delta L = an^3 + bn^2 + cn, \qquad (3)$$

where a, b, c are the coefficients of the polynomial that are determined when graduating the meter with respect to radiation of known wavelength. Polynomial (3) with defined coefficients is also introduced into the program of calculations of computer store ЭКВМ.

For operation of the device in the range of 0.4-1.1 μm, the Fabry-Perot interferometer uses silvered mirrors with reflectivity of 0 98 and an FEU-62 photomultiplier. To get unambiguous information, the length of the interferometer is selected from the condition that its region of dispersion must exceed the absolute value of preliminary wavelength determination. The interval between two adjacent interference maxima is determined in the device by the method described above with relative error of 0.02, and consequently the error of determining $\lambda_{пр}$ on the short-wave boundary of the spectral band ($\lambda = 0.4$ μm) is $0.02\ \lambda/2 = 0.004$ μm. The interferometer length calculated from this value should not exceed 20 μm. An interferometer is installed in the device with patently greater dispersion region ($L \cong 14$ μm); certification of its length is by the interference method of Ref. 5.

The error of the instrument was determined in experimental measurements of known wavelengths of emission of He-Ne, He-Cd and certain lines of He-Ar lasers. The relative error of the instrument determined in this way was 10^{-4}. Time of one measurement was 1 s.

In structure, the device consists of an optical module, three electronic modules (including power supplies) made in standard casings of the Nadel type, and the Iskra 123 computer store. The optical module of the instrument, including the interferometer and photomultiplier, is accommodated on a pedestal with aligning devices for bringing its optical axis into registration with the laser emission axis.

Instability of radiation power of the investigated laser leads to chaotic noises in the interference patterns registered by the photomultiplier. Studies showed that when noises amount to more than 10% of the useful signal amplitude, there may be malfunctions in shaper Φ. An optical isolater is used to prevent the influence of optical feedback between the interferometer and laser cavity, which can also lead to interruptions of operation.

REFERENCES

1. Drozhbin, Yu. A. et al., IZMERITEL'NAYA TEKHNIKA, No 6, 1980.

2. Byer, R. L. et al., "Laser Spectroscopy 3", Proc. 3-rd Int. Conf., Jackson Lake Lodge, Wyoming, 1977, Berlin e. a., 1977.

3. Snayder, D. D., KVANTOVAYA ELEKTRONIKA, Vol 5, No 8, 1978.

4. Salimbeni, R., Pole, R. V., OPT. LETT., Vol 5, No 2, 1980.

5. Gustyr', L. Ya. et al., Soviet Patent No 748125, BYULLETEN' IZOBRETENIY, No 26, 1980.

6610
CSO: 1862/38

UDC 535.87+621.373:535

EFFECT OF TEMPERATURE ON PHASE ANISOTROPY OF DIELECTRIC LASER MIRRORS

Leningrad OPTIKA I SPEKTROSKOPIYA in Russian Vol 51, No 4, Oct 81 (manuscript received 23 Jun 80) pp 724-725

[Article by V. G. Gudelev and V. M. Yasinskiy]

[Text] Multilayered dielectric laser mirrors that work with oblique incidence of radiation have linear phase anisotropy [Ref. 1] that has a considerable effect on the polarization-frequency characteristics of precision measurement laser systems (ring lasers, polarization interferometers and so on). Instability of the phase anisotropy of the mirrors due to heating during the working process may be detrimental to the characteristics of such systems.

To study the influence of temperature on phase anisotropy of mirrors, the intracavity frequency method of measuring anisotropy has been used [Ref. 2]. The measurements were made in an amplitude-isotropic corner-reflector laser cavity. Under ordinary conditions the sensitivity of measurement of phase anisotropy by such a method is limited by instability of cavity length, modal composition and radiation power, and does not exceed 10^{-3} rad, which precludes observation of temperature influence on phase anisotropy of mirrors [Ref. 3]. To improve measurement sensitivity, the laser was operated on a single transverse mode. A transverse magnetic field ($B \cong 7$ mT) was superimposed on the active element of the laser [Ref. 4] to stabilize lasing of two orthogonally linearly polarized waves with a slight frequency difference proportional to the linear phase anisotropy of the mirror Δ. To compensate for amplitude anisotropy of the mirror, a weak partial polarizer was placed in the cavity. To stabilize the frequency of laser radiation with respect to the center of the amplification line, an AFC system described in Ref. 5 was used. A high-voltage current stabilizer with dynamic output impedance of ~400 MΩ was used for supply of the active element. These steps improved the sensitivity of measurements of phase anisotropy to 10^{-5} rad with intermode range of 315 MHz, which corresponds to instability of the difference frequency of ±1 kHz. Slight misalignments of the cavity and fluctuations of air density that arise during measurements due to heating of the investigated mirror reduced the sensitivity of measurements of phase anisotropy to 10^{-4} rad at a mirror temperature of ~60°C

An investigation was made of the temperature dependence of phase anisotropy of dielectric mirrors made by thermal sputtering of ¼-wave layers of ZnS and MgF_2 on a K8 glass backing. Measurements were done at an angle of incidence of 30° on a lasing wavelength of 1.153 μm in the temperature range of 25-55°C.

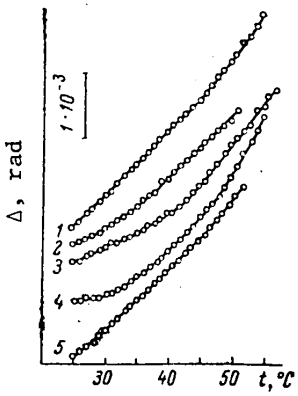

Temperature dependence of phase anisotropy of mirrors with different initial anisotropy. Δ, rad: 1-- 0.038; 2--0.033; 3-- -0.026; 4-- -0.033; 5-- -0.035

The figure shows the resultant curves for phase anisotropy of five mirrors of different manufacturing batches, having different initial anisotropy $\Delta=\delta_s-\delta_p$ at 25°C, where δ_s and δ_p are phase jumps that arise upon reflection of s- and p-polarized waves from the mirror coating. For the sake of convenience in comparison, all curves are placed in a row. It can be seen from the results that phase anisotropy of multilayered dielectric mirrors is appreciably dependent on temperature. The average slope of the dependence of anisotropy of the mirror on temperature is 10^{-4} rad/K. For a qualitative explanation of the behavior of these curves, it is convenient to use the theoretical dependence of phase anisotropy of a mirror on the parameter λ_0/λ given in Ref. 1, where λ_0 is the wavelength for which the layers of the mirror are ¼-wave layers, and λ is laser emission wavelength. When the mirror is heated, there is a change in optical thicknesses of the layers, which is equivalent to displacement of λ_0, and to a corresponding change in phase anisotropy of the mirror. Therefore, when λ_0 is a linear function of temperature, the temperature dependence of Δ is also linear. Quantitative comparison of experimental results with calculation is difficult because of a lack of reliable data on thermo-optical constants of films of sputtered materials. Besides, the coefficients of refraction of the layers due to porosity depend on the technology of mirror manufacture, i. e. on the packing density of the sputtered material and the degree of filling of pores with moisture [Ref. 6]. This apparently explains the slight differences in the behavior of curves for different mirrors.

Thus, these measurements enable us to detect and study the influence of temperature on the phase anisotropy of dielectric laser mirrors that work with oblique incidence of radiation.

REFERENCES

1. Rybakov, B. V., Skulachenko, S. S., Chumichev, R. F. and Yudin, I. I., OPTIKA I SPEKTROSKOPIYA, Vol 25, 1968, p 572.

2. Kotova, A. I., Rubanov, V. S., in: "Gazorazryadnyye pribory. Materialy tret'yey Vsesoyuznoy nauchno-tekhnicheskoy konferentsii po elektronnoy tekhnike" [Gas-Discharge Devices. Materials of the Third All-Union Scientific and Technical Conference on Electronics], Moscow, No 2(18), 1970, p 35.

3. Gudelev, V. G., Zuykova, N. V., Shchevtsova, A. I., ZHURNAL PRIKLADNOY SPEKTROSKOPII, Vol 30, 1979, p 735.

4. Morris, R. H., Ferguson, J. B., Warniak, J. S., APPL. OPT., Vol 14, 1975, p 2808.

5. Gudelev, V. G., Yasinskiy, V. M., PRIBORY I TEKHNIKA EKSPERIMENTA, No 1, 1980, p 215.

6. Ogura, S., Sugawara, N., Hiraga, R., THIN SOLID FILMS, Vol 30, 1975, p 3.

6610

CSO: 1862/48

UDC 535.214

DECELERATION OF ATOMS AND REARRANGEMENT OF ATOMIC VELOCITIES BY RESONANT LASER RADIATION PRESSURE

Moscow IZVESTIYA AKADEMII NAUK SSSR: SERIYA FIZICHESKAYA in Russian Vol 45, No 6, Jun 81 pp 1047-1058

[Article by V. I. Balykin and V. G. Minogin, Institute of Spectroscopy, USSR Academy of Sciences]

[Text] Introduction

The main features of movement of atoms in a resonant light field are determined by the velocity dependence of the force of light pressure and the velocity diffusion tensor [Ref. 1-6]. Both the force and the diffusion tensor in the case of a monochromatic traveling wave are resonant, reflecting the resonant interaction between atom and light field. A direct consequence of the resonant nature of the force and tensor of velocity diffusion is that the force and diffusion change the velocities of atoms mainly in the narrow range $\Delta v \sim \Delta\omega/k$ determined by the width of the absorption line $\Delta\omega$. In this connection, while the diffusion of atomic velocities does not depend on the direction of wave propagation and symmetrically broadens the velocity distribution of resonant atoms, the force of light pressure, singling out a direction in space, forms an asymmetric distribution. As a result, in the case where atoms propagate along the light wave the center of the velocity distribution is shifted into the region of velocities that are greater than the resonant velocity, while in the case of contrary propagation the center of this distribution is shifted toward lower velocities. At the same time, due to the nonlinear dependence of the force of light pressure on velocity, the displacement of the velocity distribution is always accompanied by narrowing, i. e. by monochromatization of atomic velocities.

This redistribution of atomic velocities is of interest in the case of deceleration of atomic beams by an opposed light field [Ref. 7, 8] since slow monochromatic atomic beams are ideal objects both for direct use in experimental practice and for injection into atomic traps [Ref. 9-11].

Two methods can be pointed out for decelerating atoms by resonant laser emission. One of them uses scanning of the frequency of laser radiation along the Doppler contour of the atomic transition. In this case the effect of the radiation on the atoms is due to continuous tuning of the laser emission frequency to the resonant frequency of the atom being decelerated. Such a method can be used for

generating pulses of cold atoms. The other method of radiative deceleration, which enables generation of steady-state streams of cold atoms, is head-on exposure of atomic beams to fixed-frequency laser emission. This method was recently analyzed for the ideal case of a monochromatic traveling wave in Ref. 8.

Our paper gives experimental and theoretical results of an investigation of the two methods mentioned above for radiative deceleration of atoms. All studies were done in a beam of sodium atoms interacting with laser radiation on transition $3S_{1/2}-3P_{3/2}$.

1. Formulation of the Problem

As a basis for our experimental study of the evolution of atomic velocities, we have chosen registration of the deformation of velocity distribution with respect to change of intensity of fluorescence of atoms that are in resonance with laser emission. When atoms are excited on a transition with frequency ω_0 by a head-on light wave with frequency $\omega < \omega_0$, the fluorescence signal is proportional to the number of atoms with velocity $v_{рез} = -(\omega - \omega_0)/k$. Therefore the change in the fluorescence signal directly reflects the change in the distribution function of the atoms $w(z, v, t)$ at longitudinal velocity $v_z = v = v_{рез}$. A more direct experiment would be to use a probe light beam to excite fluorescence and record the latter both at different distances from the point of entry of atoms into the decelerating laser field, and at different instants of time. This method can give adequate information on the change in distribution function of the atoms $w(z, v, t)$. Because of limitations on experimental capabilities, we chose a simpler arrangement (Fig. 1), in which the fluorescence detector was situated at a fixed distance $z = l$ from the source of the atomic beam, and the fluorescence itself arose due to the same radiation that was used for decelerating the atoms.

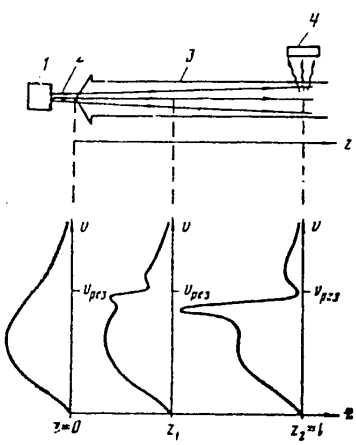

Fig. 1. Deformation of velocity distribution of atomic beam exposed to a head-on resonant light wave: 1--source; 2--atomic beam; 3--laser beam; 4--detector

The arrangement with scanning of the frequency of laser radiation enabled observation of the contour of fluorescence of the atomic beam, which determines the velocity distribution of the atoms at point $z = l$. At laser emission intensity $I_л \ll I_s$ (where I_s is the saturation intensity), the action of the force of light pressure on translational motion of atoms is insignificant. In this connection, when $I_л \gg I_s$ the curve for the fluorescence signal as a function of laser emission frequency copies the velocity distribution of the initial atomic beam. At intensity $I_л \gg I_s$, the radiation frequency dependence of the fluorescence signal represents the velocity distribution deformed by the laser emission. The degree of deceleration and monochromatization of the atomic beam can be determined by comparing two distributions with low and high intensity $I_л$.

In the arrangement with fixed frequency of laser emission, all information on the evolution of velocity distribution is contained in the behavior of fluorescence

Intensity as a function of the time of exposure. The curve describing this behavior has two distinguishing features. First, because of the drift of atoms into the region of lower velocities, it is a decreasing function of time. Secondly, the drop in the curve is always only to a certain level since for a fixed interaction length $\Delta z = l$ the velocity distribution is deformed to a certain limit.

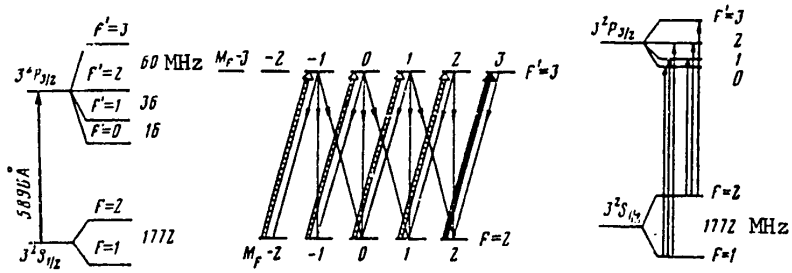

a b c

Fig. 2. Diagrams of cyclic interaction of sodium atoms with laser radiation: a--energy diagram of hyperfine structure of the D_2-line of the sodium atom; b--optical orientation of atom by circularly polarized laser emission; c--resonant transition in two-frequency excitation of atom

These methods of studying deformation of velocity distribution can in principle be applied to any atoms, assuming that they are made to interact cyclically with the light field. In the case of sodium atoms, the cyclicity of interaction can be achieved either by using circularly polarized radiation for optical orientation of the atoms, as was done in Ref. 7 (see also Ref. 12), or by exciting the atoms with a two-frequency light field (Fig. 2). The latter version is preferable since for any polarizations of laser emission it provides reliable excitation of atoms from any sublevel F = 1, 2 of the hyperfine structure of the ground state $3S_{1/2}$. However, it can be used only in the arrangement with fixed frequency of laser radiation since it is rather difficult to realize simultaneous scanning of two laser modes with fixed distance between them. In our experiments we used two axial modes of a cw dye laser as the two-frequency light field. One of the modes excited sodium atoms on transition $3S_{1/2}(F=1)-3P_{3/2}$, and the other excited atoms on transition $3S_{1/2}(F=2)-3P_{3/2}$ (Fig. 2c).

Clearly, the use of the two-frequency light field in principle could have altered the above-described simple pattern of deformation of velocity distribution since two light waves can act on different velocity groups of atoms. Actually, at the temperatures of the source of atoms that we used, the overlap of absorption lines on transitions $3S_{1/2}(F=1)-3P_{3/2}$ and $3S_{1/2}(F=2)-3P_{3/2}$ could be disregarded. In this connection, the low-frequency mode of laser radiation with frequency ω_1 excited atoms only from state F = 2, while the high-frequency mode with frequency $\omega_2 = \omega_1 +$ 1772 MHz excited atoms almost exclusively from state F = 1. Since in addition the frequency interval between modes $\omega_2 - \omega_1$ coincided with the frequency difference

of the two resonant transitions $\omega_{20}-\omega_{10} = 1772$ MHz, both modes acted on the same velocity group of atoms, and deformed the velocity distributions on levels F = 1,2 in the same way.

2. Experimental Facility

A diagram of the experimental facility is shown in Fig. 3. It consists of the following principal components: cw dye laser (1), a cell with sources of main (11) and reference (10) atomic beams, a system (5, 6) for recording the signal of fluorescence from the atoms (photomultiplier, oscilloscope), laser frequency scanning

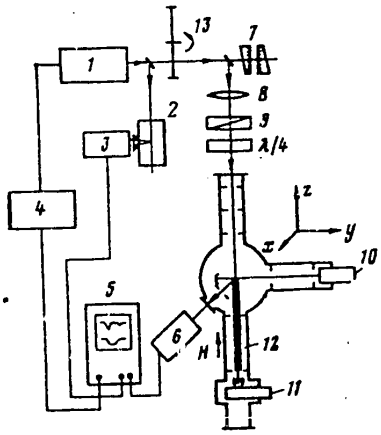

Fig. 3. Diagram of experimental setup: 1--dye laser; 2--control cell with sodium; 3, 6--photomultipliers; 4--laser frequency scanning module; 5--oscilloscope; 7--interferometer; 8--lens; 9--polarizer; 10, 11--ovens of atomic beams; 12--region of interaction of atomic and laser beams; 13--radiation interrupter

module (4), control cell with sodium vapor (2), and a system for monitoring the frequency of the laser and the scanning mode. The polarizer (9) and ¼-wave plate produced circularly polarized radiation in single-mode operation of the laser. The mechanical interrupter (13) ensured switching of laser radiation in the two-frequency mode of operation.

A Spectra-Physics 580A laser was used to get single-mode scanned radiation. A system with scanning rate of 1400 MHz/ms was made on the basis of the 481A scanning module of this laser.

The two-frequency lasing mode was achieved in the following way. The optical length of the laser cavity was selected such that the spacing between components of the hyperfine structure of the ground state of the sodium atom was a multiple of the spacing between frequencies of adjacent axial modes of the laser cavity:

$$\Delta\omega_c = \Delta\omega_{hfs}/m,$$

where m = 1, 2, 3 . . . . In our experiment, $\Delta\omega_c = 354$ MHz, m = 5. The lasing spectrum was prenarrowed to about 2 GHz by using three Fabry-Perot etalons inside the optical cavity. The effect of spatial burnout of inversion [Ref. 13] and a thin absorbing metal film inside the cavity (Troitskiy collector) [Ref. 14] were used to isolate from among the six or seven axial modes emitted by the laser two that were separated by distance $\Delta\omega_{hfs} = 1772$ MHz, and to suppress the remaining modes.

The dye laser radiation was sent to a vacuum cell with the atomic beam source (Fig. 3). The chamber was evacuated to a pressure of $p = 5 \cdot 10^{-6}$ mm Hg. The atomic beam was collinear with the laser beam. Its aperture was determined by a set of irises, the maximum diameter of the irises being greater than that of the laser beam; therefore the zone of interaction of laser radiation with the atomic beam was determined by the aperture of the laser beam. The diameter of the laser beam near the output aperture of the source of atoms was equal to $d_1 = 0.9$ mm, and in the region of fluorescence signal registration $d_2 = 1.1$ mm. The length of the interaction region was 38 cm. The working temperature of the atomic beam source $t = 300°C$.

When the mechanical interruptor (13) was used, the time of switching of the laser radiation was $\tau_{sw} = 12$ μs, which is appreciably less than the average time of flight of the atoms through the interaction space ($\tau_{fl} = 0.4$ ms). The duration of exposure of the atomic beam with the modulator open was 2.5 ms. The region of intersection of the main and reference atomic beams was imaged on the photomultiplier cathode. The fluorescence signal could be recorded both from atoms of the main atomic beam and from the atoms of the reference beam, or both together. The main atomic beam was collinear with the laser beam, and the reference beam was perpendicular. The reference atomic beam was for the purpose of absolute and relative calibration of the frequency scale. A weak magnetic field of about 1 gauss was applied along the laser beam in the cell. This field prevented redistribution of the populations of magnetic sublevels by scattered light.

3. Results of Experiments

A. Scanning of laser emission frequency

In recording deformation of the velocity distribution of the atomic beam with respect to a change in absorption line shape (fluorescence line shape), frequency-tunable circularly polarized single-mode laser radiation was used. Since in this case all information on the change of velocity distribution is contained in the shape of the fluorescence line, our principal interest was in comparing two curves for fluorescence intensity as a function of laser emission frequency: one corresponding to the velocity distribution of the initial beam, and the other corresponding to the deformed velocity distribution. The first curve could be obtained by scanning the laser frequency along the absorption line contour under two fundamentally different sets of experimental conditions. In the first instance the absorption line contour corresponding to the undeformed velocity distribution could be recorded at weak laser intensity ($I_Л \ll I_S$) where the influence of the force of light pressure on the motion of atoms is negligible. In the second instance this same contour could be produced at moderate radiation intensities ($I_Л \sim I_S$) if the rate of scanning $d\omega_Л/dt$ of the emission frequency was sufficiently slow. Actually, for appreciable deformation of the velocity distribution by the force of light pressure

$$F = -\hbar k \gamma \frac{G}{1 + G + (\Omega(t) + kv)^2/\gamma^2}, \qquad (1)$$

where $\hbar k$ is photon momentum, 2γ is the width of the absorption line, $G = I_Л/I_S$ is the saturation parameter, and $\Omega(t) = \omega_Л(t) - \omega_0$ is the mismatch of the emission frequency relative to the frequency of the atomic transition, at each instant the following condition must be met:

$$\omega_л(t) = \omega_0 - kv, \qquad (2)$$

that maximizes force (1). Differentiating (2) with respect to time and using (1), we find from condition (2) that the optimum scanning rate is

$$\frac{d\omega_z}{dt} = k\gamma v_r \frac{G}{1+G} \approx \frac{\hbar k^2 \gamma}{M} \approx 1600 \text{ MHz/ms}. \qquad (3)$$

Thus we would expect the most appreciable deformation of velocity distribution at scanning rate (3), while at lower scanning rates the shape of the absorption line ought to be little different from the undeformed line shape.

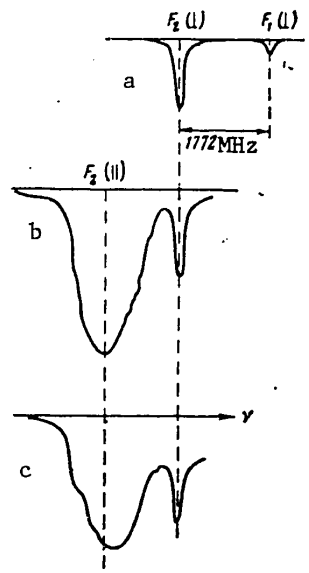

Fig. 4

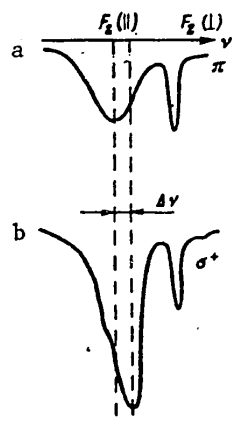

Fig. 5

Fig. 4. Absorption lines of atoms: a--in perpendicular atomic beam; b, c--in perpendicular and parallel atomic beams. Frequency scanning rates: b--46 MHz/ms, c--370 MHz/ms. Intensity of laser radiation 50 mW/cm^2

Fig. 5. Absorption line shape in parallel and perpendicular atomic beams: a--excitation by linearly polarized emission; b--excitation by circularly polarized emission

Experimental absorption line shapes are shown in Fig. 4, 5. Fig. 4a shows the contour of the absorption line of atoms in a perpencidular beam, which was used for calibrating the frequency scale. The two absorption maxima correspond to hyperfine broadening of the ground state of the sodium atom. The position of frequency maximum $F_2(\perp)$ corresponds to the rate of absorption of atoms from a parallel atomic beam with zero velocity.

Fig. 4b shows joint contours of absorption of atoms in perpendicular and parallel beams at a slow rate of scanning of laser emission frequency (46 MHz/ms). At such

a scanning rate the effects of resonant interaction cannot influence the motion of atoms, and the curves are the absorption contours of the atoms in both beams.

As an example of the influence of the force of light pressure on the motion of atoms, Fig. 4c shows line deformation in a parallel beam at a scanning rate of 370 MHz/ms. When this line is compared with that in Fig. 4b, it can be seen that the maximum of the absorption line is shifted into the region of frequencies corresponding to slower atoms.

Fig. 5 shows the shapes of the absorption line of atoms in parallel and perpendicular beams at laser radiation frequency scanning rate of $\dot{\omega}_{\Pi} = 370$ MHz/ms for different polarizations of laser radiation.

In the case of linear (π) polarization of radiation under the conditions of our experiment, multiple interaction of an atom with radiation is impossible because of the drift of atoms to sublevel F = 1. With a change to emission with circular polarization (σ^+), optical orientation of the atom takes place, and as a result the atom may interact repeatedly with radiation. This should lead to development of an appreciable force of light pressure on atoms in the beam, i. e. to deceleration of atoms, which is demonstrated by displacement of the line maximum, the maximum displacement being equal to $\frac{1}{4}v_{pr}$ (Fig. 6).

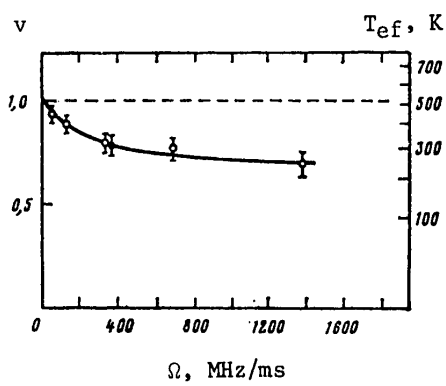

Fig. 6. Displacement of the absorption line center in a parallel atomic beam as a function of laser frequency scanning rate (black dots correspond to Fig. 4c). Scale to the right is effective temperature of atoms interacting with radiation, which was determined with respect to the maximum of the absorption line

The longitudinal temperature of atoms was determined in terms of the rms velocity of the group of atoms:

$$T = \frac{M}{2k_B}\langle (v - \langle v \rangle)^2 \rangle, \qquad (4)$$

where

$$\langle v \rangle = \frac{1}{N_0}\int_0^\infty vN(v)\,dv, \quad N_0 = \int_0^\infty N(v)\,dv,$$

<v> is the mean velocity of atoms, N(v) is the velocity distribution of atoms that results from interaction with radiation. The maximum change of temperature of atoms during interaction with radiation was determined from (4) by numerical integration. The temperature change was 73°C.

The main factors that prevent more effective deceleration and monochromatization (cooling) of atoms in this experiment are discussed in detail in Ref. 7.

B. Fixed frequency of laser emission

Fig. 7 [photo not reproduced] shows the measured dependence of the fluorescence signal of atoms on the time of interaction with laser emission at a radiation intensity of $I_л = 0.42$ W/cm^2 (saturation parameter $G = I_л/I_s = 42$, where $I_s = 0.01$ W/cm^2 is saturation intensity). The time behavior of fluorescence intensity is in complete accord with that expected on the basis of qualitative ideas. In the case of rapid switching of laser emission (the lower horizontal lines correspond to a zero fluorescence signal), fluorescence reaches the maximum value corresponding to undeformed velocity distribution. Then deformation of the velocity distribution (Fig. 1) accompanied by a reduction in the fraction of resonant atoms leads to a drop in the fluorescence signal. The latter takes place over a characteristic time of deformation of distribution that coincides with the time of flight of atoms through the light beam. On the oscillogram of Fig. 7 the time of fluorescence signal reduction is 0.5 ms, which coincides with good accuracy with the mean time of flight of atoms through the interaction space. After the mean time of flight, the fluorescence signal stabilizes on the level corresponding to the deformed distribution.

As was pointed out in Secion 1, the amount of change in the fluorescence signal determines the extent of deformation of the absorption line of the atoms, and hence the degree of deformation of velocity distribution of the atomic beam. We measured

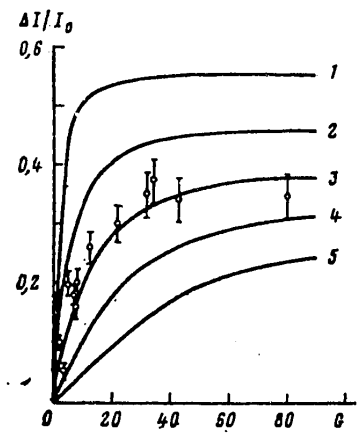

Fig. 8. Relative change of the fluorescence signal of sodium atoms as a function of intensity of laser radiation. Solid curves show the calculated behavior at different Δω: 1--30; 2--50; 3--70; 4--90; 5--110 MHz

the dependence of the change in the fluorescence signal on the intensity of laser radiation. The results of the measurements are shown by the points on Fig. 8. At an emission intensity of up to 800 mW/cm^2 ($G = 80$) used in the experiment, the relative change in the fluorescence signal reached $\Delta I/I = 0.36$.

4. Evolution of Atomic Velocities at Fixed Frequency of Laser Emission

The experimental results given above are in complete agreement with the theory of motion of atoms in a resonant light field. In the case of interest to us, where the natural width of the absorption line 2γ ($2\gamma = 10$ MHz for transition 3S-3P of the sodium atom) exceeds the recoil energy r (r = 25 kHz), a detailed description of atomic motion can be obtained from the kinetic equation for the distribution function w(z, v, t) [Ref. 2, 15, 16]. For an ideal two-level atom and traveling monochromatic wave in the case of one-dimensional motion of atoms along the z-axis counter to the light wave, this equation takes the form [Ref. 15, 16]

$$\frac{\partial w}{\partial t}+v\frac{\partial w}{\partial z}+\frac{\partial}{\partial v}(Aw)=\frac{\partial^2}{\partial v^2}(Dw), \tag{5}$$

where

$$A=-\gamma v_r\frac{G}{1+G+(\Omega+kv)^2/\gamma^2} \tag{6}$$

is the acceleration of the atom under the influence of the force of light pressure, and

$$D=\frac{1}{2}\gamma v_r^2\left(1+\alpha+G\frac{(\Omega+kv)^2/\gamma^2-3}{[1+G+(\Omega+kv)^2/\gamma^2]^2}\right) \tag{7}$$

is the component of the velocity diffusion tensor along the z-axis. In (5), (6) $v_r=\hbar k/M$ is the recoil velocity, $G=I_л/I_s$, $\Omega=\omega_л-\omega_0$, the parameter α determines the z-component of the continuous diffusion tensor [Ref. 15].

Based on equation (5), let us consider the case of deceleration of atoms by a two-frequency light field of fixed frequency. In doing this, it must be said from the start that strictly speaking equation (5) cannot be directly applied to description of the motion of atoms in the experimental arrangement described above. In the first case, this arrangement used two light waves (two axial modes) with different frequencies ω_1 and ω_2. In the second case, both modes of laser emission had a finite width of the frequency spectrum $\Delta\omega_л$ comparable with the natural width of the atomic transition. Finally, due to the presence of a hyperfine structure in the excited state $3P_{3/2}$, each of the modes in essence interacted with several coupled two-level atomic systems (Fig. 2c).

However, it can be shown that accounting for the former circumstance does not change the form of the equation. Actually, to describe two-frequency excitation of sodium atoms on two different transitions $3S_{1/2}(F=1)-3P_{3/2}$ and $3S_{1/2}(F=2)-3P_{3/2}$ we need to write two equations of type (5). However, as was explained in Section 1, since every atoms actually interacts with only one of the laser radiation modes, and since the parameters of the equations coincide, by combining these equations we again arrive at equation (5).

To account for fluctuations of the frequency of laser emission, equation (5) must be averaged over time interval τ exceeding the inverse width of the frequency spectrum: $\tau \gg \Delta\omega_л^{-1}$. In carrying out such averaging, we note that the function w(z, v, t) is already an averaged function of time since it describes a set of atoms in

the time scale $\Delta t \gg \gamma^{-1}$ [Ref. 15]. Finally, taking into consideration that under the conditions of the experiment $\Delta\omega_{\text{Л}} \sim \gamma$, we arrive at the conclusion that when averaging equation (5) it is necessary to average only its coefficients A and D. Since in addition the time dependences of A and D are determined only by the time dependence of frequency $\omega_{\text{Л}}$, it is actually sufficient to average the coefficients of the equation with respect to frequencies $\omega_{\text{Л}}$.

Averaging of acceleration A and diffusion D with respect to the frequency spectrum of laser radiation gives a simple means of accounting for the presence of a hyperfine structure in the upper level of the resonant transition. Since the width of the line of laser emission $\Delta\omega_{\text{Л}} = 10$ MHz is comparable with the intervals of the hyperfine structure of state $3P_{3/2}$, it can be assumed with sufficient accuracy for experimental purposes that the presence of a hyperfine structure is equivalent to random scatter of resonant frequencies ω_0 within the limits of the effective width of the hyperfine structure $\Delta\omega_{hfs}$. Then accounting for the finite width of laser radiation $\Delta\omega$ and the hyperfine structure of state $3P_{3/2}$ reduces to averaging the coefficients of equation (5) with respect to mismatches $\Omega = \omega_{\text{Л}} - \omega_0$.

Before explicitly writing out the averaged equation, let us note further that an estimation of the role of diffusion in the averaged equation shows that for the length l of the interaction space used in the experiments and the effective interaction width $\Delta\omega$, the contribution of diffusion to deformation of velocity distribution is small compared with that of the force of light pressure. Therefore, limiting ourselves to consideration of only the latter, we finally write out the principal equation that describes the experiment with fixed radiation frequency:

$$\frac{\partial w}{\partial t} + v\frac{\partial w}{\partial z} + \frac{\partial}{\partial v}(\langle A\rangle w) = 0, \qquad (8)$$

where the average acceleration <A> in the simple assumption of rectangular profile of distribution of mismatches Ω in effective region $\Delta\omega$ is

$$\langle A\rangle = \frac{1}{\Delta\omega}\int_{-\Delta\omega/2}^{+\Delta\omega/2} A\, d\Omega - \gamma v_r\left(\frac{\gamma}{\Delta\omega}\right)\frac{G}{(1+G)^{1/2}}\,\mathrm{arctg}\,\frac{(\Delta\omega/\gamma)(1+G)^{1/2}}{1+G+(\Delta\omega/2\gamma)^2+(\bar{\Omega}+kv)^2/\gamma^2}. \qquad (9)$$

In (9) the quantity $\bar{\Omega} = \bar{\omega}_{\text{Л}} - \bar{\omega}_0$ has the meaning of the average mismatch that is the difference between the central frequency of laser radiation $\bar{\omega}_{\text{Л}}$ and the frequency $\bar{\omega}_0$ of the atomic transition that is the average value with respect to the hyperfine structure.

The evoluation of velocity distribution w(v) of an atomic beam calculated by equation (8) for $z = l = 38$ cm and $\Delta\omega = 70$ MHz is shown on Fig. 9a. As a time unit we chose the quantity $(kv_r)^{-1} = 3.2\cdot10^{-6}$ s. In the case of long times ($t \gg \tau_{int}$) due to the finiteness of the length of the region of interaction of atoms with laser radiation, distribution w(v) approaches the steady state. The time dependence of fluorescence intensity corresponding to time deformation of w(v) is shown on Fig. 10 for different values of G. Since I_f at $t = 0$ corresponds to undeformed distribution, the change in I_f as time varies from $t = 0$ to $t = \infty$ characterizes the deformation of velocity distribution.

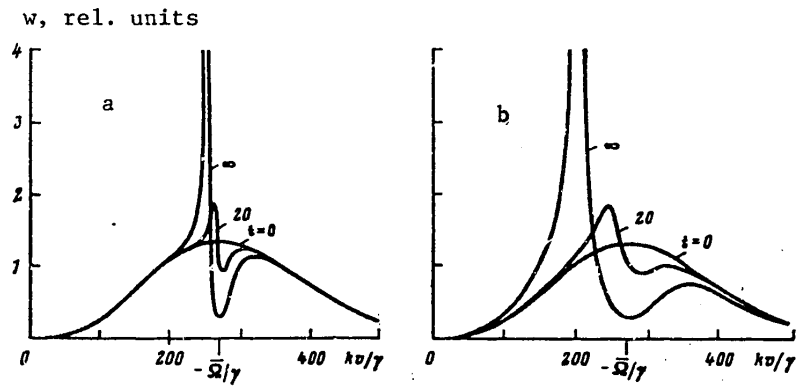

Fig. 9. Change in velocity distribution at point $z = 38$ cm as a function of interaction time t at $\bar{\Omega} = -270\gamma$, $\Delta\omega = 14\gamma$ and $G = 30$ (a), $G = 1000$ (b). Average thermal velocity of atoms $\bar{v} = 220\gamma/k = 6.5 \cdot 10^4$ cm/s ($2\gamma = 10$ MHz, $G = I/I_s$, $I_s = 10$ mW/cm^2). Time unit $(kv_r)^{-1} = 3.2 \cdot 10^{-6}$ s

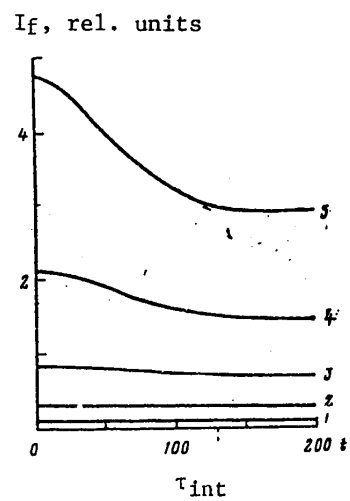

Fig. 10. Fluorescence signal of sodium atoms in the beam as a function of time of interaction with resonant laser emission for $z = 38$ [cm] at $\bar{\Omega} = -270\gamma$, $\Delta\omega = 14\gamma$, $\bar{v} = 220\gamma/k$ and $G = 1$ (1), 9 (3), 27 (4) and 81 (5)

Fig. 8 shows the behavior of the fluorescence signal as a function of the intensity of laser radiation at different values of the parameter $\Delta\omega$ as calculated from the curves of Fig. 10. The best approximation of the experimental points is realized at $\Delta\omega = 70$ MHz. This value agrees well with the mean value of the interval of the hyperfine structure $\Delta\omega_{hfs} \sim 74$ MHz.

Conclusion

Our studies show that resonant laser emission of moderate intensity ($I_л \sim I_s \sim 10$ mW/cm^2) is an effective means of controlling the translational state of atoms. When atoms are made to interact cyclically with radiation, the latter can be successfully used in particular for decelerating atomic beams and for considerably narrowing their velocity distributions. Such an application of resonant light pressure opens up real possibilities for generating beams of cold atoms and injecting them into atomic traps [Ref. 3, 9-11].

REFERENCES

1. Ashkin, A., PHYS. REV. LETTS, Vol 25, 1970, p 1321.

2. Baklanov, Ye. V., Lubetskiy, B. Ya., OPTIKA I SPEKTROSKOPIYA, Vol 41, 1976, p 3.

3. Letokhov, V. S., Minogin, V. G., Pavlik, B. D., ZHURNAL EKSPERIMENTAL'NOY I TEORETICHESKOY FIZIKI, Vol 72, 1977, p 1328.

4. Stenholm, S., APPL. PHYS., Vol 15, 1978, p 287.

5. Stenholm, S., J. JAVANAINEN APPL. PHYS., Vol 16, 1978, p 159.

6. Krasnov, I. V., Shaparev, N. Ya., ZHURNAL EKSPERIMENTAL'NOY I TEORETICHESKOY FIZIKI, Vol 77, 1978, p 899.

7. Balykin, V. I., Letokhov, V. S., Mishin, V. I., PIS'MA V ZHURNAL EKSPERIMENTAL'NOY I TEORETICHESKOY FIZIKI, Vol 29, 1979, p 614; ZHURNAL EKSPERIMENTAL'NOY I TEORETICHESKOY FIZIKI, Vol 78, 1980, p 1376.

8. Minogin, V. G., OPT. COMMUNS, Vol 34, 1980 p 265.

9. Ashkin, A. OPT. LETTS, Vol 4, 1979, p 161.

10. Gordon, J. P., Ashkin, A., PHYS. REV., Vol 21A, 1980, p 1606.

11. Letokhov, V. S., Minogin, V. G., OPT. COMMUNS, Vol 35, 1980, p 199.

12. Balykin, V. I., OPT. COMMUNS, Vol 33, 1980, p 31.

13. Hertel, I. V., Stamatovie, A. S., IEEE J. QUANT. ELECTRONICS, Vol QE-11, 1975, p 210; Beterov, I. H., Kirin, Yu. M., Yurshin, B. Ya., OPT. COMMUNS, Vol 13, 1975, p 238.

14. Gondina, N. D., Zakharov, M. I., Troitskiy, Yu. V. ZHURNAL PRIKLADNOY SPEKTROSKOPII, Vol 10, 1979, p 43.

15. Minogin, V. G., ZHURNAL EKSPERIMENTAL'NOY I TEORETICHESKOY FIZIKI, Vol 79, 1980, p 2044.

16. Cook, R. J., PHYS. REV., Vol A22, 1980, p 1078.

6610
CSO: 8144/0354

UDC 621.317.757

LOW-FREQUENCY SPECTRUM ANALYZER OF CORRELATION TYPE

Moscow PRIBORY I TEKHNIKA EKSPERIMENTA in Russian No 5, Sep-Oct 81 (manuscript received 29 Jan 80) pp 85-89

[Article by V. A. Kaznacheyev, I. M. Butenko, G. G. Bunin, K. M. Bykov and N. M. Zaytsev]

[Text] The paper describes a portable two-channel spectrum analyzer of correlation type. Frequency band 10 Hz-60 kHz; band of analysis 5 Hz; spectral threshold sensitivity ~1 nV/$\sqrt{\text{Hz}}$; dynamic range 100 dB. Provisions are made for measuring the modulus and phase of the complex correlation coefficient between spectral components of two steady-state random processes.

Results of measurements of the spectra of low-frequency (l.f.) noises in radio signals when these spectra contain discrete components that considerably exceed the levels of fluctuation noises in the frequency band of analysis will be inexact or even erroneous in the case of a narrow dynamic range and a wide band of analysis of the spectrum analyzer. Discrete components in the noise spectrum arise in the case of vibrational and audio acoustic effects, under pulsed working conditions, and when there are strong pulsations of power supply voltage. The fluctuational noises of instruments and devices under such conditions can be measured between the frequencies of discrete components of the spectrum by l.f. spectrum analyzers with narrow band of analysis and wide dynamic range.

The search for major noise sources in the signal at the output of an instrument or device is considerably facilitated by measuring correlation coefficients between spectral components of noises of the output signal and the noises of individual components of the instrument or subassemblies of the device. Such measurements can be made by two-channel l.f. spectrum analyzers with correlators at the output.

It should be noted that quite often when measuring the l.f. noises of low-noise microwave instruments and devices, the set noises of microwave detectors are comparable with the noise being studied. The influence that l.f. noises of detectors have on results of measuring noises of microwave devices is considerably reduced by using correlational fluctuation meters [Ref. 1-9]. These meters have higher sensitivity than single-channel meters.

This article gives the results of development of a two-channel spectrum analyzer of correlation type that has better spectral threshold sensitivity and a greater dynamic range than analogs made in the Soviet Union and elsewhere (see the table).

Major characteristics of best l.f. spectrum analyzers

Type of analyzer	Distinguishing features	Principal characteristics				References
		Frequency range, Hz	Spectral sensitivity, nV/$\sqrt{Hz}$	Dynamic range, dB	Band of analysis, Hz	
Described here	Two-channel correlational analyzer with automatic normalization in measurement of correlation coefficient	$10-6 \cdot 10^4$	1	100	5	-
S4-48	Single-channel	$10-2 \cdot 10^4$	17	70	5, 150	10
SK4-56	" "	$10-2 \cdot 10^4$	17	80	3	11
HP-3580A	" "	$5-5 \cdot 10^4$	30	80	1	12
HP-8553B	" "	$10^3-110 \cdot 10^6$	-	130*	10	12
IF-1	Two-channel correlational analyzer with manual normalization in measurement of correlation coefficient	$10^3-5 \cdot 10^5$	15	-	200, 400	3

*Assuming that the l.f. set noises of the spectrum analyzer in the frequency range from 10 Hz to 1 kHz change according to a 1/F law (flicker noise), the dynamic range of this spectrum analyzer on analysis frequency of 10 Hz will not exceed 90 dB.

This paper gives designs for improved technical characteristics of the spectrum analyzer: spectral threshold sensitivity of ~1 nV/$\sqrt{Hz}$, dynamic range of 100 dB, automatic normalization of spectral density of the reciprocal spectrum. The amplitude-frequency characteristics of the input amplifiers and mixers of the spectrum analyzer enable displacement of the lower limit of the frequency band to a fraction of a hertz. To do this it is sufficient to change the filters that determine the frequency band of the analysis for more narrow-band filters.

Specifics of Major Components of the Circuitry. The spectrum analyzer consists of two identical amplification channels that are superhet receivers with double frequency conversion (Fig. 1). A block diagram of one amplification channel is shown in Fig. 2.

Low threshold sensitivity on low frequencies is enxured by KT3107L low-noise transistors with high current gain ($\beta \geqslant 100$) at low collector working currents ($I_C \approx$ 0.1-1 mA) [Ref. 13]. Similar results are achieved when KT203B transistors are used for the input amplifiers.

The upper frequency of flicker noises of amplifiers using transistors of these types does not exceed 30 Hz when the impedance of the signal source is less than

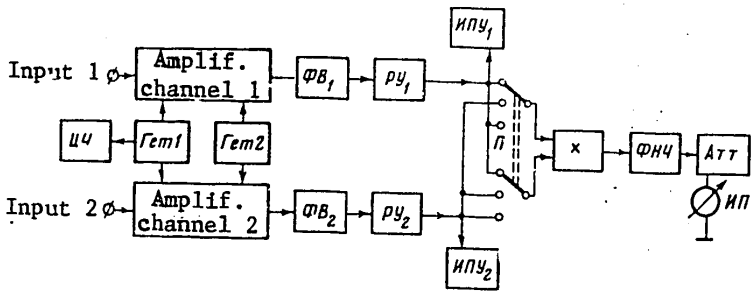

Fig. 1. Block diagram of spectrum analyzer: *Гет 1*--first heterodyne; *Гет* 2--second heterodyne (200 kHz); $ФВ_1$, $ФВ_2$--phase shifters; $РУ_1$, $РУ_2$--devices for manual and automatic gain control; $ИПУ_1$, $ИПУ_2$ --multiplier overload indicators; П--analyzer mode selector; X--multiplier; ФНЧ--low-frequency filter; ИП--meter; ЦЧ--digital frequency meter; Атт--multiplier attenuator

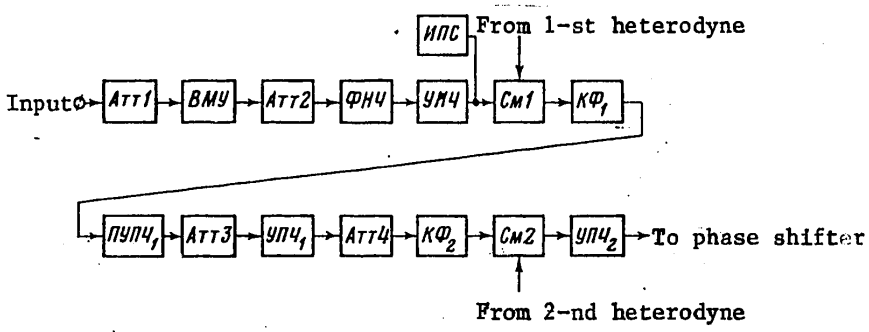

Fig. 2. Block diagram of one amplification channel; Атт1-Атт4--attenuators; ВМУ--low-noise input amplifier with stepwise gain control; УНЧ--low-frequency amplifier with continuous gain control; ИПС--mixer overload indicator; См1--first mixer (128 kHz); $КФ_1$--quartz filter with passband of 5 Hz on frequency of 128 kHz; $ПУПЧ_1$--preamplifier of first i-f voltages; $УПЧ_1$--first i-f voltage amplifier; $КФ_2$--second quartz filter with passband of 30 Hz on frequency of 128 kHz; См2--second mixer; $УПЧ_2$--second i-f voltage amplifier (72 kHz)

10 kΩ. A diagram of the amplifier is shown in Fig. 3. The experimental curve for the noise factor as a function of frequency is shown in Fig. 4. The wide dynamic range (>100 dB) is attained by making the low-frequency amplifiers in a differential circuit with deep negative feedback (>60 dB). Commutation of the input attenuator and feedback circuits is done in such a way that the input impedance of the channel is 100 kΩ on all measurement ranges.

A schematic diagram of the mixer is shown in Fig. 5. The mixer operates as follows. In the differential stage based on K1NT591 microcircuit and KT312B transistor the input voltage is changed to antiphase collector currents of the transistors of chip K1NT591. The current switches alternately connect the antiphase currents to the 2.2 kΩ load resistors. In this way the input signal is multiplied by the pulse signals of the heterodyne with 1 V peak-to-peak amplitude (from cycle to cycle).

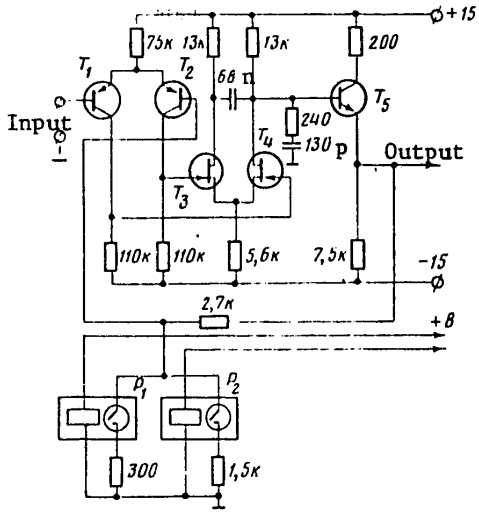

Fig. 3. Schematic diagram of low-noise input amplifier: P_1, P_2--sealed-contact relays; T_1, T_2--KT3107L; T_3, T_4--KP303B; T_5--KT3102V

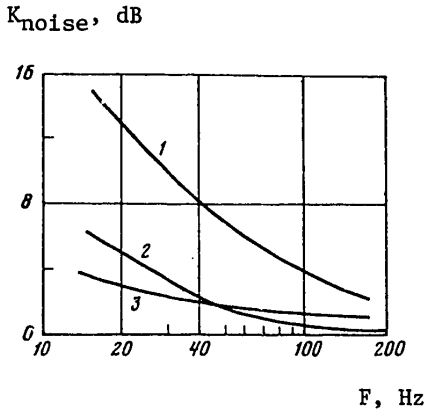

Fig. 4. Noise factors of amplification channel in 5 Hz band at different signal source impedances: 1--47 kΩ, 2--4.7 kΩ, 3--540 Ω

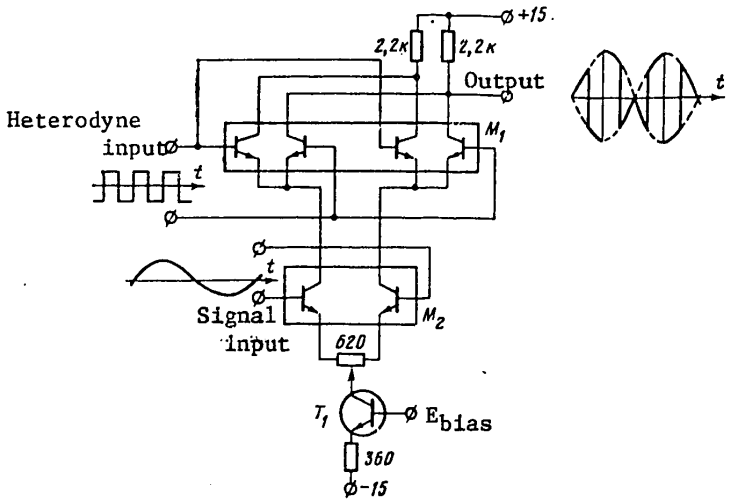

Fig. 5. Schematic diagram of mixer: M_1--K217NT3; M_2--K1NT591 T_1--KT312B

The wide dynamic range of the mixer (>100 dB in a frequency band of 5 Hz in combination with quartz filter PF2P-34) is achieved by using deep negative feedback (620 Ω resistor) in the differential stages based on chip K1NT591, and switch operation of the transistors of chip K217NT3. An advantage of the switching mode of mixer operation is that the i-f voltage amplitude is independent of fluctuations of the heterodyne amplitude. The balanced circuit of the mixer keeps the heterodyne voltage on a low level in the intermediate-frequency channel (≤40 dB over the noise level in this channel at $f_{het} = f_{i-f}$).

The dynamic range of the mixer is less than that of the preceding amplifiers since the mixer as a whole cannot be covered by feedback. Under these conditions the dynamic range of the amplification channel (together with the mixer) depends on the ratio of the transfer factor of the first quartz filter to the noise voltage of the intermediate-frequency channel normalized to the input of the intermediate-frequency preamplifier (IFPA). The higher this ratio, the wider will be the overall dynamic range. The above presentation is realized in the described spectrum analyzer in the following way: the ratio of the transfer factor of the quartz filter to the noise voltage of the intermediate-frequency channel is brought to about 1/40 nV^{-1} by selecting resistors to match the input of the quartz filter to the output impedance of the signal source (2.2 kΩ), and to match the output to the load (5.6 kΩ); the developed IFPA circuit has a noise factor of <2 dB.

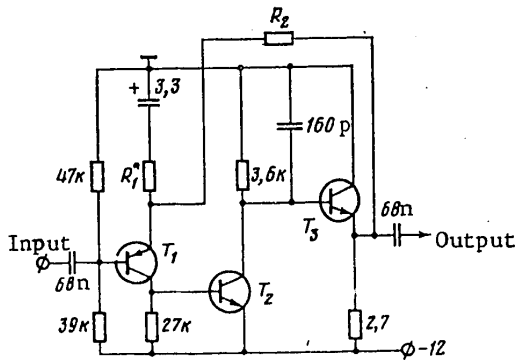

Fig. 6. Schematic diagram of IFPA: T_1--GT322V; T_2, T_3--KT301Ye

The maximum dynamic range of the amplification channel is realized at an effective signal amplitude of ~40 mV at the mixer input. This level is established by continuous gain control of the low-frequency amplifier, and is monitored by the mixer overload indicator. The indicator is a peak detector with time constant of 1 s. A schematic of the first i-f voltage preamplifier is shown in Fig. 6. To stabilize gain (40 dB), the IFPA is covered by negative feedback (R_1, R_2). R_1 is selected during tuning.

The noise level of the amplifier (~20 nV in a frequency band of 5 Hz) is determined mainly by the quartz filter load resistance. The required gain of the intermediate-frequency channel should be ≥130 dB since the optimum voltage across the inputs of the multiplier is ~150 mV. Resistance to self-excitation of the intermediate

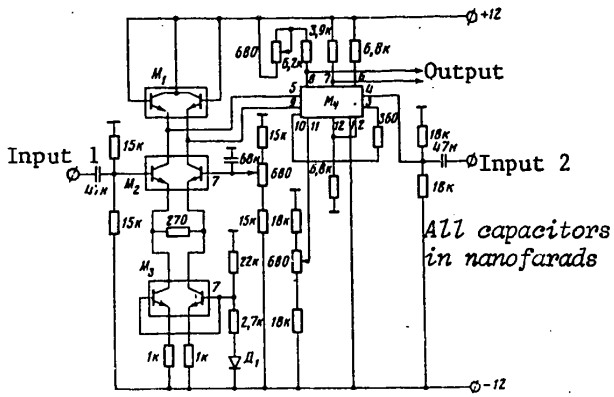

Fig. 7. Schematic of multiplier: M_1--101KT1; M_2, M_3--K1NT591; M_4--140MA1; $Д_1$--D223

frequency channel is ensured by using a second frequency converter. This facilitates tuning of the circuit and simplifies the design of the device (by reducing shielding requirements for stages of the intermediate-frequency channel).

The gain of the first intermediate-frequency (i-f) channel (128 kHz)--from the input of the IFPA to the input of the second mixer--is 70 dB; the gain of the second i-f channel (72 kHz)--from the input of the second mixer to the input of the multiplier--is 60 dB. The second quartz filter with frequency band of 30 Hz installed in the first i-f channel is intended for suppressing the noises of this channel that lie outside the 5 Hz frequency band of the first quartz filter. The second mixer is made in the same circuit as the first.

The phase shifter is built in a bridge circuit [Ref. 14, p 240]. The phase of the input signal is shifted by changing the current through diodes connected in the phase-shifting arm of the bridge. Maximum phase shift is 135°. The signal multiplier with current normalization [Ref. 15] is based on a 140MA1 microcircuit (Fig. 7). A logarithmic stages based on 101KT1 and 159NT1 microcircuits expands the range of voltages of the multiplied signals. Optimum voltages across the multiplier inputs (~150 mV) are established by regulating the gain of the low-frequency and intermediate-frequency channels, and are monitored by the readings of multiplier overload indicators.

A correlational gain in noises of the correlator (the multiplier together with the integrator) by a factor of ~5-10 with band of analysis of 5 Hz is realized at an integrator averaging time of ~10-40 s. The integrator is an RC integrating circuit with time constants of 1, 3, 10 and 45 s.

When measuring the modulus of the complex correlation coefficient between the spectral components of two random processes by the phase shifter in one channel of the spectrum analyzer, the signal phase is varied by an amount such that the indicator reading is maximized. This reading corresponds to the sought modulus, and the rotation of the phase by the phase shifter corresponds to the phase shift between the spectral components of the processes on the given frequency of the spectrum.

The real part of the complex correlation coefficient is read out directly from the scale of the meter, the zero position being in the middle of the scale. When measuring correlation coefficients in both channels, automatic gain control is switched in to obviate the need for laborious calibration of the device on each frequency of analysis.

Each heterodyne has two frequency tuning bands: a wide band from 128 to 188 kHz with frequency stability of $3 \cdot 10^{-5}$ over 15 minutes, and a narrow band from 128 to 131 kHz with frequency stability of $2 \cdot 10^{-6}$ over 15 minutes. The wide-band heterodyne is a master LC-oscillator with thermocompensation. It is tuned over a frequency band of 1.2-1.9 MHz. The frequency of the waveforms at the heterodyne output is obtained by dividing the frequency of the master oscillator by 10. The frequency of the heterodyne output signal in both ranges is varied by tuning the frequency of the master oscillator. In the narrow band the heterodyne frequency is stabilized by phase AFC.

The heterodyne frequency is monitored by a digital frequency meter with liquid crystal display. The error of frequency measurement by this meter is no more than ±0.1 Hz. Undivided frequency is sent to the frequency meter to accelerate operation by a factor of 10. KEM-2B sealed contacts are used to commutate the circuits in the attenuators, feedback in the input amplifiers, the frequency bands of the heterodyne and the time constant in the RC circuit of the multiplier.

The described spectrum analyzer can be used to measure the "fine" structure of the spectrum of low-frequency noises of electronic instruments in real applications, in particular at high levels of pulsations of supply voltages and their harmonics. Correlational analysis of the noises of devices and of the noises in circuits where they are used reveals fundamental sources of noises, and accordingly enables determination of possible ways to reduce them. Thus the wide dynamic range and the two-channel arrangement with correlator at the output are the major advantages of the given spectrum analyzer.

The authors thank V. G. Gorbas' for furnishing the frequency meter.

REFERENCES

1. Kornilov, S. A., Timasheyev, R. G., Filippov, E. V., VOPROSY RADIOELEKTRONIKI, Ser. 1, No 1, 1965, p 302.

2. Kornilov, S. A., VOPROSY RADIOELEKTRONIKI, Ser. 1, No 2, 1965, p 114.

3. "Tekhnicheskoye opisaniye i instruktsiya po ekspluatatsii izmeritelya fluktuatsiy i koeffitsiyenta korrelyatsii IF-1" [Technical Description and Operating Instructions of the IF-1 Device for Measuring Fluctuations and Correlation Coefficient], 1971.

4. Lange, F., "Korrelyatsionnaya elektronika" [Correlational Analysis], translated from German, edited by V. I. Klyachkin, Leningrad, Sudpromgiz, 1963.

5. Bunin, G. G., Kiyanov, Ye. P., Pugachev, G. A., Yazykov, Yu. D., USSR Patent No 364040, published in BYULLETEN' IZOBRETENIY No 4, 1973, p 125.

6. Kornilov, S. A., Skabovskiy, M. S., VOPROSY RADIOELEKTRONIKI, Ser. 1, No 3, 1965, p 132.

7. Kornilov, S. A., Skabovskiy, M. S., VOPROSY RADIOELEKTRONIKI, Ser. 1, No 2, 1965, p 102.

8. Bunin, G. G., Shuvalov, B. A., ELEKTRONNAYA TEKHNIKA, Ser. 1, No 8, 1979, p 50.

9. Sal'nichenko, A. Ya., PRIBORY I TEKHNIKA EKSPERIMENTA, No 5, 1976, p 97.

10. "Tekhnicheskoye opisaniye i instruktsiya po ekspluatsii analizatora spektra S4-48" [Technical Description and Operating Instructions for S4-48 Spectrum Analyzer], 1975.

11. "Katalog-prospekt Radioizmeritel'nyye pribory 1979 g." [Catalog-Prospectus on Electronic Measuring Instruments for 1979], Moscow, Central Branch Agency of Scientific and Technical Information, 1979.

12. "Hewlett-Packard Catalog", 1977.

13. Zhalud, V., Kuleshov, V. N., "Shumy v poluprovodnikovykh ustroystvakh" [Noises in Semiconductor Devices], Moscow, Sovetskoye radio, 1977, p 81.

14. Alekseyenko, A. G., "Osnovy mikroskhemotekhniki" [Principles of Microcircuitry], Moscow, Sovetskoye radio, 1977.

15. Yakubovskiy, S. V., ed., "Analogovyye i tsifrovyye integral'nyye skhemy" [Analog and Digital Integrated Circuits], Moscow, Sovetskoye radio, 1979, p 231.

6610
CSO: 1862/46

OPTOELECTRONICS

PRIZ IMAGE CONVERTER: ITS USE IN OPTICAL DATA PROCESSING SYSTEMS

Leningrad ZHURNAL TEKHNICHESKOY FIZIKI in Russian Vol 51, No 7, Jul 81 (manuscript received 18 Jun 80) pp 1422-1431

[Article by M. P. Petrov, A. V. Khomenko, M. V. Krasin'kova, V. I. Marakhonov and M. G. Shlyagin, Physicotechnical Institute imeni A. F. Ioffe, USSR Academy of Sciences, Leningrad]

[Text] The paper gives the results of a study of the new PRIZ optically controlled space-time light modulator. The transverse linear electro-optical effect in a $Bi_{12}SiO_{20}$ crystal is used for light modulation in this device. The authors examine the working principle of such a modulator, and give the results of measurement of its parameters. It is shown that with respect to all major parameters the PRIZ modulator is superior to the PROM modulator using the same crystal. Besides, the new device can be easily used for outlining, sectoral filtration and dynamic selection of images. A new method is proposed for describing the effect of dynamic light modulators that is used for describing the effect of dynamic selection of images that has been discovered in the PRIZ modulator. It is demonstrated that holograms can be recorded from such a modulator, and that it can be used for compressing LFM signals.

Optical methods are advisable for processing large masses of information, and in particular information in the form of two-dimensional images. It is most effective in such cases to use optical data processing systems that operate in real time. However, realization of systems of this kind requires an active element--what is called a space-time light modulator enabling efficient high-speed recording, readout and erasure of the initial image. In many cases of practical importance it is sufficient that the block of information imaged on the modulator and the pace of operation correspond to the television standard (number of resolvable elements 10^5-10^6, frame frequency 20-30 Hz).

At the present time, several space-time light modulators have been developed, e. g. modulators based on liquid crystals [Ref. 1], the Phototitus [Ref. 2], PROM [Ref. 3] and others. Nonetheless, up until now no modulator has yet been developed that would simultaneously satisfy the entire set of requirements to be met.

This paper is a report on the results of studies of a new modulator--the PRIZ image converter--that has high parameters and can be used for such operations as spatial differentiation and sectoral filtration by an extremely simple and effective method. In addition, this modulator has shown an effect of dynamic selection of images, enabling differentiation of the time-variable part of two-dimensional information blocks.

Working Principle

Operation of the PRIZ modulator is based on the photorefraction effect, i. e. on the change in birefringence of a crystal under the action of incident light. The same effect is used in the well known PROM device. Let us explain the working principle of both modulators by means of the structure illustrated on Fig. 1.

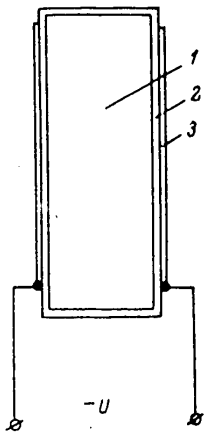

Fig. 1. Structure of PRIZ modulator

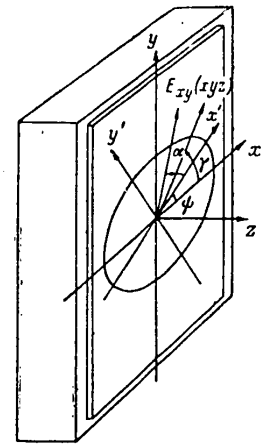

Fig. 2. Cross section of display by plane (111)

This structure consists of plate of working crystal (1) and a current feed system that includes transparent conductive coatings (3) and thin dielectric layers (2). Crystals that simultaneously show the linear electro-optical effect and photoconductivity can be used as the working material. Most suitable are cubic crystals that belong to point groups $\bar{4}3m$ and 23. Hereafter, all results will be discussed on the example of crystal $Bi_{12}SiO_{20}$ (group 23). It is on this crystal that the modulator will give the best results, although experiments were also done with $Bi_{12}GeO_{20}$ and $Bi_{12}TiO_{20}$.

The mechanism of operation of the modulator is as follows. Recording light from the blue-green part of the spectrum excites charge carriers in the crystal that drift into an electric field applied to the crystal plate. As shown in Ref. 4, this results in formation of a spatially inhomogeneous electric space charge in the crystal with distribution in the plane of the plate that reproduces the intensity distribution of the recording light. The presence of the space charge gives rise to an inhomogeneous electric field thqt has both longitudinal components

(relative to the field set up by the supply voltage) and transverse components. Since the crystal has the linear electro-optical effect, a spatial change in birefringence arises in conformity with the magnitude and direction of local internal electric fields. When polarized light from the longer-wave part of the spectrum is used for readout, the readout beam is modulated with respect to the state of polarization. An analyzer can convert modulation with respect to the state of polarization to amplitude modulation.

In order to understand the characteristic features of the PRIZ modulator that distinguish it from the PROM modulator we must go into more detail in the theory of the electro-optical effect for crystals of the given type. As is known [Ref. 5], the linear electro-optical effect in a cubic crystal that belongs to group 23 is described by the tensor of electro-optic coefficients in which only the diagonal elements r_{41}, r_{52} and r_{53} are non-zero, with $r_{41} = r_{52} = r_{63}$. Both the longitudinal and transverse field-linear electro-optical effect is possible. The electro-optical effect is termed longitudinal or transverse depending on the mutual orientation of the electric field in the medium and the direction of light wave propagation (in the longitudinal effect, these directions are parallel, and in the transverse effect they are orthogonal). In the absence of an electric field, the given crystals are isotropic, and the optical indicatrix is a spherical surface. On the other hand, if an electric field acts on the crystal, the indicatrix is deformed into an ellipsoid. To determine the birefringent properties of the crystal, it is necessary to find the cross section of the indicatrix by the plane perpendicular to the direction of propagation of the readout beam, or in our case by the plane parallel to the plane of the plate. Therefore the orientation (cut) of the plate with respect to the crystallographic axes has decisive significance in calculation of the electro-optical effect. Besides, it is important to consider that the electric field giving rise to the change in birefringence is the sum of the external applied field and the internal inhomogeneous field produced by the volumetric distribution of the charge. The phase difference between the ordinary and extraordinary beams of the reading light depends on the x and y coordinates of the plane of the crystalline plate.

Let us consider the three principal orientations of the plane of the plate (100), (110), (111). In cut (100) when the plane wave of the reading light is normally incident, only the longitudinal electro-optical effect is possible. In this case, no matter what the orientation of the electric field in the crystal, birefringence is produced only by the longitudinal field components (i. e. those along the z-axis). Hereafter, the z-axis will everywhere be taken to mean the direction of the normal to the forward surface of the crystal plate. The phase difference is

$$\Delta\varphi(x, y) = \frac{2\pi}{\lambda} n_0^3 r_{41} \int_0^{d_{\text{кр}}} E_z(x, y, z)\,dz = \frac{2\pi}{\lambda} n_0^3 r_{41} U, \qquad (1)$$

where $E_z(x, y, z)$ is the longitudinal component of the electric field, which in the case of nonuniform charge distribution in the crystal depends on the z-coordinate; $d_{\text{кр}}$ is the thickness of the crystal; U is the potential difference between surfaces of the crystal plate; n_0 is the index of refraction of the crystal.

In contrast to cut (100), in the case of cuts (110) and (111) when a plane light wave is normally incident only the transverse electro-optical effect is possible.

In cut (1110 the cross section of the optical indicatrix in the principal axes takes the form

$$\left[\frac{1}{n_0^2}-\sqrt{\frac{2}{3}}r_{41}E_{xy}(x,\ y,\ z)\right]x^2+\left[\frac{1}{n_0^2}+\sqrt{\frac{2}{3}}r_{41}E_{xy}(x,\ y,\ z)\right]y^2=1, \quad (2)$$

where $E_{xy}(x, y, z)$ is the magnitude of the projection of the electric field vector on plane (111). In the general case, E_{xy} is a function of the z-coordinate. Here the phase difference will be

$$\Delta\varphi(x,\ y)=\frac{2\pi}{\lambda}\sqrt{\frac{2}{3}}n_0^3r_{41}\int_0^{d_{\text{кр}}}E_{xy}(x,\ y,\ z)\,dz. \quad (3)$$

Thus the magnitude of birefringence is independent of the direction of the electric field projection in plane (111), and is determined only by the modulus of this projection. The angle Ψ between the principal axis of the cross section of the optical indicatrix ox and the axis [110] of the crystal, and angle γ between the projection of the electric field vector and axis [110] are related by the expression

$$2\Psi+\gamma=\pi/2. \quad (4)$$

When cut (110) is used, $\Delta\phi$ is determined both by the magnitude of the projection of the electric field vector on plane (110), and by its direction. The maximum phase difference is reached when the electric field is directed along axis [110]. In this case

$$\Delta\varphi(x,\ y)=\frac{2\pi}{\lambda}n_0^3r_{41}\int_0^{d_{\text{кр}}}[E_{xy}(x,\ y,\ z)\,dz. \quad (5)$$

At a given electric field strength, this is the maximum phase difference that can be obtained by the transverse effect in a cubic crystal [Ref. 6].

As we know, $\Delta\phi$ determines the modulation of the reading light with respect to the state of polarization. When linearly polarized reading light is used, and behind the modulator is an analyzer that isolates the component orthogonal to the initial polarization, the light is amplitude-modulated. The light intensity $I(x, y)$ behind the analyzer is described by the following expression:

$$I(x,\ y)=I_0\sin^2 2\alpha\sin^2\Delta\varphi/2, \quad (6)$$

where I_0 is the intensity of the light passing through the modulator to the analyzer; α is the angle between the direction of the field of polarization of the reading light and one of the principal axes of the optical indicatrix (Fig. 2). On the other hand, if circularly polarized light is used, the intensity of the light behind a circular analyzer (combination of ¼-wave plate and linear polarizer) does not depend on the direction of the field since $\Delta\phi$ is independent of the orientation of the electric field vector in plane (111). In recording a sine-wave grating, the magnitude of the phase difference $\Delta\phi(x, y)$ is described by the following expression:

$$\Delta\varphi(x,\ y)=\Delta\varphi_0+\Delta\varphi_{k_x}\cos k_x x. \quad (7)$$

The diffraction efficiency of the instrument η, i. e. the ratio of intensity of the beam diffracted in the first order to the intensity of the reading light incident on the modulator with consideration of (2) and (4) can be related to the amplitude of modulation of the phase difference $\Delta\phi_{k_x}$ by the following expressions:

$$\eta = J_1^2(\Delta\varphi_{k_x})\cos^2(2\psi+\gamma) \qquad (8)$$

(J_1 is a first-order Bessel function) for the case of linear polarization, and

$$\eta = J_1^2(\Delta\varphi_k) \qquad (9)$$

for the case of circular polarization. At small values of $\Delta\phi$, $J_1(\Delta\phi) \cong \Delta\phi/2$.

As we can see from relations (1)-(9), the parameters of the modulator, and as will be clear later, the functional properties depend in a radical way on the orientation of the crystal. Modulators using the transverse electro-optical effect are hereinafter called image-converter modulators in contrast to the PROM modulator where the longitudinal effect is used.

It has been noted earlier that spatial modulation of light is determined by the electric field of the space charge produced in the recording process. For the PROM modulator in which the longitudinal electro-optical effect is used, an increase in thickness of the space-charge layer leads to a sharp reduction of $\Delta\phi$ and resolution [Ref. 4]. Under the same conditions for the PRIZ modulator an increase in the effective thickness of the space charge leads to increased resolution of the device. For example, for cut (111), calculation analogous to that of Ref. 4 yields the following expression

$$\Delta\varphi_{k_x} = \frac{4\pi\sigma_0 a n_0^3 r_{41}}{\varepsilon_{\text{кр}} k_x \lambda} \times$$
$$\times\left\{1 - \frac{\varepsilon_{\text{д}}[\operatorname{ch} k_x(d_{\text{кр}}-a)+1-\operatorname{ch} k_x d_{\text{кр}} - \operatorname{ch} k_x a] - \varepsilon_{\text{кр}} \operatorname{th} k_x d_{\text{д}} \operatorname{sh} k_x a}{a k_x(\varepsilon_{\text{д}} \operatorname{th} k_x d_{\text{кр}} + \varepsilon_{\text{кр}} \operatorname{th} k_x d_{\text{д}}) \operatorname{ch} k_x d_{\text{кр}}}\right\}, \qquad (10)$$

where σ_0 is the space density of the charge produced during recording; $\varepsilon_{\text{кр}}$, $\varepsilon_{\text{д}}$, $d_{\text{кр}}$, $d_{\text{д}}$ are the permittivity and thickness of crystal [кр] and dielectric [д] respectively; a is the thickness of the space charge layer. This formula implies the following.

1) At large values of k_x ($k_x > 1/a$), $\Delta\phi \sim 1/k_x$, whereas in the case of the PROM modulator $\Delta\phi \sim 1/k_x^2$, i. e. the PRIZ modulator has smoother dependence of $\Delta\phi$ on spatial frequency k_x. This leads to an increase in the resolution of the modulator as compared with the PROM modulator.

2) At all spatial frequencies $k_x > 1\ \text{mm}^{-1}$ the magnitude for the PRIZ modulator is greater than the $\Delta\phi$ given by the PROM modulator. As a result, the diffraction efficiency of the PRIZ modulator is higher.

3) As $k_x \to 0$, $\Delta\phi \to 0$, i. e. the null space frequency is not reproduced by the PRIZ modulator. This automatically leads to spatial differentiation of images.

Results are similar for cut (110), the only difference being that a factor of the order of unity depending on angle γ shows up in formula (10). It should be noted that the external electric field in the PRIZ modulator lies in the direction of propagation of the reading beam, i. e. geometry analogous to the longitudinal electro-optical effect is externally realized in the modulator. However, in the recording process an inhomogeneous field is set up in the crystal, and the transverse components of this field are actually used to modulate the light.

Experimental Results

Fig. 3 shows the results of measurement of the diffraction efficiency of the PRIZ modulator as a function of the space frequency. The measurements were done in a logarithmic arrangement with Michelson interferometer. The space frequency was selected by varying the the angle of inclination of one of the mirrors of the interferometer. The source of recording light was either a helium-cadmium laser ($\lambda = 441$ nm) or an argon laser (λ=488 nm). It can be seen from Fig. 3 that the PRIZ has high resolution with recording by laser light. Its sensitivity in this case remains practically the same as in the case of recording by He-Cd laser light. The given experimental data agree with conclusions drawn from formula (10).

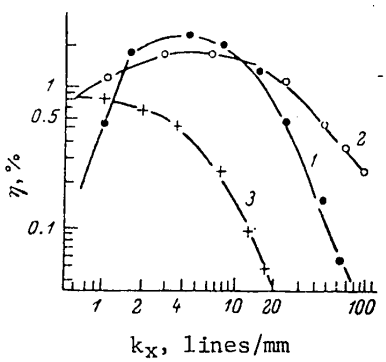

Fig. 3. Diffraction efficiency as a function of space frequency for the PRIZ modulator (1, 2) at wavelengths of the recording light of 441 nm (1) and 488 nm (2). Shown for comparison is the same curve for the PROM modulator (3), λ = 441 nm, E = 200 erg/cm^2.

Fig. 4 shows curves for diffraction efficiency as a function of the angle between the vector of the space lattice and the crystallographic axes for cut (111). The solid lines show calculated curves for η in accordance with formulas (8) and (9) for linear and circular polarization of the reading light. The space frequency of the lattice was 5 lines/mm. The plane of linear polarization was oriented along axis [11$\bar{2}$]. For linear polarization we see good agreement between the theoretical curve and the experimental data in the case

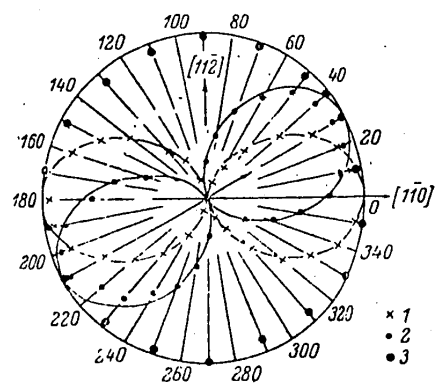

Fig. 4. Diffraction efficiency as a function of the angle between the vector of the space lattice and the crystallographic axes for circular polarization and for linear polarization parallel to axis [112]: 1--recording from the side of the negative electrode; 2--from the side of the positive linear polarization $\eta(\phi) = \eta_0 \cos^2 \phi$; 3--circular polarization $\eta(\phi) = \text{const}$

where negative potential is applied to the leading electrode with respect to the recording light. On the other hand, if "+" is applied to this electrode, the experimental values fit satisfactorily on curve $\eta = \eta_0 \cos(\gamma - 30°)$. This can be explained with consideration of the optical activity of the crystal by the fact that an inhomogeneous electric field is formed in the layer situated closer to the negative electrode [Ref. 4]. In this case, when the negative electrode is the trailing one with respect to the recording light, the plane of polarization of light is turned through an angle of ~15° due to optical activity upon passage through a crystal layer ~0.7 mm thick. In accordance with expression (8), this leads to displacement of orientational dependences through an angle of ~30°. This fact is one more confirmation of the assumption that the effective thickness of the layer responsible for modulation of light is considerably less than the thickness of the crystal.

The curves shown on Fig. 4 demonstrate that in the case of readout by linearly polarized light, the modulator does not reproduce all spatial frequencies, but rather only those whose vector lies in a certain angular sector, i. e. sectoral filtration of images is realized.

Circularly polarized light can be used for readout of images. In this case, when the crystal plate has orientation (111), the diffraction efficiency in accordance with (9) does not depend on the direction of the space lattice vector. The experimental data on Fig. 4 confirm this conclusion.

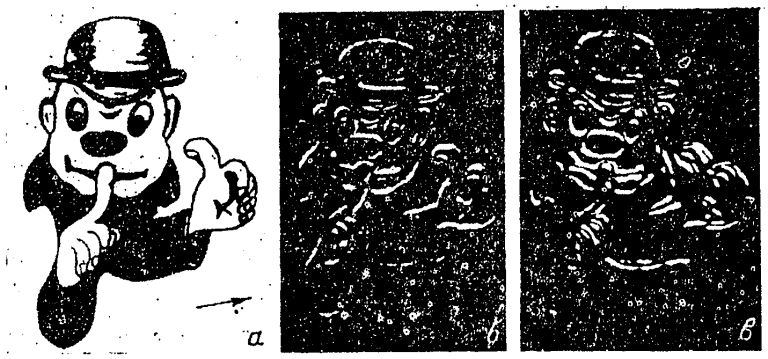

a b c

Fig. 5. Recording of hologram from PRIZ modulator: a--original image; b--image recorded on PRIZ modulator; c--image reconstructed from hologram

Fig. 5 shows a photograh of an image recorded on the PRIZ modulator that was read out by linearly polarized light. It can be seen from the figure that the null space frequency of the image was not reproduced, which led to outlining of the image. The arrow indicates the directions in which the sectoral converted image is realized; this specific feature is reflected in the name PRIZ [PReobrazovatel' IZobrazheniy: image converter].

The same figure shows an example of the image reconstructed from a hologram that was recorded by the PRIZ modulator. In this case the modulator acted as a converter of incoherent light to coherent light.

The sensitivity of the PRIZ modulator is at least an order of magnitude better than that of the PROM modulator. This means that the PRIZ can be effectively used in systems for real-time optical processing of information. Ref. 7 has reported on the use of this modulator in an optical spectrum analyzer, correlator and as a medium for recording holograms.

The PRIZ modulator can also be used for processing electrical signals, and specifically for compression of an LFM signal. In this case the signal is recorded as an LFM grid on the modulator, and readout is by coherent light. At a certain distance from the modulator, one of the diffracted beams is compressed into a narrow band. In the same plane, another diffracted light beam and the null order have remained defocused. The theoretical coefficient of compression in this case is expressed by the formula [Ref. 8]

$$k_{comp} = \frac{n}{2} + \sqrt{\frac{n^2}{4} - n}; \quad n = \Delta f l, \tag{11}$$

where Δf is the deviation of the space frequency of the grid, and l is its length. Fig. 6 shows the result of signal compression with deviation of 8 lines/mm, $l = 15$ mm, obtained by a PRIZ modulator. The signal was recorded on the modulator from photographic film by He-Cd laser light. The experimentally determined value of the coefficient of compression was ~100 (theoretical coefficient of compression of such a signal is $k_{comp} = 120$).

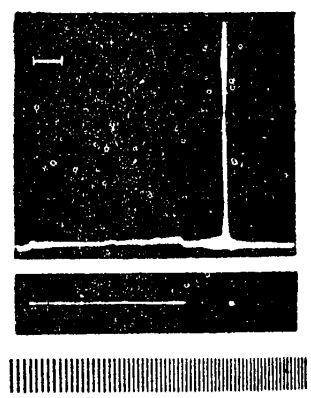

Fig. 6. Result of compression of LFM signal: a--image of LFM signal; b--image of null order and compressed signal; c--scanogram of zero order and compressed signal

Dynamic Properties

Thanks to high sensitivity ($-5 \cdot 10^{-7}$ J/cm^2 per 1% of diffraction efficiency) and the capability for fast erasure by a flashlamp when the electrodes are shorted, the PRIZ modulator ensures speed of the order of the television standard (20-30 frames per second) or more. The working mode corresponds to the usual well-known cycle: recording - readout - erasure. However, on modulators with a modified current-conducting system, another mode of operation is possible as well, i. e. a mode that does not require image erasure. Since some experimental results that explain this mode have already been published [Ref. 9], we give here only the diagram of Fig. 7. As we can see from this diagram, when the recording light is energized an image arises in the modulator that begins to fade within a certain time (in the given specific example within about 0.5 s), but flares up again when the recording light is switched off. Thus a time-variable image (or part of one) is isolated in the modulator. These effects can be attributed to redistribution of the space charge as the image changes, and they determine the entire dynamics of operation of the device.

Available experimental results of investigation of the response of the PRIZ modulator to unsteady controlling pulses show that this modulator is actually dynamic,

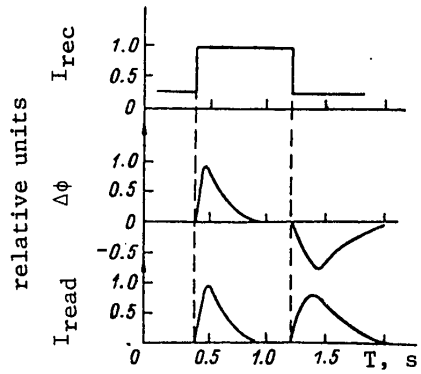

Fig. 7. Response of device to change of light intensity in image being recorded

and can provide time-continuous image processing, whereas in most known cases, discrete frame by frame processing is realized. In this connection, the problem arises of describing the characteristics of a modulator that adequately reflects their unsteady nature.

In the scope of our research, a phenomenological approach is developed to description of a dynamic modulator within the framework of the theory of linear systems. The microscopic nature of the processes that take place in the modulator, as well as its functional capabilities in devices for processing unsteady two-dimensional signals will not be discussed here.

Let us consider the response of a dynamic optically controlled modulator to the action of light that has distribution of intensity in the plane of the modulator F(x, y, t). We will take the modulator as fairly thin to avoid accounting for the three-dimensional nature of data recording. In the general case, the action of the modulator on the reading light can be described by a tensor of second rank $\hat{P}(x, y, t)$. If the reading light has the corresponding wavelength and does not influence the parameters of the modulator, then the amplitude of the reading light immediately behind the modulator $\vec{E}_{out}(x, y, t)$ is related to the amplitude of the reading light $\vec{E}_{read}$ before the modulator by the expression

$$\vec{E}_{out}(x, y, t) = \hat{P}(x, y, t)\vec{E}_{read}. \qquad (12)$$

Under the influence of the recording light there will be a change in $\hat{P}(x, y, t)$, so that we can write

$$\hat{P}(x, y, t) = \hat{P}_0 + \Delta\hat{P}(x, y, t). \qquad (13)$$

As we know, $\hat{P}_0$ is a Jones matrix. Hereafter we will consider only $\Delta\hat{P}(x, y, t)$.

In accordance with the theory of linear systems, the response of the system $\Delta\hat{P}(x, y, t)$ to signal F(x, y, t) can be represented as

$$\Delta\hat{P}(x, y, t) = \iiint_{-\infty}^{\infty} \hat{\kappa}(k_x, k_y, \omega)\, S(k_x, k_y, \omega)\, e^{-i(\omega t + k_y y + k_x x)} dk_x dk_y d\omega, \qquad (14)$$

where k_x, k_y and ω are the spatial and time frequencies respectively; $S(k_x, k_y, \omega)$ is the three-dimensional Fourier transform of the function $F(x, y, t)$, and $\kappa(k_x, k_y, \omega)$ is the Fourier transform of the function of response of the modulator to the recording light $\Delta P_\delta(x, y, t)$

$$\Delta\hat{P}_\delta(x, y, t) = \iiint_{-\infty}^{\infty} \hat{\kappa}(k_x, k_y, \omega) e^{-i(k_x x + k_y y + \omega t)} dk_x dk_y d\omega. \qquad (15)$$

The function $\hat{\kappa}(k_x, k_y, \omega)$ characterizes the response of the modulator to the recording light. It is related to the transfer characteristic with respect to the reading light by the expression

$$\mathcal{H}(k_x, k_y, t) = \int_{-\infty}^{\infty} \hat{\kappa}(k_x, k_y, \omega) S(k_x, k_y, \omega) e^{-i\omega t} d\omega, \qquad (16)$$

which is thus a function of time. An important quantity in the experimental respect is the diffraction efficiency

$$\eta(k_x, k_y, \omega) = |\kappa(k_x, k_y, \omega) S(k_x, k_y, \omega)|^2. \qquad (17)$$

The difference between this case and the traditional case where the recording of steady-state time-independent images is considered is that the unsteady images are distributed with respect to traveling rather than steady-state waves. And the response of the modulator is also represented as a sum of traveling waves with amplitude $\kappa(k_x, k_y, \omega)S(k_x, k_y, \omega)$. Since in our case the action of the recording light gives rise to a change in the index of refraction (photorefraction effect), apparently traveling waves also represent the photorefraction waves.

As can be seen from comparing formulas (8) and (17), for low intensities of the recording light when the system meets conditions of linearity, the diagonal elements of the transfer characteristic $\kappa(k_x, k_y, \omega)$ coincide with $\Delta\varphi_{k_x, k_y \omega}$ except for a coefficient that depends on angles α and ψ.

It is important to emphasize the difference in the two stages of analysis. The first stage examines the linear response of the medium to the intensity of the recording light, i. e. the recording of the image. Fourier analysis is done with respect to three variables, and the transfer characteristic is the function $\hat{\kappa}(k_x, k_y, \omega)$, while the response function is $\Delta\hat{P}(x, y, t)$. In readout, the transfer characteristic of the device is the function $\mathcal{H}(k_x k_y, t)$ (16), which depends on time as a parameter.

For experimental determination of $\kappa(k_x, k_y, \omega)$, blue light was used to record on the modulator an image of the form

$$F(x, y, t) = B(1 + m \cos k_x x \cos \omega t). \qquad (18)$$

The intensity of diffraction of He-Ne laser light was measured at the same time. Based on (17) and (18) we can easily find that the intensity of light in the first diffraction order is

$$\eta_{k_x, 0, \omega} = \frac{B^2 m^2}{16} |\kappa(k_x, 0, \omega)|^2. \qquad (19)$$

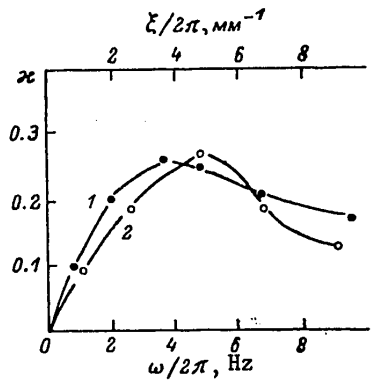

Fig. 8. Dependence of κ on temporal and spatial frequencies: 1--$\omega/2\pi = 2$ Hz; 2--$\xi/2\pi = 5$ mm^{-1}

Fig. 8 shows the values of $|\kappa(k_x, 0, \omega)|$ as a function of k_x at fixed ω and as a function of ω at fixed k_x for a modulator in which the (110) cut is used, and $k_x \parallel [110]$. It can be seen from the figure that the frequency response $\kappa(k_x, 0, \omega)$ vanishes at $\omega = 0$, and increases linearly at small ω. This type of behavior of the frequency characteristic means that the PRIZ modulator in the given mode of operation does not transfer null temporal frequencies, i. e. steady-state images, but ensures continuous isolation of unsteady parts of the image, thus realizing dynamic image selection. At small ω in the 0-3 Hz range, the operation of dynamic selection coincides with differentiation of images with respect to time.

REFERENCES

1. Kompanets, I. N., Parfenov, A. V., Popov, Yu. M., Preprint No 114, Physics Institute imeni P. N. Lebedev, Moscow, 1979.

2. Grenot, M., Pergrale, J., Donjon, J., Marie, G., APPL. PHYS. LETT., Vol 21, 1972, p 83.

3. Oliver, D. S., OPT. ENG., Vol 17, 1978, p 288.

4. Petrov, M. P., Khomenko, A. V., Berezkin, V. I., Krasin'kova, M. V., MIKROELEKTRONIKA, Vol 8, 1979; Khomenko, A. V., Petrov, M. P., Krasin'kova, M. V., PIS'MA V ZHURNAL TEKHNICHESKOY FIZIKI, Vol 5, 1979, p 334; Petrov, M. P., Khomenko, A. V., Berezkin, V. I., Krasin'kova, M. V., FERROELECTRICS, Vol 22, 1978, p 651.

5. Sonin, A. S., Vasilevskaya, A. S., "Elektroopticheskiye kristally" [Electro-Optical Crystals], Atomizdat, Moscow, 1971.

6. Mustel', Ye. R., Parygin, V. N., "Metody modulyatsii i skanirovaniya sveta" [Methods of Light Modulation and Scanning], "Nauka", Moscow, 1970.

7. Petrov, M. P., Marakhanov, V. I., Shlyagin, M. G., Khomenko, A. V., Krasin'kova, M. V., ZHURNAL TEKHNICHESKOY FIZIKI, Vol 50, 1980, p 1311.

8. Shirman, Ya. D., "Razrezheniye i szhatiye signalov" [Expansion and Compression of Signals], "Sov. radio", Moscow, 1974.

9. Petrov, M. P., Khomenko, A. V., Marakhanov, V. I., Shlyagin, M. G., PIS'MA V ZHURNAL TEKHNICHESKOY FIZIKI, Vol 6, 1980, p 385.

6610
CSO: 1862/54

PLASMA PHYSICS

UDC 533.93/.95

RADIATION RELATIVISTIC GAS DYNAMICS OF HIGH TEMPERATURE PHENOMENA

Moscow RADIATSIONNAYA RELYATIVISTSKAYA GAZODINAMIKA VYSOKOTEMPERATURNYKH YAVLENIY in Russian 1981 (signed to press 6 Feb 81) pp 2-4, 87-88

[Annotation, foreword and table of contents from book "Radiation Relativistic Gas Dynamics of High Temperature Phenomena", by Vladimir Sergeyevich Imshennik and Yuriy Ivanovich Morozov, Atomizdat, 1065 copies, 88 pages]

[Text] On the basis of relativistic covariant equations of radiation transport, which include processes of absorption and scattering of photons in matter, the authors derive various approximations of radiation relativistic gas dynamics: radiative heat conduction with local thermodynamic equilibrium, nonequilibrium Thomson coherent scattering of photons and Compton scattering of photons. Expressions are obtained for the energy-radiation pulse tensor. Diffusion approximations of radiation relativistic gas dynamics are examined. The authors derive completely closed nonrelativistic diffusion equations of Compton radiation gas dynamics which generalize the ordinary approximation of radiative heat conduction for the case when photon scattering processes predominate.

The book is intended for scientific workers in the fields of high-temperature-plasma physics and relativistic astrophysics. It can be used by graduate students and senior course students in physics.

The bibliography contains 49 references.

Foreword

Relativistic effects during the movement of a gas interacting with occurrent radiation play a very substantial role in many problems of high temperature gas dynamics. Equations of radiation relativistic gas dynamics must be employed in order to take these effects into account when diverse physical phenomena with a high energy density are being investigated. One can mention in this case powerful electrical discharges in plasma of the plasma focus type and compression and heating of targets by laser radiation, relativistic electron beams or beams of high-energy heavy ions. For phenomena like these it is necessary to account for such effects as the part radiation plays in pulse transport, the effect of macroscopic movement of matter on radiation transport of energy, the influence of various effects of interaction between radiation and matter on gas dynamic characteristics of movement and so on. Especially important is the consideration of relativistic effects in a number of

astrophysics problems, such as the propagation of strong shock waves in stellar envelopes toward the star surface, typical in the gravitational collapse of stars and in supernovae outbursts; high-speed fluxes of matter in the surface layers of stars and the sun, of the stellar wind and solar wind type; the development of flare activity of the sun and stars and so on.

A detailed, comprehensive investigation of these problems necessarily touches upon a broad range of questions of a theoretical nature which call for a well-grounded presentation on the method used to obtain approximations of the equations of radiation gas dynamics in relativistic covariant form, and on their merit and limits of applicability.

The basis for the study of radiation transport in a medium moving at relativistic velocities was set forth in the classic work of Thomas [1]. Cited works [2-6] are devoted to various forms of covariant formulation of the Thomas equations within the framework of the special theory of relativity. In the work of Lindquist [7], equations of relativistic radiation gas dynamics are obtained in a general covariant form which holds for general relativity theory. Characteristic of the works along this line is that most of them rely on the representation of radiation in the form of a photon gas and on the use of the Boltzmann equation, whereby the effects of the radiation's interaction with matter are viewed phenomenologically--in terms of the coefficients of radiation absorption and scattering, the effective opacity of the medium and the function of the source. This approach enables linking the relativistic covariant description of the effects of radiation-matter interaction with the well developed formalism of classical transport theory. Moreover, for many practically important cases it enables finding effective methods of solving the equations using angular and spectral moments of the radiation's intensity.

However, many aspects of relativistic radiation gas dynamics which are important in regard to high-temperature media are treated inadequately or not rigorously enough in the pertinent literature. This is particularly so as concerns coverage of the role of radiation scattering effects, which are a governing factor for certain processes occurring in such media. It addition, it is necessary to mention the rather complicated way of deriving relativistic covariant equations of radiation gas dynamics which relies in certain cases [7] on a mathematical apparatus scarcely accessible to a lot of physicists. Meanwhile, a simple and effective method of obtaining the equations of radiation relativistic gas dynamics using widely known formal procedures of special relativity theory is entirely feasible, a method which enables properly allowing for a number of important effects described at present on the basis of a specific tetradic formulation of general relativity theory.

The purpose of this book is to simply and comprehensibly set forth certain complex problems of the radiation relativistic gas dynamics of high temperature phenomena and to formulate the equations of radiation relativistic gas dynamics in a number of practically important approximations.

Contents

5454
CSO: 1862/29

STRESS, STRAIN AND DEFORMATION

UDC 534.222.2

CALCULATING INTERNAL STRUCTURE OF DETONATION WAVE

Moscow DOKLADY AKADEMII NAUK SSSR in Russian Vol 260, No 5, 1981 (manuscript received 23 Apr 81) pp 1154-1157

[Article by S. K. Aslanov and O. S. Golinskiy, Odessa State University imeni I. I. Mechnikov]

[Text] It has been experimentally shown [Ref. 1-3] that the detonation propagation process has a pulsation structure. This is explained by instability of the detonation wave relative to unsteady perturbations that curve its wavefront and result in formation of Mach configurations there. Their complete calculation, in particular determination of the frequency Ω of appearance of the configurations and the size Δy of inhomogeneities that they generate must be based on nonlinear analysis of perturbations. Such an approach to investigation of stability runs up against serious analytical difficulties. Therefore we will try in this paper to find estimates for the principal structural elements Ω and Δy of the detonation wave on the basis of linear stability theory. While this theory cannot lay claim to any final conclusions, nonetheless the quantitative estimates that it yields explain some known experimental factors.

In studying detonation stability relative to perturbations $\sim\exp(\beta x + ihy - i\omega t)$, Ref. 4 used the Zel'dovich model [Ref. 5, 6] with chemical kinetics of the delta function type $\delta(t-\tau)$. To solve the equation derived in Ref. 4 relative to ω, we use the hypersonic asymptotic form of Ref. 7, which gives a good approximation up to shock-wave Mach numbers $M_0 \gtrsim 3$. By taking the number M_1 in the induction zone [Ref. 8] as a small parameter, we obtain for analysis of instability the dimensionless form of expansion of the eigenvalue $\zeta = \zeta_0 + \zeta_1 M_1^2 + \ldots$ ($\zeta = i\omega\tau$, τ is the induction period) and an equation relative to principal term ζ_0 of the following form:

$$(1) \quad e^{-\zeta_0} F + \Phi = 0,$$

F, Φ are algebraic functions of ζ_0, E/RT, ξ, M_0, M_g, κ_1, κ_2, where $\xi = hL = 2\pi L/\lambda$, $L = V_1\tau$, E is the activation energy, R is the gas constant, T is temperature, V is velocity, κ is the ratio of specific heats, λ is the perturbation wavelength (Fig. 1), L is the thickness of the detonation front, subscripts 1 and 2 refer to gasdynamic quantities of the induction zone and detonation products.

The transcendental factor $e^{-\zeta_0}$ shows the presence of a vibrational spectrum of unstable pertturbations expressed by an infinite sequence of complex roots $\zeta_0 = a + ib$.

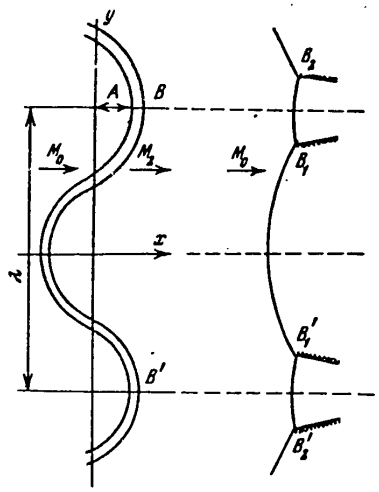

Fig. 1

Depending on the value ξ of the geometric dimension of the perturbation, two types of instabilities may develop on the front: one-dimensional ($\xi = 0$) and two-dimenaional ($\xi \neq 0$). The former is associated with the predominantly one-dimensional nature of initial perturbations and the galloping mode of propagation of the process. The frequency spectrum for this case was studied in Ref. 8.

The two-dimensional type of instability is associated with development of curvatures of the detonation front and arisal of breaks there formed by Mach configurations that ignite the mixture in the transverse direction. Generally speaking, perturbations may take place in this process with arbitrary value of the parameter $\xi \neq 0$. However, such breaks should be generated primarily by the perturbation that develops with accompanying maximum curvature of the detonation front. This curvature is determined both by the initial level of the perturbation and by its wavelength λ. The only way to determine the parameter figuring in equation (1) is from the standpoint of the overall average level for principal initial perturbations.

The quantative characteristic of the curvature that the perturbed front acquires in time t is the ratio of the amplitude of its displacement $A(t) \sim \exp[\mathrm{Re}(-i\omega t)]$ to the dimension of the given perturbation $\lambda \sim 1/\xi$ (Fig. 1). With reference to the curvature of the detonation wave as a whole (as a wavefront), it makes sense to consider time intervals at least as long as the characteristic time τ of the process. It is to this parameter that we refer the characteristic curvature of the detonation front introduced above, which in the logarithmic scale takes the form $c(\xi) = a + \ln \xi$. Then the maximum of $c(\xi)$ uniquely determines the quantity ξ_m, i. e. the wavelength λ_m of the perturbation with the most rapidly increasing curvature of the wavefront, reaching its maximum value at points B (B'). It is precisely in the vicinity of such points that we should primarily expect the breaks B_1, B_2 (B_1', B_2') as perturbations develop, with formation of the triple configurations experimentally observed by the wake and optical method [Ref. 1-3]. Numerical analysis has shown that the maximum of $c(\xi)$ is weakly sensitive to selection of the time interval.

Solution of equation (1) has been numerically confirmed on a computer with initial isolation of roots for the limiting case $\xi = 0$. The calculations were done on the basis of the example of detonations in a mixture of $2H_2 + O_2$ (κ_1=1.4, κ_2 = 1.3, T_0 = 293 K) for the following cases: 1) self-maintained mode M_2 = 1 at p_0 = 760, 300, 100 and 45 mm Hg; 2) overdriven mode (oblique Mach wave at the tip of the spin nucleus for p_0 = 45 mm Hg [Ref. 3]), M_0 = 6.05, M_{0n}=5.88, M_{2n} = 0.553.

Activation energy E was taken as 18 kcal/mole [Ref. 9, 10], the speed of sound in the initial mixture was 514 m/s, and the detonation rate was based on experimental dependence on p_0 from Ref. 3.

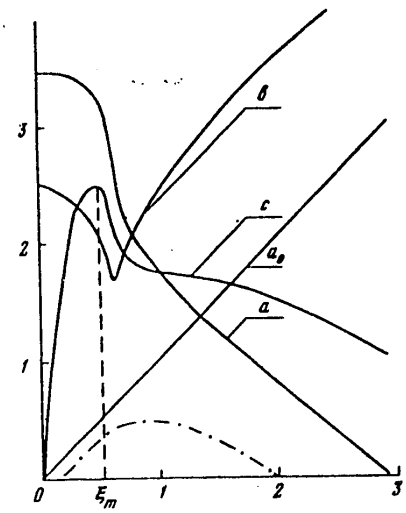

Fig. 2

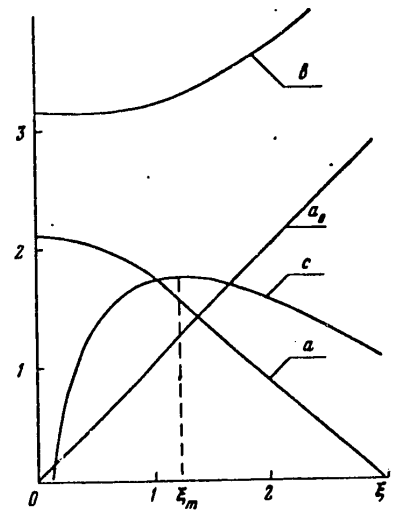

Fig. 3

Results of calculation are given only for characteristic cases: $p_0 = 760$ and 45 mm Hg. Accordingly, Fig. 2 and 3 show curves for the distribution with respect to wave number ξ of the fundamental harmonic of the eigenvalue $\zeta_0(a, b)$, as well as the only real root a_0 of equation (1) that is associated with aperiodic instability, and the value of $c(\xi)$. The dot-and-dash curve of $a(\xi)$ for overdriven compression given for comparison on Fig. 2 clarifies the experimentally observed stabilizing action of this mode on the detonation process.

The value of ξ_m found in each case corresponds to a certain value of the frequency parameter $\nu_0 = b/(2\pi\tau)$ that characterizes the frequency Ω of appearance of inhomogeneities in the detonation front. Their average dimension Δy can be estimated by using $\lambda_m/2$, since Fig. 1 shows that an average of two Mach configurations (B_1', B_2') develop over the extent of one wavelength.

Determining T_1 from the enthalpy of the shock-compressed mixture [Ref. 3], and using experimental values of τ recalculated for the pressure of the mixture ($\tau \sim 1/p_1$) [Ref. 9], we get the following final results. For $p_0 = 760$ mm Hg ($M_0 = 5.45$; $\tau = 2 \cdot 10^{-7}$ s): $\xi_m = 0.5$; $b = 1.95$, i. e. $\lambda_m/2 = 0.68$ mm and $\nu_0 = 1.5$ MHz. Data of experiments [Ref. 3, 9]--$\Delta y = 0.6$ mm and $\Omega = 1.3$-1.4 MHz. For $p_0 = 300$ mm Hg ($M_0 = 5.25$; $\tau = 7.2 \cdot 10^{-7}$ s): $\xi_m = 0.57$; $b = 2.33$, i. e. $\lambda_m/2 = 2.1$ mm and $\nu_0 = 0.52$ MHz for experimental $\Delta y \cong 1.8$ mm and $\Omega = 0.4$-0.5 MHz. At $p_0 = 100$ mm Hg ($M_0 = 4.55$; $\tau = 5 \cdot 10^{-6}$ s): $\xi_m = 1.05$; $b = 3.04$, i. e. $\lambda_m/2 = 7.3$ [mm], and $\nu_0 = 92$ kHz (experiment $\Delta y = 6.6$ mm; $\Omega = 85$ kHz).

In case $p_0 = 45$ mm Hg ($M_0 = 4.28$; $\tau = 1.4 \cdot 10^{-5}$ s), $\xi_m = 1.23$; $b = 3.3$, i. e. $\lambda_m/2 = 16.7$ mm, and $\nu_0 = 39$ kHz. The initial data for this case correspond to the spin mode in a tube 16 mm in diameter, with experimentally observed spin frequency of 44 kHz. The interesting fact that $\lambda_m/2$ remains close to the diameter and is greater than the diameter is evidence of the possibility that a single break may exist in the cross section of the tube, which ensures spin detonation.

With a further reduction in the initial parameters of the mixture (beyond the region of the spin mode), τ rises rapidly, and a slight change in ξ_m ensures a strong increase in λ_m, which may considerably exceed the diameter of the tube as the characteristic transverse dimension of the wavefront. If the detonation limits are not reached in this case, the instability becomes one-dimensional, resulting in galloping of the process with periodic pulsation of extinguishing and ignition of the mixture behind the shock wave (with frequency ν_0 at $\xi = 0$).

Thus we have shown on the basis of the phenomenological theory developed above that each set of parameters of the initial fuel mixture, and in particular the value of the initial pressure p_0, has a definite natural frequency that characterizes the internal pulsation structure of the detonation wave and the size of the inhomogeneities that develop there.

The authors are sincerely grateful to Ya. B. Zel'dovich for constructive discussions of the work and useful remarks.

REFERENCES

1. Denisov, Yu. N., Troshin, Ya. K., DOKLADY AKADEMII NAUK SSSR, Vol 125, No 1, 1959, p 110.

2. Voytsekhovskiy, B. V., Kotov, B. Ye., Mitrofanov, V. V., Topchiyan, M. Y., IZVESTIYA SIBIRSKOGO OTDELENIYA AKADEMII NAUK SSSR, No 9, 1958, p 44.

3. Shelkin, K. I., Troshin, Ya. K., "Gazodinamika goreniya" [Gasdynamics of Combustion], Izdatel'stvo AN SSSR, Moscow, 1963, p 44.

4. Aslanov, S. K., DOKLADY AKADEMII NAUK SSSR, Vol 163, No 3, 1965, p 667.

5. Zel'dovich, Ya. B., ZHURNAL EKSPERIMENTAL'NOY I TEORETICEHSKOY FIZIKI, Vol 10, 1940, p 542.

6. Zel'dovich, Ya. B., Kompaneyets, A. S., "Teoriya detonatsii" [Detonation Theory], Gostekhizdat, Moscow, 1965.

7. Chernyy, G. G., "Techeniye gaza s bol'shoy sverkhzvukovoy skorost'yu" [Gas Flow at High Supersonic Velocity], Fizmatgiz, Moscow, 1969, pp 1-5.

8. Aslanov, S. K., DOKLADY AKADEMII NAUK UKRAINSKOY SSR, Series A, No 4, 1977, p 313.

9. Shchetinkov, Ye. S., "Fizika goreniya gazov" [Physics of Combustion of Gases], Nauka, Moscow, 1965, p 129.

10. Soloukhin, R. I., "Udarnyye volny i detonatsiya v gazakh" [Shock Waves and Detonation in Gases], Fizmatgiz, Moscow, 1963, p 115.

6610
CSO: 1862/59

MISCELLANEOUS

SURVEY OF RESEARCH IN PHYSICS AND ASTRONOMY

Moscow USPEKHI FIZICHESKIKH NAUK in Russian Vol 134, No 3, Jul 81 pp 469-483, 512-517

[Table of contents, introduction, concluding remarks and bibliography from article by V. L. Ginzburg, Physics Institute imeni P. N. Lebedev, USSR Academy of Sciences: "What Problems of Physics and Astronomy are now of Particular Importance and Interest? (Ten Years Later)"]

[Excerpts] Table of Contents page

I. Introduction

In 1971 in the "Present-Day Physics" section of USPEKHI FIZICHESKIKH NAUK, an article [Ref. 1] was published with the same title as the present article, but of course without the subtitle ("Ten Years Later"). Ref. 1 was expanded into a small booklet that was subsequently translated into several languages, and has now been published in the Soviet Union in a third edition in 1980 [Ref. 2]. It seems to me that such a fate of Ref. 1 leaves no doubt that the formulation of the problem contained therein and its discussion is of real interest to many, and apparently primarily to young physicists and astronomers. At the same time, it is quite obvious that setting apart some small class of problems to be elevated to the ranks of those of special importance and interest is an arbitrary matter, and must not result in neglect of the enormous number of other problems. It is also clear that the author's selection is subjective, and no claim was then or is now made that Ref. 1, 2 are anything more than popular science articles. All this has been fairly well stated in Ref. 1, 2, and there is no need here to go into any more detail in developing these remarks. However, I should note the following: if Ref. 1 were being written from the start, in order to avoid irritating some readers (if we assume that everyone who has criticized the article has actually read it), a more neutral title would have been chosen (such as "Some Interesting and Important Problems of Physics and Astrophysics"). Unfortunately, from the very nature of this, the second article, it is impossible to change the title.

It is clear from the foregoing that for ten years the author in reworking Ref. 1 for new publications has been following the transformation of certain trends and topics in the area of physics and astrophysics. Thus in a natural way the idea has arisen of writing the present article, which has the purpose of reflecting the changes that have taken place in physics and astrophysics over the past ten years. But, of course, we are not speaking of physics and astrophysics as a whole, but rather principally only the problems discussed in Ref. 1. Therefore the organization of the article is as in Ref. 1, which singled out 17 problems; in Ref. 2 there were 21 areas, but some of them should have been broken down. On the whole, in this article we will deal with approximately 25 problems and scientific areas.

Finally, I would like to emphasize the following. This article is obviously not what physicists refer to as a "research paper", but neither is it a review of the literature. Therefore it should not be expected to meet requirements that are appropriate for other cases. For example, in the first place the author assumes that we can dispense with questions of priority in the article proper and in the list of references. Numerous names or citations of priority would be bothersome to the reader. Besides, time and again we have had to come to the conclusion that priority citations in the literature "adapted by repetition" are frequently inexact or even incorrect. And to undertake a special priority search with respect to the history of the numerous citations would be entirely out of place. Secondly, the author does not follow the "impersonal style" of exposition favored in scientific literature, especially in Russian. According to the tenets of this style, not only is it forbidden to use personal pronouns (I, me, etc.),

but the author must in general be hidden as far as possible from the eyes of the reader. I remember how L. D. Landau was always interrupting speakers who had started to say what they thought or assumed with the comment: "Don't forget, your wife is the only one interested in your biography." The impersonal style has come into being as a result of lengthy experience in the development of science and I consider it perfectly appropriate in scientific papers, surveys, monographs and textbooks (I daresay my own practice is no contradiction). But another matter entirely are journalistic articles, memoirs or articles like the one I am writing, and I wouldn't know what genre it belongs to. At any rate, this article is already "personal" in its very inception (i. e. it is subjective by definition), being devoted to my own idea of certain trends and directions in physics and astrophysics. I know some people who would find such an approach in itself inappropriate or immodest. Others disagree with many of my opinions. All this is their own business and their right. I would be the last to make any categorical claims regarding my opinions, and moreover I myself feel that some remarks of mine are quite controversial. I only reserve the right to have such opinions and not be afraid to express them. In such a situation, the author cannot and does not mean to "keep his innocence and still make a profit." Therefore I will have to use personal pronouns, and to some extent not hide my "biography." I very much hope that this form of exposition will not invoke a negative response on the part of readers.

II. Macrophysics

Macrophysics as a whole is grounded on a firm foudation (classical and quantum mechanics, classical and quantum electrodynamics, including the special theory of relativity). Therefore it is natural that the development of macrophysics in qualitatively new principles is taking place more slowly and less dramatically than in the case of microphysics and astronomy (including cosmology). To be sure, we anticipated events somewhat [see Ref. 1, 2] in putting nuclear physics in the category of macrophysics, as this field borders closely on microphysics. On the other hand, the general theory of relativity (having in mind Einstein's classical theory) is in its essence a part of macrophysics, but it operates in full force only in outer space, and is therefore discussed in the astrophysics section of the article. But even when we consider the advances in nuclear physics and general relativity theory over the past decade, macrophysics is not up to microphysics in quantity of profound and important new results. However, advances and results in science cannot be weighed out on scales, much of this progress being poorly commensurable anyway. Therefore we will not divide up "places" and will rather get on with the specific problems.

1. Controlled Nuclear Fusion

This problem has been dealt with for 30 years now. The initial "rosy optimism" was quickly replaced by what could often be taken as even pessimistic views after it was learned how capricious hot plasma could be, how difficult it is to contain in traps. But it gradually became clear that with careful control over the homogeneity of the magnetic field (to be more precise there must be no field inhomogeneities that are unforeseen in calculations), and also when heavier impurities are removed from a hydrogen plasma, various magnetic traps (tokamaks, stellarators and some others) operate in general in accord with expectations [Ref. 3a]. As a

result, there is no longer any doubt as to the possibility of success in systems with magnetic plasma containment. But to check calculations and overcome difficulties, it is necessary to build ever larger facilities. Naturally this requires considerable money, effort and time. Tokamaks are currently the favorite, but as far as I can judge, their superiority over, say, stellarators has not been demonstrated. Research is also continuing on "open" magnetic traps, called "mirrortrons" in the jargon. There is scarcely anyone who would try to assure us that open systems, in some ways the simplest and most convenient, will never be able to compete with toroidal facilities.

Over the past decade there has been an upsurge of interest in systems with inertial plasma containment involving micro-implosion of motes (droplets) of a mixture of deuterium $D \equiv d$ and tritium $T \equiv t$ (of course, we cannot rule out the use of pure D as well in the future). In principle, the initial implosion of the mote can be accomplished by light (lasers) and by electron and ion beams [Ref. 3b]. Electrons are especially difficult to use, at the present time laser systems have been most thoroughly studied, and interest in the use of ion beams is increasing. Unfortunately, as in the case of magnetic traps, generally speaking, very large facilities are needed for studying the capabilities of the "inertial thermonucleus." In general, research on possibilities of controlled nuclear fusion in the seventies has to a greater extent than formerly turned from a physical problem simultaneously into an engineering problem of industrial scale. However, physics is still leading as competition goes on between rival principles and methods of plasma containment, and no operating reactor that delivers power has yet been produced on any of the roads being taken.

2. High-Temperature Superconductivity

This problem was formulated, at least on modern principles, in 1964. The purpose is clear: to develop or find superconductors or some kind of inhomogeneous superconducting "components" that would remain superconductive at least at the temperature of liquid nitrogen $T_{b,N_2} = 77.4$ K (the boiling point of nitrogen at atmospheric pressure). However, the state of superconductivity theory, despite its enormous advances in certain directions, is still not such that it could predict the critical temperature of superconductive transition T_c for more or less complicated compounds or dielectric-metal-dielectric "sandwiches." Therefore, any recommendations that can be made with respect to the search for high-temperature superconductors are qualitative and not overly precise. To some extent under the influence of these recommendations (exactly to what extent it would be hard to say), a fairly large number of quasi-one-dimensional and laminar (quasi-two-dimensional) compounds have been synthesized, and several new superconductors have been found. But so far (with a stipulation relative to CuCl and CdS that will become clear from the following) the compound Nb_3Ge has the highest critical temperature of $T_c \approx 23.2$ K, which was learned in 1973. At the same time, we must point out that the search for new superconductors has turned up such interesting results as the discovery of metallic conductivity (and superconductivity with $T_c \approx 0.3$ K) in polymeric sulfur nitride $(SN)_x$, which obviously does not contain metal atoms. In 1980, superconductivity was discovered in the organic crystal ditetramethyltetraselenafulvalene-hexafluorophosphate $[(TMTSF)_2PF_6]$. To be sure, this crystal has metallic conductivity at low temperature, as well as superconductivity with $T_c \sim 1$ K, only under pressure of several kilobars [Ref. 4]. Nonetheless, we are apparently

dealing with a new class of metals and semiconductors since it is known to be comparatively easy in some cases to vary organic compounds. Besides, there are certain grounds for expecting attainment of rather high critical temperatures for organic compounds [Ref. 5]. Of course, no guarantee of success can be given in this respect, but the occurrence of a new class of superconductors is of interest even if they are low-temperature superconductors. Also worthy of mention here are experiments that have led to the conclusion of superconductivity in sulfur (S) under high pressure and with specific pressure treatment, T_c lying in a range of 26-31 K [Ref. 6].

Returning directly to the problem of high-temperature superconductivity, it must be noted that theoretical analysis gives no grounds for rejecting the possibility of existence of equilibrium (or perhaps metastable) materials with $T_c \lesssim 300$ K. At the same time, it is clear that rather severe conditions must be met to attain critical temperatures $T > T_{b,N_2} = 77.4$ K, and no guarantee of success can be given. In this area we must try, seek, check out all new materials, sandwiches and so on for superconductivity.

It is possible that success has already been achieved on this path. In 1978 there were reports [Ref. 7] of "superdiamagnetism"* in appropriately prepared copper chloride (CuCl) held under a pressure of several kilobars. The "superdiamagnetism" effect was observed at temperatures exceeding 150-200 K. Whether the observed effect is genuinely new, or is a result of experimental error or simulation of real superdiamagnetism is unfortunately not yet quite clear. If superdiamagnetism in CuCl has actually been observed, it might have been due to the occurrence of a high-temperature superconductive phase, possibly arising in principle upon transition of certain semiconductors or semimetals to the superconductive state [Ref. 5, chapter 5]. Another possibility is the formation of "sandwiches" of Cu and CuCl, or the occurrence of true surface conductivity [Ref. 8]. However, another entirely different hypothesis has been suggested: apparently there may be substances of a type as yet unknown with spontaneous currents that must have superdiamagnetism, but are different from ordinary superconductors [Ref. 8]. The latter possibility is not yet quite clear even in its theoretical formulation, to say nothing of experiment. However, it must be noted that even though further investigation of CuCl has not cleared up the problem, high-temperature superdiamagnetism in this material has nevertheless been confirmed by one other laboratory under conditions that are so far unclear [Ref. 9]. The difficulty of getting a clear idea of the behavior of CuCl is nothing exceptional, as I feel is rightly pointed out in the survey of Ref. 10. There are precedents for complications of this kind (e. g. in the case of some semiconductors) when dealing with materials that have properties difficult to control. And here the problem may be impurities, or

*A sufficiently weak magnetic field does not penetrate deep into an ideal superconductor (this property is called the Meissner effect). Formally, it can be stated that in the case of the Meissner effect, the magnetic susceptibility, just as for an ideal diamagnetic material, is $\chi_{id} = -1/4\pi$. In ordinary diamagnetic materials $\chi \sim 10^{-4}$-10^{-6}. I call superdiamagnetics (appropriately, I believe) those materials for which χ is comparable with $\chi_{id} = -1/4\pi$, let us say if $\chi \sim (0.01$-$0.1)$ times $1/4\pi$. Although superconductors are superdiamagnetics, the reverse may not be true, i. e. superdiamagnetism may not necessarily be accompanied by superconductivity (in the sense of zero resistance to flow of electric current) [Ref. 8].

various lattice defects or residual stresses. Therefore it is not at all ruled out that high-temperature superconductivity is what has been observed in CuCl.

And moreover, in 1980 a strong diamagnetic effect analogous to that described for CuCl was observed at liquid nitrogen temperature (T_{b,N_2}=77.4 K) in CdS crystals treated by the method of pressure quenching. In this technique, a pressure of about 40 kbar was relieved at a rate of greater than 10^6 bar/s [Ref. 11]. No details are given in the article on the method used for preparing the specimens (which might be attributable to the worksite of the authors--U. S. Army Armament Research and Development Command, Large Caliber Weapons Systems). Doubtless the result for CdS raises interest both in CuCl and generally in any still totally enigmatic mechanism of high-temperature superdiamagnetism.

The search for high-temperature superconductors, in contrast to studies in the area of controlled nuclear fusion, does not require building gigantic facilities. Therefore success may come in a small laboratory and be a complete surprise to other physicists. Moreover, perhaps such success has already been achieved in the case of CuCl and CdS. If this is actually the case, we can assume that there is the brightest outlook for obtaining and studying high-temperature superconductors.

3. New Substances (Problem of Creating Metallic Hydrogen and Some Other Substances)

Development of new materials is usually the province of material science or chemistry. But the situation changes when dealing with materials like metallic hydrogen. Without argument, this is a physics problem, and the solution is unknown.

There is no doubt that a metallic phase of hydrogen exists at pressures exceeding 1.5-2 Mbar. Probably metallic hydrogen will be superconductive at high temperatures ~100-200 K, which makes this metal even more interesting. The literature has already mentioned production of metallic hydrogen (see bibliography of Ref. 2), but on the whole the question is not clear. Specifically, it is not completely certain that the metallic phase of hydrogen has actually been observed, and most importantly its properties (in particular with respect to superconductivity) still remain admittedly unknown. The main difficulty involves setting up pressures greater than 2-3 Mbar. This can easily be done by using shock waves, but generally speaking this is accompanied by heating, to say nothing of the difficulties of measuring a number of parameters of the metal in a very short time. On the other hand, under quasi-equilibrium conditions the necessary pressure can be produced by simple presses in small volumes (between miniature anvils), but there are no suitable materials for doing this. Even diamond begins to "flow" at such pressures [Ref. 12]. Apparently a new approach is needed here. One way or another, it is still a long way off before we make a "piece" of metallic hydrogen.

As another example of an "exotic" material, Ref. 1 mentioned anomalous (superdense or polymeric) water, whose existence was being widely debated in the literature at that time. For this reason, it was remarked in Ref. 1 that "the question must be considered open, although in my opinion, research [references to the literature were given here--*V. G.*] does not offer much hope for the existence of pure polymeric (superdense) water. But regardless of the final outcome, studies

that have already been done clearly show how difficult it is to solve even such a problem as the possibility of occurrence of a new phase of one of the most widespread substances... This example is instructive in many respects, in particular as a reminder that any discovery should be considered finally established only after repeated and comprehensive verification."

This quotation, expressing doubt in the existence of anomalous water, even though the question as a whole was considered open, prompted some authors of papers on anomalous water to write to USPEKHI FIZICHESKIKH NAUK (special letter, Vol 105, 1971, p 179). In this letter I was advised "not to draw hasty negative conclusions that may be tempting because of simplicity, but are based on incomplete, biased and uncritical use of literature on the question." However, just a short time has elapsed, and the question on anomalous water has been "closed": it turns out that the liquid being studied was ordinary water containing a number of impurities.

I have taken up this episode here only because I wanted once more to emphasize how important it is to verify experimental data from many aspects, particularly when far-reaching conclusions are being drawn on the basis of such data. The authors of pertinent papers are right to publish them, for they risk more than anyone else in so doing. In addition to being objective, it is still more important that the publication permits more rapid verification in other laboratories. Therefore, in my opinion one should not severely denounce (as is sometimes done) authors who have published incorrect work if, of course, they have made a mistake in good faith, and their experiments have been done on the whole at a proper level. But by the same token, no one has a right to demand that "discoveries" be recognized as such before they have been confirmed in several places. Within reasonable limits, authors have a right to err; but those around them have no less of a right to be dubious.

4. Metallic Exciton (Electron-Hole) Liquid in Semiconductors

In Ref. 1, the topic of this section was set apart from others in the field of semiconductor physics, and I feel that there were grounds for doing this. But now the problem has been basically solved (or, if you will, "earned our confidence"): metallic exciton liquid has been created in semiconductors and to a great extent has been studied. This problem has even been covered in a special monograph [Ref. 13a] that came out in the English original in 1977. To be sure, the situation is far from complete (but this can be said in nearly all cases); some essentially new problems have arisen (involving quasi-one-dimensional and quasi-two-dimensional semiconductors; see Ref. 2 and the literature cited there). Nonetheless, we would scarcely be justified today in citing the problem of metallic exciton liquid as the sole representative of semiconductor physics and almost all of solid state physics. Metal-dielectric phase transitions and disordered semiconductors are of great interest and are being studied on a broad front [Ref. 13b]. We could also mention here the so-called spin glasses and quantum crystals, as well as laminar and straight-chain compounds (materials).

5. Phase Transitions of the Second Kind (Critical Pressures). Some Examples

Strictly speaking, phase transitions are not a single problem, but something broader. To be sure, since all phase transitions have common features, we can

single out a general theory of phase transitions. In such a theory, typical transitions of the first kind in which (and near which) the thermodynamic potentials of phases have no singularities, are in no way remarkable (unless we are dealing with superheating and supercooling, formation of nuclei and the kinetics of transitions). But transitions of the second kind, transitions of the first kind that are close to them (having in mind for example a fairly low latent heat of transition, which is zero for transitions of the second kind) and critical points do have singularities, and have attracted considerable attention for a long time. To be sure, the singularity in the thermodynamic potential is by no means always sharply pronounced, and in a number of cases (as an example for the transition to the superconducting state, and usually for magnetic and ferroelectric transitions) a fairly simple theory is applicable in which fluctuations are disregarded and the singularity is ignored. Such an approach, which can be traced back to van der Waals, Weiss and others, was systematically developed by Landau, and is frequently called the Landau theory of phase transitions [Ref. 14]. The fact that such a theory diverges from experiment near the critical point in a liquid was noted even at the turn of the century [Ref. 15a]. A clear example of a transition to which the Landau theory cannot be applied is the λ-transition in liquid helium (meaning the transition HeI⇄HeII in liquid ^{4}He).

The creation of a theory of phase transitions of the second kind and critical phenomena that properly accounts for fluctuations and generally enables description at least in principle of all real transitions, has turned into one of the most fundamental problems of the physics of condensed media. The task has been formidable. Nevertheless, even in the sixties some progress was made, and this success has been reinforced in the past decade. The introduction of so-called critical indices, the use of gage invariance hypotheses, the development of rather powerful methods of approximate calculation of critical indices in combination with numerous more exact measurements of different quantities close to transition points--all has brought about a considerable advance in the theory of phase transitions. Since the principal achievements of theory in this field have been reflected in the theoretical physics course of Ref. 14a (see also Ref. 14b), we will not take them up here.

The problem that we must not overlook here is as follows: to what extent can the theory of phase transitions at the present time be considered basically complete? Of course, the answer to this question does not at all demand the capability of exact calculation, say, of the critical indices--any exact calculation of specific constants or coefficients in the field of physics of the condensed state is the exception rather than the rule. But certainly we ought to be able to ask that the theory give us the capability of unified examination of all thermodynamic and kinetic processes and phenomena in the near vicinity of a transition point. In this connection, the coefficients in the corresponding equations can be matched within certain limits on the basis of experimental data. If we approach the theory of phase transitions even with such somewhat constraining requirements, we cannot but acknowledge that this theory is still far from complete. Without going into kinetics, even in the thermodynamic aspect when using critical indices, the questions of the region of applicability of given limiting laws with increasing distance from the transition point frequently remain unanswered.* But the main

*For example, the density of the superfluid part of HeII near the λ-point, which corresponds to temperature T_λ, is written in the form $\rho_s(T)=\text{const}(T-T_\lambda)^2\beta$,

point is that the theory is usually limited to homogeneous medium, whereas there are numerous cases that are of interest in which there are granules or defects, inhomogeneous external fields are present, and so on. Finally, there are a number of kinetic and dynamic problems (flow in liquid crystals and in helium, propagation of sound, relaxation of some quantities) that must be solved even near the phase transition point, and in fact are of particular interest just when they are close to this point. In the light of such natural requirements, the imperfections in the theory of phase transitions are particularly glaring. This can be seen specifically in research on superfluidity in helium II near the λ-point [Ref. 16], although in this case the theory has apparently advanced further than in other areas.

Thus the problem of phase transitions remains outstanding and significant within the framework of development of the general theory as well. But in addition to this, the problem pertains to some extent both to specific transitions, and to some phenomena near transition points. An example of such phenomena is light scattering that has a number of interesting peculiarities close to transition points [Ref. 17]. The same thing can be said about scattering of x-rays and neutrons.

As to individual phase transitions, or even transitions in a whole class of substances, the past decade has indeed brought much that is new. Let us mention here the "disproportionate" phases in ferroelectric and magnetic materials [Ref. 15b], phase transitions in liquid crystals, quasi-one-dimensional and quasi-two-dimensional materials, phase transitions on a surface, phase transitions in liquid ^{3}He and in atomic hydrogen. A separate article could and should be devoted to each of these questions, as has already been partly done in the pages of USPEKHI FIZICHESKIKH NAUK and other journals. Therefore, I shall not even attempt to explain anything with regard to all the enumerated cases, but will restrict myself to a few comments on liquid ^{3}He and atomic hydrogen (however, see section 6 below).

The possibility that "pairs" of two atoms with integral spin might be formed in liquid ^{3}He (as occurs in superconductors) has a long history of discussion. The formation of pairs with integral spin and their subsequent Bose-Einstein condensation should lead to superfluidity analogous to superconductivity (as we know, superconductivity can be considered as superfluidity of a charged electron fluid in metals, or of a proton fluid in neutron stars). However, theoretical attempts have been unsuccessful in getting reliable estimates of the temperature of superfluid transition, and experimental results have been in large measure unexpected. For example it was found in 1972 and 1973 [Ref. 18] that not just one, but two phase transitions occur in liquid ^{3}He (albeit at a pressure exceeding 34 atm) at temperatures of approximately $2.6 \cdot 10^{-3}$ and $2.0 \cdot 10^{-3}$ K respectively. Then it was learned that it was a matter of transition to superfluid states differing from one another in the total angular momentum of "pairs". The attraction leading to pair formation is apparently mainly exchange interaction (forces of the same type lead to ferromagnetism). Studies of superfluidity and other effects in liquid ^{3}He (and we should say that this isotope is quite rare; its occurrence in nature

---

where the critical index β is close to 1/3 (experimental data imply $2\beta = 0.67 \pm 0.01$). But what is the accuracy of such an expression for $\rho_s(T)$, especially with increasing distance from the λ-point?

is several orders of magnitude less than that of isotope ^{4}He) that have been done in recent years are striking in their subtlety and scope [Ref. 18]. After all, this work involves temperatures less than 3 mK away from absolute zero, and an object (superfluid ^{3}He) distinguished by great complexity (compared with superfluid ^{4}He) due to the presence of orbital and spin moments. I am inclined to think that in the physics of condensed media the advances in research on liquid ^{3}He are perhaps the most impressive over the last ten years.

Let us also take up the possibility of superfluid transition in atomic hydrogen gas, since this example is fairly interesting, although apparently of much less general physical significance than transitions in ^{3}He. Atomic hydrogen gas, if it is somehow produced, under ordinary conditions is rapidly converted to molecular hydrogen gas (H_2). However, atomic hydrogen gas can "last" for several minutes at a low temperature $T \lesssim 1$ K in a vessel whose walls are covered with superfluid helium II. And if the gas in addition is held in a fairly strong magnetic field, the stability of atomic hydrogen is enhanced [Ref. 20], and apparently under attainable conditions we can disregard recombination (the reason for this is well known: in the H_2 molecule the spins of the electrons are directed opposite to one another; in a strong magnetic field the spins of all electrons are in the same direction, and to form the H_2 molecule the spin of one of the atoms must be flipped, which is not easy to do). Atoms of H with parallel spins in the ground state repel one another (more precisely, there is some van der Waals attraction between atoms at great distances, but it is weak). Therefore such a gas at atmospheric pressure is not liquefied right down to absolute zero. At the same time, in a Bose gas of H atoms at low temperature depending on its density, Bose-Einstein condensation should take place, and the resultant phase should be superfluid (here it is significant that the gas is not ideal, and accounting for the corresponding interaction is what leads to superfluidity).

There is no doubt that the problem of phase transitions on the whole remains one of the main directions in physics.

6. Surface Physics

The physics of surfaces and of various processes and effects on a surface has been under study and development for more than a decade. It is already clear from quite general considerations that atoms and electrons on and near a surface are under different conditions than in the volume, and therefore there are grounds for assuming that on the surface there may be new phases, different transitions between these phases, new types and branches of excitations, and so on. In this connection, "new" is understood to mean phases and excitations different from those that are volumetric. For example on the surface (including the thin layer near the surface), the crystal lattice may have another structure and/or parameters, there may be magnetic ordering in the surface layer that is absent in the volume at a given temperature and so on. The possibility of propagation of a variety of surface waves is also known (acoustic waves, polaritons, magnons) [Ref. 21]. Closely related are the properties of thin films and layers, especially monomolecular layers, as well as the question of surface behavior of individual atoms, molecules, defects and inhomogeneities.

Nonetheless, ten years ago in Ref. 1 there was no section on surface physics, and although it did show up later in Ref. 2, it was quite modest. It is, of course,

debatable whether such inadequate attention to surface physics was justified in Ref. 1 and the booklet [Ref. 2]. And the same applies to a number of other problems that have been set apart here. But one way or the other, special mention and emphasis of the role of surface physics at the present time is absolutely necessary. The reason in general is that in recent years what has seemed merely possible is becoming a reality because of progress in experimental techniques. We have learned, at least in some cases, how to produce a clean surface and check its state (degree of roughness and the like), methods have been newly developed or considerably improved for studying the surface and near-surface layer, atoms on the surface and surface inhomogeneities (steps and so on). Let us mention such methods as the LEED technique (low energy electron diffraction), ARPS (angle resolved photoemission spectroscopy), inelastic scattering of ions with energy of the order of 1 MeV, electron microscopy, analysis of surface acoustic waves and surface polaritons (surface electromagnetic waves [Ref. 22]). Also known are some other methods involving the use of light, x-rays and neutrons.

A great deal of progress has already been made. Surface magnetic ordering has been observed. Particularly noteworthy are studies of inversion layers on the $Si-SiO_2$ interface, properties of electrons on the surface of liquid helium [Ref. 22], investigation of surface polaritons [Ref. 21] and reconstruction of some crystal surfaces [Ref. 22, 23].

Here we take surface reconstruction to mean a change in lattice parameter for atoms that are situated on the surface. For example on the surface of Si (face 111) under certain conditions the lattice parameter is seven times greater than in the volume. It is possible that in examining the effect of reconstruction in many cases it is important to consider the role of surface electron levels.

Studies of phase transitions in two-dimensional and quasi-two-dimensional systems are impressive both in scale and in significance. Strictly speaking, this problem is not new, but is, so to speak, gathering momentum [Ref. 22, 24, 25]. The tasks here are quite diverse, and are of course intimately related to surface physics.

There is no doubt that surface physics is on a steep climb and will bring us much that is new.

7. Behavior of Matter in Ultrastrong Magnetic Fields. Investigation of Very Large Molecules. Liquid Crystals

The problems mentioned in the heading of this section have little relation to one another, none of them was mentioned in Ref. 1, but they were included in Ref. 2. Unification of these three problems in a single section stems merely from the reluctance to go into any of them in detail. At the same time, I did not wish to simply omit them as I have done with many others that go beyond the scope of this article.

Ultrastrong magnetic fields are those in which the structure of atoms, molecules or condensed substances formed from them are determined to a great extent by the magnetic field rather than by Coulomb forces. Such a situation arises when the Zeeman (magnetic) splitting between levels exceeds the distance between the levels in the absence of a magnetic field. For the hydrogen atom the characteristic

difference of energies between levels in the absence of a field (or in a weak field) is $E_a \sim e^4 m/2\hbar^2 \sim 10$ eV. On the other hand, Zeeman splitting is $E_H \sim e\hbar/mc \sim 10^{-8}H$ eV (here field strength H is measured in oersteds or gausses since H could also mean magnetic induction B). Obviously $E_H \gg E_a$ when $H \gg e^3 m^2 c/\hbar^3 = (e^2/\hbar c)^2 \times (mc/e\hbar)mc^2 \sim 3 \cdot 10^9$ Oe. For heavy atoms, the right-hand member of this equation contains a factor Z^3 (Z is atomic number).

As is clear from this estimate, the problem of the behavior of matter in ultrastrong magnetic fields was to some extent abstract before the discovery of pulsars (1967-1968). But we now know that on the surface of magnetized neutron stars (pulsars) the magnetic field reaches values of $H \sim 10^{12}$-10^{13} Oe. Thus the surface layer of neutron stars, and especially of pulsars is in a strong field (the field at the surface of some neutron stars may not be so strong). If iron is predominant in this layer, as is quite probable, such iron is a material quite unlike anything that we know, apparently consisting of Fe_2 molecules stretched out along the field, forming some kind of polymer structure with large binding energy. The latter is significant for the entire electrodynamics of pulsars since it determines the possibility of electrons and ions being torn from the surface (see some literature cited in Ref. 2).

Fortunately, the matter is not limited to the surface properties of neutron stars so far away. While we cannot set up ultrastrong magnetic fields for atoms and molecules (in the sense described above) in the laboratory, there are situations where the effect of a magnetic field is stronger than the influence of Coulomb forces in fields that are accessible right here on earth. For example, the binding energy of hydrogen-like excitons in semiconductors is $m_{eff}/m\varepsilon^2$ times less than for the hydrogen atom (here m_{eff} is the effective mass of an electron and a hole, m is the mass of the electron and ε is the permittivity of the material). Splitting of levels in a magnetic field in this case is m/m_{eff} times greater than for the atom. As a result, the field is ultrastrong for the condition $H \gg 3 \cdot 10^9 \times m_{eff}^2/m^2\varepsilon^2$ Oe. At values of $m_{eff} \sim 0.1m$, $\varepsilon \sim 10$, which are completely realistic for a semiconductor, the action of the field predominates at $H \gg 3 \cdot 10^5$ Oe, i. e. even in accessible fields. In general, "exciton matter" can be studied in strong and even ultrastrong fields in the laboratory.

It is to be hoped that even this discussion will give an idea of the diversity and extraordinary nature of the problem of the behavior of matter in ultrastrong magnetic fields.

Despite the exceptional importance of biological problems for science and for the development of all human society, we completely omit them here, just as in Ref. 1 and 2. By way of justification, if such is needed, suffice it to quote the well-known advice not to try to bound the unbounded. There are two reasons that we mention giant molecules here (proteins, nucleic acids) though they are mainly of biological importance. First of all, such molecules occupy a certain intermediate place between "ordinary" molecules and a condensed medium, or droplets and filaments of condensed medium. With certain stipulations, the concepts of phase transitions, ordering, conduction bands and so on can be applied under such conditions. Secondly, as far as I can judge, there is still a great lag (compared with some other areas of physics) with respect to developing effective methods of analyzing the structure of giant molecules, especially under conditions where

they are few in number and are in solution or in a mixture with other molecules. The potential importance of pertinent research is so great that physicists ought not to forget it.

Liquid crystals have been known for a long time. But I remember when physicists treated them as a sort of oddity: will wonders never cease--crystal and liquid at the same time. The availability of a large number of simpler objects for research, lack of engineering applications brought about a situation leaving the study of liquid crystals in the dark. Now the situation is quite different. Liquid crystals are extensively used in technology, play a large part in biology, and finally, liquid crystals of various types and the phase transitions in them have been of interest for various studies in the field of physics of condensed media. The interest in liquid crystals is unabating.

8. X-Ray, Gamma and New Kinds of Optical Lasers

This section was also missing in Ref. 1, despite the fact that interest in lasers in science and engineering is enormous, and has not slackened for about twenty years. However, although the development of laser technology as well as applications of lasers (including nonlinear optics) comprises an extensive physical and technical problem, there is still little to choose from when it comes to material for this article. Lasers of fundamentally new types and those with powers several orders of magnitude greater than conventional lasers are another matter (it is quite probable that attainment of such high powers will require new methods and principles).

And by the way, here we can clearly see the arbitrary nature of any list of "Particularly important and interesting problems." In nearly every field of physics and astrophysics, a jump by several orders of magnitude, and sometimes even by one order, is a big problem in itself, though far from always realistic. One of many examples is in high-pressure physics. Pressures right up to about 1 Mbar have generally been mastered, but as we pointed out in section 3, we have not managed to go much further in the static mode, and here we are running into fundamental difficulties. Getting to static pressures of 10 Mbar in volumes that are not too small and with control would be a breakthrough. But there is no such problem in our list (at least not in explicit form) since an actual physical problem is more than mere wishes and conversations.

Returning to our topic, we note than in recent years a great deal is being written about free electron lasers [Ref. 26]. This refers to realization, and in some cases considerable development of the rather old idea of generating electromagnetic waves by a beam of relativistic electrons passing through an undulator or wiggler (in the simplest version, this is a system of magnets that creates an alternating field along the beam, shaking the electrons in the beam). It is difficult to see the analogy with lasers in systems of this type, and the term "free electron laser" seems a misnomer. But of course we are not dealing with names. It is quite possible that the "free electron laser" will be of practical interest in the field of microwaves and optics. As to the transition to the x-ray region of the spectrum, here the effectiveness of a device of the undulator type using dense relativistic beams still remains entirely problematical.

It should be noted that the problem of making very powerful x-ray sources has in general been solved by using synchrotrons (the same end can be attained by using an electron linac combined with an undulator, or by setting up an undulator section in the synchrotron). But usually this means incoherent emission of individual electrons. However, one would like to use coherent emission as in the laser, and to have the capability of achieving a high degree of monochromaticity. Such a device, the analog of the laser in the x-ray region, could be called the xaser, and in the case of gamma rays the term gaser could be used.*

In systems with an electron beam, coherence "works" only in sufficiently dense beams, and under a number of other conditions that are hard to realize in the x-ray region. It is in this sense, i. e. in the sense of a coherent "free electron laser" that we called attention above to lack of clarity in the transition to the x-ray region of the spectrum (and it is only when coherence is used that the name makes any sense).

Besides dense electron beams, it has been suggested that xasers could be made by using atomic transitions, and gasers could use transitions in atomic nuclei. Ref. 2, section 7 contains some information relating to this. As far as we know, there have been no important advances in this field recently. All the same, the paths that have been brought to light already in the literature are very complex (it is reasonable to include among such paths, for example, those associated with the use of atomic explosions).

Not all dreams become reality and are of practical interest besides. Therefore it is entirely possible that xasers and gasers will never be built, or in any event will not find wide application. But who knows... Some unexpected idea, as has often happened in the history of physics, could in principle radically alter the situation.

9. Superheavy (Far Transuranium) Elements. "Exotic" Nuclei

In Ref. 1, nuclear physics was not only included in the "macrophysics" section, but was represented only by a single problem (superheavy elements). Both were debatable, and it is now clear that there are more problems of "particular importance" in the area of nuclear physics in any event. Therefore, Ref. 2 already contained the heading "exotic nuclei."

The problem of the search for superheavy elements has not undergone any appreciable changes (with a reservation that will be clear from the following). To be sure, a report appeared in 1976 in one of the most prestigious physics journals (PHYSICAL REVIEW LETTERS) on occurrence of quite stable elements with $Z = 116$, 126 and others. However, this paper was in error. But the only ones safe from error are those who do nothing. We already pointed out in section 3 that such errors should not be dramatized. Articles cited in Ref. 2 shed light on the ways

*As we know, the word "laser" is an acronym formed by the first letters of words in the phrase "light amplification by stimulated emission of radiation." Therefore it would be inconsistent to use the terms "x-ray laser" and "gamma laser." The words "xaser" and "gaser" result from substituting "x" (x-ray) and "g" (gamma ray) for the letter "l" (light) in "laser." But of course terminology is a secondary matter, the moreso as we are not yet dealing with actual devices in the case of xasers and gasers.

being used in attempts or hopes to synthesize or detect superheavy elements. We can add here only that a report appeared in late 1980 [Ref. 27] on possible observation of a track of a nucleus with $Z \geqslant 110$. The track was detected in an olivine crystal of meteoric origin.

Nuclei that are part of cosmic rays leave tracks in crystals that are revealed by special treatment (in particular by etching and annealing). The length of the tracks depends on the atomic number of the nucleus. In Ref. 27, about 150 tracks of nuclei of the uranium group were observed with lengths of 180-240 μm. In addition, the above-mentioned single track was observed with length of 365 μm, which corresponds to a nucleus with $Z \geqslant 110$. Of course this result must be confirmed by finding other such tracks, and also by additional proof of the statement that we are actually dealing with a nucleus with $Z \geqslant 110$. If the observed track indeed belongs to a nucleus with $Z \geqslant 110$, then the occurrence of such nuclei relative to the occurrence of uranium nuclei is of the order of 10^{-3}.

As concerns other problems from the field of nuclear physics, it should be noted that investigation of the nucleus in some cases sheds light on the interaction between nucleons, and between nucleons and leptons [Ref. 28]. Considerable attention is being given to nuclear matter, which exists primarily in neutron stars. Here there is an obvious connection with astrophysics (see for example Ref. 29). Of considerable interest is the possibility being discussed in the literature of existence of nuclear matter and atomic nuclei with density exceeding the usual value by a factor of two or more (see some citations given in Ref. 2). In known nuclei, such a dense phase is apparently not realized, but prospects are being discussed for observing its "precursors" in certain nuclei (it is known that a phase transition influences the properties of matter even before the transition point is reached) [Ref. 30a]. Considerable attention is being given in recent years to collisions of relativistic heavy nuclei. In general, there is no doubt that investigation of the atomic nucleus, as formerly, is associated with a number of fundamental physical problems (see also Ref. 30b).

V. Concluding Remarks

Before the author's mental gaze, and I hope that of my readers as well, has flashed a decade full of intense work by physicists and astronomers. Ten years is a long time to a person. For a young person, because ten years ago he might not yet have been an adult. For an older person, a decade in science is also a long time, but for quite another reason: there is less and less chance of prolonged participation in the development of science, or even keeping track of such development. However, if we can set aside our subjective perception of time and its passage, a decade in sciences is not so much. Let us recall that special relativity theory is about 75 years old, general relativity theory--65, and quantum mechanics--55. And at the same time, it is these theories that lie at the foundation of contemporary physics. Superconductivity was discovered in 1911, and cosmic rays in 1912. Yet even today both these problems are at the center of attention, and are being studied by many more people than in the first two or three decades after their discovery. Thus the time scale in contemporary physics is longer than an active human lifetime, to say nothing of a decade. Let us add that the complexity of some modern experimental facilities (accelerators, space-station observatories, ground-based optical and radio telescopes, and so on) is such that at least

ten or fifteen years have elapsed between the time of the initial planning stage and final completion.*

In light of what has been said, it is natural that over the decade separating Ref. 1 from the present article, even though much that is new has occurred, still most of the problems remain on our list. It is true that considerable changes have occurred in microphysics, but this apparently makes the intervening years exceptional (however, many of the new ideas came up earlier, e. g. the quark hypothesis in 1963-1964).

Thus a decade in the development of physics and astronomy, though not extremely long, nevertheless has been witness to much that is new.

Therefore, it seems to me, if this article was worth writing at all as a kind of continuation of Ref. 1, then it has been appropriate to do it just now, ten years later. But should these articles have been written? I leave that to others to judge. Let me just say that the writing has been an interesting challenge for me. The burst of growth in physics and astronomy has been so great that it is no easy matter to trace that growth in even a score of areas and problems, as have been singled out in this article. On the other hand, in any given period it is possible to treat only one or two problems profesionally, so to speak, going into details. In this regard, work on an article such as this one gives occasion to become acquainted, if only fleetingly, with a lot of material of wide scope. One learns much that is interesting, the trees no longer overshadow the forest, the outlook for the future can be seen, the latitude and at the same time the profound unity of physics, the wealth of its content become clearer. If some of my readers share these feelings to any extent, the purpose of the article will have been achieved. I invite constructive criticism from those who read the article but are partly dissatisfied or even irritated. Such criticism, I feel, should come down to the writing of other articles, short or long, in which various problems and questions are treated otherwise than here, put in a new light. I think that this is just what many readers of USPKHI FIZICHESKIKH NAUK want.

In conclusion, I want to take this opportunity to thank all those who made comments after reading the article in manuscript. Just as in Ref. 1, their names are not mentioned lest I impose upon others, even indirectly, the responsibility for the content and inadequacies of the article.

REFERENCES**

---

*To avoid overloading the article, we will not make any other comments here relating to the development of physics and astronomy. The author's opinion on this account is clear from Ref. 2, 78 (let me note that I have changed my mind regarding the nature of the "second astronomical revolution" as expressed in Ref. 2, and now hold the view presented in Ref. 78).

**A rather large number of references to the literature on almost all of the questions dealt with in this article can be found in Ref. 2. Besides, in many cases additional references can be found by looking through the indexes of articles published in USPEKHI FIZICHESKIKH NAUK. Such indexes are published each year in the December issue of the journal.

1. Ginzburg, V. L., USPEKHI FIZICHESKIKH NAUK, Vol 103, 1971, p 87.

2. Ginzburg, V. L., "O fizike i astrofizike (kakiye problemy predstavlyayutsya seychas osobenno vazhnymi i interesnymi?)" [Physics and Astrophysics (What Problems are now of Particular Importance and Interest?)], Moscow, Nauka, 1980.

3. a) "Novosti termoyadernykh issledovaniy v SSSR: Operativnaya informatsiya" [News of Fusion Research in the USSR: Operational Information], Moscow, Institute of Atomic Energy, 1980, 1981.

   b) Ionass, Dzh., USPEKHI FIZICHESKIKH NAUK, Vol 133, 1981, p 159.

4. Jerome, D., Mazaud, A., Ribault, M., Bechgard, K., J. DE PHYS., (PARIS), LETT., Vol 41, 1980, p 95.

   Andres, K., Wudl, F., McWhan, D. B., Thomas, G. A., Nalewajek, D., Stevens, A. L., PHYS. REV. LETTS, Vol 45, 1980, p 1449.

   Greene, R. L., Engler, E. M., Ibid., p 1587.

5. Ginzburg, V. L., Kirzhnits, D. A., ed., "Problema vysokotemperaturnoy sverkhprovodimosti" [Problem of High-Temperature Superconductivity], Moscow, Nauka, 1977; see also USPEKHI FIZICHESKIKH NAUK, Vol 118, 1976, p 315.

6. Stepanov, G. N., Yakovlev, Ye. N., PIS'MA V ZHURNAL EKSPERIMENTAL'NOY I TEORETICHESKOY FIZIKI, Vol 32, 1980, p 657.

7. Brandt, N. G. et al., Ibid., Vol 27, 1978, p 37.

   Chu, C. W. et al., PHYS. REV., SER. B, Vol 18, 1978, p 2116.

8. Volkov, B. A., Ginzburg, V. L., Kopayev, Yu. V., PIS'MA V ZHURNAL EKSPERIMENTAL'NOY I TEORETICHESKOY FIZIKI, Vol 27, 1978, p 221.

   Volkov, B. A., Kopayev, Yu. V. et al., Ibid, p 615; Vol 30, 1979, p 317.

   Ginzburg, V. L., SOL. STATE COMM., 1981 (in press).

9. Lefkowitz, I., Manning, J. S., Bloomfield, P. E., PHYS. REV., SER. B, Vol 20, 1979, p 4506; see also PHYS. REV., SER. B, Vol 23, 1981, p 3022.

10. Gebale, T. I., Chu, C. W., COMM. SOL. STATE PHYS., Vol 9, 1979, p 115.

11. Brown, E., Homan, C. G., MacCrone, R. K., PHYS. REV. LETTS, Vol 45, 1978, p 478.

12. Stishov, S. M., USPEKHI FIZICHESKIKH NAUK, Vol 127, 1979, p 719; see also PIS'MA V ZHURNAL EKSPERIMENTAL'NOY I TEORETICHESKOY FIZIKI, Vol 33, 1981, p 136.

13. a) Rays, T., Khensel, Dzh., Fillips, T., Tomas, G., "Elektronno-dyrochnaya zhidkost' v poluprovodnikakh" [Electron-Hole Liquid in Semiconductors], Moscow, Mir, 1980.

b) Sadovskiy, M. V., USPEKHI FIZICHESKIKH NAUK, Vol 133, 1981, p 223.

14. a) Landau, L. D., Lifshits, Ye. M., "Statisticheskaya fizika" [Statistical Physics], Part 1, Moscow, Nauka, 1976.

b) Ma, Sh., "Sovremennaya teoriya kriticheskikh yavleniy" [Modern Theory of Critical Phenomena], Moscow, Mir, 1980.

15. a) Levelt Sengers, J. M. H., PHYSICA SER. A., Vol 82, 1976, p 319.

b) Levanyuk, A. P., Sannikov, D. G., USPEKHI FIZICHESKIKH NAUK, Vol 132, 1980, p 694.

16. Ginzburg, V. L., Sobyanin, A. A., USPEKHI FIZICHESKIKH NAUK, Vol 120, 1976, pp 153, 733; PHYS. LETT. SER. A, Vol 69, 1979, p 417.

17. Fabelinskiy, I. L., "Molekulyarnoye rasseyaniye sveta" [Molecular Light Scattering], Moscow, Nauka, 1965.

Ginzburg, V. L., Levanyuk, A. P., Sobyanin, A. A., USPEKHI FIZICHESKIKH NAUK, Vol 130, 1980, p 615; PHYS. REPT., Vol 57, 1980, p 153.

18. "Sverkhtekuchest' geliya-3. Sbornik statey" [Superfluid ^{3}He. Collection of Articles], Moscow, Mir, 1977.

"Kvantovyye zhidkosti i kristally. Sbornik statey" [Quantum Liquids and Crystals. Collection of Articles], Moscow, Mir, 1979.

19. Hardy, W. N. et al., PHYS. REV. LETTS, Vol 45, 1980, p 453.

Cline, R. W. et al., Ibid., p 2117.

20. Walraven, J. T. M., Silvera, I. F., Mattey, A. P. M., PHYS. REV. LETTS, Vol 45, 1980, pp 449, 915.

21. Agranovich, V. M., Ginzburg, V. L., "Kristallooptika s uchetom prostranstvennoy dispersii i teoriya eksitonov" [Crystal Optics With Regard to Spatial Dispersion, and Exciton Theory], Moscow, Nauka, 1979.

22. "Proc. Intern. School on Condensed Matter Physics", Varna, Bulgaria, 1980.

23. Tabor, D., SURFACE SCI., Vol 89, 1979, p 1.

24. Pokrovsky, V. L., ADV. PHYS., Vol 28, 1979, p 595.

25. Nelson, D. R., in: "Proc. Summer School in Statistical Mechanics", Enschede, Netherlands, 1980.

26. Brantman, V. L., Ginzburg, N. S. [sic], Petelin, M. I., OPTICS COMMUNS, Vol 30, 1980, p 409.

27. Perelygin, V. P., Stetsenko, S. G., PIS'MA V ZHURNAL EKSPERIMENTAL'NOY I TEORETICHESKOY FIZIKI, Vol 32, 1980, p 622.

28. Blin-Stoyle, R. J., CONTEMP. PHYS., Vol 20, 1979, p 377.

Nikolayev, N. N., USPEKHI FIZICHESKIKH NAUK, Vol 134, No 3, 1981.

29. Pines, D., USPEKHI FIZICHESKIKH NAUK, Vol 131, 1980, p 479.

Pines, D., SCIENCE, Vol 207, 1980, p 597; J. DE PHYS., Vol 41, 1980, p C2-111.

30. a) Alberico, W. M. et al., PHYS. REV., SER. B, Vol 92, 1980, p 153.

Vasak, D. et al., Ibid., Vol 93, 1980, p 243.
Mohan, L. R. R., Minich, R. W., Ibid., p 467.

b) Sliv, L. A., USPEKHI FIZICHESKIKH NAUK, Vol 153, 1981, p 337.

31. Einstein, A., Collected Scientific Papers Vol 2, Moscow, Nauka, 1966, p 406.

32. Salam, A., USPEKHI FIZICHESKIKH NAUK, Vol 132, 1980, p 229.

33. Vaynberg, S., Ibid., p 201.

Glashow, S., Ibid., p 219.

34. Cleine, D., Rubbia, C., PHYS. TODAY, Vol 23, No 8, 1980, p 44.

35. Iliopoulos, J., CONTEMP. PHYS., Vol 21, 1980, p 159.

t'Hooft, G., SCI. AMERICAN, Vol 242, No 6, 1980, p 90.

36. Berger, Ch. et al., PHYS. REV., SER. B, Vol 86, 1979, p 418; PHYS. REV. LETTS, Vol 43, 1979, p 830.

Azimov, Ya. I., Dokshitser, Yu. L., Khoze, V. A., USPEKHI FIZICHESKIKH NAUK, Vol 132, 1980, p 443.

37. Vaynshteyn, A. I., Zakharov, V. I., Shifman, M. A., USPEKHI FIZICHESKIKH NAUK, Vol 131, 1980, p 537.

38. Georgiand, H., Glashow, S. L., PHYS. TODAY, Vol 33, No 9, 1980, p 30.

39. Okun', L. B., USPEKHI FIZICHESKIKH NAUK, Vol 134, 1981, p 3; see also Okun', L. B., "Leptony i kvarki" [Leptons and Quarks], Moscow, Nauka, 1981.

40. Rikhter, B., USPEKHI FIZICHESKIKH NAUK, Vol 125, 1978, p 201.

Ting, S., Ibid., p 227.

41. Lederman, L., USPEKHI FIZICHESKIKH NAUK, Vol 128, 1979, p 693.

42. Bartel, W. et al., PHYS. REV., SER. B, Vol 89, 1979, p 136.

Barber, D. P. et al., PHYS. REV. LETTS, Vol 44, 1980, p 722.

43. Chanowitz, M. S., Ibid., p 59.

44. Heisenberg, W., USPEKHI FIZICHESKIKH NAUK, Vol 121, 1977, p 657.

45. Nambu, Y., USPEKHI FIZICHESKIKH NAUK, Vol 124, 1978, p 147.

Drell, S. D., PHYS. TODAY, Vol 31, No 6, 1978, p 23.

46. Yang, Ch., USPEKHI FIZICHESKIKH NAUK, Vol 132, 1980, p 169.

47. Pais, A., REV. MOD. PHYS., Vol 15, 1979, p 861.

48. Vaynberg, S., USPEKHI FIZICHESKIKH NAUK, Vol 118, 1976, p 505; Vol 120, p 677.

Cleine, D., Mann, A., Rubbia, C., USPEKHI FIZICHESKIKH NAUK, Vol 120, 1976, p 97.

Iliopoulos, J., USPEKHI FIZICHESKIKH NAUK, Vol 123, 1977, p 565.

Slavnov, A. A., USPEKHI FIZICHESKIKH NAUK, Vol 124, 1978, p 487.

49. Kirzhnits, D. A., USPEKHI FIZICHESKIKH NAUK, Vol 125, 1978, p 169.

50. Rikhter, B., USPEKHI FIZICHESKIKH NAUK, Vol 130, 1980, pp 707, 717.

Wilson, R. R., SCI. AMERICAN, Vol 242, No 1, 1980, p 26.

51. Barkov, L. M., Zolotarev, M. S., Khriplovich, I. B., USPEKHI FIZICHESKIKH NAUK, Vol 132, 1980, p 409.

52. Bogdanov, Yu. V., Sobel'man, I. I., Sorokin, Yu. N., Struk, I. I., PIS'MA V ZHURNAL EKSPERIMENTAL'NOY I TEORETICHESKOY FIZIKI, Vol 31, 1980, pp 234, 556.

53. Azimov, Ya. I., Khoze, V. A., USPEKHI FIZICHESKIKH NAUK, Vol 132, 1980, p 379.

54. Dolgov, A. D., Zel'dovich, Ya. B., USPEKHI FIZICHESKIKH NAUK, Vol 130, 1980, p 559.

55. Markov, M. A., USPEKHI FIZICHESKIKH NAUK, Vol 111, 1973, p 719.

56. Fridman, D., van N'yuvenkheyzen, P., USPEKHI FIZICHESKIKH NAUK, Vol 128, 1979, p 135.

57. Lyubinov,V. A. et al., Preprint ITEP, Moscow, 1980; PHYS. REV., SER. B, Vol 94, 1980, p 266.

Kozik, V. S. et al., YADERNAYA FIZIKA, Vol 32, 1980, p 301.

58. Reines et al., PHYS. REV. LETTS, Vol 45, 1980, p 1307.

Barger, V. et al., PHYS. REV., SER. B, Vol 93, 1980, p 194.

59. Bilen'kiy, S. M., Pontekorvo, B. M., USPEKHI FIZICHESKIKH NAUK, Vol 123, 1977, p 181.

60. Gunn, J. E. et al., ASTROPHYS. J., Vol 243, 1981, p 1.

61. Drell, S., USPEKHI FIZICHESKIKH NAUK, Vol 130, 1980, p 507.

62. Bartel, W. et al., PHYS. REV., SER. B, Vol 92, 1980, p 206.

63. Ginzburg, V. L., PIS'MA V ZHURNAL EKSPERIMENTAL'NOY I TEORETICHESKOY FIZIKI, Vol 22, 1975, p 514.

Ginzburg, V. L., Frolov, V. P., PIS'MA V ASTRONOMICHESKIY ZHURNAL, Vol 2, 1976, p 474.

64. Nikol'skiy, S. I., Feynberg, Ye. L., Avakyan, V. V. et al., USPEKHI FIZICHESKIKH NAUK, Vol 132, 1980, pp 392, 394, 395.

Feynberg, Ye. L., VESTNIK AKADEMII NAUK SSSR, No 1, 1981, p 25.

65. "Problema narusheniya *CP*-invariantnosti" [Problem of CP-Invariance Violation], USPEKHI FIZICHESKIKH NAUK, Vol 95, 1968, p 401.

Nanopoulos, D. V. et al., ANN. PHYS., N. Y., Vol 127, 1980, p 126.

66. Nikishev, A. A., Ritus, V. I., "Quantum Electrodynamics of Phenomena in Intense Field", TRUDY FIZICHESKOGO INSTITUTA IMENI P. N. LEBEDEVA AKADEMII NAUK SSSR, Vol 111, 1979.

67. Linde, A. D., REPT. PROG. PHYS., Vol 42, 1979, p 389.

68. Turner, M. S., Schramm, D. N., PHYS. TODAY, Vol 32, No 9, 1980, p 42.

69. Ginzburg, V. L., Man'ko, V. I., FIZIKA ELEMENTARNYKH CHASTITS I ATOMNOGO YADRA, Vol 7, 1976, p 3.

70. Oppenheimer, J. R., Snyder, H., PHYS. REV., Vol 56, 1939, p 455; a Russian translation of this article can be found in the collection "Al'bert Eynshteyn i teoriya gravitatsii" [Albert Einstein and the Theory of Gravitation], Moscow, Mir, 1979, p 353.

71. Rees, M. J., CONTEMP. PHYS., Vol 21, 1980, p 99.

72. Vessot, R. F. C., Levine, M. W., GENERAL RELATIVITY AND GRAVITATION, Vol 10, 1979, p 181; see also PHYS. REV. LETTS, Vol 45, 1980, p 2081.

73. Reasenberg, R. D. et al., ASTROPHYS. J. LETT., Vol 34, 1979, p L219.
Will, C. M., PROC. ROY. SOC. SER. A, Vol 268, 1979, p 5

74. Ginzburg, V. L., USPEKHI FIZICHESKIKH NAUK, Vol 128, 1979, p 435; this article was also published in the collection: Ginzburg, V. L., "O teorii otnositel'nosti" [Relativity Theory], Moscow, Nauka, 1979.

75. Mukhanov, V. F., USPEKHI FIZICHESKIKH NAUK, Vol 133, 1981, p 729.

Chaffee, F. H., SCI. AMERICAN, Vol 243, No 5, 1980, p 60.

76. Braginskiy, V. B., USPEKHI FIZICHESKIKH NAUK, Vol 132, 1980, p 387; ZEMLYA I VSELENNAYA, No 3, 1980, p 28.

Rudenko, V. N., USPEKHI FIZICHESKIKH NAUK, Vol 126, 1978, p 361.

77. Taylor, J. H. et al., NATURE, Vol 277, 1979, p 437.

78. Ginzburg, V. L., VOPROSY FILOSOFII, No 12, 1980, p 24.

79. Bernshteyn, I. M., Shvartsman, V. F., ZHURNAL EKSPERIMENTAL'NOY I TEORETICHESKOY FIZIKI, Vol 79, 1980, p 1617.

80. Bond, J. R. et al., PHYS. REV., Vol 45, 1980, p 1980 [sic].

81. Linde, A. D., PHYS. REV., SER. B, Vol 92, 1980, pp 119, 327, 394.

Kirzhnits, D. A., Linde, A. D., PRIRODA, Vol 11, 1979, p 20.

Kighuchi, M., PROGR. THEOR. PHYS., Vol 63, 1980, p 146.

Nanopoulos, D. V., Weinberg, S., PHYS. REV. SER. D., Vol 20, 1979, p 2484.

82. Bekenstein, J. D., Meisels, A., ASTROPHYS. J., Vol 237, 1980, p 342.

83. Gurovich, V. Ts., Starobinskiy, A. A., ZHURNAL EKSPERIMENTAL'NOY I TEORETICHESKOY FIZIKI, Vol 77, 1979, p 1683; see also PIS'MA V ZHURNAL EKSPERIMENTAL'NOY I TEORETICHESKOY FIZIKI, Vol 30, 1979, p 719.

Frolov, V. P., Vilkovisky, G. A., "Intern. Center for Theoretical Physics Preprint IC/79/69", Miramare, Trieste, 1979.

Zel'dovich, Ya. B., USPEKHI FIZICHESKIKH NAUK, Vol 133, 1981, p 479.

Mukhanov, V. F., Chibisov, G. V., PIS'MA V ZHURNAL EKSPERIMENTAL'NOY I TEORETICHESKOY FIZIKI, Vol 33, 1981, p 549.

84. Gurskiy, G., Van den Khevel, E., USPEKHI FIZICHESKIKH NAUK, Vol 118, 1976, p 673.

85. Manchester, R., Taylor, J., "Pul'sary" [Pulsars], Moscow, Mir, 1980.

Smith, F. G., "Pul'sary", Moscow, Mir, 1979.

Ter Khaar, D., USPEKHI FIZICHESKIKH NAUK, Vol 119, 1976, p 525.

86. Lamb, V. K., "Pulsars", IAU Symp. No 95, Bonn, West Germany, August, 1980. The materials of this symposium represent the latest detailed summary of data on pulsars (the materials of IAU symposia are usually published by D. Reidel, Netherlands).

87. Ginzburg, V. L., Zheleznyakov, V. V., ANN. REV. ASTRON. AND ASTROPHYSICS, Vol 13, 1975, p 511.

Ochelkov, Yu. P., Usov, V. V., PIS'MA V ASTRONOMICHESKIY ZHURNAL, Vol 5, 1979, p 180.

Machabeli, G. Z., Usov, V. V., Ibid., p 445.

88. Landau, L., Lifshits, Ye. M., "Teoriya polya" [Field Theory], Moscow, Nauka, 1973.

89. Hawking, S. W., NATURE, Vol 248, 1974, p 30; PHYS. REV. SER. D, 1976, Vol 13, p 191.

90. Frolov, V. P. USPEKHI FIZICHESKIKH NAUK, Vol 118, 1976, p 479; in: the Einstein Collection, 1975-1976, Moscow, Nauka, 1978, p 82.

"Chernyye dyry" [Black Holes], collection of articles, Moscow, Mir, 1978.

91. Kirzhnits, D. A., Frolov, V. P., PRIRODA, 1981.

92. Laytman, A. P., Syunyayev, R. A. et al., USPEKHI FIZICHESKIKH NAUK, Vol 126, 1978, p 515.

93. Ku, W. H. M., Helfand, D. J., Lucy, L. B., NATURE, Vol 88, 1980, p 323.

94. Ginzburg, V. L., Ozernoy, L. M., ASTROPHYS. AND SPACE SCI., Vol 48, 1977, p 401.

95. Dokuchayev, V. I., Ozernoy, L. M., PIS'MA V ASTRONOMICHESKIY ZHURNAL, Vol 3, 1977, p 391; ASTRONOMICHESKIY ZHURNAL, Vol 55, 1977, p 27.

Gurzyadyan, V. G., Ozernoy, L. M., PIS'MA V ASTRONOMICHESKIY ZHURNAL, Vol 5, 1979, p 630.

Duncan, M. J., Wheeler, J. C., ASTROPHYS. J. LETT., Vol 237, 1980, p L27.

96. Berezinsky, V. S., Ginzburg, V. L., MON. NOT. RQS, Vol 194, 1981, p 3.

97. Longeir, M. S., Einasto, J., ed., "The Large Scale Structure of the Universe", IAU Symposium No 79 (a Russian translation is being done).

98. Ginzburg, V. L., Ptuskin, V. S., USPEKHI FIZICHESKIKH NAUK, Vol 117, 1975, p 585.

99. "Origin of Cosmic Rays", IUPAP/IAU Symposium No 94, Bologna, Italy. D. Reidel, Amsterdam, 1980.

"VII Yevropeyskiy simpozium po kosmicheskim lucham" [Seventh European Symposium on Cosmic Rays], Leningrad, 1980.

100. Helfand, D. J. et al., NATURE, Vol 283, 1980, p 337.

Baity, W. A., Pterson, L. E., ed., "X-Ray Astronomy" (COSPAR), Oxford, Pergamon Press, 1979.

101. Gal'per, A. M., Luchkov, B. I., Prilutskiy, O. F., USPEKHI FIZICHESKIKH NAUK, Vol 128, 1979, p 313.

Pinkau, K., NATURE, Vol 277, 1979, p 17.

USPEKHI FIZICHESKIKH NAUK, Vol 132, 1980, pp 700, 702, 704.

102. Rozental', I. L., Usov, V. V., Estulin, I. V., USPEKHI FIZICHESKIKH NAUK, Vol 127, 1979, p 135.

Levental, M., McCallum, C. J., SCI. AMERICAN, Vol 243, No 1, 1980, p 50.

103. Swanenberg, B. N. et al., "Second COS-B Catalog of High-Energy Gamma-Sources", Preprint, 1980.

104. Mazets, Ye. P. et al., PIS'MA V ASTRONOMICHESKIY ZHURNAL, Vol 6, 1980, pp 609, 706.

105. Mazets, E. P. et al., NATURE, Vol 282, 1979, p 587; Vol 290, 1981, p 378.

Terrell, J. et al., NATURE, Vol 285, 1980, p 383.

106. Ramaty, R. et al., NATURE, Vol 287, 1980, p 122.

107. NATURE, Vol 284, 1980, p 507.

108. Bahcall, J. M., SPACE SCI. REV., Vol 24, 1979, p 227.

109. "Neutrino-77. Proc. of the Intern. Conference on Neutrino Physics and Neutrino Astrophysics", Moscow, Nauka, Vol 1, 1978.

110. Berezinskiy, V. S., PRIRODA, No 3, 1981, p 13; USPEKHI FIZICHESKIKH NAUK, Vol 133, 1981, p 545.

111. La Rue, G. S., Phillips, J. D., Fairbank, W. M., PHYS. REV. LETTS, Vol 46, 1981, p 967.

112. Georgi, H., SCI. AMERICAN, Vol 244, No 4, 1981, p 40.

6610
CSO: 8144/0499

UDC 519.95

OPTIMUM CONTROL OF SYSTEMS WITH INDEFINITE INFORMATION

Sverdlovsk OPTIMAL'NOYE UPRAVLENIYE SISTEMAMI S NEOPREDELENNOY INFORMATSIYEY in Russian 1980 (signed to press 12 Sep 80) pp 2, 145, 147, 149, 151

[Annotation and abstracts of articles from book "Optimum Control of Systems With Indefinite Information", edited by L. N. Petlenko, Ural Science Center, USSR Academy of Sciences, 1000 copies, 152 pages]

[Text] An examination is made of mathematical problems of control and observation under conditions of uncertainty. The articles of this collection can be put into three major divisions. The first of these comprises papers in which an investigation is made of problems of observation, the properties of information sets are studied, problems of identifying the parameters of controlled systems are examined. The second division presents results relating to the theory of differential games. Here an investigation is made of solutions of positional game problems of control based on program iterations, optimum strategies are constructed for some types of differential games. The third division contains papers where an investigation is made of game problems of control in the case of incomplete phase information and problems of controlling information sets.

The collection may be of interest to specialists working in the field of mathematical control theory and its applications.

UDC 519.9

APPROACH TO DEFINING DYNAMIC GAMES IN THE LANGUAGE OF GENERALIZED DYNAMIC SYSTEMS

[Abstract of article by Baydosov, V. A.]

[Text] It is shown that any family of motions with Markov properties that is generated by the strategy of one of the players uniquely determines a generalized dynamic system. This enables formulation and investigation of problems of dynamic games by using generalized dynamic systems. References 6.

UDC 517.9

MINIMAX PROGRAM CONSTRUCTION IN DIFFERENTIAL GAME

[Abstract of article by Batukhtin, V. D.]

[Text] The author considers a procedure for constructing sets of minimax positional absorption in a nonlinear game problem of approach. A relationship is established

between minimax positional and programmed absorption. A model example is presented. References 4.

UDC 519.9

EVALUATING WEIGHTING FUNCTIONS OF LINEAR CONTROLLED SYSTEMS FROM MEASUREMENT RESULTS, PART 2

[Abstract of article by Isakov, A. I.]

[Text] An examination is made of the problem of evaluating the parameters of linear controlled systems from results of observation of a linear signal that delivers information on the phase vector of the system. Equations are presented for determining the compatible region of weighting functions. References 8.

UDC 519.9

INFORMATION SETS OF QUASILINEAR SYSTEMS

[Abstract of article by Kayumov, R. I.]

[Text] The author examines a system with motion described by a differential equation with indefinite interference that appears nonlinearly in the second member of the equation. Some properties of information sets of such systems are studied. References 5.

UDC 519.9

SOME STABLE BRIDGES FOR LINEAR CONTROLLED SYSTEMS

[Abstract of article by Kryazhimskiy, A. V.]

[Text] The author points out an auxiliary construction used for solving some classes of linear game problems. References 6.

UDC 519.9

CONSTRUCTION OF OPTIMUM CONTROL OF MOTION IN A PLANE POTENTIAL FIELD

[Abstract of article by Kukushkin, A. P.]

[Text] An examination is made of the speed problem for a material point moving under the action of a potential force and a controlling force normal to the trajectory. Equations of the principle of the maximum are reduced to a second-order linear differential equation. A relation is demonstrated between the initial problem and the solution of the equation for normal variation of the trajectory and also the curvature of the generalized bachistochrone. References 6.

UDC 517.9

AN EXTREMUM TARGETING METHOD IN A MINIMAX DIFFERENTIAL GUIDANCE GAME

[Abstract of article by Loginov, M. I.]

[Text] The author proposes a modification of the method of extremum targeting in the guidance problem for a conflict-controlled system that is linear with respect to phase coordinates and nonlinear with respect to controls. When conditions of regularity are met, a method is given for forming the strategy of one of the players that guarantees this player a game result no worse than in the programmed maximin problem for the initial position. References 6.

UDC 519.9

CONSTRUCTION OF EQUILIBRIUM SETS OF STRATEGIES IN POSITIONAL MANY-PLAYER DIFFERENTIAL GAMES

[Abstract of article by Lutmanov, S. V.]

[Text] An examination is made of linear differential games of several players. Based on a suggested programmed construction, an equilibrium set of strategies is synthesized for all players without assuming pairwise nonintersection of maximum stable bridges. References 3.

UDC 519.9

METHOD OF CONSTRUCTING STABLE SETS IN DIFFERENTIAL-DIFFERENCE GAMES

[Abstract of article by Maksimov, V. I.]

[Text] The author gives a method of constructing stable sets for a differential-functional approach game. The technique is based on a dynamic programming procedure, and involves the use of smooth functionals that act as a potential. References 10.

UDC 519.9

CONTROL PROBLEM WITH VECTOR QUALITY CRITERION UNDER CONDITIONS OF UNCERTAINTY

[Abstract of article by Nikonov, O. I.]

[Text] The problem of controlling an ensemble (tube) of signal-compatible trajectories is considered for a linear controlled system that functions under conditions of uncertainty. A vector quality criterion is assumed that has components depending on the realization of cross sections of this ensemble and the time for occurrence of the process. References 7.

UDC 519.9

POSITIONAL CONTROL THEORY IN NONLINEAR SYSTEMS WITH DISTRIBUTED PARAMETERS

[Abstract of article by Okhezin, S. P.]

[Text] The author distinguishes a class of conflict-controlled systems described by ordinary differential equations in Banach spaces. The theorem of the alternative in the approach-evasion problem is valid for this class of systems. References 9.

UDC 517.9

MINIMAX PROGRAMMED CONSTRUCTION IN APPRACH PROBLEM

[Abstract of article by Ruzakov, V. Ya.]

[Text] The author considers an auxiliary minimax construction. A condition is given such that the approach problem is solved when this condition is met by an iteration process. References 8.

UDC 519.9

IRREGULAR INFORMATION GAME PROBLEM

[Abstract of article by Serov, V. P.]

[Text] The author considers a model example of an information game problem of guidance. An investigation is made of a linear controlled system with interference that has dynamics of the "boy and crocodile" type. Control is synthesized from the results of observation of part of the phase coordinates. Solution of the control synthesis problem is based on extremum constructions of the theory of game problems of dynamics. A strategy is found that ensures a game result that is optimum with respect to the minimax of a functional. Figures 3, references 6.

UDC 519.9

GAME PROBLEM OF GUIDANCE IN THE CASE OF INFORMATION DELAY

[Abstract of article by Filippov, S. D.]

[Text] A game problem of guidance with delay of information is considered for a linear system of general type. An alternative statement on possible outcomes of the game is proved on the basis of an analog of the method of extremum targeting with total recall. References 8.

UDC 519.9

INFORMATION SETS OF PARABOLIC SYSTEMS WITH QUADRATIC CONSTRAINT

[Abstract of article by Khapalov, A. Yu.]

[Text] An examination is made of a problem of a posteriori observation for a distributed parabolic system with unknown perturbations at input and output. Two different methods of observation are discussed. An analytical description is derived for information sets $X(\theta, y(\cdot))$ $(\theta > 0)$ that are compatible at time θ with the realized signal $y(t)$ $(t \in [0. \theta])$. References 11.

UDC 519.9

OPTIMALITY CONDITIONS OF DISCRETE-CONTINUOUS SYSTEMS

[Abstract of article by Chebykin, L. S.]

[Text] Necessary conditions of optimality of controls are obtained in the form of a maximum principle for a system whose behavior on a given time segment is described by a set of differential and finite-difference equations. It is shown that in the case of a linear system these conditions are sufficient as well. References 6.

UDC 519.9

PROGRAMMED CONSTRUCTIONS IN DIFFERENTIAL GAMES WITH INFORMATION STORE

[Abstract of article by Chentsov, A. G.]

[Text] An examination is made of iteration methods of constructing a stable system of functional sets and values of a game as a functional on histories of a controlled process for corresponding nonlinear differential games with information storage. Different iteration methods are compared and an example is proposed of a differential game with continuous criterion functional that does not have an equilibrium situation in positional strategies. References 6.

6610
CSO: 1862/42

END